Starch granule number and size in *Arabidopsis thaliana* leaves

Matilda Crumpton-Taylor

A thesis submitted to the University of East Anglia for the degree of Doctor of Philosophy

John Innes Centre
Norwich
September 2010

Abstract

The aim of my work was to understand the variation of starch granule number and size in *Arabidopsis thaliana* leaves. I describe first the development of methods to measure the number of starch granules per chloroplast. My work reveals that at a given developmental stage the number of granules per unit volume of stroma is much more conserved than the number of granules per chloroplast.

In this study I explore the role of STARCH SYNTHASE4 (SS4) in granule initiation and the control of granule numbers, by analysing the phenotype of the *Arabidopsis ss4* mutant. My results support and extend the observation that SS4 is required for starch synthesis in young leaves, and provide new information about its influence on the starch phenotype of the whole plant. In the absence of SS4, synthesis of glucan polymers as a whole seems to be blocked in the young leaves, indicating that SS4 may be responsible for the production of a small malto-oligosaccharide that is required as a primer for the polymerising activity of the other starch synthases and starch branching enzymes.

I describe the use of the *accumulation and regulation of chloroplast* (*arc*) mutants of *Arabidopsis* to explore the possibility that components of the chloroplast division apparatus could play an important role in granule initiation and/or starch metabolism. My results show that mutations in the chloroplast division components ARC3, ARC5, ARC6, *At*FtsZ1-1, *At*MinD1 and *At*MinE1 are not important and/or involved in starch metabolism.

Taken as a whole my results show that starch granule number within *Arabidopsis* chloroplasts is related to stromal volume. I suggest that the most likely mechanism of granule initiation is via spontaneous crystallisation when the concentration of suitable glucans or malto-oligosaccharides within a volume of stroma reaches a critical level.

Table of Contents

List of Figures

List of Tables

Acknowledgements

I want first to thank my supervisor Professor Alison Smith for her continuous support through all the little ups and downs during the past four years. I want to express my appreciation for all the helpful discussions, for her guidance and invaluable advice. I would also like to thank my supervisory committee members Professor Rob Field and Dr. David Laurie for supporting my work with valuable suggestions and constructive advice.

I would like to say a big thank you to all the past and present members of Alison's research group, for providing a great working environment and many enjoyable hours at work. I would like to thank Dr. Vas Andriotis and Dr. Thomas Howard for sharing their microscopy and technical knowledge. I want to say a special thank you to Dr. Marilyn Pike, Dr. Paul Barratt, Dr. Sylviane Comparot-Moss and Dr. Alex Graf for all their expertise. I would like to thank them for taking the time to help me with technical problems, for discussing my project with me, and explaining ideas and techniques clearly. I also wish to thank my other colleagues Brendan Fahy, Steve Mackay and Freddy Cook for the enjoyable lunches.

I would like to thank Kim Findlay and Susan Bunnewell for all their help with electron microscopy, including training, sample preparation and imaging. Thanks also to Ken Png and Scott Grandison for collaborating with me and helping produce interesting data to work with.

A warm thanks to Eva Thuenemann, Lucy Foulston, Dr. Liz Alvey and Dr. Yuki Yasumura for their friendship, for helping me to settle into Norwich and making it feel like home. I would like to thank my whole family and especially my parents, Jane and Leslie Crumpton-Taylor for their encouragement and support throughout my PhD. Last but not least, a big thank you to Alex Brown, to whom I am deeply grateful for his love, patience and support and for being the best friend I could have ever hoped for.

Abbreviations

ADG	ADPglucose pyrophosphorylase
ADP	Adenosine 5'-diphosphate
ADPG	Adenosine 5'-diphosphoglucose
AGPase	Adenosine 5'-diphosphoglucose pyrophosphorylase
AMY	α-amylase
ARC	Accumulation and Regulation of Chloroplasts
ATP	Adenosine 5'-triphosphate
BAM	β-amylase
BiFC	Bimolecular fluorescence complementation
BSA	Bovine serum albumin
cDNA	Complementary DNA
CDT1	Cdc10-dependent transcript 1
CIB	Chloroplast isolation buffer
Col	Columbia
CPE	Chloroplast processing enzyme
DAG	Days after germination
DBE	Debranching enzyme
Dex	Dexamethasone
DNA	Deoxyribonucleic acid
DP	Degree of polymerisation
DPE	Disproportionating enzyme
DTT	Dithiothreitol
EDTA	Ethlenediamineteteraacetic acid
EOD	End of day
EON	End of night
Fructose-6-P	Fructose 6-phosphate
FBPase	Fructose bisphosphatase
FIB-SEM	Focused Ion Beam-Scanning Electron Microscopy
FRET	Fluorescence Resonance Energy Transfer
FtsZ	Filamentary temperature-sensitive
FW	Fresh weight
GBSS	Granule Bound Starch Synthase
GCAM	Granule per Chloroplast Approximation Method
GC	Giant chloroplast
GFP	Green fluorescent protein
Glucose-1-P	Glucose-1-phosphate
Glucose-6-P	Glucose-6-phosphate
Glc	Glucose
GWD	Glucan water dikinase
HEPES	N-(2-hyroxyethyl)-piperazine-N'-(2-ethanesulfonic acid)
IEM	Inner Envelope Membrane
ISA	Isoamylase
LB	Luria-Bertani broth
LDA	Limit-dextrinase
L*er*	Landsberg *erecta*
LSF	LIKE SEX4
LUC	Luciferase
MCD	Multiple chloroplast division site

MEX1	Maltose exporter (maltose excess1)
MOS	Malto-oligosaccharides
MS	Murashige and Skoog
MTLS	Microtubule-like structures
NAD^+/NADH	Nicotinamide adenine dinucleotide oxidised/reduced form
$NADP^+$/NADPH	Nicotinamide adenine dinucleotide phosphate oxidised/reduced form
PAGE	Polyacrylamide gel electrophoresis
PARC	Paralog of ARC
PCR	Polymerase chain reaction
PDV	Plastid division
3-PGA	3-phosphoglycerate
PGI	Phosphoglucose isomerase
PGM	Phosphoglucomutase
PGSIP1	Plant glycogenin-like starch initiation protein 1
Pho1	Plastidial α-1,4-glucan phosphorylase
PHS	*Arabidopsis* homolog of Pho1
P_i	Inorganic orthophosphate
PP_i	Inorganic pyrophosphate
PWD	Phosphoglucan water dikinase
RNA	Ribonucleic acid
RNAi	RNA interference
RT-PCR	Reverse transcription - polymerase chain reaction
SAXS	Small-angle X-ray scattering
SBD	Starch Binding Domain
SBE	Starch Binding Enzyme
SDS	Sodium dodecyl sulphate
SE	Standard error of the mean
SEM	Scanning Electron Microscopy
SEX	Starch Excess
SnRK1	Sucrose non-fermenting-1-related protein kinase-1
SOC	Super Optimal broth with Catabolite repression
SS	Starch Synthase
SuSy	Sucrose synthase
TEM	Transmission Electron Microscopy
T_m	Melting temperature of primers
Trehalose-6-P	Trehalose-6-phosphate
Tris	3-N-tris (hydroxymethylaminomethane)
UDPG	Uridine 5-diphosphoglucose
v/v	Volume by volume
Ws	Wassilewskija
WT	Wild Type
w/v	Weight by volume
YFP	Yellow fluorescent protein

1 Introduction

1.1 Aim

The principal aim of my work is to understand the variation of starch granule number and size in *Arabidopsis* leaves. Although the structure of starch and the synthesis and degradation of its component polymers in the leaves of *Arabidopsis thaliana* is relatively well characterised, almost nothing is known about the variation in starch granule size and number and the extent to which these parameters are under genetic and environmental control. It seems likely that granule size and or number may be important in the control of starch degradation, which in turn is vital for normal plant growth. Evidence for this is as follows.

Arabidopsis maintains approximately linear rates of degradation through the night, such that starch is almost exhausted at dawn (Gibon *et al.,* 2004; Gibon *et al.,* 2009; Lu *et al.,* 2005). This controlled pattern of degradation is essential for normal growth. *Arabidopsis* mutants impaired in starch degradation, for example *starch excess4* (*sex4*) (Kötting *et al.,* 2009; Zeeman *et al.,* 1998a) and *glucan water dikinase1* (*gwd1,* also called *sex1*) (Caspar *et al.,* 1991; Yu *et al.,* 2001) and mutants unable to accumulate starch, for example *ADPglucose pyrophosphorylase1* (*adg1*) (Lin *et al.,* 1988) and *phosphoglucomutase1/ starch-free1* (*pgm1/stf1*) (Caspar *et al.,* 1985; Kofler *et al.,* 2000; Streb *et al.,* 2009) have a reduced growth rate. In the above mutants, the lack of provision of sugars from starch during the night leads to transcriptional changes indicative of carbon starvation, and a reduction or cessation of growth for several hours (Gibon *et al.,* 2004; Schulze *et al.,* 1994; Smith and Stitt 2007; Comparot-Moss, S. JIC unpublished; Wiese *et al.,* 2007). The availability of carbohydrate affects both the leaf growth cycle and the elongation of roots (Smith and Stitt 2007; Wiese *et al.,* 2007).

Control of starch degradation in leaves at night requires starch to be in the form of granules, rather than amorphous glucans. For example the *isoamylase1* (*isa1*) mutation reduces the synthesis of starch granules and increases the production of a highly branched, soluble glucan called phytoglycogen. At night, phytoglycogen is broken down in an exponential manner, and reserves of this glucan are exhausted before dawn.

In contrast, granular starch in the *isa1* mutant is degraded linearly and lasts until dawn (Delatte *et al.,* 2005; Streb *et al.,* 2008; Zeeman *et al.,* 1998b).

Plants are able to adjust the rate of starch degradation in response to an unexpected early night (Graf *et al.,* 2010; Lu *et al.,* 2005). For example, starch accumulated during an unexpectedly shortened day is degraded at a rate so that reserves last until dawn, even though both the length of the night and the amount of starch available at the end of the day are altered relative to the previous night (Graf *et al.,* 2010). This adjustment requires information about both the length of the night and the amount of granular starch present at the end of the day. Measurement of night length is likely to be a function of the circadian clock (Graf *et al.,* 2010). The nature of any mechanisms that monitor or measure starch content is unknown, but it is reasonable to speculate that the size, shape and number of starch granules may be important.

The starch granules from leaves are flattened and disc like and on average between 1 and 2 µm in diameter, regardless of species (Grange *et al.,* 1989b; Santacruz *et al.,* 2004; Steup *et al.,* 1983; Wildman *et al.,* 1980). This contrasts in several respects with storage starches that show a huge variation in size (0.3 µm to over 100 µm, Lindeboom *et al.,* 2004), and shape from the smooth, oval potato starch to the irregular polygonal shaped granules of the Chinese taro (Jane *et al.,* 1994). The variation in storage starch indicates that there are species specific controls over how storage starch is accumulated and the granules are constructed. The conservation in size and shape of granules in leaves may imply that these parameters are important in diurnal starch turnover in plants in general. However, very little is known about how starch granule morphology and final size are determined or how important they may be in control of starch turnover.

In this chapter I describe the background to my research. First I discuss how starch is both synthesised and degraded, and the structure of the starch granule. I then review the present state of knowledge on how the starch granule is initiated and how starch granule number and morphology are determined. Finally I provide a rationale for my experimental approaches, described in the remainder of the thesis.

1.2 Starch Synthesis and Structure

Starch is present as semi-crystalline granules throughout the Plant kingdom and in some orders of the Protozoa kingdom. For example, starch granules have been observed in the protozoan *Toxoplasma gondii* (Guérardel *et al.,* 2005), *Eimeria brunetti* (Ryley *et al.,* 1969) and *Sarcocystis muris* (Sheffield *et al.,* 1977) all of which belong to the suborder Eimeriorina (Cavalier-Smith 1999). Granular starch is absent from the Animal, Bacteria, Chromista and Fungi kingdoms, although some species of fungi have been reported to contain non-granular starch-like material resembling short chain amylose molecules in their cell walls (Dodd and McCracken 1972; McCracken and Dodd 1971; Meeuse and Hall 1973).

1.2.1 How starch is synthesised

In photosynthetic organs (Figure 1.1A), starch is made in the chloroplasts during the daytime from the Calvin cycle intermediate fructose 6-phosphate (fructose-6-P) (reviewed in Zeeman *et al.,* 2007b). Within the chloroplast, phosphoglucose isomerase (PGI, EC 5.3.1.9) catalyses the reversible isomerisation of fructose-6-P and glucose 6-phosphate (glucose-6-P) (Neuhaus *et al.,* 1989; Yu *et al.,* 2000). Phosphoglucomutase (PGM, EC 5.4.2.2) then catalyses the conversion of glucose-6-P to glucose 1-phosphate (glucose-1-P) (Caspar *et al.,* 1985; Lytovchenko *et al.,* 2002).

In non photosynthetic organs, starch is synthesised in amyloplasts (non-photosynthetic plastids) from sucrose imported from the leaves (Figure 1.1B) (reviewed in Smith 2001). Sucrose is converted to glucose-6-P in the cytosol and then transported into the amyloplasts where it is converted to glucose-1-P (Harrison *et al.,* 1998; Hill and Smith 1991; Kammerer *et al.,* 1998; Neuhaus *et al.,* 1993; Tauberger *et al.,* 2000).

Starch synthesis in chloroplasts and amyloplasts is dependent on ADPglucose pyrophosphorylase (AGPase, EC 2.7.7.27), which catalyses the synthesis of adenosine 5'-diphosphate glucose (ADPG) and pyrophosphate (PP_i) from ATP and glucose-1-P (Lin *et al.,* 1988; Neuhaus and Stitt 1990; Wang *et al.,* 1998). ADPG is the substrate used by the starch synthases for the extension of glucan chains (Baba *et al.,* 1987; Recondo and Leloir 1961; Szydlowski *et al.,* 2009). In cereal endosperms ADPG is also

made in the cytosol by a cytosolic isoform of AGPase and then transported into the amyloplast (Ballicora *et al.,* 2000; Beckles *et al.,* 2001; Denyer *et al.,* 1996b; Shannon *et al.,* 1998).

An alternative starch synthesis pathway has been suggested in which the starch precursor molecule, ADPG, can be produced in the cytosol by sucrose synthase (SuSy) and be imported into the chloroplast (Baroja-Fernandez *et al.,* 2004; Munoz *et al.,* 2005; Munoz *et al.,* 2006). However, evidence for this alternative model has been criticised as being circumstantial and the model is not considered consistent with existing genetic and biochemical evidence (Neuhaus *et al.,* 2005; Streb *et al.,* 2009; Zeeman *et al.,* 2007b). Any contribution by SuSy to the ADPG pool in leaves is minor since SuSy is not required for transitory starch synthesis in the leaves (Barratt *et al.,* 2009).

Linear and branched chains of glucose molecules are referred to collectively as glucans. Starch granules contain two types of glucan polymer; amylopectin and amylose. Amylopectin consists of linear chains of α-1,4 linked glucoses joined by α-1,6 links that create branch points. Amylose consists of longer linear chains of α-1,4 linked glucoses with much less frequent α-1,6 links. The ratio of amylopectin to amylose within the granule varies between species and organs. However, amylopectin is the major component of the granule, forming the semi-crystalline granule matrix. The amylose content of starch from *Arabidopsis* leaves at the end of a 12 hour photoperiod is approximately 6% (Zeeman *et al.,* 2002b); whereas in tobacco leaf starch amylose makes up 15 to 20% of the granule (Matheson 1996) and in storage starches amylose makes up between 15 and 35% of the granule (Flipse *et al.,* 1996; Mohammadkhani *et al.,* 1998; Raeker *et al.,* 1998; Tomlinson and Denyer 2003). Synthesis of amylopectin requires three different types of enzyme, starch synthases (SS), starch branching enzymes (SBE) and debranching enzymes. On the other hand, extensive studies in maize, pea and potato prove that amylose is synthesised almost exclusively by one particular isoform of starch synthase, granule bound starch synthase (GBSS) (Denyer *et al.,* 1995; Denyer *et al.,* 1996a; Denyer *et al.,* 1999; Edwards *et al.,* 2002; Fulton *et al.,* 2002; Hovenkamp-Hermelink *et al.,* 1987; Kuipers *et al.,* 1994; MacDonald and Preiss 1985; Nelson and Rines 1962; Shure *et al.,* 1983; Sivak *et al.,* 1993).

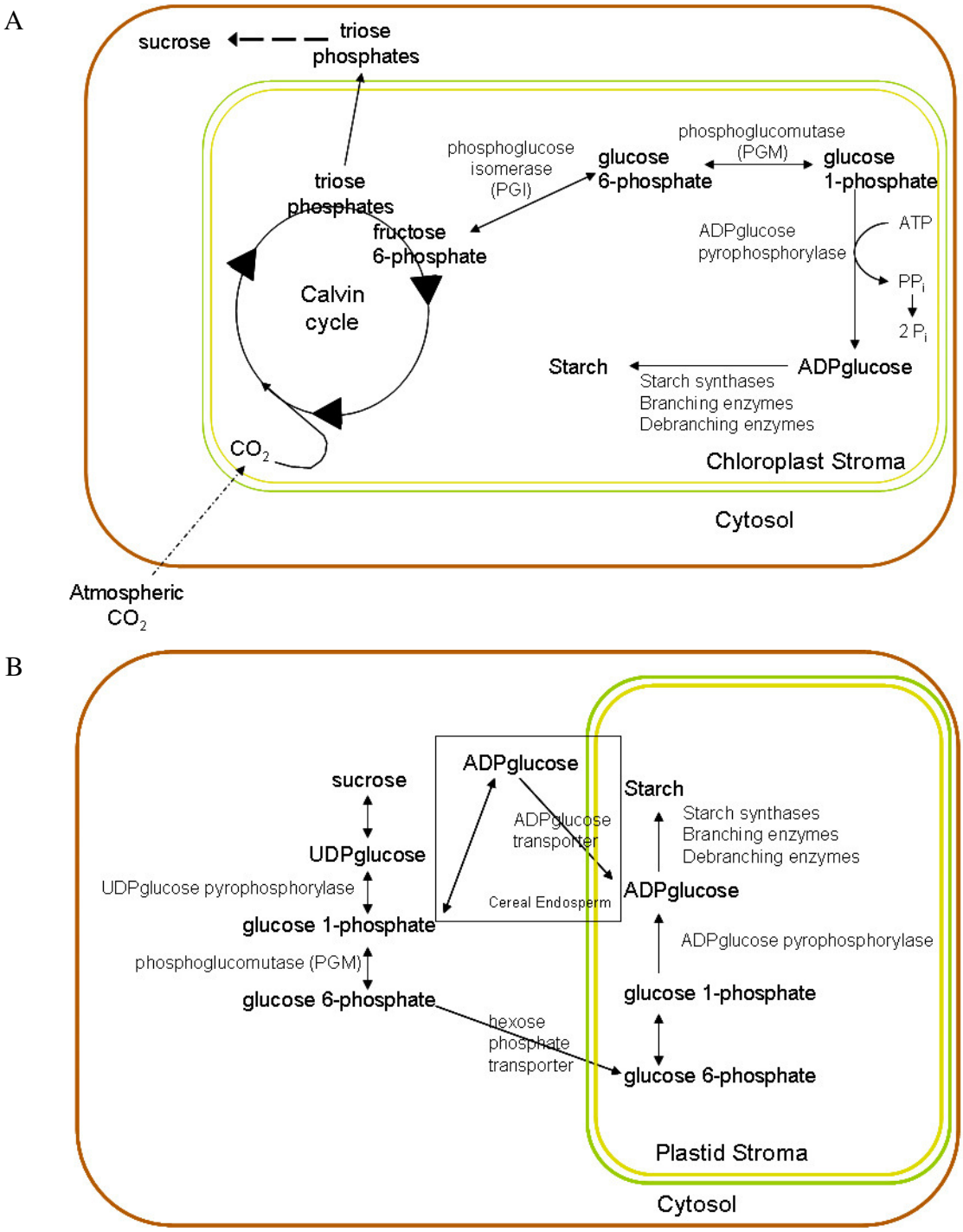

Figure 1.1: Pathways of starch synthesis. (A) Starch synthesis in photosynthetic organs (adapted from Zeeman *et al.,* 2007b). (B) Starch synthesis in non-photosynthetic organs (adapted from Smith *et al.,* 1997).

Based on amino acid sequence the starch synthases can be split into five major classes: SS1, SS2, SS3, SS4 and GBSS (Patron and Keeling 2005). The SSs (EC 2.4.1.21) elongate glucan polymers by catalysing the addition of glucose residues from ADPG to the non-reducing end of an α-1,4-linked glucan chain. All the SSs, excluding GBSS, are exclusively involved in amylopectin synthesis. The multiple isoforms of starch synthases are present in all higher plants and have been conserved across distantly related species, suggesting that they each have a distinct role in starch synthesis (Patron and Keeling 2005). Analysis of mutant plants and in vitro studies of the enzymes from species including maize, pea, potato, rice and *Arabidopsis* showed that SS1 preferentially elongates the shortest chains of amylopectin (degree of polymerisation (DP) 6-12), SS2 medium-length chains (DP 12-28) and SS3 longer chains (DP 60+) (Commuri and Keeling 2001; Craig *et al.,* 1998; Delvallé *et al.,* 2005; Edwards *et al.,* 1999; Fujita *et al.,* 2007; Zhang *et al.,* 2005; Zhang *et al.,* 2008). The contribution made by the starch synthase classes during granule formation varies between species and plant organs. For example, while both pea embryos and potato tubers contain SS2 (Denyer and Smith 1992; Edwards *et al.,* 1996; Edwards *et al.,* 1995), loss of SS2 has a large effect on pea embryo starch, but a small effect on potato tuber starch (Craig *et al.,* 1998; Edwards *et al.,* 1995). Loss of SS3 from rice endosperm results in smaller, rounder and less crystalline granules, while loss of SS3 from *Arabidopsis* leaves results in an increase in starch synthesis, but no alteration of granule size or shape (Fujita *et al.,* 2007; Ryoo *et al.,* 2007; Zhang *et al.,* 2005). Amylose synthesis occurs within the amylopectin matrix using malto-oligosaccharides (MOS) as primers and binding of GBSS to the starch granule is necessary for its activation (Denyer *et al.,* 1993; Tatge *et al.,* 1999; Zeeman *et al.,* 2002a).

SBEs (EC 2.4.1.18) are responsible for cutting α-1,4 linkages between glucose units and then adding the cleaved portion to another chain via an α-1,6 link to create a branch point (Borovsky *et al.,* 1975). Isoforms of SBEs fall into two classes I (or B) and II (or A), which have different roles in amylopectin synthesis (Burton *et al.,* 1995; Morell *et al.,* 1997; Rahman *et al.,* 2001). SBE class I enzymes preferentially cleave and transfer longer chains than class II enzymes (Guan and Preiss 1993; Takeda *et al.,* 1993). In addition, a study in barley revealed that the different isoforms of SBEII (SBEIIa and SBEIIb) play specific roles in determining the branching pattern and chain length distribution of glucan chains in the endosperm in vivo (Regina *et al.,* 2010). In general

mutations affecting class II SBEs in storage organs such as seeds and tubers reduce starch synthesis and result in amylopectin with longer chains and fewer branches (Bhattacharyya *et al.,* 1990; Blauth *et al.,* 2001; Jobling *et al.,* 1999; Mizuno *et al.,* 1993). Knocking-out the two SBE genes in *Arabidopsis* (which both encode class II SBEs) appears to prevent starch granule synthesis in the leaves (Dumez *et al.,* 2006). Maize mutants lacking SBEIIa are unable to degrade leaf starch effectively and the leaves tend to senesce (Blauth *et al.,* 2001). Mutations in class II SBEs also affect the rate of starch synthesis in pea leaves (Smith *et al.,* 1990; Tomlinson *et al.,* 1997). These results emphasise the importance of class II SBEs in starch granule formation and turnover in leaves. In contrast, mutations in SBEI have little effect on starch structure or chain length distribution (Blauth *et al.,* 2002; Safford *et al.,* 1998; Satoh *et al.,* 2003). Expression of all possible combinations of the three isoforms of SBE (SBEI, SBEIIa and SBEIIb) from maize in a *Saccharomyces cerevisiae* line lacking host branching enzymes, showed that the SBEs have very strong synergistic effects, with each combination of enzymes producing different polysaccharide structures (Seo *et al.,* 2002). For example, SBEI expression on its own has little affect on the host glucan accumulation, nor does SBEI expression in conjunction with either SBEIIa or SBEIIb. However, when all three SBEs are present there was a significant increase in branching compared to that seen with just SBEIIa and SBEIIb expression (Seo *et al.,* 2002). Therefore, SBEI does have an important role in influencing glucan structure, but only when the other SBEs are present.

Starch de-branching enzymes, isoamylase (ISA; EC 3.2.1.68) and limit-dextrinase (LDA; EC 3.2.1.142) cleave α-1,6 links in branched glucans. Both types of enzyme are able to debranch amylopectin, while LDA is also able to digest the yeast glucan, pullulan and ISA can debranch the bacterial and animal glucan, glycogen. The isoforms of ISA fall into three groups: ISA1, ISA2/DBE1 (DEBRANCHING ENZYME1) and ISA3 (Hussain *et al.,* 2003; Rahman *et al.,* 2003). ISA1 and ISA2 have been shown to be involved in starch synthesis (Bustos *et al.,* 2004; James *et al.,* 1995; Streb *et al.,* 2008; Wattebled *et al.,* 2005; Zeeman *et al.,* 1998b), whereas ISA3 is only involved in starch degradation (Delatte *et al.,* 2006; Dinges *et al.,* 2003). The role of ISA and LDA in starch synthesis will be discussed in more detail later.

In the single celled green alga *Chlamydomonas reinhardtii,* α-1,4 glucanotransferase or disproportionating enzyme (D-enzyme; EC 2.4.1.25) is required for normal starch granule biogenesis (Colleoni *et al.,* 1999a; Colleoni *et al.,* 1999b) and was therefore proposed to play a role in amylopectin biosynthesis (Wattebled *et al.,* 2003). However, in *Arabidopsis* and potato leaves loss of D-enzyme activity primarily affects starch degradation. It is thought to be involved in malto-oligosaccharide metabolism during starch degradation (Critchley *et al.,* 2001; Lloyd *et al.,* 2004; Takaha *et al.,* 1998).

1.2.2 Control of starch synthesis

As discussed earlier, the starch granules that form in chloroplasts are small and transitory, enlarging during the day and being degraded at night to provide sugars for maintenance and growth (Caspar *et al.,* 1985; Gibon *et al.,* 2004; Lu *et al.,* 2005). Starch has historically been seen as a short term "buffer" between the rate of CO_2 assimilation and the rate of sucrose synthesis or export. In other words, leaf starch was considered to be an overflow product of photosynthesis, which accumulated when the rate of carbon assimilation exceeded the sink demand for sucrose or assimilate transport capacity (Eichelmann and Laisk 1994; Komor 2000; Stitt and Quick 1989) .

As discussed previously, AGPase is responsible for the first committed step in starch synthesis, the production of ADPG. AGPase activity in the plant is modulated by light and sugars, which act indirectly to alter its redox state and as a result its sensitivity to activation by 3-phosphoglycerate (3-PGA) and inhibition by inorganic phosphate (P_i) (Ballicora *et al.,* 2000; Hendriks *et al.,* 2003; Tiessen *et al.,* 2002; Tiessen *et al.,* 2003). For example, AGPase is reduced and activated when sucrose accumulates (Hendriks *et al.,* 2003; Tiessen *et al.,* 2002). Therefore, feedback from sucrose synthesis can lead to the stimulation of starch synthesis. As sucrose levels increase in leaf cells during the day this leads to phosphorylation and inhibition of sucrose phosphate synthase (SPS; EC 2.4.1.14) or the conversion of sucrose to hexose phosphate via invertase (EC 3.2.1.26) and hexokinase (EC 2.7.1.1), both of which result in an increase in hexose phosphates (Huber and Huber 1996; Lunn and Hatch 1997; Stitt *et al.,* 1987; Trevanion *et al.,* 2004). The increase in hexose phosphate leads to an increase in fructose 2,6-bisphosphate (Fru2,6BP) which inhibits cytosolic fructose bisphosphatase (FBPase; EC 3.1.3.11) (Huber and Huber 1996; Stitt 1990). This reduces the export rate of triose

phosphate from the chloroplast and recycling of P_i from the cytosol into the chloroplast (Huber and Huber 1996; Stitt 1990; Stitt *et al.,* 1987). This causes a depletion of chloroplast P_i and an accumulation of 3-PGA, which activates AGPase (Ballicora *et al.,* 2004; Kleczkowski 1999; Preiss 1988).

The signalling pathways that link sugar levels to AGPase activation are not fully understood, but are likely to involve sucrose non-fermenting-1-related protein kinase-1 (SnRK1). This enzyme has been implicated in multiple functions and mechanisms including the signalling pathway leading to redox regulation of AGPase and the flux of carbon into starch (Jossier *et al.,* 2009; Tiessen *et al.,* 2003). For example, antisense repression of SnRK1 in potato tubers prevented the sucrose-dependent redox activation of AGPase (Tiessen *et al.,* 2003). Likewise, when SnRK1 activity is increased in transgenic potato tubers, both the expression levels and activity of AGPase increase, leading to a significant increase in starch content (McKibbin *et al.,* 2006). SnRK1 over expression in *Arabidopsis* leaves modified the activity of enzymes and the expression of genes involved in various sugar signalling pathways (Jossier *et al.,* 2009). However, SnRK1 appears to have different functions in sink and source tissues, with overexpression of SnRK1 in *Arabidopsis* leaves leading to a reduction in starch (Jossier *et al.,* 2009).

It is now recognised that the starch accumulated in leaves during the day is essential for normal metabolism and growth at night (Naegele *et al.,* 2010). Control of starch turnover, i.e. control of the rate of starch synthesis during the day and of the rate of degradation at night, is considered critical for normal plant growth and development (Caspar *et al.,* 1985; Corbesier *et al.,* 1998; Geiger *et al.,* 2000; Schulze *et al.,* 1994). As described earlier, starchless mutants have reduced growth rates (Caspar *et al.,* 1985; Lin *et al.,* 1988). In addition, in starchless mutants of *Arabidopsis* the shoot to root ratio is shifted in favour of root growth (Schulze *et al.,* 1991), the timing of flowering is delayed (Bernier *et al.,* 1993) and the allocation of resources to seed formation is disturbed (Schulze *et al.,* 1994). The control mechanism or mechanisms that match the partitioning of photosynthate between sucrose and starch during the day to the anticipated length of the night are unknown.

The signalling metabolite trehalose-6-phosphate (trehalose-6-P) has a role in carbohydrate utilisation and is critical for normal growth and development (Schluepmann *et al.,* 2003). It has been suggested that trehalose-6-P links the level of AGPase activation and hence the rate of starch synthesis during the day to the plant's demand for carbon during the night (Smith and Stitt 2007). An increase in trehalose-6-P levels increases the activation of AGPase and enhances the amount of freshly assimilated carbon partitioned into starch (Kolbe *et al.,* 2005; Lunn *et al.,* 2006). This causes the rate of starch synthesis relative to sugar synthesis to increase, preparing the plant for a long period of darkness during the subsequent night (Smith and Stitt 2007).

Further evidence of coordination between daytime synthesis and carbon requirement at night comes from the fact that under long term growth in short day conditions (up to 3 h light/ 21 h dark), starch accumulation rates are increased during the light period and starch degradation rates are decreased at night relative to plants grown under a 12-h light/12-h dark regime (Gibon *et al.,* 2009). Likewise, plants grown in long days partition less of their assimilate into starch than plants grown in short days, and have a faster rate of starch degradation (Lu *et al.,* 2005). During both long and short day growth conditions the rate of starch accumulation and degradation is such that starch reserves at night last until dawn. Plants therefore avoid a starvation response and an increase in trehalose-6-P levels experienced following an extended night, as discussed above. The mechanisms by which the length of the day and night control the partitioning of carbon into starch during the day are not fully understood. It is possible that the circadian clock is involved. The circadian clock is entrained to day/night cycles by photoreceptors (phytochromes and crypochromes). The circadian clock can then measure a day length of 24 h, so when the night begins the timing of dawn can be anticipated and appropriate physiological responses can occur in advance (reviewed in Imaizumi 2010; McClung 2001). If dawn and as a result photosynthesis occur later than anticipated, this information may be used to adjust the partitioning of photosynthate into starch during the next day. This adjustment is likely to take place via modulation of AGPase. This is supported by the fact that the shorter the photoperiod under which plants are grown, the greater the diurnal changes in AGPase activity (Gibon *et al.,* 2009). However, the mechanisms that might link the circadian clock to AGPase modulation are completely unknown. The known involvement of the circadian clock in

the control of the rate of starch degradation will be discussed at the end of the following section.

1.2.3 Starch degradation and its control

As previously discussed control of the rate of starch degradation in leaves is essential for normal plant growth. Knowledge of the starch degradation pathway is fundamental for understanding how starch turnover is controlled. In the following section I will summarise the current understanding of the starch degradation pathway in *Arabidopsis* leaves at night.

Starch degradation begins after transition from light to dark. The mechanism by which it is switched on by the light to dark transition is not known, but may involve sugar sensing mechanisms responding to the depletion of leaf sugars (Chia *et al.,* 2004; Moore *et al.,* 2003; Rolland *et al.,* 2006; Zeeman and ap Rees 1999). Other possible mechanisms to initiate starch degradation are the redox and pH changes that occur in the stroma at the light to dark transition. It is unlikely that starch is degraded in the light, in the experimental conditions used for growing *Arabidopsis* (Streb *et al.,* 2009; Zeeman *et al.,* 2002b). During starch degradation the surface of the granule is attacked by β-amylases (BAM; EC 3.2.1.2), which remove successive maltose units from the non-reducing ends of glucan chains (Fulton *et al.,* 2008; Streb *et al.,* 2008; Yu *et al.,* 2005) and the debranching enzyme ISA3 which removes short branches from the granule surface (Delatte *et al.,* 2006). The linear malto-oligosaccharides released by ISA3 can be acted upon by BAM or plastidic disproportionating enzyme1 (DPE1; also known as D-enzyme). BAM is unable to act upon chains of less than four glycosyl residues (Lizotte *et al.,* 1990). Any maltotriose (three glucosyl residues) produced can be acted on by DPE1, which converts two maltotriose molecules, rearranging them to produce one glucose and one maltopentaose, the latter of which can act as a substrate for BAM (Critchley *et al.,* 2001).

The main product of the above pathway is maltose, while a little glucose is also produced (Lu *et al.,* 2005; Lu and Sharkey 2006; Lu *et al.,* 2006; Weise *et al.,* 2004). Maltose is exported from the chloroplast via the maltose exporter (maltose excess1; MEX1) located in the chloroplast envelope (Niittylä *et al.,* 2004), while glucose can be

transported via a chloroplast-envelope glucose transporter (Schafer *et al.,* 1977; Servaites and Geiger 2002; Weber *et al.,* 2000). Within the cytosol, a transglucosidase releases one of the glucosyl moieties of maltose, to be acted on by hexokinase and glucokinase (EC 2.7.1.2), and transfers the other to an acceptor, probably a water-soluble heteroglycan (Fettke *et al.,* 2006). Cytosolic glucan phosphorylase (designated as PHS2 in *Arabidopsis*; EC 2.4.1.1) is probably responsible for release of the glucosyl moiety from the heteroglycan as glucose-1-P (Chia *et al.,* 2004; Fettke *et al.,* 2006; Lu *et al.,* 2006; Steichen *et al.,* 2008).

Loss of α-amylase 3 (AMY3; EC 3.2.1.1), the only α-amylase located in the chloroplast, does not affect the starch degradation rate, indicating that under normal wild-type conditions AMY activity is not required for starch degradation in *Arabidopsis* leaves (Yu *et al.,* 2005). However, under certain conditions, for example the absence of ISA3, the starch granule can be degraded via a hydrolytic route catalysed by AMY3 (Delatte *et al.,* 2006; Zeeman *et al.,* 2007a). The products of the AMY3 hydrolytic degradation can then be acted upon by the debranching enzyme LDA, followed by DPE1 and BAM to ultimately produce maltose and glucose for export from the chloroplast.

The phosphorylation and dephosphorylation of the starch granule is essential for normal starch degradation (Caspar *et al.,* 1991; Comparot-Moss *et al.,* 2010; Kötting *et al.,* 2009; Yu *et al.,* 2001; Zeeman *et al.,* 1998a). A cycle of glucan phosphorylation and dephosphorylation is thought to uncoil the amylopectin double helices, causing rearrangement of the granule surface into a less ordered and more hydrated state and as a result facilitate the attack on the starch granule by BAM and ISA3 (Edner *et al.,* 2007; Hansen *et al.,* 2009; Hejazi *et al.,* 2008; Kötting *et al.,* 2009). GWD1 phosphorylates glucose moieties in starch at the C6-position (Mikkelsen *et al.,* 2006; Yu *et al.,* 2001) and phosphoglucan water dikinase (PWD; EC 2.7.9.5) phosphorylates glucose moieties in starch granules which have previously been phosphorylated in the C6-position, at the C3-position (Baunsgaard *et al.,* 2005; Kötting *et al.,* 2005; Ritte *et al.,* 2006).

Dephosphorylation of the granule is also required for starch degradation because BAM is unable to efficiently hydrolyse phosphorylated glucans (Edner *et al.,* 2007). The phosphoglucan phosphatase SEX4 (EC 3.1.3.48) dephosphorylates the starch granule surface, allowing BAM to further hydrolyse the glucan branches (Gentry *et al.,* 2007;

Hejazi *et al.,* 2010; Kerk *et al.,* 2006; Kötting *et al.,* 2009; Niittylä *et al.,* 2006). LIKE SEX4 (LSF1) may also be involved in the dephosphorylation of the starch granule surface (Comparot-Moss *et al.,* 2010). LSF1 is believed to be either a phosphoglucan phosphatase, removing phosphate groups from starch or a protein phosphatase (EC 3.1.3.16), dephosphorylating and activating enzymes involved in starch degradation (Comparot-Moss *et al.,* 2010).

The cycle of glucan phosphorylation and dephosphorylation may play a role in controlling the rate of starch degradation (Stitt *et al.,* 2010). As previously described, evidence from extended night experiments and mutants with altered glucan accumulation indicate that plants integrate information about the amount of starch present in the leaves at the end of the day and the length of the night ahead to set a linear rate of starch degradation (Delatte *et al.,* 2005; Gibon *et al.,* 2004; Graf *et al.,* 2010; Lin *et al.,* 1988; Lu *et al.,* 2005; Streb *et al.,* 2008; Zeeman *et al.,* 1998b). As described above, the cycle of glucan phosphorylation and dephosphorylation is thought to open up the glucan structure to degrading enzymes (Hansen *et al.,* 2009; Hejazi *et al.,* 2008; Kötting *et al.,* 2009). If the rate at which the glucans were phosphorylated and dephosphorylated was controlled then this would control the degradation rate during the night.

The circadian clock is the timing mechanism that controls the rate of starch degradation, so that starch reserves last until the anticipated dawn (Graf *et al.,* 2010). The involvement of the circadian clock in the timing of starch degradation is supported by three keys pieces of evidence: Firstly, the maintenance of normal starch degradation rates at night following skeleton light periods, secondly, the degradation rate in clock mutants grown under 24 h days coordinating with their own internal clock and thirdly, the inability of wild-type plants to adjust their degradation rate when grown under 28 h or 17 h days (Graf *et al.,* 2010). A skeleton light period consists of a period of darkness (5 h in the experiments of Graf *et al.* (2010)) interrupting the usual 12 h light period. If plants are grown under these conditions from germination, their pattern of degradation is unaffected and they maintain a linear rate of starch degradation during the night, so that starch reserves last until the normal dawn. The circadian clock of wild-type plants has a period of 24 h, whereas the clock of the *lhy/cca1* mutants has a period of 17 h. If the *lhy/cca1* mutants are grown under 24 h days the rate of starch degradation at night

proceeds too quickly, and starch is exhausted three to four hours early, at the dawn anticipated by the fast running clock of the mutants, rather than the actual dawn. However, if the mutants are grown under 17 h days, the linear rate of degradation means that the starch reserves last until the actual dawn. Likewise, if wild-type plants are grown in abnormal day lengths (e.g. 17 or 28 h days), starch is exhausted 24 hours after the last dawn rather than at the actual dawn. For example, if wild-type plants are grown under 28 h days, the degradation rate is too fast and starch is exhausted before dawn. However, if wild-type plants are grown under17 h days, the degradation rate is too slow and 40% of the starch remains at the end of the night (Graf *et al.,* 2010).

As discussed above, the correct setting of the rate of starch degradation during the night requires not only information about the anticipated length of the night, but also information about the starch content of the leaf. It is important to note that it is unknown how information about the starch content at the end of the day is measured and then integrated with the timing information to determine the degradation rate.

Although it is clear that the circadian clock is the timing mechanism that controls the rate of starch degradation (Graf *et al.,* 2010), the molecular nature of this timing mechanism is unknown. While the expression levels of several starch-metabolising genes appear to be under circadian control (Harmer *et al.,* 2000; Ni *et al.,* 2009; Schaffer *et al.,* 2001), transcript changes are not always reflected in the protein levels or enzyme activity, indicating that post-transcriptional mechanisms rather than transcriptional regulation is responsible for the control of starch-metabolising enzyme activity (Gibon *et al.,* 2006; Lu *et al.,* 2005; Smith *et al.,* 2004; Usadel *et al.,* 2008; Weise *et al.,* 2006; Yu *et al.,* 2001). For example, transcript levels of the starch phosphorylating enzyme GWD1 show large diurnal and circadian changes but the level of protein does not change over the day/night cycle. A potential post-translation control could be a feedback regulation from the intermediates of starch degradation, for example malto-oligosaccharides may inhibit enzymes involved in the degradation of the starch granule (Lizotte *et al.,* 1990; Smith *et al.,* 2005; Zeeman *et al.,* 2007b). An alternative post-translational control mechanism is redox activation of starch degradation enzymes via a light-independent thioredoxin (Balmer *et al.,* 2006; Mikkelsen *et al.,* 2005). GWD1 and some BAM isoforms have been shown to be activated by reduction in vitro (Mikkelsen *et al.,* 2005; Sparla *et al.,* 2006). However, it

is not obvious how this could contribute to control of starch degradation in vivo. If redox mechanisms exerted an important influence on the activation state of these enzymes in vivo, then they would be expected to be in a more oxidised and hence inactive state during the night (Mikkelsen *et al.,* 2005; Sparla *et al.,* 2006). A post-translational control mechanism could feed into the glucan phosphorylation and dephosphorylation mechanism discussed above by regulating the activity of SEX4, GWD1, PWD or LSF1, to control the rate at which the starch granule is degraded during the night.

1.2.4 The structure of starch

In order to understand how the starch granule initiates and grows, we must first understand the structure of the granule. The internal organisation of amylopectin within the starch granule is thought to be less variable than overall granule morphology (Gallant *et al.,* 1997; Kossmann and Lloyd 2000; Tomlinson and Denyer 2003).

Amylopectin consists mainly of clusters of short glucan chains 12 to 16 glucose units long (Figure 1.2A) (French 1984; Hizukuri 1986; Jenkins *et al.,* 1993). Double helices form from adjacent short chains. These pack together parallel to each other, forming crystalline arrays (crystalline lamellae). Short chain clusters are linked together along the long axis of the molecule via longer chains about 40 and 70 glucose units long, that span two or three crystalline lamellae (Hizukuri 1986). Non-crystalline regions (amorphous lamellae) occur between the crystalline lamellae; these contain branch points that link together the chain clusters. Alternating layers of crystalline lamellae and amorphous lamellae form the semi-crystalline regions of the starch granule. Amylose has no organised structure and tends to be distributed throughout the starch granule amongst the amylopectin (Jane *et al.,* 1992).

Small-angle X-ray scattering (SAXS) studies of starch granules revealed a single small-angle peak in the pattern which corresponds to a 9 nm repeat (Donald 2001 and references therein). The 9 nm represents the combined distance of one crystalline and one amorphous lamella repeat (Figure 1.2A and B). Jenkins *et al.* (1993) studied starch from a variety of biological sources and found the repeat distance of 9 nm (±0.3 nm) to be consistent across all the species studied. Depending on the length of the glucose

chains within a cluster and the position of the branch points two different types of amylopectin crystal with different packing of helices are formed; A-type has short average chain lengths and B-type has longer average chain lengths (Figure 1.3) (Hanashiro *et al.,* 2002; Jane *et al.,* 1997; Tang *et al.,* 2001a; Tang *et al.,* 2002; Tang *et al.,* 2001b). An intermediate between the two types of crystallinity is known as C-type (Hanashiro *et al.,* 2002; Tang *et al.,* 2002).

Microscopy revealed that amylopectin molecules could organise into super-helices and then into blocklets (Gallant *et al.,* 1997; Oostergetel and van Bruggen 1993; Ridout *et al.,* 2002). For a detailed review of blocklet properties see Tang *et al.* (2006). Depending on the botanical source of the starch and location in the granule, blocklets vary in diameter from 10 to 500 nm (Baker *et al.,* 2001; Ridout *et al.,* 2003; Szymonska and Krok 2003). Blocklets stacked on top of each other are thought to make up a growth ring of the starch granule (Figure 1.2B) (Gallant *et al.,* 1997). Concentric growth rings a few hundreds of nm in width, of alternating hard and soft material, can be observed using scanning electron microscopy when starch granules are cracked open and partially digested with α-amylase (Figure 1.2C) (Gallant *et al.,* 1992; Pilling and Smith 2003). The hard material, which is not readily digestible by α-amylase, is thought to be made up of larger blocklets, while the soft material, which is easily digested by α-amylase, consists of smaller blocklets (Buléon *et al.,* 1998; Gallant *et al.,* 1997).

Starch granules are considered to grow by 'apposition'; the gradual addition of layers of material from the outside (Badenhuizen and Dutton 1956; Yoshida *et al.,* 1958). However, evidence from a recent study suggests that synthesis may not exclusively occur at the surface of the starch granule. Mukerjea *et al.* (2009) peeled successive layers off storage starch granules and found that all layers contained starch synthase enzymes. Therefore, if ADPG is able to diffuse freely through the granule, glucan chains can be elongated throughout the starch granule (Mukerjea *et al.,* 2009). Leaf starch granule thickness changes very little with granule diameter, suggesting that glucose residues are added and removed to a greater extent at the edges of the granules (Grange *et al.,* 1989b).

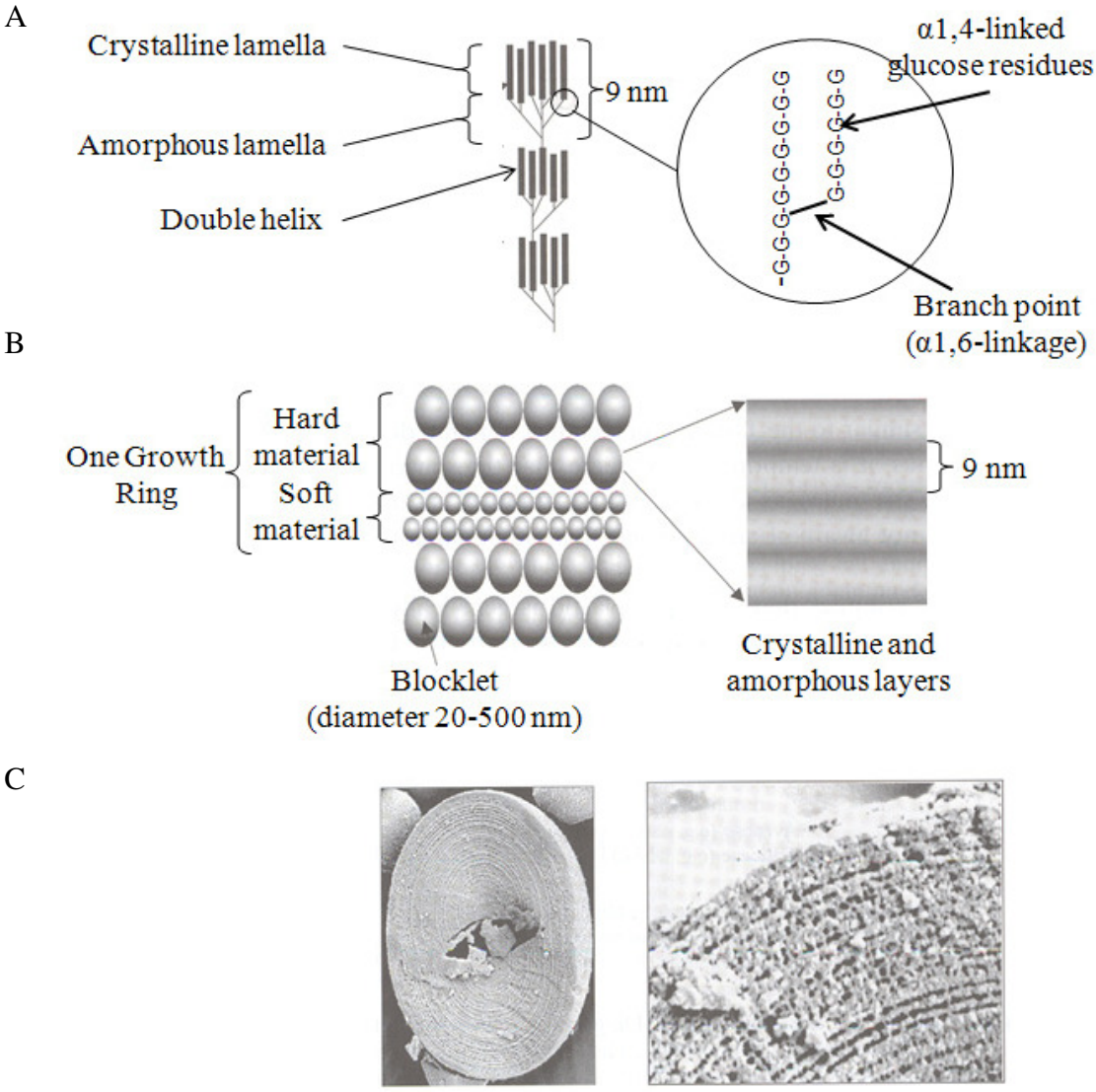

Figure 1.2: Starch granule structure. (A) Amylopectin structure with double helices connected by a backbone and branch points. (B) Proposed blocklet arrangement. (C) Growth rings of potato starch granule under two magnifications using scanning electron microscopy. Starch granule cracked open and treated with α-amylase. Growth rings approximately 100 nm apart. (Figure 7 from Tomlinson and Denyer 2003).

Models have been constructed that focus on physical explanations for amylopectin polymer self-assembly onto the existing starch granule (Oostergetel and van Bruggen 1993; Waigh *et al.,* 1999; Waigh *et al.,* 2000). The double helices of amylopectin align parallel to each other due to the antagonism from the entropy of the backbone (Warner 1989). In this case the 'backbone' refers to a long glucan chain in the amylopectin molecule, within the amorphous lamellae, to which the shorter side chains are linked.

The ordering of the side chains guides further polymerisation of amylopectin in the next layer. Waigh *et al.* (1999) suggested that the model of backbone repulsion explains why A and B-type starches still have 9 nm repeats, despite B-type having longer glucose side chains (Hizukuri 1986) (Figure 1.3). If starch has long spacing branches (A-type) then only shorter chain lengths are required for the lamellae to crystallise because the chains are less coupled to the motions of the backbone. Conversely in B-type starches, longer chain lengths are required because the shorter spacing branches mean the chains are more coupled to backbone motions. For a detailed review of the glucan structures within starch see Damager *et al.* (2010).

While the self-assembly of amylopectin molecules onto the surface of the starch granule helps explain how the existing granule grows, it does not explain how the granule itself initiates. In the next section I discuss the existing evidence on how the starch granule and the glucan chains of which it consists are initiated.

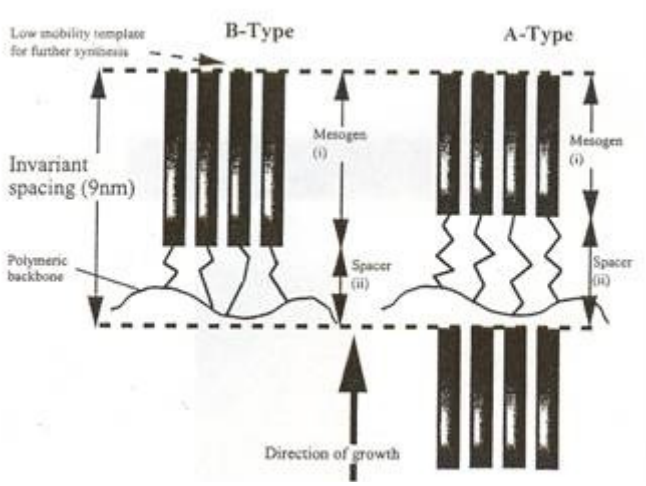

Figure 1.3: Diagram to represent lamellar spacing in A and B-type starches (Figure 11 from Waigh *et al.,* 1999). 'Mesogens' are the glucan chain double helices (crystalline lamellae) and 'spacers' are the longer glucan chains and branch points that link the chain clusters (amorphous lamellae). This terminology come from the field of liquid crystalline polymers: Waigh *et al.* (1999) consider amylopectin to have the properties of a side chain liquid crystalline polymer. A-type starches have short mesogens and long spacers. The opposite is true of B-type starches.

1.3 Starch Granule and Glucan Chain Initiation

As described above, the structure and synthesis of starch is relatively well known. However the process of granule initiation and amylopectin polymer initiation remains a mystery. In the following section I will discuss theories on how the granule is initiated, including the possibility that glucans with an ordered branching pattern spontaneously crystallise into a granule. I will also discuss a number of possible theories on how the amylopectin polymer is initiated, including the possibility that there is a self-glucosylating protein in plants with the ability to initiate a chain of glucose residues.

To my knowledge there have been no reports of starch granule production in vitro or in transgenic non-starch-producing organisms. SBEs play an important role in amylopectin structure and subsequent granule formation (section 1.2.1). For example, as previously discussed knocking-out the two SBE genes in *Arabidopsis* appears to prevent starch granule synthesis in the leaves (Dumez *et al.,* 2006), while mutations in individual SBEs affects the rate of starch synthesis in leaves (Smith *et al.,* 1990; Tomlinson *et al.,* 1997). Guan *et al*. (1995) hypothesised that if eukaryotic SBEs are expressed within bacteria, this might be sufficient to create a starch granule instead of amorphous glycogen. Guan *et al.* (1995) expressed maize SBEI and SBEIIb in *E. coli* cells deficient in glycogen branching enzyme but retaining the rest of the glycogen synthesis enzymes. The *E. coli* cells produced glucan polymers that resembled glycogen rather than amylopectin and no granules were produced. However, the branching pattern did vary from that of glycogen from wild-type *E. coli*. Therefore, there are additional factors in planta that are necessary for the initiation of the starch granule. In theory both genetic and physical factors could be responsible for glucan chain and starch granule initiation.

1.3.1 Genetic Controls

There is a strong argument for the genetic control of both glucan chain and granule initiation. Different species and different organs have different numbers of granules per plastid. For example, maize endosperm amyloplasts contain only a single starch granule (McCullough *et al.,* 1992), while the amyloplasts in rice and oat endosperm contain multiple granules (Buttrose 1962; Hinchman and Gordon 1974). The endosperm amyloplasts of wheat seeds contain two different types of starch granule. One disc

shaped A-type granule (≥10μm) generally forms in the centre of the plastid, then the smaller more spherical B-type granules (≤10μm) form in the stromule regions, tubular projections that stem from the plastid and sometimes connect to other plastids (Bechtel and Wilson 2003; Bechtel *et al.,* 1990; Langeveld *et al.,* 2000; Parker 1985). The two types of granule initiate in two waves; A granules in the first 5-7 days following fertilisation and B granules 12-15 days after fertilisation (Briarty *et al.,* 1979). This tight regulation of initiation indicates a genetic and developmental control over starch granule initiation (Shewry and Morell 2001).

Starch biosynthesis enzymes form complexes which may provide an environment for ordered construction of amylopectin polymers (Hennen-Bierwagen *et al.,* 2008), potentially aiding the formation, or even initiation of, starch granules. Examples of starch synthesis enzyme complexes include a SSI-SSII-SBEII complex in wheat endosperm (Tetlow *et al.,* 2008) and a 670 kD complex consisting of SSIII, SSIIa, SBEIIa and SBEIIb in maize endosperm (Hennen-Bierwagen *et al.,* 2009). The expression of starch synthesis genes and hence the formation of these complexes is likely to be under genetic control. For example, studies of the expression profiles of starch synthesis genes led Tsai *et al*. (2009) to propose a common mechanism for the transcriptional co-regulation of starch synthesis genes via specific cis-elements in the gene promoters. Thus far however, nothing is known about the importance and function in vivo of complexes of starch biosynthetic enzymes.

The four main genetic factors that have been proposed to be involved in glucan chain and/or granule initiation are ISA, α-1,4-glucan phosphorylase, SS4, and glycogenin, all of which are discussed below.

1.3.1.1 Isoamylase (ISA)

The debranching enzymes ISA1 and ISA2/DBE1 play an essential role in normal starch granule initiation and production. The ISA enzymes are responsible for cleaving α-1,6 links in branched glucans, not creating links, therefore it is not intuitively obvious why these enzymes are required for granule synthesis. Nonetheless, there is a large amount of evidence for an absolute requirement for these enzymes in the formation of semi-crystalline granules. *T. gondii* is a protozoan parasite which contains crystalline storage

polysaccharides analogous to amylopectin (Guérardel *et al.,* 2005). The *T. gondii* genome does not contain the complexity of genes responsible for starch synthesis in higher plants. For example, while *Arabidopsis* has five SS genes, *T. gondii* contains only one (Coppin *et al.,* 2005). However, *T. gondii* does retain a copy of ISA, which may suggest that ISA is required for normal granule production (Coppin *et al.,* 2005). It must be pointed out that it is unknown whether the ISA occurring in *T. gondii* plays a role in starch synthesis or whether, like higher plant ISA3, it is involved in degradation. In general, mutations in ISA1 and ISA2 of higher plants reduce the synthesis of starch granules and increase the production of a highly branched, soluble glucan phytoglycogen. There are examples of *isa* mutants in a variety of organisms including maize (Dinges *et al.,* 2001; James *et al.,* 1995; Pan and Nelson 1984), rice (Kubo *et al.,* 1999; Nakamura *et al.,* 1997), barley (Burton *et al.,* 2002), *Arabidopsis* (Delatte *et al.,* 2005; Streb *et al.,* 2008; Zeeman *et al.,* 1998b) and green algae (Dauvillée *et al.,* 2001; Mouille *et al.,* 1996). There are two proposed models which seek to explain the way ISA may operate in starch synthesis, both of which are based on interpretations of the phenotypes of plants lacking ISA or with reduced ISA levels.

The first model, proposed by Mouille *et al.* (1996), Ball *et al.* (1996) and Myers *et al.* (2000) suggests that ISA is responsible for making amylopectin from a hypothetical amylopectin precursor, pre-amylopectin. The pre-amylopectin molecule is suggested to have a branching structure which is unable to organise itself into a starch granule. ISA is responsible for removing certain branches from pre-amylopectin, for example branch points that are very close to other branch points, so that the structure is able to crystallise and form amylopectin (Streb *et al.,* 2008). In the *isa* mutants the pre-amylopectin is not processed properly into amylopectin, so the SSs and SBEs continue to act on the pre-amylopectin and produce phytoglycogen.

The second model, in which ISA is indirectly involved in granule initiation, was proposed by Zeeman *et al.* (1998b). In this model ISA is responsible for the degradation of α-glucans in the stroma. Small soluble glucans in the stroma compete with the amylopectin for SS and SBE activity. SSs and SBEs can act on the soluble glucans to produce phytoglycogen. The role of ISA is to clear the stroma of small glucans and prevent the formation of phytoglycogen. In *isa* mutants α-glucans accumulate, directing glucan synthesis away from the granule surface; as a result phytoglycogen is produced.

Originally it was thought that the amylopectin structure of *Arabidopsis isa* mutants was similar to that of wild-type, supporting the indirect role of ISA in granule synthesis (Zeeman *et al.,* 1998b). However, it is now known that both the chain length distribution and branching frequency is altered in the mutant amylopectin (Delatte *et al.,* 2005; Wattebled *et al.,* 2005). In the *Atisa1* mutant there is an increase in the number of short glucan chains with a DP between 3 and 8 and a decrease in slightly longer chains (DP 9-16) compared to wild-type (Delatte *et al.,* 2005). These data indicate that ISA may directly affect the branching pattern of the amylopectin molecules which form the granules, thus supporting the first model described above.

The consequences of ISA loss vary between plants, organs and cells. For example, the *Chlamydomonas* (*sta7*) *isa* mutant, accumulates phytoglycogen and almost no starch (<3% of glucan compared with the wild-type is found as starch), (Mouille *et al.,* 1996), while barley *isa* mutants accumulate approximately 60% of their glucans as starch and 40% as phytoglycogen (Burton *et al.,* 2002). Chloroplasts in the mesophyll cells of the *Arabidopsis isa1* mutant contain predominately phytoglycogen, while plastids in the epidermal, guard and bundle sheath cells contain well-defined starch granules (Delatte *et al.,* 2005; Streb *et al.,* 2008). Within the grains of the rice *isa* mutant, *sugary1*, there is a large variation in the ratio of starch to phytoglycogen (Kubo *et al.,* 1999; Nakamura *et al.,* 1997). The endosperms of some allelic lines of *sugary1* mutants consisted only of phytoglycogen, whereas other lines had a transition from phytoglycogen in the endosperm centre to starch in the outer sections. In the barley *isa* mutant Risø 17 there is variation in the phytoglycogen content even between plastids within the same cell (Burton *et al.,* 2002). Evidence from the mutants described above indicates that ISA has a significant role in granule initiation, but the importance of this role varies depending upon a large number of unknown factors within the plastid where ISA is acting.

The apparent differences in the impact of ISA loss on starch production could be due to redundancy occurring in certain species or organs, which does not occur in others. For example, in *Arabidopsis* starch granules, albeit abnormal, are still produced when any one of the de-branching enzymes (ISA1, ISA2, ISA3 and LDA) remain (Streb *et al.,* 2008). Thus although ISA3 and LDA are primarily involved in starch degradation, they can function in starch synthesis when ISA1 and ISA2 are absent. In *Arabidopsis* loss of ISA3 or LDA does not result in the production of phytoglycogen and their main roles

are in starch degradation (Delatte *et al.,* 2006; Wattebled *et al.,* 2005). Despite this, loss of LDA in maize, rice and *Arabidopsis* enhances the phytoglycogen-accumulation phenotype of *isa* mutants (Dinges *et al.,* 2003; Kubo *et al.,* 1999; Wattebled *et al.,* 2005). In *Arabidopsis,* only when all four de-branching enzymes are lost are starch granules completely absent, indicating that debranching is a mandatory step for normal amylopectin synthesis and granule initiation (Streb *et al.,* 2008).

Evidence suggests that ISA1 and ISA2 function together. In potato tubers and *Arabidopsis* leaves the mutant phenotypes of *isa1* and *isa2* are indistinguishable from each other (Bustos *et al.,* 2004; Delatte *et al.,* 2005; Wattebled *et al.,* 2005). In potato tubers, maize endosperm, kidney bean seeds and rice endosperm ISA1 and ISA2 have been shown to exist together in a heteromeric complex (Bustos *et al.,* 2004; Hussain *et al.,* 2003; Ishizaki *et al.,* 1983; Kubo *et al.,* 2010; Takashima *et al.,* 2007; Utsumi and Nakamura 2006). ISA2 is considered to be enzymatically inactive due to conserved variations in certain amino acids and is therefore thought to have a regulatory role in most species (Deschamps *et al.,* 2008; Hussain *et al.,* 2003), perhaps helping to control the number and size of granules (Kubo *et al.,* 2010). In the endosperm of maize and rice, ISA1 also occurs as homomeric complex and can act independently of ISA2, resulting in wild-type starch levels in seeds of an *isa2* mutant (Kubo *et al.,* 2010; Utsumi and Nakamura 2006).

Loss of ISA affects both the number of granule initiations and the timing of granule initiation. For example, potato antisense lines with reduced ISA levels contain starch granules of wild-type appearance, but also contain phytoglycogen and a very large number of very small granules, often attached to the surface of the large granules (Figure 1.4) (Bustos *et al.,* 2004). In maize endosperm, loss of ISA2 does not affect the starch level but results in greater numbers of smaller granules (Kubo *et al.,* 2010). This further emphasises the importance of ISA in wild-type granule initiation, as its removal eliminates normal control of both the number and timing of granule initiation.

A B

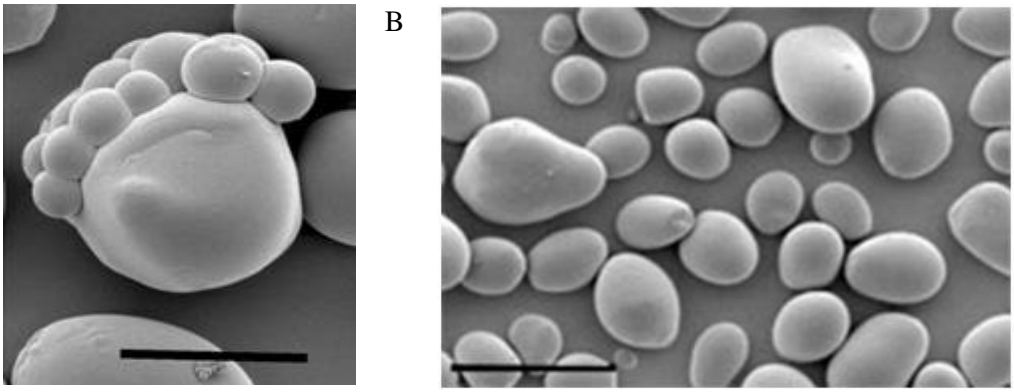

Figure 1.4: Isolated starch granules from control and transgenic potato tubers (from Bustos *et al.,* 2004). (A) Stisa2 antisense line with strongly reduced activity of ISA2. Scale bar = 20µm. (B) Control. Scale bar = 50 µm.

To date, no model to explain the role of ISA in amylopectin synthesis has been proven. However, the majority of evidence presented from *isa* mutants appears to favour the first model described above, in which the ISAs are responsible for creating an amylopectin molecule with the branching pattern required to crystallise into a starch granule. The 9 nm repeat observed in semi crystalline starch granules (see section 1.2.4) can only form if the amylopectin side chain branches attached to the amylopectin backbone have sufficient mobility to form double helices (Donald 2001). These amylopectin double helices form the basis of crystalline lamellae structure. When there is insufficient plasticity of these side chains, the double helices pull apart and the ordered crystalline structure is lost (Donald 2001). ISA1 may act in granule synthesis to maintain the flexibility of these side chains by removal of excess branch points. The observed variation in *isa* mutants demonstrates that the role of ISA in granule production is not straight forward and is likely to involve interaction with other starch synthesis proteins. Investigation into the interaction of ISA with other genes involved in starch synthesis may provide further information into its role in starch granule initiation.

1.3.1.2 Plastidial α-1,4-glucan phosphorylase

Plastidial α-1,4-glucan phosphorylases (EC 2.4.1.1) participate primarily in metabolizing unbranched oligoglucans, by catalysing the reversible transfer of a glucosyl unit from the non-reducing end of an α-1,4-glucan chain to orthophosphate (P_i)

to produce glucose-1-P. Plastidial α-1,4-glucan phosphorylase (Pho1 or PHS1) plays different roles in photosynthetic and non photosynthetic organs.

In storage organs it has been shown that α-1,4-glucan phosphorylase can play a role in starch synthesis in addition to its primary role in starch degradation (Fettke *et al.,* 2010). Evidence from wheat, rice, potato and green algae suggests that Pho1 is potentially involved in starch synthesis; either directly synthesising glucans or indirectly by shortening long unbranched side chains of pre-amylopectin molecules (Albrecht *et al.,* 2001; Dauvillee *et al.,* 2006; Satoh *et al.,* 2008; Schupp and Ziegler 2004). In potato leaves the expression pattern of Pho1 closely corresponds to starch accumulation (Albrecht *et al.,* 2001) and in wheat endosperms Pho1 activity coincides with the accumulation of storage starch (Schupp and Ziegler 2004). The strongest evidence for Pho1 playing a role in starch synthesis comes from mutations in *C. reinhardtii* and rice endosperm (Dauvillee *et al.,* 2006; Satoh *et al.,* 2008). The loss of Pho1 from rice endosperm resulted in reduced starch accumulation and smaller starch granules with modified amylopectin structure (Satoh *et al.,* 2008). In addition to a role in starch synthesis Pho1 may also be involved in glucan chain and granule initiation. Mutation of PhoB, one of the two plastidial α-1,4-glucan phosphorylases in *C. reinhardtii*, results in a reduced starch content, with abnormal granules and modified amylopectin structure (Dauvillee *et al.,* 2006). Pho1 has been found to synthesise α-1,4-glucan chains in the absence of an added glucan primer, suggesting that it may be elongating an endogenous primer tightly associated with the enzyme (Albrecht *et al.,* 2001; Sivak 1992). However, it remains possible that this "unprimed" activity could have been due to oligosaccharide contamination of assay components. Potentially, if real, the unprimed glucan biosynthesis of Pho1 could be involved in the initiation of amylopectin chains.

However, overall the evidence for the involvement of α-1,4-glucan phosphorylase in starch synthesis, beyond a minor role, is not strong and has not been proven in a wild-type plant. There is no evidence in *Arabidopsis* or any leaf tissue that α-1,4-glucan phosphorylase is involved in starch synthesis or glucan chain initiation. In fact, evidence from *Arabidopsis* and potato leaves suggest that α-1,4-glucan phosphorylase is not involved in starch synthesis or degradation, but plays a role in tolerance to abiotic stress (Sonnewald *et al.,* 1995; Zeeman *et al.,* 2004). The *Arabidopsis* mutant deficient in plastidial α1,4-glucan phosphorylase (*Atphs1*), displayed no change in starch

synthesis or degradation and starch structure or composition (Zeeman *et al.,* 2004). Reducing the activity of Pho1 by expression of antisense RNA in potato leaves had no major impact on starch accumulation (Sonnewald *et al.,* 1995). In knock-out or antisense lines lacking AGPase there is a drastic reduction in starch synthesis in *Arabidopsis* (Lin *et al.,* 1988; Neuhaus and Stitt 1990) indicating that PHS1 cannot compensate for loss of starch synthesis via the AGPase starch synthesis route.

1.3.1.3 Glycogenin

The synthesis of glycogen, the highly branched glucan polymer present in yeast and animals, requires a specific, protein primer called glycogenin. Glycogenin (EC 2.4.1.186) is a Mn^{2+}/Mg^{2+}-dependent Uridine 5-diphosphoglucose (UDPG) requiring glucosyltransferase (reviewed in Alonso *et al.,* 1995; Smythe and Cohen 1991). Glycogenin glucosylates itself to create a chain of up to eight α-1,4-linked glucose residues that are covalently linked via a tyrosine residue to the glycogenin molecule (Cheng *et al.,* 1995; Lomako *et al.,* 1992; Lomako *et al.,* 1993; Pitcher *et al.,* 1988; Whelan 1998). Glycogen synthase (EC 2.4.1.11) and glycogenin form a complex (Pitcher *et al.,* 1987; Skurat *et al.,* 2006); allowing glycogen synthase to elongate the glucan chain attached to glycogenin. However, it is worth noting that the synthesis of glycogen in bacteria does not involve a glycogenin. The components of plant starch synthesis are of prokaryotic origin (Patron and Keeling 2005) so there is no a priori reason to suppose that plant starch synthesis requires a glycogenin-like protein.

There has been much interest in the possibility that a glycogenin-like protein is a primer for amylopectin biosynthesis in plants. Proteins with the ability to autoglucosylate using UDPG have been detected or purified from some plant tissues, for example potato tubers (Ardila and Tandecarz 1992; Lavintman and Cardini 1973; Lavintman *et al.,* 1974), carrots (Quentmeier *et al.,* 1987), wheat (Langeveld *et al.,* 2002) and maize endosperm (Rothschild and Tandecarz 1994). However, evidence suggests that these proteins are involved in the synthesis of polysaccharide components of the cell wall rather than amylopectin (Delgado *et al.,* 1998; Dhugga *et al.,* 1997; Langeveld *et al.,* 2002). Singh *et al.* (1995) attempted to find an amylopectin primer in sweet corn. They found a protein which they named amylogenin, which utilised UDPG and self-glucosylated in vitro. However, amylogenin showed no homology to glycogenin from

mammals and they were unable to demonstrate that it was required for starch synthesis. Factors such as the location of amylogenin outside of the plastid and its creation of a glycosidic link between glucose and arginine, as opposed to the glucose-tyrosine link in glycogenin, brought into question its involvement in starch granule priming (Singh *et al.,* 1995). A chloroplast localised glycogenin-like protein, plant glycogenin-like starch initiation protein 1 (PGSIP1), was reported to be involved in starch metabolism and possibly amylopectin initiation in *Arabidopsis* (Chatterjee *et al.,* 2005). Iodine staining of leaves showed that transgenic plants with undetectable levels of PGSIP1 RNA had reduced starch content at the end of the light period compared to wild-type leaves (Chatterjee *et al.,* 2005). However, no self-glucosylation ability was demonstrated and further studies are required to substantiate the claims that PGSIP1 is involved in starch synthesis or glucan chain initiation.

The search for glycogenin-like proteins responsible for amylopectin initiation in plants is underway (Kolasa 2007). A recent BLAST search of the TAIR *Arabidopsis* database showed 15 genes with predicted amino acid sequence similarity to the human glycogenin protein (Table 1.1). Sequence similarity is compared using the E-value, which gives the statistical significance of each alignment result, i.e. how many amino-acid matches are expected by chance. The lower the E-value, the more likely the alignment is significant. In a biochemical study, two starch granule-bound proteins with self-glucosylating activity were discovered, but the proteins responsible have yet to be identified (Denyer, K. JIC, personal communication). Burton *et al.*(2002) suggested that a plant equivalent of glycogenin might be the site of action of ISA during starch synthesis This theory is supported by evidence from Lomako *et al.* (1992), who demonstrated in vitro that the α-glucan chain of glycogenin from rabbit muscle could be removed by bacterial ISA, making glycogenin incapable of priming glycogen synthesis. ISA may prevent the initiation of large numbers of granules and phytoglycogen by cleaving off α-glucan chains bound to the glycogenin-like molecule. According to this theory, in the *isa* mutant, multiple initiations occur because the level of glucosylation of the glycogenin-like molecule is not regulated. There is currently no evidence for an interaction between a glycogenin-like protein and ISA in plants. Only after the discovery of 'amylogenin' could an interaction with ISA be tested.

Gene Name	Description	E-value
AT1G77130	PLANT GLYCOGENIN-LIKE STARCH INITIATION PROTEIN 2 (PGSIP2)	$4e^{-21}$
AT3G18660	PLANT GLYCOGENIN-LIKE STARCH INITIATION PROTEIN 1 (PGSIP1)	$1e^{-20}$
AT5G18480	PLANT GLYCOGENIN-LIKE STARCH INITIATION PROTEIN 6 (PGSIP6)	$2e^{-20}$
AT4G33330	PLANT GLYCOGENIN-LIKE STARCH INITIATION PROTEIN 3 (PGSIP3)	$1e^{-19}$
AT1G08990	PLANT GLYCOGENIN-LIKE STARCH INITIATION PROTEIN 5 (PGSIP5)	$2e^{-18}$
AT2G47180	ARABIDOPSIS THALIANA GALACTINOL SYNTHASE 1 (ATGOLS1)	$7e^{-18}$
AT1G60450	ARABIDOPSIS THALIANA GALACTINOL SYNTHASE 7 (ATGOLS7)	$6e^{-17}$
AT1G54940	PLANT GLYCOGENIN-LIKE STARCH INITIATION PROTEIN 4 (PGSIP4)	$3e^{-15}$
AT1G60470	ARABIDOPSIS THALIANA GALACTINOL SYNTHASE 4 (ATGOLS4)	$3e^{-15}$
AT1G09350	ARABIDOPSIS THALIANA GALACTINOL SYNTHASE 3 (ATGOLS3)	$7e^{-15}$
AT1G56600	ARABIDOPSIS THALIANA GALACTINOL SYNTHASE 2 (ATGOLS2)	$1e^{-14}$
AT4G16600	glycogenin glucosyltransferase (glycogenin)-related	$7e^{-13}$
AT2G35710	glycogenin glucosyltransferase (glycogenin)-related	$3e^{-12}$
AT4G26250	ARABIDOPSIS THALIANA GALACTINOL SYNTHASE 6 (ATGOLS6)	$2e^{-11}$
AT5G23790	ARABIDOPSIS THALIANA GALACTINOL SYNTHASE 5 (ATGOLS5)	$4e^{-10}$

Table 1.1: Results of a TBLASTN search of the human glycogenin protein sequence against the *Arabidopsis thaliana* genome using TAIR (www.arabidopsis.org). The expect value (E-value) is the equivalent to a p-value in a statistical test. E-value is an indication of similarity between two sequences and gives the statistical significance of each alignment, i.e. how many amino-acid matches are expected by chance. The lower the E-value the more likely the alignment is significant and does not occur by chance.

1.3.1.4 Starch Synthase IV (SS4)

SS4 appears to have a specific function related to granule initiation and growth that is not shared by the other SSs. Loss of SS1, SS2 or SS3 from *Arabidopsis* has only moderate effects on starch content and granule size, shape and structure (Delvallé *et al.,* 2005; Szydlowski *et al.,* 2009; Zhang *et al.,* 2005). Chloroplasts of the triple mutant *ss1 ss2 ss3* contain the wild-type number of starch granules (Szydlowski *et al.,* 2009). Loss

of SS1 from *Arabidopsis* results in a 56% reduction in starch synthase activity, but the granule itself is similar to wild-type apart from a reduction in the number of shorter glucan chains in the amylopectin molecules, a slight increase in amylose content and a slightly elongated shape (Delvallé *et al.,* 2005). However, loss of SS4 from *Arabidopsis* has a massive effect on the starch phenotype. In the *ss4*, *ss1 ss4* and *ss2 ss4* mutants and the triple mutant *ss1 ss2 ss4* on average only a single, large granule per chloroplast is produced compared with estimates of about five in wild-type chloroplasts (Roldan *et al.,* 2007; Szydlowski *et al.,* 2009). This suggests that SS4 may be involved in controlling the number and size of starch granules. The massive effect on starch when SS4 is lost, not seen when the other SSs are lost, is surprising since SS4 is a minor SS, in the sense that it makes up a small percentage of starch synthase activity. For example, SS3 is readily detectable on native gels of wild-type leaf extracts stained for starch synthase activity, SS4 is not. SS3 accounts for 15 to 30% of the total soluble SS activity in *Arabidopsis* leaves, whereas there is no detectable decrease in SS activity in *ss4* relative to wild-type leaves, indicating that the activity of SS4 is below levels detectable in starch synthase assays (Szydlowski *et al.,* 2009).

The larger size of the granules in *ss4* mutants may be a consequence of there being a reduced number of granules initiated, since all the available ADPG is channelled into fewer granules (Roldan *et al.,* 2007). There is a reduced rate of both starch synthesis and degradation in the *ss4* mutant (Roldan *et al.,* 2007). Roldan *et al.* (2007) proposed that the reduction in overall granule surface area and surface:volume ratio results in reduced granule surface area available for starch synthesis or degradation enzyme activity.

SS4 has little role in the determination of amylopectin structure (Szydlowski *et al.,* 2009) and the amylose to amylopectin ratio is unaffected in the *ss4* mutant (Roldan *et al.,* 2007). There were only minor modifications to chain length distributions (a slight reduction in the number of short chains of degree of polymerisation (DP) = 7-10) (Roldan *et al.,* 2007), indicating that the other starch synthases continue to act as normal and the major function of SS4 is not to elongate amylopectin chains. Roldan *et al.* (2007) noted the presence of a less electron-dense zone at the core of the *ss4* mutant granule in transmission-electron microscopy images, which could indicate the presence of a cavity in the hilum.

Taken together the evidence suggests that SS4 is involved during the establishment of the initial structure of the starch granule (Roldan *et al.,* 2007). However, there is obviously redundancy, since the mutants are still able to form granules. The *ss3 ss4* double mutant fails to accumulate measurable amounts of starch, suggesting that an active class 3 or class 4 starch synthase is mandatory for the synthesis of transitory starch in *Arabidopsis* leaves (Szydlowski *et al.,* 2009).

It is possible that the function of SS4 is to synthesise short glucan polymers. For example, SS4 has a high activity when using maltotriose as a primer (>90% of the activity observed with amylopectin) that is not observed for the other SSs (Szydlowski *et al.,* 2009). SS4 could also use other MOS as primers but with a much lower efficiency (Szydlowski *et al.,* 2009). MOS are generated all the time during starch synthesis, and are then turned over quickly (Niittylä 2003). This process is absent in *pgm* and *pgi* mutants, indicating that MOS are made either from glucose-1-P, the substrate for ADPG synthesis, or from ADPG itself (Niittylä 2003). It is possible that SS4 could be making these MOS, for the other SSs to then act upon to create glucan chains. Thus in the absence of SS4 glucan synthesis and hence perhaps glucan initiation is severely limited by lack of short glucan chains as substrates for the other SS isoforms.

SS4 might conceivably self-glucosylate, acting as a glycogenin (see section 1.3.1.3) and initiating glucan synthesis, although this has not been demonstrated experimentally (Szydlowski *et al.,* 2009). Purified SS4 proteins incubated with radioactively labelled ADPG failed to incorporate any radioactivity, indicating that under these experimental conditions SS4 does not display ADPG-dependent self-glucosylating activity (Szydlowski *et al.,* 2009). Alternatively SS4 might be the only starch synthase that can act on a glycogenin-like primer.

1.3.2 Physical Controls

Physical factors could be involved in granule initiation. The initiation of the starch granule could be a spontaneous event, with amylopectin molecules crystallising and self-assembling into the ordered lamellae structure. It has been shown that in vitro low molecular weight or lightly branched starch polymers can spontaneously form spherulites, similar to starch granules in their three-dimensional morphology,

crystallinity and the exhibition of a Maltese cross when viewed under polarised light (Helbert *et al.,* 1993; Nordmark and Ziegler 2002a; Nordmark and Ziegler 2002b; Ring *et al.,* 1987). Being semi-crystalline, starch granules exhibit birefringence when viewed between polarised light (Gallant *et al.,* 1997). The granules will not show birefringence if the crystalline regions are randomly orientated, even if the granule is constructed of a highly crystalline polymer (Geddes and Greenwood 1969). Spherulites are small, usually spherical bodies consisting of radiating crystals. The crystallinity of spherulitic crystals, observed under polarised light, is weak and less orientated than the outer regions of native starch granules, similar to the hilum and core region of native starch granules (Ziegler *et al.,* 2005). The hilum is the point of granule initiation from which the granule grows out. Ziegler *et al.* (2005) proposed that granules initiate via spherulitic crystallization of lightly branched or linear glucose polymers, such as amylopectin intermediates, produced early in starch synthesis.

The primary nucleation event responsible for the initial formation of the starch granule could be either homogeneous or heterogeneous nucleation (Geddes and Greenwood 1969). In homogeneous nucleation, polymer molecules - in the case of starch this is short glucan chains - are in constant motion and align portions of themselves together with a small degree of order. Above a certain size the organised state becomes stable and acts as a nucleus for growth. Alternatively, during heterogeneous nucleation a foreign particle has a stabilising affect on polymer molecules, acting like a seed or nucleus for growth. In the chloroplast stroma there are many structures and proteins that could potentially act as stabilisers.

It has been suggested that starch crystallizes out from a coacervate (Badenhuizen 1963; Macmasters *et al.,* 1946). A coacervate is a tiny spherical droplet of assorted organic molecules which is held together by hydrophobic forces from a surrounding liquid. Coacervates measure 1 to 100 micrometers across, possess osmotic properties and form spontaneously from certain dilute organic solutions. Their name derives from the Latin coacervare, meaning to assemble together or cluster. Doi (1965) speculated that because the protein concentration of the plastid is so high, amylopectin molecules newly synthesized in the plastid go into a separate phase, appearing as droplets or particles. Doi (1965) attempted to reproduce the natural conditions of starch granule formation in a ‘gelatin gel’ (an aqueous gelatin solution). He showed granules forming from

amylopectin, but the granules had poor crystallinity and did not show polarization. He was able to produce amylopectin and amylose like polysaccharides in a gelatin gel by combining glucose-1-P, α-glucan phosphorylase, 1,4-alpha-glucan branching enzyme and a primer. However, no granular structures were formed.

Spontaneous crystallisation could be responsible for both the initiation and the growth of starch granules. Throughout the day, in addition to the extension of the glucan chains at the periphery of the granule by SSs, new amylopectin molecules may be initiated in the stroma, which then spontaneously crystallise onto the surface of the existing granules. If starch granules are initiated via physical means e.g. spherulitic crystallisation, as discussed above, the question still remains about which molecule or molecules is responsible for initiating the glucan chains required for the initial crystallization.

1.3.3 Other possible controls

One of the smallest photosynthetic eukaryotes (0.8 μm in diameter), the unicellular chlorophyte *Ostreococcus taurii*, has been proposed as a new model system for studying starch metabolism, since it has a small genome (10.2 Mb) and yet displays all the major features of other plant cells (Hicks *et al.,* 2001). *O. taurii* only ever contains one starch granule, which is synthesised in the centre of the plastid (Ral *et al.,* 2004). *O. taurii* cells elongate and divide centrally, during which the starch granule appears to constrict or degrade at the division plane, to form two granules, one of which is inherited by each daughter cell (Figure 1.5). This division is thought to be explained by localised degradation of the granule at the site where the plastid constricts, possibly involving LDA activity (Ral *et al.,* 2004). During prolonged incubation in darkness *O. taurii* died before the starch was completely degraded (Ral *et al.,* 2004). The above observations led Ral *et al.* (2004) to propose that all granules are derived from a parental granule, which grows and then divides between the daughter cells. Therefore in *O. taurii,* granule initiation and potentially glucan initiation are unnecessary. The division of granules and allocation between daughter chloroplasts may occur in other species, removing the requirement for new granules to be initiated; although there is no evidence for this. Interestingly, *O. taurii* does not contain an SS4 gene (Leterrier *et al.,* 2008); further suggesting a critical role for SS4 in starch granule initiation. As *O. taurii*

evolved the mechanism described above, whereby the need for initiation of a new starch granule is eliminated, this may have removed the need for SS4, and *O. taurii* may have lost its copy of the *SS4* gene over time.

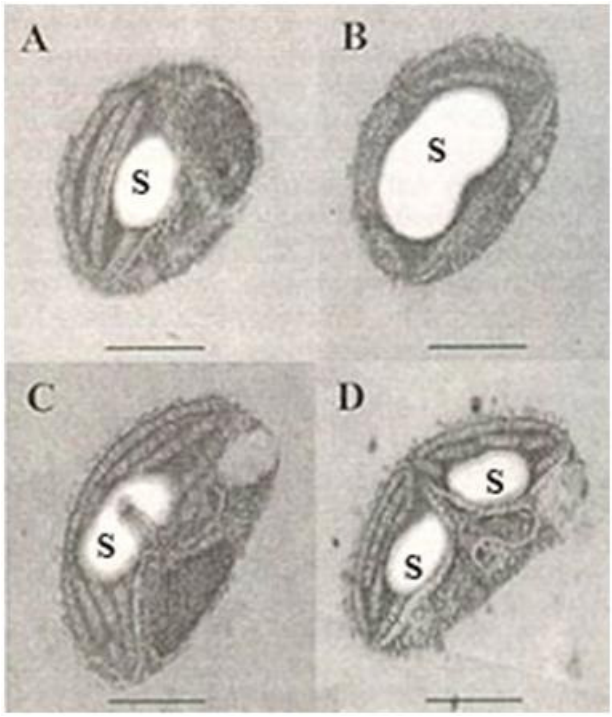

Figure 1.5: Starch division in *Ostreococcus taurii* with central starch granule. (A - D) Transmission electron micrographs of dividing *O. taurii* cells. s = starch granule. Bar = 0.4 µm (Figure 6 from Ral *et al.,* 2004).

1.4 Controls over starch granule number and morphology

The variability of starch granules across species is remarkable considering that the basic chemistry of all starches is the same. This variability suggests a complex set of interacting factors which contribute to the production of starch in plants, but very little is known about how differences in starch granule morphology, size and number between species and organs are determined. In other words, it is unknown which factors alter the standard pattern of starch production from the basic chemical reactions of the starch synthesis pathway, to produce the variety of shapes that occur in different

species. It is likely that a number of genetic factors are responsible for controlling the number, size or morphology of granules formed. Borem *et al.,* (1999) identified a region on chromosome two in Barley containing quantitative trait loci (QTL) which affected a number of starch parameters, including the overall mean granule volume and the roundness of the small B-type granules. Shewry and Morell (2001) suggested that the primary biosynthetic enzymes of different species may have differences in their properties which result in different granule shapes. Alternatively, they hypothesised that it was the unique combination of physical environment and substrate supply in each species and organ that contributed to differences in granule morphology. Plants with mutations in starch metabolism genes often have altered granule size, morphology and occasionally number, as previously discussed for SS4. These mutants provide us with clues, not only into their primary function in starch metabolism but also into the controls over how the starch granule is constructed. A number of these mutants are discussed below.

Changes in starch content due to mutations often change the size of granules and not the number, implying that control over granule number is independent of granule size. For example, the *sex* mutants of *Arabidopsis* have reduced starch degradation and depending on the time of day can contain three to four times more starch than wild-type plants. Both *sex4* and *gwd1* have larger granules than wild-type plants (Sokolov *et al.,* 2006; Zeeman *et al.,* 2002b), indicating that the plant maintains some control over the number of granules that initiate, so the increase in starch accumulation results in larger granules. This contrasts to the phenotype found in the *lsf1* mutant, which has a starch excess phenotype, but the granules are a similar size and shape to wild-type granules (Comparot-Moss *et al.,* 2010), implying an increase in granule number. Therefore, under certain mutant conditions the plant is unable to control the number of granules initiated. Alternatively, in the *lsf1* mutant the plant may have retained an ability to restrict the growth of granules, initiating new granules and channelling the excess glucans into these new granules. Ji *et al.* (2004), were able to reduce the size of potato starch granules by over-expressing starch-binding domain2 (SBD2) derived from *Bacillus circulans* cyclodextrin glycosyltransferase in an amylose-free potato mutant. The total starch yield was equal to wild-type, indicating that there was a greater number of smaller starch granules. Ji *et al.* (2004) hypothesised that SBD2 binds to the starch granule surface. When levels are high enough, the starch granule is completely covered,

preventing SS and SBE from accessing the granule surface. This may force additional granule initiations, due to the action of the SSs and SBEs on available glucans in the stroma. This is in line with the theory of how ISA acts during starch synthesis proposed by Zeeman *et al.* (1998b), in which the stroma contains soluble glucans that can be acted upon by SSs and SBEs.

Change in granule size sometimes alters granule shape, but not always, implying that the control over granule shape is partially linked to size. For example, in *sex4* the granules are not only larger, but also more spherical and occasionally have irregular protrusions (Sokolov *et al.,* 2006; Zeeman *et al.,* 2002b). This contrasts with the starch granules of *gwd1,* which are larger but remain disc shaped and resemble wild-type granules (Zeeman *et al.,* 2002b). Therefore, the increase in starch accumulation does not always result in altered granule shape, implying that under some mutant conditions the plant is able to maintain normal control over granule shape.

Many mutations alter granule morphology as a result of changes to the amylopectin polymers from which the granule is constructed, for example mutations that knock out SBEs (Bhattacharyya *et al.,* 1990; Boyer *et al.,* 1976) and SSs (Craig *et al.,* 1998; Fujita *et al.,* 2007; Ryoo *et al.,* 2007) or cause alterations in the amylose content (Buléon *et al.,* 1997; Delrue *et al.,* 1992; Fulton *et al.,* 2002; Wattebled *et al.,* 2002). Amylose is not essential for normal starch granule formation in higher plants (Buléon *et al.,* 1998; Kim *et al.,* 2003; Kuipers *et al.,* 1994). However, *C. reinhardtii gbss* mutants that lack amylose, have smaller granules with more irregular shapes than wild-type (Delrue *et al.,* 1992) and SS2 defective mutants that have an increased amylose content, show a large variety of distorted granule shapes (Buléon *et al.,* 1997). In *C. reinhardtii* amylose may be involved in granule formation, potentially affecting the packaging of the amylopectin molecules and altering the crystallinity of the granules. Using an in vitro system Wattebled *et al.* (2002) investigated the impact amylose synthesis had on isolated *C. reinhardtii* starch granules, in the absence of amylopectin synthesising enzymes. They supplied ADPG to isolated granules, as a substrate for GBSS contained in the matrix of the granules. While the amount of A-type starch remained constant, the amount of B-type starch increased; suggesting that GBSS either synthesises material that then crystallizes into B-type starch, or converts amorphous amylopectin already in the system into B-type starch. After a number of incubations the resulting granules

appeared highly distorted and slightly fused together into a network (Wattebled *et al.,* 2002). Therefore, in *C. reinhardtii* GBSS is able to synthesise long amylopectin chains and as a result is involved in granule formation, affecting the branching pattern of the amylopectin molecules and altering the granule morphology.

There is no evidence in higher plants of changes in granule morphology brought about by reduction or elimination of amylose. However, abnormal amounts of amylose can have an influence on the crystalline packing of amylopectin in higher plants. For example, in potato plants loss of SS3 is accompanied by an increase in GBSS activity (Fulton *et al.,* 2002). The increase in GBSS activity resulted in larger amylose molecules and an increase in the proportion of very long amylopectin chains (Fulton *et al.,* 2002). The increase in long glucan chains was reported to result in disruption of the semi-crystalline packaging of the amylopectin molecules leading to altered granules in the *ss3* mutant that contained fissures. In conclusion, the impact of a GBSS mutation or overexpression and the resulting amylose loss or excess upon granule morphology, depends upon the contribution of GBSS to amylopectin structure under wild-type conditions. In *C. reinhardtii,* GBSS normally contributes to the synthesis of long chains in amylopectin, meaning both an increase and a decrease in amylose has an impact upon granule morphology. However, in potato plants the contribution of GBSS to long chains of amylopectin is small, so only a large increase in amylose content affects the granule morphology.

1.4.1 The environment within the plastid

As previously mentioned, Shewry and Morell (2001) hypothesised that it may be the unique combination of physical environment and substrate supply in each species and organ that contributed to differences in granule morphology. In other words, the environment within which the starch granules are made may influence granule size, morphology and initiation.

In some algae, bryophytes and protozoa the pyrenoid may be involved in the physical construction of the starch granule, influencing final granule morphology. The pyrenoid is a proteinaceous structure mostly consisting of Rubisco and is thought to be a centre of carbon dioxide fixation, either within the chloroplast or the cytosol. For example, the

starch granules of *C. reinhardtii* typically surround the pyrenoid and adopt a shape dictated by the pyrenoid (Libessart *et al.,* 1995). The Cryptomonads, for example *Guillardia theta*, synthesise starch granules in their periplastidial space, rather than within their chloroplasts (Kugrens *et al.,* 2000). The starch granules are globular with an unusual round cavity, which is suspected to be due to close association between the granules and the pyrenoid during synthesis (Figure 1.6) (Deschamps *et al.,* 2006). In the algae *Chlorella kessleri* both pyrenoid-associated and stromal starch forms (Izumo *et al.,* 2007). The two types of starch vary not only in morphology, but also in size and chain length distribution (Izumo *et al.,* 2007). In a similar way, the shape of transitory starch granules formed in chloroplasts could be dictated by the space available between the thylakoids (Badenhuizen 1969).

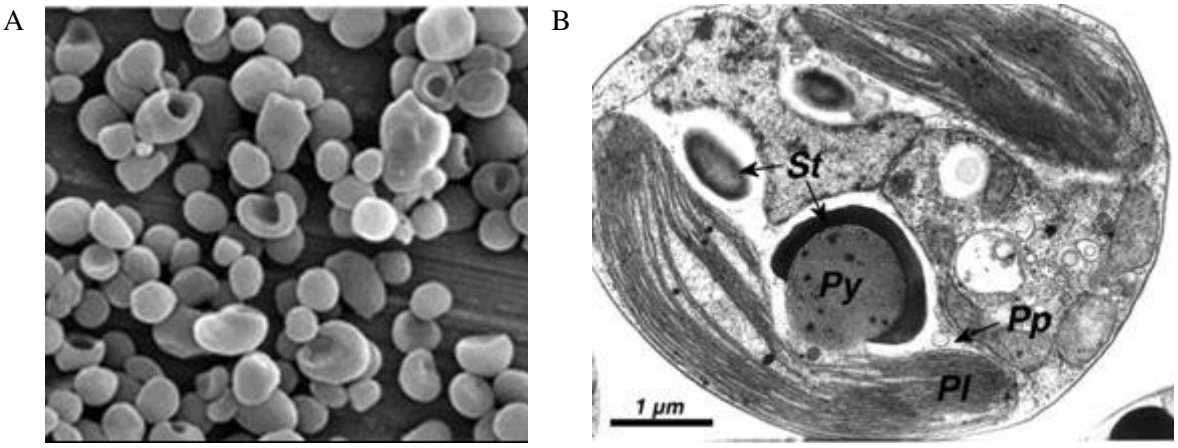

Figure 1.6: *Guillardia theta* starch. (A) Scanning electron microscopy of starch granules, including some with unusual round cavities. (B) Transmission electron microscopy of *G. theta* showing both pyrenoid associated starch and free starch granules. Pl= plastid; Py = pyrenoid; Pp = periplast; St = starch (Deschamps *et al.,* 2006).

Badenhuizen (1969) suggested that substances in the stroma determine how starch granules are assembled and control granule morphology, but location within the chloroplast is not essential for granule initiation and growth. During evolution of photosynthesising organisms some of the enzymes involved in granule synthesis have

moved to different cellular compartments in some lineages (Patron and Keeling 2005). For example, in red algae, the SSs and ISA are originally derived from the plastid; however, they now act in the cytosol. Red algae such as *Cyanidionschyzon merolae* produce what is known as floridean starch, which is synthesised outside the plastid in the cytosol (Viola *et al.,* 2001). Patron and Keeling (2005) suggested that the ancestor of the green and red algae synthesised starch in the plastid and that in the red algae the pathway became relocated to the cytosol. Despite minor differences in chain length distributions, floridean starch is structurally more similar to higher plant amylopectin than to glycogen (Yu *et al.,* 2002). The starch synthesising machinery in the dinoflagellates, such as *Crypthecodinium cohnii* is thought to have originated from a red algal ancestor following secondary or tertiary endosymbiosis of a red algal ancestor (Coppin *et al.,* 2005; Morden and Sherwood 2002). Approximately 50% of dinoflagellates contain chloroplasts, but starch granules are produced in the cytosol (Dodge and Lee 2000).

It has been suggested that the 'plastoskeleton', a filamentous network of proteins within plastids, may provide the framework which organises the enzymes involved in starch synthesis (Reski 2002; Tomlinson and Denyer 2003). 'Plastoskeleton' is a term coined by Kiessling *et al*. (2000) to describe the scaffold of microtubule-like filaments made from Filamentary temperature-sensitive (FtsZ) molecules, within the chloroplasts of the moss, *Physcomitrella patens*. The *Arabidopsis* genome contains two families of homologs of FtsZ, both of which are critical for chloroplast division (Osteryoung *et al.,* 1998 and references therein), although it is important to note that no plastoskeleton has been identified in the chloroplasts of higher plants. The potential interaction between the chloroplast division components and starch will be discussed in more detail in Chapter 5.

1.4.2 Potential mechanisms for sensing leaf starch content

As discussed above, setting the correct rate of starch degradation in leaves at night requires measurement of both the length of time until dawn and the amount of starch present (Gibon *et al.,* 2004; Graf *et al.,* 2010; Lu *et al.,* 2005). To set the appropriate rate of degradation the amount of starch present at the end of the day must be divided by the length of the night. The mechanism for measuring the amount of starch present is

unknown. Possible methods include mechanisms that monitor the total flux into starch during the day, or mechanisms that directly or indirectly measure the starch volume or surface area.

If the starch pathway produced a small amount of a side product in the form of a signalling molecule, in direct proportion to the major flux into starch, then the flux into starch could be measured (Stitt, M. personal communication). For example, AGPase catalyses synthesis of ADPG from ATP and glucose-1-P (Lin *et al.,* 1988). If AGPase had a very low affinity for a substrate other than ATP, for example GTP, then GDPglucose might be produced from glucose-1-P at a very low rate. GDPglucose production would therefore be proportional to the rate of glucose 1-P consumption and the rate of starch synthesis. Hence at the end of the day, the GDPglucose concentration in the stroma would relate directly to the amount of starch present. Sensing and signalling systems would be required to feed this information to the mechanism that sets the starch degradation rate. A method for removing GDPglucose from the plant at night would also be required.

Evidence against such a system for measuring the flow of carbon into the starch synthesis pathway comes from the *isa* mutants. As previously discussed, the *isa* mutants accumulate only a small fraction of the starch that wild-type does and the rest of the glucans accumulate as phytoglycogen (Delatte *et al.,* 2005; Zeeman *et al.,* 1998b). Phytoglycogen degradation occurs at an exponential rate, while despite the reduction in starch levels, the rate of starch degradation is still linear and such that reserves last almost exactly until dawn (Delatte *et al.,* 2005; Streb *et al.,* 2008; Zeeman *et al.,* 1998b). If the rate of starch degradation was set by the flux through AGPase into glucan production then starch degradation would be expected to occur at a much faster rate. Therefore, the rate of starch degradation appears to be related to the amount of granular starch present at the beginning of the night, not the flux into glucans during the day.

A mechanism may exist that directly measures the starch volume or surface area. Caspar *et al.* (1991) suggested the existence of a regulatory mechanism that measures the actual size of the starch pool accumulated or some constituent of starch such as the number of non-reducing ends, although they did not propose how this mechanism may function. Alternatively, if a stromal molecule were absorbed or adsorbed by the starch granules as

they grow, then the amount of this molecule in the stroma or on the surface of the granule would directly reflect the amount of starch present. There are no obvious candidates for what this stromal molecule might be and where or how it might be sensed. The molecule might control granule degradation directly, by inhibiting granule degrading enzymes (e.g. GWD) in the stroma. Absorption of the molecule into the granule as it grows during the day would reduce its concentration in the stroma, setting the activity of the degradation enzymes at the beginning of the night. Alternatively, the activity of granule degrading enzymes might be promoted or inhibited by absorption of the stromal signalling molecule onto the granule surface.

A mechanism may exist that monitors the starch volume indirectly. For example as the granule volume increases during the day, the chloroplast volume may also increase. Mechanosensitive ion channels in the inner chloroplast envelope (Haswell and Meyerowitz 2006; Pyke 2006) or components of the chloroplast cytoskeleton-like network (Kiessling *et al.,* 2000) may detect the alterations in volume. *Arabidopsis* mutants that have altered chloroplast development could be used to explore mechanisms that might exist to regulate or control starch granule initiation and accumulation in the chloroplasts of *Arabidopsis* leaves. The mechanism of chloroplast division and its possible impact on starch accumulation will be described in more detail in the introduction section of Chapter 5.

1.5 Justification for experimental approach

In order to shed light on the variation of starch granule number and size in *Arabidopsis* leaves I first established new and quantitative techniques to examine starch granule numbers on a chloroplast basis in *Arabidopsis* leaves, and to establish how these change over the day\night cycle and as the leaf ages. This work is described in Chapter 3. I then used two different approaches to understand factors that control granule numbers. These approaches were based on clues from existing research about factors that may be important in granule size and initiation, described above. In Chapter 4 I describe experiments in which I used the *ss4* mutant to study the involvement of SS4 during the establishment of the initial structure of the starch granule and in the control of granule number per chloroplast. In Chapter 5 I describe the use of the *accumulation and regulation of chloroplast* (*arc*) mutants to explore the impact of altered chloroplast

division machinery and chloroplast size on the composition and quantity of starch granules.

2 Materials and Methods

2.1 Plant Material

Experiments were conducted on plants of *Arabidopsis thaliana* L. (Heynh) accessions Columbia (Col-0; N1093: referred to below as the wild-type), Wassilewskija (Ws; N1602) and Landsberg *erecta* (L*er*; N1686) which were originally provided by the Nottingham Arabidopsis Stock Centre (NASC) (University of Nottingham, UK).

The *accumulation and regulation of chloroplast* (*arc*) mutants *arc1*, *arc3*, *arc5*, *arc6*, *arc11* and *arc12* were kindly provided by Dr. Kevin Pyke (University of Nottingham, UK). The *ss4* mutant, SALK_096130, carrying a T-DNA insertion in At4g18240, was obtained through NASC and the homozygous line was isolated by Chris Hylton (JIC). The *isa1* mutant, SALK_042704, carrying a T-DNA insertion in At2g39930, was kindly provided by Prof. Sam Zeeman (ETH, Zurich).

Segregating populations of seeds carrying one of the following T-DNA insertions in the listed genes were obtained from NASC; SALK_057144 and SALK_012892 in At1g75010, SAIL_71_D11 in At3g19720, SAIL_693_G04 in At5g42480 and SALK_073878 in At5g55280.

2.2 Growth conditions

2.2.1 Plant tissue culture

Media were autoclaved and allowed to cool to 50^{o}C before the addition of antibiotics. Media were poured into 90 mm or 140 mm Petri dishes and air-dried for 30 min. Plates were stored at 4^{o}C and used within 2 weeks. Seeds were surface-sterilised by soaking them for 5 min in 5% (v/v) bleach (5% available chlorine e.g. Parazone; Jeyes, Thetford, UK) and then washing in ddH_2O. Seeds were air-dried on sterile filter paper and sown onto plates. Plates were sealed with micropore surgical tape, stored at 4^{o}C for 3 days and transferred to a controlled environment room (CER).

2.2.2 Plant growth conditions

Unless otherwise stated, *Arabidopsis* seeds were sown onto compost (Levington's F2, Levington Horticulture, Suffolk, UK), in 24-, 40- or 60-cell trays (21 x 35 cm). Trays were covered with propagator lids and stored at 4°C for three days, then moved to a CER at a constant temperature of 20°C, 75% relative humidity, with a 12 hour photoperiod. The light intensity was 180 µmol quanta m^{-2} s^{-1} throughout the growing period. Propagator lids were removed after approximately 8 days.

For experiments involving the determination of luciferase activity (section 2.12), following the 4°C treatment plants were transferred to growth cabinets (Sanyo GallenKamp). The conditions were the same as described above except that the light intensity was 160 µmol m^{-2} s^{-1}.

Unless otherwise stated, leaf tissue was harvested at 3-4 weeks, equivalent to the principal growth stage 1.14 (3.50/3.70) according to Boyes *et al.* (2001). For seed propagation, plants were grown in a CER (under the conditions described above) and seeds harvested by bagging inflorescences before the siliques ripened and split open. Newly harvested seed was allowed to dry at room temperature for at least 2 weeks before sowing.

2.3 Bacteria and yeast strains

Plasmids were constructed and amplified in *Escherichia coli* strain TOP10, transferred to *Agrobacterium tumefaciens* GV3101 (Table 2.1), and introduced into wild-type *Arabidopsis* (Col-0) by floral dipping as described in sections 2.9 and 2.10.

Strain	Antibiotic Resistance	Genotype/Properties	Source
Escherichia coli			
TOP10	Str^R	F- *mcr*A Δ(*mrr-hsd*RMS-*mcr*BC) φ80*lac*ZΔM15 Δ*lac*X74 *rec*A1 *ara*D139 Δ(*ara-leu*)7697 *gal*U *gal*K *rps*L *end*A1 *nup*G λ-	Invitrogen Ltd; http://www.invitrogen.com
Agrobacterium tumefaciens			
GV3101	Rif^R, $Gent^R$	pMP90 (pTiC58ΔT-DNA), genes for nopalin biosynthesis	Van Larebeke *et al.* (1973)

Table 2.1: Bacterial strains.

2.4 Media and antibiotics

The composition of plant and bacterial media for the sterile growth of seedlings on plates and the growth of bacterial cultures respectively is described in Table 2.2.

Media	Composition
Plant growth medium	
MS medium	0.5 x Murashige and Skoog plant salt mixture (Duchefa Biochemie, Ipswich, UK), 50 mg l^{-1} *myo*-inositol, 0.5 mg l^{-1} thiamine, 0.25 mg l^{-1} pyridoxine, 0.25 mg l^{-1} nicotinic acid, 0.25 g l^{-1} 2-[N-morpholino]-ethanesulphonic acid (MES), 0.8% (w/v) Bacto agar (Difco™; BD Diagnostics; http://www.bd.com/uk/), pH 5.7 (pH adjusted with 1 M KOH), sucrose was added to a final concentration of 30 mM for selection of transgenic plants
Bacterial growth medium	
Luria-Bertani Broth (LB) medium	10 g l^{-1} Bacto-tryptone, 5 g l^{-1} bacto-yeast extract, 10 g l^{-1} NaCl, pH 7.0, for solid medium Bacto agar (Difco) was added to a final concentration of 1.5% (w/v)
Super Optimal broth with Catabolite repression (SOC)	20 g l^{-1} Bacto-tryptone, 5 g l^{-1} bacto-yeast extract, 0.5 g l^{-1} NaCl, 0.186 g l^{-1} KCl, pH 7.0, medium was autoclaved prior to addition of glucose to a final concentration of 20 mM and $MgCl_2$ to a final concentration of 2 mM.

Table 2.2: Media used for plants and bacteria.

Antibiotics were used for selection of *E. coli*, Agrobacterium *tumefaciens* and during the selection of transgenic *Arabidopsis* lines. The final concentrations of antibiotics used are listed in Table 2.3.

Antibiotic	**Final concentration**	**Dissolved in**	**Effect on**
Gentamycin (Gent)	50 µg/ml	dH_2O	Gram-negative bacteria
Rifampicin (Rif)	10 µg/ml	methanol	Bacteria
Spectinomycin (Spc)	100 µg/ml	dH_2O	Bacteria
Hygromycin (Hyg)	50 µg/ml	dH_2O	Bacteria, fungi and plants

Table 2.3: Antibiotic concentrations in selection media

2.5 Cloning vectors

The empty vectors used for cloning or as controls are listed in Table 2.4. Gateway vectors were transformed into *E. coli* DB3.1 for propagation and maintenance using the antibiotic resistance shown. *E. coli* Top10 cells were transformed with the plasmid carrying the gene of interest.

Gateway Vector	Resistance	Description	Source
pCR8/GW/ TOPO TA	SpcR	Vector for cloning DNA fragments with terminal 3' A-overhangs	Invitrogen
pOpoff2 Hyg	Hyg	Vector system for the production of dexamethasone-inducible RNAi lines. LhGR transcription factor is constitutively expressed but activates transcription from the pOp6 promoter only when dexamethasone is present. pOp6 promoter drives expression of a hairpin RNA cassette.	Wielopolska *et al.* (2005) Craft *et al.* (2005)

Table 2.4: Gateway vectors

2.6 Oligonucleotides

Oligonucleotide primers (from Sigma-Aldrich Ltd, Haverhill, UK; (http://www.sigmaaldrich.com/united-kingdom.html) were resuspended in dH_20 to obtain a 100 µM stock solution. For the standard Polymerase Chain Reaction (PCR), primers were diluted to a working solution of 10 µM. Oligonucleotides used in this work are listed in Table 2.5 and 2.6.

Oligonucleotide	**Oligonucleotide sequence (5'-3')**
pOpOff2(hyg)::SS4A	
SS4_P4_LP	GGATTGGCACTGTTGAAGGT
SS4_P4_RP	CCGGACTGAAGAAGCAACTC
pOpOff2(hyg)::SS4B	
SS4_P6_LP	TTGGAGCGAGCATTTAATCA
SS4_P6_RP	CTCACGTGCGATTAGGAACA
pOpOff2(hyg)::SS4C	
SS4_P1_LP	AACCCATGGATTAGCAGGAA
SS4_P1_RP	GGGAGCCTTTCTTGACCTCT
pOpOff2(hyg)::SS4D	
SS4_P5_LP	TGGACTTTCTTCAGCGGAGT
SS4_P5_RP	GAATATGTGGAACCGGGCTA
semi-quantitative RT-PCR	
Tubulin 5-1	CCTGATAACTTCGTCTTTGG
Tubulin 3-1	GTGAACTCCATCTCGTCCAT
Fragments in PCR8 plasmid	
M13Fwd	CGACGTTGTAAAACGACGGCCAGT
M13Rev	CACACAGGAAACAGCTATGACCATG
Screening of T-DNA insertion mutants	
LBa2Salk	TGGACCGCTTGCTGCAACT
LBb1Salk	GCGTGGACCGCTTGCTGCAACT
LB3 SAIL	TAGCATCTGAATTTCATAACCAATCTCGATACAC
GK_LB	CCCATTTGGACGTGAATGTAGACAC
SALK_057144_LP	CAAGTCGATGCCAACTGAGA
SALK_057144_RP	TACAGCATTGCCGGATGATA
SALK_012892_LP	AGCCTGATCTGGAGCCTAAAG

SALK_012892_RP	TCTCAGTTGGCATCGACTTG
SAIL_71_D11_LP	TGTGTTGGATGCCCTTAAGAC
SAIL_71_D11_RP	TGTCACCTGATGAAGGAAAGG
SAIL_693_G04_LP	AACGCTACTCTCTGAGACCCC
SAIL_693_G04_RP	TAAATGGTTTAAGCGGTGTGC
SALK_073878_LP	CAGAGCTTGCGAATCCGTGTT
SALK_073878_RP	AAGCATGCGCAAAGTCAGTCG
SALK_042704_LP	GGTTTCATGCCAAATGTGATG
SALK_042704_RP	AGTGAAACGAGCTTTGAGCAG
SALK_096130_LP	GTGACATTACTTGAGGAGCGG
SALK_096130_RP	GAATTTGCTTGGATGTTGAGGTTC

Table 2.5: Oligonucleotides

Mutant Name	T-DNA Insertion Line	Oligonucleotide 1	Oligonucleotide 2
arc3-2	SALK_057144	SALK_057144_RP	LBa2Salk
arc3-3	SALK_012892	SALK_012892_LP	LBa2Salk
arc5-2	SAIL_71_D11	SAIL_71_D11_RP	LB3 SAIL
arc6-5	SAIL_693_G04	SAIL_693_G04_RP	LB3 SAIL
arc10-2	SALK_073878	SALK_073878_LP	LBb1Salk
ss4	SALK_096130	SALK_096130_LP	LBa2Salk
isa1	SALK_042704	SALK_042704_LP	LBa2Salk

Table 2.6: Oligonucleotide combinations used during screening to amplify T-DNA insertion regions.

2.7 General Molecular Methods

2.7.1 Isolation of DNA

2.7.1.1 Isolation of plasmid DNA from *E. coli*

Plasmid DNA from bacterial cultures grown overnight was isolated using the QIAprep Spin Miniprep Kit according to the manufacturer's instructions (Qiagen Ltd.; Crawley, UK).

2.7.1.2 Isolation of genomic DNA from plants

For plant DNA extraction approximately 50 mg leaf tissue was harvested and frozen in liquid nitrogen. Samples were pulverised while still frozen using a mixer mill (Retsch; Haan, Germany). The frozen powder was extracted at 4°C in DNA extraction buffer (200 mM Tris-HCl pH 9, 400 mM LiCl, 25 mM EDTA, 1% SDS (w/v)). Samples were centrifuged at 20,000 *g* for 5 min to pellet the debris. One volume isopropanol was added to the supernatant and mixed by inversion. DNA was collected by centrifugation at 20,000 *g* for 10 min. The pellet was washed with 500 µl of 70% (v/v) ethanol, followed by centrifugation at 20,000 *g* for 2 min. The pellet was air dried and dissolved in 50 µl ddH_2O.

2.7.2 Polymerase chain reaction (PCR)

PCR was performed using Taq DNA polymerase (Qiagen, catalogue number 201203). Reactions were prepared in a final volume of 20 µl: 50-100 ng DNA template, 2.5 U polymerase, polymerase reaction buffer and 0.2 µM of each primer and 0.2 mM dNTPs. All PCR amplifications were conducted in a DYAD Thermal Cycler (BioRad; Hemel Hempstead, UK). An initial denaturation step of 94°C for 3 min was followed by 25 to 35 cycles of 94°C for 30 s; 50-60°C for 30 s and 72°C for 1 min per kb of target DNA and a final elongation step of 72°C for 10 min.

2.7.3 Genotyping of mutants

To select homozygous mutants and wild-type segregants as controls, genomic DNA was isolated (section 2.7.1.2). PCR on genomic DNA was performed using gene-specific primers as listed in Section 2.6. The primers used amplified PCR fragments of the sizes listed in Table 2.7:

Mutant Name	T-DNA insertion line	Wild-type band size (bp)	T-DNA insertion approximate band size (bp)
arc3-2	SALK_057144	967	684
arc3-3	SALK_012892	1249	686
arc5-2	SAIL_71_D11	1145	601
arc6-5	SAIL_693_G04	1018	466
arc10-2	SALK_073878	909	448
isa1	SALK_042704	999	764
ss4	SALK_096130	1037	767

Table 2.7: Expected PCR product size when genotyping T-DNA insertion mutants.

On first use of the primers, PCR products were excised from the agarose gel and sequenced (section 2.7.5) to confirm amplification of the correct fragment was occurring and to check the location of the T-DNA insertion. Wild-type plants contained no PCR product when amplifying the T-DNA insertion region, and no wild-type PCR product was detected using DNA from homozygous mutants.

2.7.4 Agarose gel electrophoresis

PCR products were mixed with 5 x loading dye (50% (v/v) glycerol, 5 mM EDTA, 0.04% (w/v) bromophenol blue, 0.04% (w/v) xylene cyanol FF, 10 mM NaCl). PCR products were loaded onto a 1% agarose gel, prepared using 1 x TAE buffer (40 mM Tris, 20 mM acetic acid, 1 mM EDTA, pH 8.0) supplemented with 0.01% (v/v) ethidium bromide. DNA was detected by fluorescence of the bound ethidium bromide when exposed to ultraviolet (UV) light from a transilluminator and photographed using a Gel Doc 1000 system (Bio-Rad).

2.7.5 DNA sequencing

PCR products were excised from agarose gels and DNA extracted using the QIAquick® Gel Extraction kit (Qiagen; Catalogue Number 28704) according to the manufacturer's instructions. Cycle sequencing reactions were carried out using the ABI prism BigDye terminator kit v3.1 (Applied Biosystems, Foster City, CA, USA) according to the

manufacturers' instructions. A final volume of 10 µl contained about 100 ng of template DNA, 1.6 µl of 2 µM sequencing primer, 1.5 µl Big Dye sequencing buffer and 1 µl ABI BigDye version 3.1 sequencing mix. Samples were run as described in Table 2.8. Analysis of the reaction products was performed by the John Innes Centre Genome Laboratory on AbiPrism 3730XL and 3730 capillary sequencers (Applied Biosystems). DNA sequences were analysed using ContigExpress and aligned using the AlignX function of the Vector NTI Advance Suite 11 (Invitrogen; http://www.invitrogen.com).

Step	**Temperature**	**Time**
1	96^{o}C	10 s
2	55^{o}C	5 s
3	60^{o}C	4 min
4	Repeat steps 1 to 3, 25 times	
5	Cool to 8^{o}C	

Table 2.8: Sequencing reaction

2.7.6 RNA extraction

For plant RNA extraction approximately 50 mg leaf tissue was harvested and frozen in liquid nitrogen. Samples were pulverised while still frozen using a mixer mill (Retsch). RNA was isolated using the RNeasy™ Plant Mini kit (Qiagen) according to the manufacturer's instructions. The RNA concentration and quality was determined by measuring absorbance at 260 nm and 280 nm using a NanoDrop ND-1000 spectrophotometer (NanoDrop Technologies/ Thermo Fisher Scientific Inc. http://www.nanodrop.com/).

2.7.7 cDNA synthesis

Following RNA isolation, traces of DNA were removed by digestion with RQ1-DNAse (Promega; http://www.promega.com/uk/) using the following reaction mix:

Amount	Ingredient
x µl	1 µg RNA
1 µl	10x RQ1 DNase buffer
1 µl	RQ1 DNAse (1 u μl^{-1})
0.5 µl	RNAsin Plus RNase inhibitor (Promega)
x µl	DEPC treated H_2O to a final volume of 10 µl

The mixture was incubated at 37ºC for no longer than 15 min. Samples were placed on ice and 1 µl of 25 mM EDTA was added. To inactivate the DNase, samples were incubated at 65ºC for 10 min and then placed on ice.

The DNase treated samples were used to synthesise cDNA. Two µl of oligo(dT)16-18 primer (50 ng/µl) were added and samples were incubated for 5 min at 70ºC, then placed back on ice. The SuperScript III Reverse Transcriptase (RTase) kit (Invitrogen) was used for reverse transcription of RNA. The following was added to each sample:

Amount	Ingredient
4 µl	5x First Strand Buffer
1 µl	dNTP mix (10 mM each)
1 µl	DTT (100 mM)
1 µl	SuperScript III RTase blend

Samples were mixed by inverting, pulse centrifuged and incubated at 47 ºC for 60 min followed by heat inactivation of the RTase enzyme at 75ºC for 10 min. The first strand cDNA was then used for semi-quantitative reverse transcription polymerase chain reaction (semi-quantitative RT PCR).

2.7.8 Semi-quantitative reverse transcription polymerase chain reaction (RT-PCR)

Semi-quantitative RT-PCR was used to assess the transcript levels of the *SS4* gene. RNA was extracted from plants (section 2.7.6), converted to cDNA (section 2.7.7) and then amplified using the standard PCR cycle (section 2.7.2), except that 21, 25, 28 or 35 amplification cycles were used. Two sets of primers were used to amplify different

regions of the SS4 cDNA to ensure a robust result (section 2.6). Primers SALK_096130_LP and SALK_096130_RP amplified a 645 bp region of cDNA, 1257 bp from the start codon. Primers SS4_P5_LP and SS4_P6_RP amplified a 629 bp region of cDNA, 2495 bp from the start codon. Primers that amplified a region of the tubulin gene were used as a control to ensure equal cDNA concentrations and gel loading. PCR products were run on an agarose gel (section 2.7.4) and relative expression levels analysed on an image of the gel using Adobe Photoshop (section 2.15).

2.7.9 Protoplast isolation

Arabidopsis leaf protoplasts were isolated from 4-week-old plants. Leaf tissue was sliced with a sharp razor and incubated in protoplast buffer (400 mM sorbitol, 20 mM MES-KOH (pH 5.2), 0.5 mM $CaCl_2$) for 30 min with illumination, and then incubated for a further 3 h in protoplast buffer containing 1% (w/v) Cellulase R-10 and 0.25% (w/v) Macerozyme R-10 (Yakult, Tokyo, Japan). Protoplasts were released by gentle agitation with a glass rod. Note: Enzymes were desalted before use by applying them to a PD-10 desalting column containing Sephadex G-25 medium (GE Healthcare; http://www.gelifesciences.com) and eluting in a small volume of protoplast buffer.

2.7.10 Chloroplast isolation

Intact chloroplasts were isolated using the Sigma Chloroplast Isolation Kit (CP-ISO http://www.sigmaaldrich.com) according to manufacturer's guidelines. All steps performed at 4^{o}C. For mechanical isolation of chloroplasts approximately 4 g of leaves were harvested, washed in deionized water and cut into approximately 1 cm^2 pieces. The pieces were macerated in a blender (Multi-moulinette, Moulinex, UK; http://www.moulinex.co.uk/) with 6 ml g^{-1} of Chloroplast Isolation Buffer (CIB) plus 0.1% (w/v) BSA using four bursts of 1 s each. The macerated leaves were filtered through a 100 µm mesh and whole cell and cell wall material removed from the filtrate by centrifugation at 200 *g* for 3 min. The supernatant was transferred to fresh tubes and centrifuged at 1000 *g* for 7 min. The supernatant was discarded and the pellet gently resuspended using a soft paintbrush in 2 ml CIB with 0.1% (w/v) BSA. The resuspended solution was loaded on top of a Percoll gradient. The Percoll gradient

consisted of two steps: Step 1 (volume 1.25 ml) 80% Percoll solution: 20% CIB, 0.1% (w/v) BSA; step 2 (volume 2.5 ml) 40% Percoll: 60% CIB, 0.1% (w/v) BSA. The Percoll gradient was centrifuged at 4°C for 15 min at 1500 *g* to separate intact from ruptured chloroplasts. After centrifugation chloroplasts in the band between the two Percoll layers were collected using a Pasteur pipette and the total volume made up to 200 µl with CIB.

Chloroplast intactness was assayed by measuring NADP-dependent glyceraldehyde-3-phosphate (GAP) dehydrogenase activity before and after rupturing the chloroplasts by osmotic shock (Batz *et al.,* 1995). Isolated chloroplasts were stored on ice and used immediately.

2.7.11 Preparation of protein extracts for SDS-PAGE

Approximately 200 mg leaf tissue was harvested at the end of the light period, weighed and immediately frozen in liquid N_2. Frozen samples were powdered, then extracted at 4°C in protein loading buffer (6 ml of protein loading buffer g^{-1} fresh $weight^{-1}$). The protein loading buffer consisted of 0.125 M Tris (pH 6.8); 4% (w/v) SDS; 20% (v/v) Glycerol (Analar grade); 0.2 M DTT and 1% (v/v) Protease inhibitor cocktail (SIGMA). Extracts were centrifuged at 20,000 *g* for 10 min at 4°C. The supernatant was removed and stored at -20°C.

2.7.12 Western blot analysis

A rabbit antiserum was raised previously by Chris Hylton (JIC) against a 14-amino-acid fragment of SS4 protein corresponding to a region that displays no similarity with all other SS isoforms (from Asp149 to Thr162).

Equal quantities of leaf extract on a fresh weight basis (see section 2.7.11) were loaded onto a 7.5% SDS-polyacrylamide gel. Proteins were transferred from the SDS-polyacrylamide gel to a nitrocellulose membrane by Western blotting in a Trans-Blot SD transfer cell (Bio-Rad) according to the manufacturer's instructions. Membranes were incubated with the rabbit anti-SS4 serum at a dilution of 1:300 followed by alkaline phosphatase-conjugated goat anti-rabbit antiserum (Sigma) according to

Denyer *et al.* (1993). Alkaline phosphatase activity and hence the SS4 protein was detected using the SIGMAFAST™ BCIP®/NBT reagent (Sigma).

To check the equal loading of gels used for western blotting a gel was run at the same time, using the same extracts as used for the western blot and stained with Coomassie® InstantBlue™ stain (Expedeon; http://www.expedeon.com).

2.7.13 Gateway Cloning

The Gateway Technology was used as an efficient way to move DNA sequences into multiple vector systems for functional analysis and protein expression (Hartley *et al.,* 2000).

2.7.13.1 A-tailing of PCR products

Cloning of a PCR product into the GATEWAY-ready pCR8/GW/TOPO TA plasmid (Invitrogen) requires 3' A-overhangs at the end of the DNA double strand. To allow cloning of amplified PCR products into pCR8/GW/TOPO an A-tailing reaction was performed using the following reaction mix:

Final concentration	**Ingredient**
-	5 µl PCR product
1X	5X GoTaq Flexi Buffer (Promega)
1 mM	Deoxyadenosinephosphate (dATPs)
1 mM	$MgCl_2$
0.1 U	GoTaq Flexi polymerase 5 U μl^{-1} (Promega)
	ddH_2O to 10 µl

Samples were incubated for 10 min at 72°C then run on and purified from an agarose gel (Section 2.7.4 and 2.7.5).

2.7.13.2 Cloning of PCR fragments into pCR8/GW/TOTO TA

Cloning of PCR fragments into pCR8/GW/TOPO TA (Invitrogen) was performed using the following reaction mix:

Amount	**Ingredient**
1 to 2 µl	PCR product /A-tailing product
0.5 µl	Salt Solution (1.2 M NaCl, 60 mM $MgCl_2$)
0.5 µl	Vector (pCR8/GW/TOPO TA)
x µl	ddH_2O to 4 µl

Samples were incubated for between 10 min and 1 h at room temperature and transformed into chemically competent Top10 *E. coli* cells (Section 2.9.1). Successful cloning was confirmed by colony-PCR using sequence specific primers or the M13Fwd and Rev primers (Section 2.6 and 2.7.2).

2.7.13.3 LR reaction

During the LR reaction the clonase enzyme LR Clonase II (Invitrogen) recombines and thereby exchanges the sequences within the attL and attR sites which flank the gene in the pCR8 entry plasmid (Section 2.7.13.2) and the GATEWAY cassette in the destination plasmid (Section 2.5) respectively.

To perform the LR reaction, 50 to 150 ng of pCR8 plasmid containing the fragment of interest was mixed with the same amount of destination vector (pOpoff2Hyg: section 2.5). TE buffer (10 mM Tris-HCl, 0.1 mM EDTA, pH 8.0) was added to make a total volume of 4.5 µl and then 0.5 µl of LR Clonase II was added to the LR reaction. Samples were mixed thoroughly and left at room temperature for 4 h to 16 h. To terminate the LR reaction, 1 µl of proteinase K solution (20 mg ml^{-1}, 20 units mg^{-1}, Invitrogen) was added to each sample and samples incubated at 37°C for 10 min. Subsequently, *E. coli* Top10 cells were transformed with 2.5 µl of each LR reaction (Section 2.9.1) and successful recombination was confirmed by colony-PCR (Section 2.7.2).

2.8 Measurement of starch content

2.8.1 Enzymes and Chemicals

Unless otherwise stated, enzymes for biochemistry methods were from Roche (http://www.roche-applied-science.com), SIGMA (http://www.sigmaaldrich.com), Megazyme (http://secure.megazyme.com/Homepage.aspx) or BDH (https://www.vwrsp.com/).

2.8.2 Extraction of starch from *Arabidopsis* leaves

To determine the starch content in Arabidopsis leaves, starch was separated from other material using the perchloric acid method. Approximately 50 – 150 mg leaf tissue was harvested in 2 ml tubes containing a steel ball (4 mm diameter) and rapidly frozen in liquid nitrogen. Samples were pulverised while still frozen using a mixer mill (Retsch) at 30 strokes per s for 1 min. The frozen powder was resuspended in 1 ml 0.7 M perchloric acid ($HClO_4$) at 4°C and mixed vigorously. The extract was then centrifuged at 3000 *g* for 10 min at 4°C to separate insoluble from soluble glucans. The term 'insoluble glucans' includes starch and other glucans pelleted by centrifugation at 3000 *g*, while 'soluble glucans' include phytoglycogen and smaller oligosaccharides.

The supernatant was transferred to clean tubes and one-half adjusted to pH 7 (for sugar measurements) and the other half to pH 5 (for phytoglycogen measurements), with ice-cold 2 M KOH, 0.4 M MES, 0.4 M KCl. Samples were centrifuged at 3000 *g* for 10 min at 4°C and the supernatant transferred to a clean tube. Phytoglycogen was precipitated overnight at 4°C by the addition of 600 µl 75% (v/v) methanol (containing 1% (w/v) KCl) to 200 µl of the supernatant adjusted to pH 5. The precipitate was collected by centrifugation, resuspended in 1 ml of ddH_2O and stored at -20°C until required for enzymatic digestion of phytoglycogen. The neutralised supernatant was stored at -20°C until required for assaying glucose, fructose and sucrose.

The starch-containing pellet was washed four times in 80% (v/v) ethanol (until the supernatant was colourless) to remove remaining sugars. After the final wash, the pellet was dried at room temperature for 20 min and resuspended in 1 ml ddH_2O. Samples

were either used immediately for enzymatic digestion of starch (Section 2.8.3) or stored at -20°C.

When measurements of phytoglycogen or sugars were not required, the original method described above was modified to allow high throughput sample preparation, as described in Graf (2009).

2.8.3 Enzymatic digestion of starch and phytoglycogen

To measure the starch and phytoglycogen content, samples were first solubilised by boiling for 15 min in sealed tubes, then 300 µl of each sample were transferred to two fresh tubes containing 290 µl sodium acetate (0.2 M, pH 4.8). To one tube 10 µl of ddH_2O was added and to the second tube 10 µl of a 9:1 (v/v) mixture of amyloglucosidase (10 µg μl^{-1}; catalogue number: 10102857001; Roche, Basel, Switzerland) and α-amylase (1 U μl^{-1}; catalogue number: E-ANAAM; Megazyme, Bray, Ireland) was added per sample. All tubes were mixed and incubated over night at 37°C. Samples were then used for glucose measurement or stored at -20°C. To measure sucrose, an aliquot of the neutralised supernatant (section 2.8.2) was incubated for two hours at 37°C with β-fructosidase, and then assayed for glucose.

2.8.4 Glucose Assay

Starch, sucrose, glucose and fructose were assayed enzymatically according to Chia *et al*. (2004), Smith and Zeeman (2006) and Hargreaves and ap Rees (1988). Prior to the assay all samples were mixed and then centrifuged at 4500 g. Production of NADH via the enzyme coupling system was measured at 25°C on a plate reader at 340 nm (SPECTRAmax 340PC, Molecular Devices; http://www.moleculardevices.com/home.html).

2.9 Transformation of living cells

2.9.1 Transformation of *Escherichia coli*

In each *E. coli* transformation, 20 µl of frozen competent cells were mixed with 3 µl of LR recombination reaction (Section 2.7.13.3) or 4 µl of plasmid preparation (Section 2.7.13.2). The mix was incubated on ice for 10 min. The cells were then heat shocked at 42°C for 30 to 45 s and chilled on ice for 2 min. One ml of SOC medium (Table 2.2) was added and the cells were incubated in a shaker at 37°C and 200 rpm for 1 h. Cells were collected by centrifugation at 5500 *g* for 5 min. The supernatant was removed and the pellet was resuspended in 100 µl of LB broth. Cells were then plated on LB agar medium containing the appropriate antibiotics and the plates were incubated upside down at 37°C for about 16 h. Bacterial colonies were screened using colony PCR (Section 2.7.2) to check for the correct insert. Desired colonies were re-plated on LB agar medium containing the appropriate antibiotics and the plates were incubated upside down at 37°C for about 16 h. Desired colonies were transferred to 15 ml LB liquid medium containing the appropriate antibiotics and incubated in a shaker at 37°C and 200 rpm for 16 h. Plasmid DNA was isolated from the bacterial culture using the QIAprep Spin Miniprep Kit (Section 2.7.1.1)

2.9.2 Transformation of *Agrobacterium*

In order to generate freeze/ thaw competent cells *A. tumefaciens* strain GV3101 was grown in 200 ml LB medium (Table 2.2) to an OD_{600} of 0.8 to 1.0. Cells were collected by centrifugation and washed in subsequent steps with 200 ml and 2 ml of ice-cold $CaCl_2$. Fifteen µl of competent cells were thawed on ice and 5 µl of plasmid DNA isolated with the QIAprep Spin Miniprep Kit (Section 2.7.1.1) was added and mixed carefully. Cells were incubated on ice for 5 min, and then frozen in liquid nitrogen for 5 min, before heating at 37°C for 5 min without agitation. One ml of LB medium was added to the cells and they were incubated in a shaker at 28°C and 200 rpm for at least 2 h. The cells were collected by centrifugation at 5500 g for 3 to 5 min. The pelleted cells were resuspended in 100 µl of LB broth and plated on LB agar medium containing the appropriate antibiotics. Plates were then incubated upside down at 28°C for 48 h, at which point colonies appeared. Colonies were screened using colony PCR (Section 2.7.2) to check for the correct insert. Desired colonies were re-plated on LB agar

medium containing the appropriate antibiotics and the plates were incubated upside down at 37°C for about 16 h. Plates were stored at 4°C until required.

2.10 *Agrobacterium* mediated transformation of *Arabidopsis* by floral dipping

Four or five *Arabidopsis* plants were planted per 64 cm^2 pot and grown in a CER until they flowered. The primary inflorescence was removed and plants grown for a further 8 to 10 days until most secondary inflorescences were 3 to 15 cm tall. *Agrobacterium* strains transformed with the appropriate plasmid (section 2.9.2) were grown in 200 ml LB medium containing the appropriate antibiotics at 28ºC shaking at 250 rpm to an OD_{600} of 1.0 to 1.4. Cells were pelleted by centrifugation at 5500 *g* for 10 min at 25°C and then resuspended in 200 ml of infiltration medium (5% (w/v) sucrose, 0.05% Silwet® L-77 (GE silicones; Friendly, WV, USA) in dH_2O (Clough and Bent 1998)). Plants were inverted into beakers containing the suspension such that all aboveground tissues were submerged, then agitated gently for 1 to 2 min. The infiltrated plants were placed in trays covered with clear plastic, and kept in low light or darkness overnight before being returned to the glasshouse and allowed to set seed.

2.11 Cross pollination of *Arabidopsis* plants

Young flower buds in which stigmas were still fully enclosed within the sepals from the primary or secondary inflorescences were selected as pollen acceptors. Using fine point forceps the apical meristem and all unwanted, surrounding buds and siliques were removed from the inflorescence. Flowers selected to receive the pollen were emasculated by removing the sepals, petals and stamens. The emasculated flowers were left for 1 day to ensure the stigma had not been damaged during emasculation or had not already been self pollinated. Anthers from mature flowers of the donor plant were used to very gently dust pollen onto the acceptor stigma. The pollinated siliques were left to mature and any new shoots that emerged were removed from the plant. Siliques were harvested shortly before dehiscence.

2.12 Determination of luciferase activity

An *Arabidopsis* starvation reporter line (*pAt1g10070:LUC)* produced by Graf *et al.* (2009; 2010) containing a construct consisting of a fusion of the low-sugar responsive promoter pAt1g10070 and the luciferase (*LUC*) gene was used to assess the level of carbon starvation in mutant plants harbouring the starvation reporter.

For all luciferase experiments *Arabidopsis* plants harbouring the low-sugar reporter were grown on soil, 40- or 60-cell trays (21 x 35 cm). Approximately 12 h before the first bioluminescence image was to be taken, plants were pre-treated by spraying with luciferin solution (1 mM luciferin (Promega), 0.02% (v/v) TritonX-100). For each treatment, approximately 10 ml of luciferin solution was sprayed onto each tray. Plants were sprayed again with the luciferin solution 1 h before transfer to the NightOwl CCD camera system (Berthold Technologies; http://www.berthold.com). Bioluminescence was assayed using the following settings: medium resolution, 1 min exposure time, pixel binning 4x4, single frame accumulation. For time-course experiments the plants remained in the machine for the entirety of the experiment and imaging took place every 15-20 min. Bioluminescence emission was quantified using the WinLight software (Perkin-Elmer; http://www.perkinelmer.co.uk/) according to manufacturer's instructions.

2.13 Curvature and growth studies

For gravitropic curvature and root growth studies, seedlings were grown under sterile conditions in square polystyrene Petri dishes (100 x 15mm) on 0.7% (w/v) agar containing the nutrients described in Haughn and Somerville (1986) with 1% (w/v) sucrose added. Seeds were surfaced sterilized and sown on the agar medium in horizontal rows. The seeds were incubated on the medium for 3 d in darkness at 4^{o}C. Plates were transferred to 22^{o}C under continuous illumination. The dishes were placed on their edge so that the surface of the agar was vertical, and for future reference and analysis a vertical line was drawn on the dish. Seedlings were used when roots were 5-10 mm long i.e. approximately 4 days after germination.

To quantify the extent of variation in root growth direction of vertically grown plants, the angle between the root tips and the vertical line drawn on the plates was measured

from digital photographs in 175 plants for each genotype. Angles were measured at the root tips (in this study, the final 2.5 mm of the root) using the protractor function in Image J imaging software (http://rsbweb.nih.gov/ij/).

2.14 Phenotypic analysis

2.14.1 Purification of starch granules

Plants were harvested at the end of the light period, frozen in liquid N_2, and starch extracted using a pestle and mortar in four volumes of isolation buffer: 100 mM 3-(*N*-morpholino) propanesulphonic acid (MOPS), pH 7.2, 5 mM EDTA, 2.63 mM Na-metabisulphite, 0.05% (v/v) Triton X-100 and 5 mM DTT. The homogenate was filtered through two layers of Miracloth. The insoluble material, including starch, was pelleted by centrifugation at 20000 *g* for 10 min at 4°C. The pellet was re-suspended in 5 ml isolation buffer and applied to the top of 20 ml Percoll (90% Percoll: 10% isolation buffer) in a 30 ml corex tube. Starch was pelleted by centrifugation at 5000 *g* for 10 min at 4°C. The pellet was re-suspended in 2 ml isolation buffer and applied to the top of 10 ml Percoll (90% Percoll: 10% isolation buffer) in a 15 ml corex tube. Starch was pelleted by centrifugation at 5000 *g* for 10 min at 4°C. The pellet was washed 3 times with water (10 min at 4°C and 5000 *g*) to remove residual isolation buffer. The starch pellet was re-suspended in 1.5 ml 100% ice cold acetone and centrifuged for 5 min 20000 *g* at 4°C. Starch was finally air dried for 4 h and stored at -20°C.

To crack granules for digestion and microscopy a small amount of starch was placed in a liquid N_2 cooled mortar and ground briefly. The starch was suspended in 1 ml dH_2O and frozen by adding additional liquid N_2 to the mortar. The frozen starch solution was ground until the water began to thaw and a slurry formed. The starch solution was allowed to thaw completely in the mortar and transferred to a 2 ml Eppendorf tube. Starch was pelleted by centrifugation at 20000 *g* for 10 min at 4°C then air dried for 4 h and stored at -20°C.

2.14.2 Light microscopy and Transmission Electron Microscopy (TEM)

For TEM and light microscopy, unless otherwise stated leaf samples of 25 day old plants grown under a 12-h light/12-h dark regime were collected after 9 h light. Small pieces (2 mm^2) of leaves were cut with a razor blade from the middle of the leaf (omitting the main vein) and immediately fixed in 2.5% (v/v) glutaraldehyde in 0.05 M Na cacodylate, pH 7.3. Samples were vacuum infiltrated and left overnight in fresh fixative at 4^oC. The samples were subsequently washed in 0.05 M Na cacodylate and post-fixed with 1% (v/w) osmium tetroxide in 0.05 M Na cacodylate for 1 h at 4^oC. Samples were then dehydrated in an ethanol series and infiltrated with LR White resin by successive changes of resin/ethanol mixes over 3 days at room temperature, with the last infiltration overnight in 100% fresh LR White resin. The resin was polymerised at 60^oC for 16 h. Ultrathin sections (60 nm) were prepared with a diamond knife (Leica KMR2, Leica; http://www.leica-microsystems.com) on an UC6 Leica ultramicrotome, collected on Formvar-coated 200 μM mesh nickel grids and examined under 200 kV using a FEI Tecnai G2 20 Twin transmission electron microscope (Philips, Eindhoven, The Netherlands). All embedding and ultrathin sectioning (with the exception of the initial fixative and vacuum infiltration step) was performed by Sue Bunnewell (JIC). TEM was performed by Sue Bunnewell or Kim Findlay (JIC).

For light microscopy, 0.9 µm sections of material embedded in LR White resin were prepared on a Reichert-Jung Ultracut E ultramicrotome (Leica) and dried onto glass microscope slides. Slides were stained with iodine solution [50% (v/v) Lugol's solution] for 5 min and rinsed with dH_2O immediately prior to observation. All light microscopy was performed on a Zeiss Axiophot light microscope (Carl Zeiss; www.zeiss.co.uk) and images captured using a Pixera Penguin 600 CL CCD (charge couple device) digital camera (Pixera UK; http://www.pixera.com).

2.14.3 Scanning Electron Microscopy (SEM)

Dry starch samples, isolated as described in section 2.14.1, were brushed onto the surface of double-sided, carbonated sticky stills (Leit-tabs) attached to SEM stubs. The stills and stubs were supplied by Agar Scientific Ltd. (Cambridge, UK). Mounted starch samples were sputter coated with gold for 75 s at 10 mA in an argon atmosphere, using

a high resolution sputter coater (Agar Scientific; http://www.agarscientific.com). The coated stubs were transferred to a FEI XL30 FEG SEM (Philips) and imaged at 3 kV.

2.14.4 Starch Granule measurements

Intact or cracked starch granules (section 2.14.1) were photographed using a SEM according to section 2.14.3. Measurements of granule radii were taken using Image J imaging software (http://rsbweb.nih.gov/ij/). The scale for granule measurements was set in µm.

Equations to calculate the radius and subsequently to derive the granule volume from granule radius were developed with the help of Dr. Scott Grandison (JIC and University of East Anglia). Isolated starch granules have a tendency to clump together or lie on top of one another and as a result when photographed (section 2.14.3) it is rare that a whole granule is visible. To overcome this problem an Excel spreadsheet was created to calculate the radius of a starch granule from three points placed manually around the edge of the granule in Image J, as illustrated in Figure 2.1A. The three points act as x, y coordinates, through which theoretical lines can be drawn. The points at which these three lines intercept one another is used to calculate the granule radius:

(A) $[(x1 - x2)^2 + (y1 - y2)^2] \times [(x1 - x3)^2 + (y1 - y3)^2] \times [(x2 - x3)^2 + (y2 - y3)^2]$

(B) $[(-y1 + y2) \times (x2 + x3) \times (y1 - y3) + x1 \times (-y2 + y3)]^2$

(C) $0.5 \times (\text{equation A} \div \text{equation B})^{0.5}$

The answer in equation C is multiplied by the scale calculated for each individual photo, to give the radius in µm.

To calculate the relationship between granule radius and thickness, photographs of cracked granules with exposed cross-sections were taken using a SEM and measurements of the thickness and radius taken. These measurements were plotted on a graph to calculate the relationship (the slope of the line) between the granule diameter and granule thickness (Figure 2.1B). The equation for the line was as follows:

(D) $y = 0.3278x + 0.4347$

Where 0.3278 is the gradient of the line and 0.4347 is the y axis intercept of the line. The volume of each starch granule could then be calculated using the following equation:

(E) $^4/_3 \pi r^3$ x 0.3278

The mass of an individual starch granule was calculated by converting the volume from μm^3 to cm^3 ($\div$ 1,000,000,000,000) and then multiplying the calculated volume by the known density of starch, 1.5 g/cm^3 (Dengate *et al.,* 1978; Munck *et al.,* 1988).

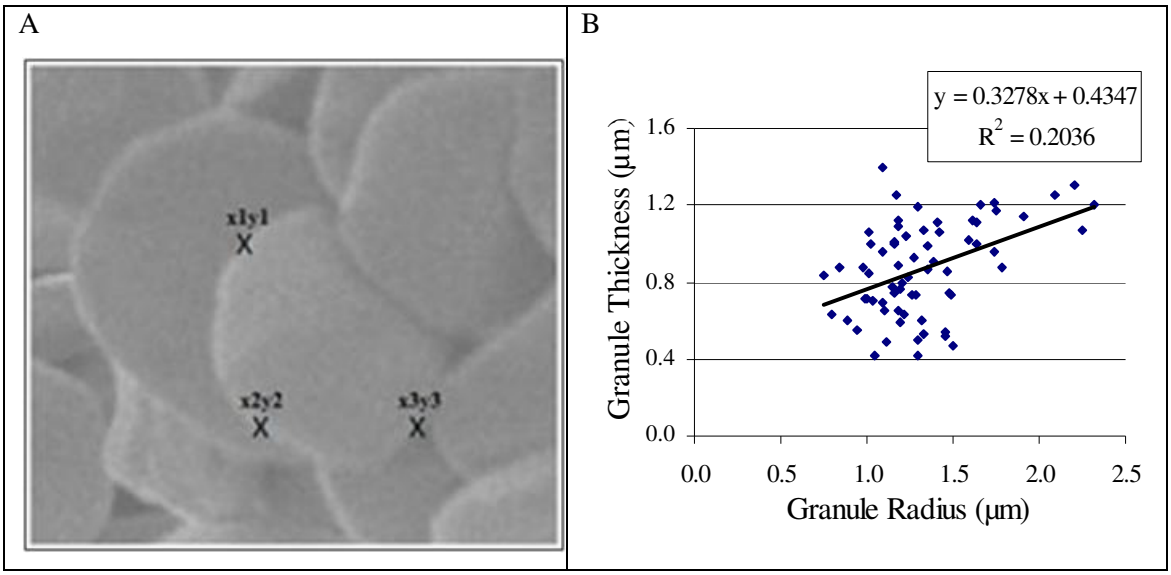

Figure 2.1: (A) Diagram to illustrate how points placed around the edge of an SEM image of a starch granule using Image J, act as x, y coordinates. 'X' marks where the point is placed, while 'x1y1' represent the coordinates used in equations A and B. (B) Measurements of granule radius and thickness from SEM photographs of cracked granules with exposed cross-sections. These measurements were plotted on a graph to calculate the relationship (the slope of the line) between the granule diameter and granule thickness.

2.14.5 Haemocytometer measurements

A double celled modified Fuchs-Rosenthal haemocytometer (Agar Scientific) was used according to the guidelines in Kouri *et al.* (2003).

2.14.6 Iodine staining of rosettes and leaves

Individual leaves or whole rosettes were harvested into 80% (v/v) ethanol, then heated at 80^{o}C until they were fully decolourised. The ethanol was removed and replaced with an iodine/ potassium iodide solution (50% (v/v) dH_2O: Lugol's solution, Sigma Aldrich) for 5 min. Leaves and rosettes were rinsed with dH_2O to remove excess stain and photographed.

2.14.7 Focused-Ion-Beam Scanning Electron Microscopy (FIB-SEM)

Leaf samples of 25-day-old plants cultured under a 12-h light/12-h dark regime were collected after 12 h light and 12 h dark. Leaf number 6 was selected for mature leaf samples and leaves 14, 15 and 16 for immature leaf samples, where leaf number 1 was the first true leaf formed and the oldest leaf of the rosette. Samples were fixed and embedded as for TEM (section 2.14.2). All FIB-SEM was performed by Ken Png (NanoVision Centre, Department of Materials, Queen Mary, University of London, UK) on an FEI Quanta 3D Environmental SEM (Philips). This work was funded by the Engineering and Physical Sciences Research Council (EPSRC).

2.15 Software Tools - Band quantification

Images of western blots and agarose gels were analysed in Adobe Photoshop. The images were converted to greyscale and the light and dark pixels were inverted. Bands of interest were individually selected using the Rectangular Marquee tool and the mean pixel intensity value gathered from the histogram information. Values from a minimum of 3 separate bands were averaged for each reading.

2.16 Statistical analysis of significance

For statistical analyses I used the software package GenStat – Tenth Edition (VSN international). The unpaired two sample Student's t-test and Analysis of Variance (ANOVA) were used throughout this thesis to calculate the significance of differences between data sets. A p-value of 0.05 or less indicated statistically significant differences.

3 The relationship between starch granules and chloroplasts in the *Arabidopsis* leaf

3.1 Introduction

3.1.1 Aim

The wide range of knowledge and molecular tools available for *Arabidopsis* makes it an ideal species for the study of starch synthesis. However, a major obstacle to the study of starch granules in leaves in general is their very small size and the difficulty of observing them in intact tissues. As a result almost nothing is known about the extent and nature of developmental, spatial and environmentally induced variation in starch granule size, shape and number in leaves. It is not known whether diurnal (day-night cycle) and environmentally induced (e.g. light level or day length) variations in starch content involve changes in granule number, or simply changes in the size of a fairly constant number of granules. Changes in granule number would require frequent de novo initiations of new granules, and would alter the surface/volume relationship of starch in the chloroplast. Both the number of granules initiated and the surface to volume ratio are potentially important to the diurnal control of starch turnover.

As a leaf grows and expands, cell size increases and the number of chloroplasts per cell increases. For example, measurements of spinach leaves showed a five-fold increase in the number of chloroplasts per cell in palisade and mesophyll cells, over a ten day growth period (Possingham and Saurer 1969) and measurements of *Arabidopsis* mesophyll cells revealed a greater than six-fold increase in the number of chloroplasts per cell between young and mature leaves (Stettler *et al.,* 2009), which means that several rounds of chloroplast division have occurred. In wild-type *Arabidopsis* (ecotype Landsberg *erecta* (L*er*)) meristematic mesophyll cells (young post-mitotic cells) contain around fifteen proplastids, destined to become chloroplasts, while fully expanded mature mesophyll cells contain around 120 chloroplasts, therefore three rounds of division must take place during cell maturation (Marrison *et al.,* 1999). It is not known if there is conservation in starch granule number per chloroplast during leaf development and whether as a result the number of starch granules per chloroplast is the same in immature and mature leaves. Conservation in starch granule number per

chloroplast through rounds of chloroplast division may suggest the existence of a mechanism that counts the number of granules, perhaps monitoring the number of granules per unit stromal volume. Starch granules would then be equally divided between daughter chloroplasts, or new granules would be initiated to achieve the parental complement in daughter chloroplasts after division.

In this chapter I describe the variation in granule size and number in chloroplasts of *Arabidopsis* leaves. As well as providing new scientific knowledge, this information is necessary as a background for other studies on starch granule initiation. First I discuss existing methods for observing and counting starch granules and provide an overview of the present state of knowledge on granule number variation. I then present my results on the development of methods to provide reproducible measurements of starch granule numbers in chloroplasts, and the application of these methods to discover how transitory starch granule numbers vary during the day-night cycle, at different developmental stages, and when plants are grown under different environmental conditions. Finally I discuss my results and describe how they compare with and add to our existing knowledge of leaf starch metabolism.

3.1.2 Granule number and size variation in leaves

There is limited information about how the wild-type plant responds in terms of granule morphology or number to changes in leaf starch content. As discussed in Chapter 1 (section 1.4) an increase in starch content does not always result in an increase in starch granule number (Sokolov *et al.,* 2006; Zeeman *et al.,* 2002b). Grange *et al.* (1989b) analysed SEM images of isolated starch granules from wild-type mature pepper leaves grown under a variety of environmental conditions that resulted in a variety of starch contents. It is important to note that these authors made no observations or measurements on leaf sections and all results were derived from equations based on measurements of leaf starch content and granule size. Grange *et al.* (1989b) found that as expected, the mean diameter of starch granules was positively correlated to daylength and leaf starch content, but interestingly the increase in granule diameter as the day proceeded was not accompanied by an increase in granule number on a leaf area basis. Initially as starch content increased the number of granules also increased, but as the starch content increased further the number of granules plateaued. This implies that at

the beginning of the day either new granules are initiated until the maximum number of granules is reached, or tiny granules, too small to detect at the end of the night, grow to detectable sizes with no new initiations. Grange *et al.* (1989b) also found that under long day growing conditions when there are slower rates of starch accumulation, there were fewer and larger granules than when starch accumulates faster during short days. All this led Grange *et al.* (1989b) to speculate that the number of starch granule initiations and therefore the number of granules in a given leaf area is controlled by the rate of starch synthesis. Nothing is known about how the starch granules vary in wild-type *Arabidopsis* plants over the diurnal cycle and with day length.

Growing plants under elevated CO_2 results in increased starch accumulation (Pritchard *et al.,* 1997; Teng *et al.,* 2009; Tipping and Murray 1999). Evidence from sections through *Arabidopsis* leaves and *Pinus palustris* (Longleaf Pine) needles suggests that the enhanced starch content under elevated CO_2 is in the form of more and larger granules, i.e. both granule number and granule size are increased (Pritchard *et al.,* 1997; Teng *et al.,* 2009). Sections through *P. palustris* seedlings grown in elevated CO_2 showed chloroplasts contained an average of 1.2 starch granules, that occupied an average cross sectional area of 6.3 μm^2 per chloroplast profile. However, chloroplasts of seedlings grown in ambient CO_2 contained on average 0.9 starch granules which occupied 2.9 μm^2 per chloroplast cross section (Pritchard *et al.,* 1997). Measurements on sections through embedded leaf material showed that when *Arabidopsis* plants are grown under elevated CO_2 compared to ambient CO_2, starch granule cross-sectional area increases by an average of 51.7% (1.32 μm^2 compared to 0.87 μm^2) and the average number of granules per chloroplast in section increases by 42.1% (2.77 granules compared to 1.95 granules) (Teng *et al.,* 2009). However, while there can be no doubt that starch granules increase in size when plants are grown under elevated CO_2, measurements of granule number taken from individual sections through embedded leaf material may not accurately record any increase in granule number. Chloroplasts grown under elevated CO_2 may in fact contain the same number of granules as those grown under ambient CO_2. The above result might be obtained because when starch granules are larger, more granules are observed in any one section, because there is more chance that a random section through a chloroplast will incorporate a larger granule than a smaller granule.

Taken as a whole, limited information is available on the relationship between starch content or plastid volume and granule size and number; this allows no firm conclusions about how these parameters may be linked. Furthermore, methods available for determining these relationships in leaves are generally unsatisfactory.

3.1.3 Existing Methods

The chloroplasts of *Arabidopsis* mesophyll cells are generally stated to contain approximately five starch granules (Zeeman *et al.,* 2007b). This estimate is based largely on transmission electron microscopy (TEM). Methods previously used to count granules and estimate the numbers of granules per chloroplast in other species include flow cytometry and fluorescence microscopy after staining with fluorescently labelled compounds such as FITC conjugated Concanavalin A. These methods are described in the following section along with other possible methods for counting granules such as Focused Ion Beam-Scanning Electron Microscopy (FIB-SEM).

3.1.3.1 Microscopy

Both TEM and SEM have been used to provide information about variation in granule size and shape. For example, early studies on starch metabolism used TEM to show that during the night starch granules decrease in size, but do not disappear entirely (Haapala 1968; Haapala 1969). Using SEM, Grange *et al.* (1989b) were among the first to compare starch granules from leaves grown under clearly defined conditions resulting in varying leaf starch contents. They found small granules were more spherical than large granules; the extra material rendered the large granules more disc-like than the small granules.

The majority of observations and measurements of starch granules have been made on TEM images of sections through mesophyll cells. TEM produces a high resolution image and can be used for basic comparisons of starch phenotype between species or growing conditions. However, TEM has its disadvantages. For example, a single section through a chloroplast may not be representative of the overall chloroplast structure and composition, because a section gives a single image of a chloroplast and cannot be used to calculate the total number of starch granules per chloroplast. A complete

reconstruction through the chloroplast would allow the exact number of granules per chloroplast in the selected cell type to be counted. However, to do this by TEM would require serial sectioning and 3D image reconstruction, involving the correct alignment of many section images; all very time consuming and technically challenging processes. Using this method it would not be possible to quickly check how the number of granules per chloroplast alters during the normal day-night cycle or under varying environmental conditions.

A possible alternative to using TEM to image through the chloroplast could be to use Focused Ion Beam-Scanning Electron Microscopy (FIB-SEM) for 3D reconstruction. FIB-SEM involves taking several hundred SEM images through an embedded sample of leaf tissue, by repeatedly imaging the block surface and then removing a thin section using an ion beam. The images do not therefore require alignment, allowing them to be entered straight into imaging software that automatically stacks the images, creating a video of successive sections through the chloroplast. An FIB-SEM is available for use at the Nano-Vision Centre, Queen Mary University of London. It is not known whether this technique is suitable for imaging starch granules, and a number of potential problems can be envisaged. For example, the resolution may not be satisfactory for counting the number of granules, particularly at the end of the night when starch granules are very small. It is unknown how the starch granules will respond to the ion beam. During the fixation process the semi-crystalline nature of the granules may not allow the fixative to penetrate into the granule. This may result in the granule melting slightly upon contact with the ion beam, destroying the sample and causing inaccurate images to be produced. There is an additional SEM based method for serial sectioning, the Gatan 3View® 3D high resolution imaging system (http://www.gatan.com), but this is not available for my use within the UK. The 3View system uses an ultramicrotome with a diamond knife mounted inside a Field Emission Gun-SEM (FEG-SEM), which allows serial sectioning and imaging of a block within the microscope chamber. Other imaging techniques that produce 3D reconstructions of biological material include confocal laser scanning microscopy and electron tomography, neither of which is suitable for reconstruction of *Arabidopsis* chloroplasts. The small size of *Arabidopsis* starch granules means that they are unlikely to be adequately resolved within chloroplasts using confocal microscopy. While starch granules are well within the resolution range of electron tomography, the technique would not be able to reconstruct

a whole chloroplast because it requires electron transparent samples, which are thinner than a whole chloroplast.

3.1.3.2 Flow Cytometry

Flow cytometry can be used for counting the number of particles of various sizes within a solution. This technique has been applied to a suspension of chloroplasts to estimate the number of starch granules per chloroplast in two species of beans, *Phaseolus vulgaris* (common bean) and *Phaseolus acutifolius* (Tepary bean) (Yang *et al.,* 2002). In this method a suspension of ruptured chloroplasts passed through the flow cytometer separates into two distinct peaks of fluorescence intensity. According to Yang *et al.* (2002) these two peaks represent the chloroplasts and the starch granules. However, the authors fail to show an example of intact chloroplasts in the system, which in theory should lack the "starch" peak Therefore, the true identity of these two peaks is unknown. Schroder and Petit (1992) and Ashcroft *et al.* (1986) both observed that suspensions of 'intact' spinach chloroplasts produced two peaks. On further analysis the two peaks were discovered to be intact and ruptured chloroplasts, while a suspension of thylakoids produced a completely separate third peak. Even if the flow cytometry process is begun with 100% intact chloroplasts, pipetting, dilution, resuspension and flowing through capillary tubes can lead to breakage, which means that it is almost impossible to view the profile of 100% intact chloroplasts in a flow cytometer (reviewed in Bergounioux *et al.,* 1992; Petit *et al.,* 1989).

Flow cytometry can be used to count starch granules in starch storing organs, such as maize kernels (Commuri and Jones 2001; Jones *et al.,* 1992), which have starch granules between 5 and 20 µm in diameter (Jane *et al.,* 1994). However, my preliminary experiments indicated that flow cytometry cannot be used to count *Arabidopsis* starch granules, because due to their small size (average 1 to 2 µm in diameter) they cannot be differentiated from other small particles in a solution of ruptured chloroplasts. This was confirmed by Nigel Miller (Department of Pathology, University of Cambridge, UK; personal communication) who has over 27 years experience in flow cytometry and currently runs the flow cytometry facility at the University of Cambridge.

3.1.3.3 Concanavalin

Schneider and Sievers (1981) showed that FITC conjugated Concanavalin A (FITC-Con A) bound specifically to the surfaces of starch granules in formaldehyde-treated cress roots. If this were also true for *Arabidopsis* leaves, counting FITC-Con A labelled objects in tissues visualised by fluorescence microscopy would provide a direct estimate of starch granule number per chloroplast (Bouchet *et al.,* 1984; Kahn 1983; Schneider and Sievers 1981). Preliminary results indicated that the binding of the FITC-Con A to sections through embedded leaf material fixed in formaldehyde was not specific for starch granules; it either appeared to bind at random or to the chloroplast membranes. Therefore, FITC-Con A cannot be used in a system to estimate the number of granules per chloroplast in *Arabidopsis* leaves.

Alternatively, specific proteins fused to fluorescent proteins such as yellow fluorescent protein (YFP) and green fluorescent protein (GFP) have been found to localise to the surface of starch granules, thus rendering the granules fluorescent (Christiansen *et al.,* 2009; Comparot-Moss *et al.,* 2010). Christiansen *et al.* (2009) were able to visualise starch granules in tobacco leaves by transient expression of the starch binding domain of GWD3 fused to YFP. YFP fluorescence was localised to the chloroplasts and confined to the starch granules. The same was true in tobacco leaves transiently expressing a LIKE SEX4 (LSF1)-GFP construct (Comparot-Moss *et al.,* 2010). However, several considerations indicate that this method may be unsuitable for estimating starch granule number per chloroplast in *Arabidopsis* leaves. First it is important to take into account that in these transiently overexpressing lines there is very high expression of the fluorescent construct, leading to the possibility of mis-localisation. Second, as with all types of microscopy there are limits of detection. The starch granules in *Arabidopsis* are smaller than those in tobacco leaves and good resolution of the number per chloroplast may not be possible using confocal laser scanning microscopy, especially at the end of the night when the average *Arabidopsis* granule diameter will be very small. The density of components within a leaf means that overlapping of chloroplasts and other cell components would be a real problem in resolution of images, and counting the number of granules may not be possible using this method. Third, the starch granules within lines over-expressing a starch-binding protein may be bigger than expected in the wild-type because the presence of large

amounts of the fluorescent protein on the granule surface may reduce starch turnover over during the diurnal cycle.

In the following section I present my results on method development, and the application of these methods to discover how transitory starch granule numbers vary during the diurnal cycle and as the leaf ages.

3.2 Results

3.2.1 Microscopy

I measured the diameter of granules from leaves harvested across the 24 h photoperiod using three methods. Method one, measurements of isolated starch granules photographed using SEM; method two, starch granules measured from light microscopy images of single sections through embedded leaf material, and method three, starch granules measured from FIB-SEM images of serial sections through blocks of embedded material (see section 2.14.7 for a detailed description of this method). FIB-SEM data were only available for the end of the day and end of the night and are therefore not included in the 24 h photoperiod data (Figure 3.1).

There is general agreement between the three methods that the mean diameter of starch granules increases during the light period, peaks at the end of the day and decreases again at night (Figure 3.1 and 3.2). However, the three methods give different impressions of the pattern and magnitude of changes. For example, the two methods in which granule diameter is recorded at several time points (isolated granules and granules in sections; Figure 3.1), give different results for changes in granule size and number throughout the day/ night cycle. There is greater difference in the mean granule diameter between the two datasets at the end of the day (0.39 µm) than the end of the night (0.07 µm) (Figure 3.1). There is no significant difference in mean granule diameter between the two datasets at the end of the night, but there is at the end of the day (Table 3.1). A greater change in granule diameter across the day is seen with the isolated granules (1.14 µm) than granules within sections (0.68 µm). For isolated starch granules, diameter increased at a much greater rate towards the end of the light period, increasing by 0.12 µm in the first three hours of light, but 0.68 µm in the last three hours of the light (Figure 3.1). The opposite is true of the granules measured in single sections. Diameter increased by 0.31 µm in the first three hours of light and only 0.07 µm during the last three hours of the light. Potential reasons for the differences between the data sets are discussed later in this chapter.

Figure 3.2A displays the range of granule diameters at the end of the day and end of the night for the three different granule measurement methods. All three methods show the same trend in granule diameter, with the granule diameter higher at the end of the day

than at the end of the night. For end of the day samples there is no significant difference in the mean diameter of isolated granules and granules observed by light microscopy on sections or FIB-SEM on blocks of embedded mesophyll tissue (Table 3.1). However, there is a significant difference in the mean diameter of granules observed in single sections and by FIB-SEM on blocks. For end of the night samples, the opposite is true. There is no significant difference in the mean diameter of granules observed in single sections and by FIB-SEM on blocks, but there is a significant difference in the mean diameter of isolated granules and granules observed in single sections or by FIB-SEM on blocks (Table 3.1). All three methods show there is a greater range in granule diameter at the end of the day than at the end of the night. Isolated starch granules have a much larger range of granule diameters (0.11 µm to 2.43 µm) than granules in single sections (0.33 µm to 2.03 µm) or granules measured from FIB-SEM images (0.24 µm to 1.80 µm).

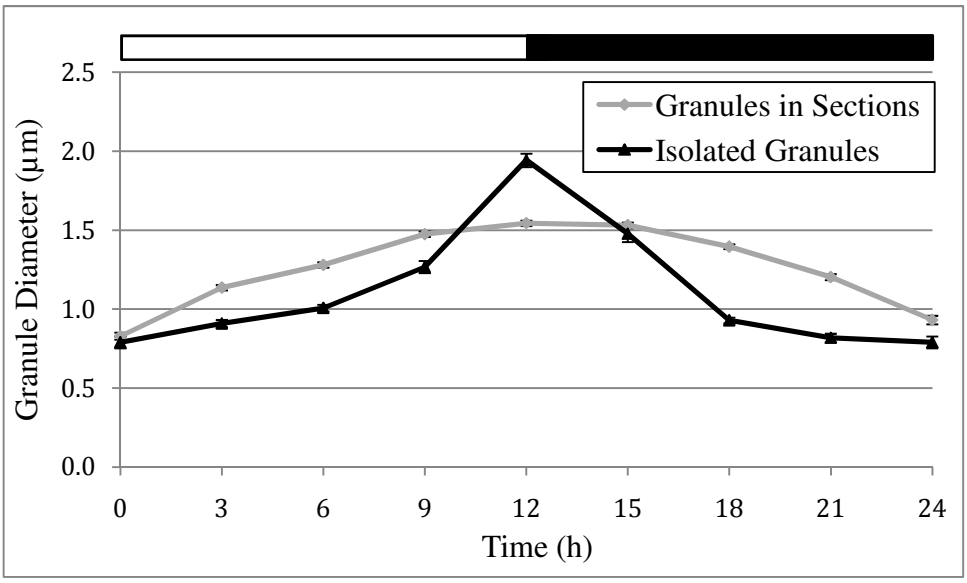

Figure 3.1: Granule size distribution over the 24 h photoperiod. The clear bar at the top of the graph represents the hours of daylight and the black bar the hours of darkness. Granules in sections (grey) = measurements taken using imaging software on light microscopy photographs of mesophyll cell sections stained with iodine solution, prepared according to section 2.14.2. Values are means of measurements on 177 to 996 granules. Sections from four mature leaves from two different rosettes (stage 3.90 (Boyes *et al.,* 2001)), harvested at each time point. Error bars represent standard error (SE). Isolated granules (black) = measurements taken using imaging software on SEM images of isolated granules, prepared according to section 2.14.3. Values are the means of measurements on 215 to 304 granules taken from ten SEM images taken at random. Granules isolated from 25-day-old plants. Starch was extracted from a pool of 40 plants per time point. Error bars represent SE. Where no error bars are visible the SE is smaller than the symbol. Statistics are displayed in Table 3.1.

A

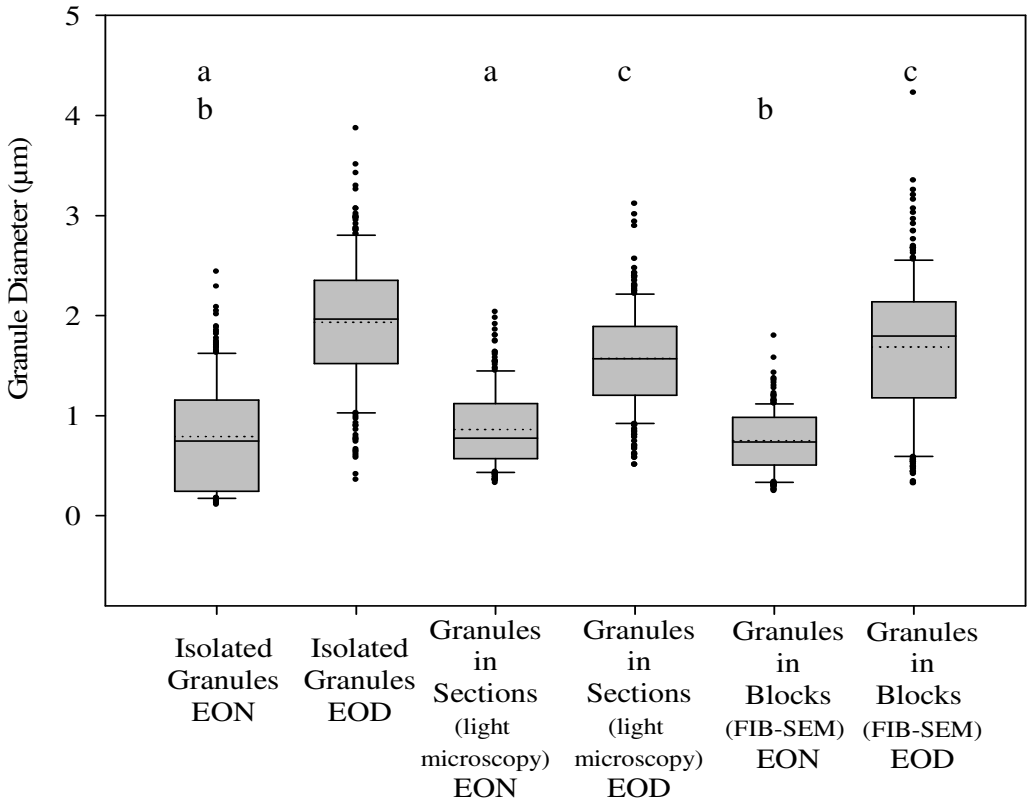

B

	Average Granule Diameter (µm)			
	EOD	SE	EON	SE
Isolated Starch Granules	1.933	0.043	0.791	0.037
Starch Granules in Sections	1.545	0.017	0.861	0.026
Starch Granules in Blocks (FIB-SEM)	1.686	0.047	0.750	0.020

Figure 3.2: Starch granule size distribution from different methods of measurement. (A) Box plot showing the range in granule diameters. The solid line in the middle of the box is the median (50th percentile). The bottom and top of the box are the 25th and 75th percentiles. The upper and lower bars represent the 90th and 10th percentiles respectively. Outliers are represented as diamonds. Mean shown as dotted line. Boxes labelled with the same letter have means which are not significantly different from one another. (B) Table of average granule diameters. Isolated starch granules = measurements taken using imaging software on SEM images of isolated granules, prepared according to section 2.14.3. Starch granules in sections = measurements taken using imaging software on light microscopy photographs of mesophyll cell sections stained with iodine solution, prepared according to section 2.14.2. Starch granules in blocks (FIB-SEM) = measurements taken using imaging software on stacked FIB-SEM images through mesophyll cells, prepared according to section 2.14.7. EON = End of Night. EOD = End of Day. For all three methods 222 granule were measured. Statistics are displayed in Table 3.1

End of Night			End of Day		
	Sections	FIB-SEM		Sections	FIB-SEM
Isolated	t (442) =-1.58 p = 0.115	t (442) = -0.96 p =0.336	Isolated	t (442) = 6.56 p <0.001	t (442) = -3.84 p <0.001
Sections		t (442) = -3.41 p <0.001	Sections		t (442) = 1.95 p = 0.052

Table 3.1: Statistics for data displayed in Figure 3.1 and 3.2. Test of the null hypothesis that the mean granule diameters of the two datasets are not different.

3.2.2 Granule per Chloroplast Approximation Method (GCAM)

As an alternative to the microscopy methods discussed above I developed the Granule per Chloroplast Approximation Method (GCAM) for calculating the number of starch granules per chloroplast. The GCAM is based on the theory that the number of starch granules per chloroplast can be calculated from knowledge, for a given sample of leaves, of the starch content, the number of chloroplasts and the starch granule size.

The first step was to develop a method for isolation of intact chloroplasts, for which there are a number of published methods for *Arabidopsis* (Aronsson and Jarvis 2002; Fitzpatrick and Keegstra 2001; Weise *et al.,* 2004). The 'chloroplast isolation kit' from Sigma was selected (section 2.7.10), which involves homogenising leaf material, filtering out leaf debris, pelleting the chloroplasts and isolating the intact chloroplasts by spinning through a Percoll gradient. Chloroplast intactness was assayed by measuring NADP-dependent glyceraldehyde-3-phosphate (GAP) dehydrogenase activity before and after rupturing the chloroplasts by osmotic shock (Batz *et al.,* 1995). Chloroplasts were estimated to be between 75% and 87.5% intact (lowest and highest level of intactness achieved from three chloroplast extractions). These values compare favourably with Aronsson and Jarvis (2002) who achieved chloroplast intactness of greater than 85%, Fitzpatrick and Keegstra (2001) who achieved 82-95% intact chloroplasts and Dorion et al. (2005) who achieved 70-75% intact chloroplasts.

The number of chloroplasts in the suspension was counted using a haemocytometer (section 2.14.5). To calculate the amount of starch in a sample of the suspension,

established enzymatic methods were used to extract and then assay the starch. To a known volume of the isolated chloroplast suspension, perchloric acid was added to a final concentration of 0.7 M. The suspension was thoroughly mixed to ensure all chloroplasts were ruptured and then the starch extracted and assayed (sections 2.8.2 and 2.8.3). The amount of starch could then be calculated as pg of glucose per chloroplast.

The next step was to measure the size of the starch granules present in the leaves from which chloroplasts were isolated. In order to extract a representative sample, starch granules were purified from leaves (section 2.14.1) harvested at the same time as the leaves used for chloroplast isolation. Granules were photographed using SEM (section 2.14.3), measured using image analysis software and the volume calculated using an equation developed with Scott Grandison (JIC and University of East Anglia) (section 2.14.4). The average mass of a granule in the sample of isolated chloroplasts was calculated by multiplying the calculated volume by the density 1.5 g/cm^3 (Dengate *et al.,* 1978; Munck *et al.,* 1988). This value of density was obtained from measurements on air-equilibrated wheat granules (Dengate *et al.,* 1978) and dry granules from storage organs of maize, wheat, rice and potato (Munck *et al.,* 1988). Although the density of *Arabidopsis* leaf starch is not known, its structure is similar to that of storage starch (Zeeman *et al.,* 2002b) and it is reasonable to assume that its density will also be similar.

The final step was to use the data gathered above (the starch content and the number of chloroplasts in a chloroplast suspension and the starch granule size in leaves from which the suspension was made) to calculate the number of granules per chloroplast.

In summary, the GCAM consisted of the following steps:

1. Isolate a suspension of intact chloroplasts (section 2.7.10):
    a. Count chloroplast number per unit volume using a haemocytometer (section 2.14.5).
2. Measure the amount of starch per unit volume of the chloroplast suspension (section 2.8).
3. Calculate the average weight of starch per chloroplast (pg glucose/chloroplast) using the values from steps 1 and 2.

4. Isolate (section 2.14.1) and then photograph (section 2.14.3), starch granules from a representative sample of leaves:
    a. Measure the radius of granules using image analysis software (section 2.14.4).
    b. Use the equation derived by Scott Grandison (JIC and University of East Anglia) to calculate the volume of a starch granule from its radius (section 2.14.4).
    c. Calculate the average mass of a starch granule by multiplying the calculated volume by the known density of 1.5g/cm^3 (Munck *et al.,* 1988).
5. Calculate the number of starch granules per chloroplast, by dividing the amount of starch per chloroplast (step 3) by the mass of an individual starch granule (step 4).

During each run of the experiment measurements on chloroplast suspensions from four samples (4 g fresh weight leaf tissue in each sample) were averaged to give the final number of granules per chloroplast.

The GCAM was tested on the *starch synthase 4* (*ss4*) mutant. From sectioning and TEM imaging it has been shown that the *ss4* mutant has an average of one starch granule per chloroplast in mature leaves (Roldan *et al.,* 2007) and no granules in its youngest leaves (Figure 4.17). At various points during the day/night cycle in both long days (16 h light/8 h dark) and normal days (12 h light/ 12 h dark) the GCAM estimated the *ss4* mutant to have an average of about 0.9 granules per chloroplast (Table 3.2). The results obtained from the GCAM thus fit with the known phenotype of the *ss4* mutant, providing confidence in the reliability of the method.

Growth conditions	Time of day	Estimated number of granules per chloroplast	SE	Leaf starch content (mg glu g^{-1} FW)	SE
12 h light/ 12 h dark	0 h light – End of Night	0.88	0.06	1.56	0.41
	6 h light – Midday	0.88	0.13	2.23	0.09
	12 h light – End of Day	0.87	0.14	5.45	0.77
16 h light/ 8 h dark	8 h light – Midday	0.97	0.12	3.72	0.50
	0 h light – End of Night	0.96	0.12	1.54	0.23

Table 3.2: Calculation of the number of starch granules per chloroplast using the GCAM for the *ss4* mutant. Sample sizes for the number of granules per chloroplast: 12 h light (12 h light/ 12 h dark photoperiod) n = 8; all other treatments n = 4, where n is a chloroplast preparation.

The GCAM was applied to wild-type plants, to examine whether granule number per chloroplast changes over the day/night cycle (0 h light, 6 h light and 12 h light; Table 3.3), under different day/night cycles (12 h light/ 12 h dark and 16 h light/ 8 h dark; Table 3.4) and under different light levels (180 µmol quanta m^{-2} s^{-1} and 245 µmol m^{-2} s^{-1}; Table 3.5). Figure 3.3 contains a summary of the results. The granule number per chloroplast stays approximately constant over a range of leaf starch contents and chloroplast starch contents (Figure 3.3A and B). For example, while starch content of the leaves varies by 40 fold over the 12 h light/ 12 h dark cycle, starch granule number per chloroplast remains approximately the same (Table 3.3). As the starch content increases the mean granule volume increases (Figure 3.3D), thus the granules change in size rather than number as starch content alters (Figure 3.3C). The following paragraphs discuss the individual datasets in more depth.

Plants grown under long days (16 h light/ 8 h dark), have the same number of granules per chloroplast as in a day/night cycle of 12 h light/ 12 h dark (Table 3.4; Statistics Table 3.6). However, there is a reduction in starch granule volume in plants grown under long days (0.48 μm^3 ± SE 0.04), compared to short days (0.84 μm^3 ± SE 0.02), even though there is no difference in the leaf starch content (Table 3.3). This suggests that under long days there are more chloroplasts in a given leaf area. This is supported by the fact that the amount of starch per chloroplast is lower in plants grown under long days (4.4 pg glu $chloroplast^{-1}$, SE 0.3) than in those grown under a 12 h day/12 h night cycle (6.7 pg glu $chloroplast^{-1}$, SE 0.4).

To examine the effect of light intensity on granule number per chloroplast, plants were grown in 12 h light/ 12 h dark conditions, under either 180 µmol m^{-2} s^{-1} or a higher light level (245 µmol m^{-2} s^{-1}) from germination, or were transferred 24 hours prior to harvest from the lower to the higher light level, while retaining the 12 h night as normal. In plants grown under a higher light level from germination, the amount of leaf starch at midday is lower than in plants under the lower light level. In plants transferred to the higher light level for the 24 hours prior to harvest the starch levels are unaltered at midday (Table 3.5). Growth under high light from germination resulted in smaller granules (0.67 μm^3 ± SE 0.02) than growth under normal light (0.98 μm^3 ± SE 0.03), but transfer to high light for 24 h prior to harvest had no effect on granule size (0.95 μm^3 ± SE 0.04). Despite the alteration in starch content and granule size in plants grown under different light levels, the number of granules per chloroplast is the same (Table 3.5).

Time of day	Estimated number of granules per chloroplast	SE	Leaf starch content (mg glu g^{-1} FW)	SE
6 h light - midday	5.06	0.33	4.98	0.74
12 h light – End of day	5.54	0.28	8.40	0.33
0 h light – End of Night	5.83	0.30	0.21	0.08

Table 3.3: Calculations of the number of starch granules per chloroplast using the GCAM for wild-type plants. Plants were grown in 12 h light/ 12 h dark conditions. Sample sizes for the number of granules per chloroplast: 6 h light n = 12; 12 h light and 0 h light n = 8, where n is a chloroplast preparation. Statistics are displayed in Table 3.6.

Time of day	Estimated number of granules per chloroplast	SE	Leaf starch content (mg glu g^{-1} FW)	SE
Midday (12 h light/12 h dark)	5.06	0.33	4.98	0.74
Midday (16 h light/8 h dark)	5.51	0.48	5.73	0.44

Table 3.4: Calculations of the number of starch granules per chloroplast using the GCAM for wild-type plants harvested at midday under different day/night cycles. Sample sizes for the number of granules per chloroplast: 12 h light/12 h dark n = 12 and 16 h light/8 h dark n = 8, where n is a chloroplast preparation. Statistics are displayed in Table 3.6.

Light conditions (µmol m^{-2} s^{-1})	Estimated number of granules per chloroplast	SE	Leaf starch content (mg glu g^{-1} FW)	SE
180	4.88	0.18	5.64	1.09
180 (245 for 24h prior to harvest*)	4.77	0.19	5.35	0.65
245	4.86	0.26	2.85	0.35

Table 3.5: Calculations of the number of starch granules per chloroplast using the GCAM for wild-type plants grown under different light intensities, harvested at midday (6 h light). *= 24 hours prior to harvest plants were transferred to the higher light level; plants still experienced the 12 h night as normal. Sample sizes for the number of granules per chloroplast: n = 4, where n is a chloroplast preparation. Statistics are displayed in Table 3.6.

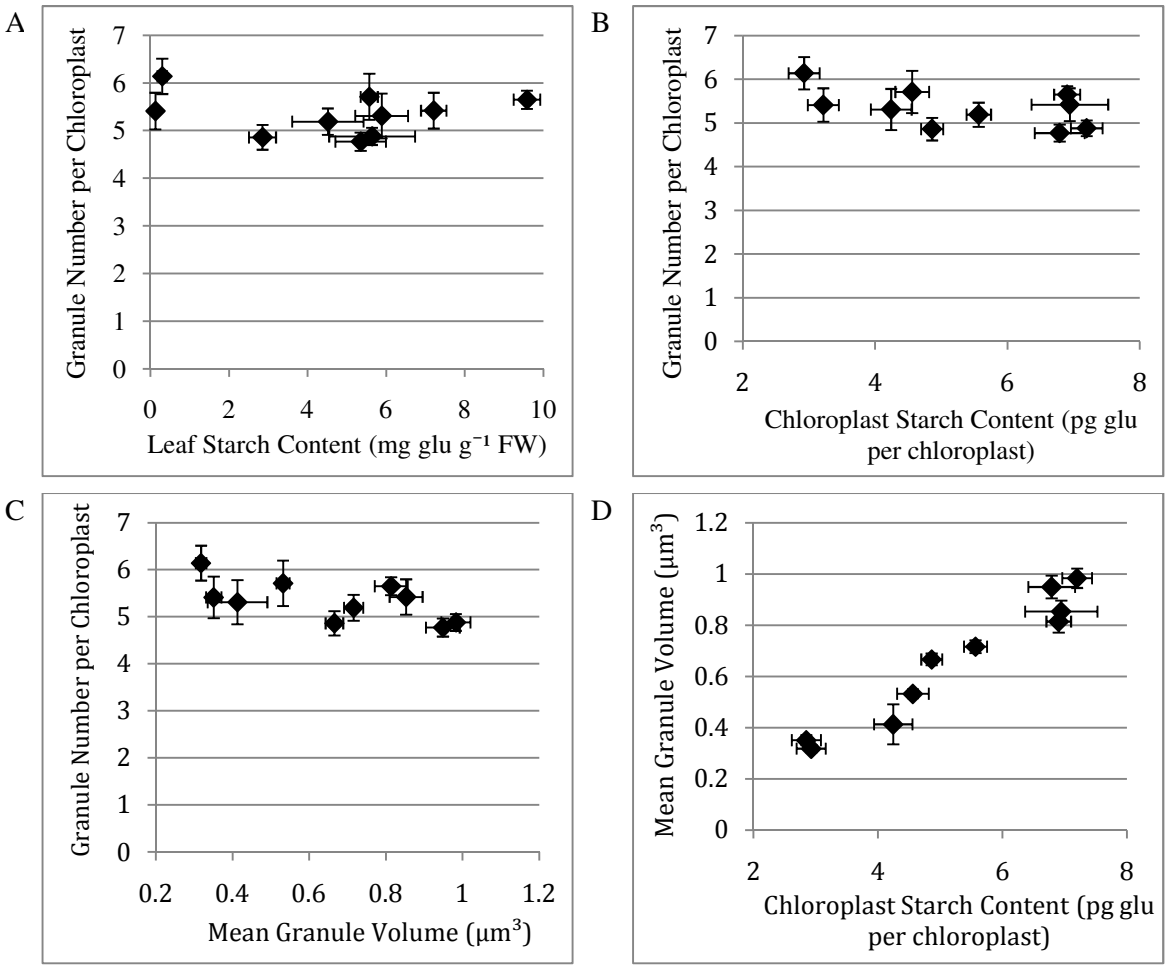

Figure 3.3: Data from the Granule per Chloroplast Approximation Method (GCAM). The graphs contain data from ten independent experiments. In six experiments samples were harvested in the middle of the light period (Table 3.3 to 3.5), in two they were harvested at the end of the night (Table 3.3) and in two they were harvested at the end of the day (Table 3.3). In eight experiments plants were grown under 12 h light-12 h dark conditions (Table 3.3 to 3.5) and in two experiments plants were grown under 16 h light-8 h dark (Table 3.4). Plants for eight experiments were grown under 180 µmol quanta m^{-1} s^{-1} (Table 3.3 to 3.5), for one experiment under 245 µmol quanta m^{-1} s^{-1} (Table 3.5) and for one experiment under 180 µmol quanta m^{-1} s^{-1} with a shift to 245 µmol 24 h prior to harvest (Table 3.5). For granule number per chloroplast, chloroplast starch content and leaf starch content n = 4. Mean granule volume n = 323-878. Values are means ± SE. Statistics are displayed in Table 3.6.

All data: Number of granules per chloroplast			ANOVA: F (6,43) = 2.05, p = 0.085		
Time of day			**Light level**		
Number of granules per chloroplast			Number of granules per chloroplast		
	EOD	midday		245 µmol m^{-2} s^{-1}	180/245 µmol m^{-2} s^{-1} shift
midday	F (2,27) = 3.11, p = 0.063		180/245 µmol m^{-2} s^{-1} shift	F (2,11) = 0.08, p= 0.924	
EON			180 µmol m^{-2} s^{-1}		
Starch content			Starch content		
	EOD	midday		245 µmol m^{-2} s^{-1}	180/245 µmol m^{-2} s^{-1} shift
midday	t (17) = 5.30, p <0.001		180/245 µmol m^{-2} s^{-1} shift	t (6) = -3.41, p = 0.014	
EON	t (14) = 16.29, p <0.001	t (17) = -10.93, p <0.001	180 µmol m^{-2} s^{-1}	t (5) = -2.78, p = 0.039	t (5) = 0.24, p = 0.817
Starch granule volume			Starch granule volume		
	EOD	midday		245 µmol m^{-2} s^{-1}	180/245 µmol m^{-2} s^{-1} shift
midday	t (1825) = -0.22 p =0.825		180/245 µmol m^{-2} s^{-1} shift	t (791) = -7.19, p <0.001	
EON	t (2051) = 15.51 p <0.001	t (2280) = -20.62 p <0.001	180 µmol m^{-2} s^{-1}	t (772) = -5.69, p <0.001	t (971) = -0.58, p = 0.563

Day length	
Number of granules per chloroplast	
	Long day 16 h/ 8 h
Normal day 12 h/ 12 h	t (18) = 1.28, p = 0.216
Starch content	
	Long day 16 h/ 8 h
Normal day 12 h/ 12 h	t (17) = 1.40, p = 0.179
Starch granule volume	
	Long day 16 h/ 8 h
Normal day 12 h/ 12 h	t (2995) = -8.55, p<0.001

Table 3.6: Statistics for comparison of the GCAM data presented in Tables 3.3, 3.4 and 3.5 and Figure 3.3. In each case the statistic tests the null hypothesis that the means of the datasets are not different.

3.2.3 Focused Ion Beam-Scanning Electron Microscopy (FIB-SEM)

To provide an independent check of the above results on the number of granules per chloroplast, I decided to use Focused Ion Beam-SEM (FIB-SEM). To the best of my knowledge this is the first time this technique has been used to address a problem of this nature. As mentioned above, FIB-SEM enables several hundred SEM images to be taken of an embedded sample of leaf tissue, by repeatedly imaging the block surface and then removing a thin section using an ion beam. The sequential images were stacked using imaging software, enabling me to scroll through and count the exact number of granules per chloroplast. I also measured granule width and length at the widest point. The depth of each section removed by the ion beam is known and therefore all dimensions of the chloroplast and starch granules can be calculated. As I showed in section 3.2.1 the resolution was sufficient to measure the granules in leaf samples embedded at the end of the day and end of the night. The ion beam did not appear to alter the structure of the starch granules.

In the work described below, the chloroplast volume and starch granule number of 150 chloroplasts (50 chloroplasts from three leaves) were measured for each time point or leaf age. Measurements of granule volume were taken from 60 of these chloroplasts (20 chloroplasts from three leaves) for each time point or leaf age. Examples of the images produced by FIB-SEM through a chloroplast from a mature and an immature leaf are shown in Figures 3.4 and 3.5 respectively. The results from FIB-SEM are summarised in Table 3.7 and Figures 3.6 and 3.7.

I first used FIB-SEM to compare the starch granule and chloroplast volumes from immature and mature leaves harvested at the end of the light period. Analysis of the FIB-SEM data reveals that immature leaves contain smaller chloroplasts than mature leaves. There is a huge variation in chloroplast size and granule number per chloroplast in mesophyll cells at both leaf ages. The chloroplasts of mature leaves range from 37.6 μm^3 to 240.4 μm^3, and contain between three and fourteen starch granules; while the chloroplasts of immature leaves are between 11.5 μm^3 and 128.8 μm^3, and contain between four and twenty-one starch granules.

In both mature and immature leaves the greater the chloroplast volume the greater the total granule volume it contains (Figure 3.6A). In general as the number of granules per

chloroplast increases, the total granule volume per chloroplast increases (Figure 3.6B). Although there was a lot of variability, in both immature and mature leaves, the greater the chloroplast volume the greater the number of granules it contains (Figure 3.6C) and the greater the volume of the individual starch granules (Figure 3.6D). The chloroplasts of immature leaves contain a greater number of smaller granules than the chloroplasts of mature leaves. The mean volume of starch per chloroplast of an immature leaf is less than half of the mean volume per chloroplast in a mature leaf. The volume of stroma per granule can be calculated by dividing the chloroplast volume by the number of granules in that chloroplast. The volume of stroma per granule is four times greater in mature leaves than in immature leaves; a highly significant difference (Table 3.7). However, the percentage of the chloroplast composed of starch is approximately the same in immature and mature leaves (Table 3.7).

I then used FIB-SEM to compare starch granule and chloroplast volumes at the end of the day and end of the night in mature leaves. At the end of the day the greater the chloroplast volume the greater the total granule volume it contains (Figure 3.7A), and the greater the number of starch granules (Figure 3.7B). These trends are not seen at the end of the night, when all chloroplasts contain low levels of starch. At the end of the night chloroplasts are smaller than at the end of the day, and they contain apparently fewer and smaller granules than at the end of the day (Figure 3.7C and D). The total granule volume per chloroplast at the end of the night is less than 10% of that at the end of the day. As a result, the percentage of the chloroplast composed of starch is significantly smaller at the end of the night, than at the end of the day (Table 3.7). However, the volume of stroma per granule is approximately the same at the end of the night and at the end of the day (Table 3.7).

FIB-SEM analysis reveals a large degree of variability across the rosette in both granule number per chloroplast and the size of granules in a chloroplast. There is no correlation between the volume of individual starch granules and the number of starch granules in a chloroplast, in either immature or mature leaves (Figure 3.8).

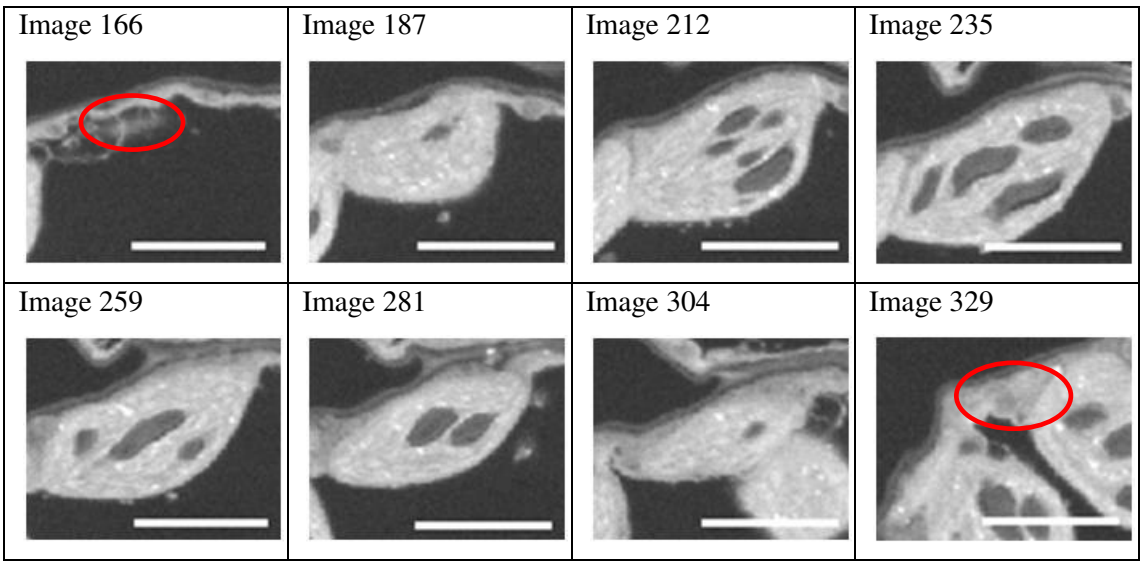

Figure 3.4: Representative FIB-SEM block images from a sequentially-numbered series through a single chloroplast in a mature leaf, harvested at the end of the day. Chloroplast: 176 μm^3 in volume; starting at image 166, 163 sections (48.54 nm each) to pass through the chloroplast. This chloroplast contains 8 granules. Red circle indicates the location of the chloroplast at the first and last sections. Bar = 5 µm

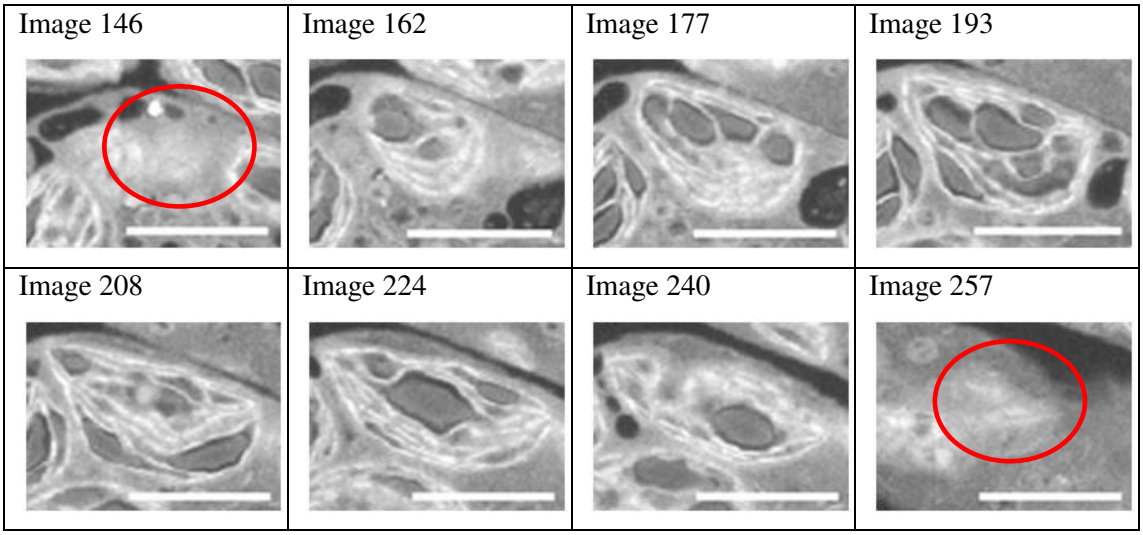

Figure 3.5: Representative FIB-SEM section images from a sequentially-numbered series through a single chloroplast in an embedded immature leaf, harvested at the end of the day. Chloroplast: 81 μm^3 in volume; starting at image 146, 111 sections (36.45 nm each) to pass through the chloroplast. This chloroplast contains 17 granules. Red circle indicates the location of the chloroplast at the first and last sections. Bar = 5 µm

A

	End of Day		**End of Night**
	Immature Leaves	Mature Leaves	Mature Leaves
Mean granule number per chloroplast	11.4 ± 0.3	6.8 ± 0.2	4.0 ± 0.1
Mean chloroplast volume	42.1 µm³ ± 2.1	96.7 µm³ ± 2.7	54.4 µm³ ± 2.1
Mean volume of individual starch granules	0.6 µm³ ± 0.03	2.0 µm³ ± 0.1	0.3 µm³ ± 0.02
Total granule volume per chloroplast	6.5 µm³ ± 0.6	14.1 µm³ ± 0.8	1.4 µm³ ± 0.1
Stromal volume per granule	3.6 µm³ ± 0.1	14.9 µm³± 0.4	15.5 µm³ ± 1.0
Percentage of the chloroplast composed of starch (%)	14.7 ± 0.7	15.1 ± 0.6	2.9 ± 0.3

B

Percentage of the chloroplast composed of starch			
	Immature leaves		EON
Mature leaves	t (118) = -0.47, p = 0.638	EOD	t (118) = 19.59, p <0.001
µm³ of stroma per granule			
	Immature leaves		EON
Mature leaves	t (298) = -25.21, p <0.001	EOD	t (118) = -0.60, p = 0.550

Table 3.7: A summary of data collected from the measurement of FIB-SEM sections is displayed in (A). Values are means ± SE. (B) Statistics for comparison of the FIB-SEM section data presented in (A) and Figure 3.6 and 3.7. In each case the statistic is a test of the null hypothesis that the means of the datasets are the same. The chloroplast volume and starch granule number of 150 chloroplasts (50 chloroplasts from three leaves) were measured for each time point or leaf age. More detailed measurements of granule volume were taken for 60 of these chloroplasts (20 chloroplasts from three leaves) for each time point or leaf age.

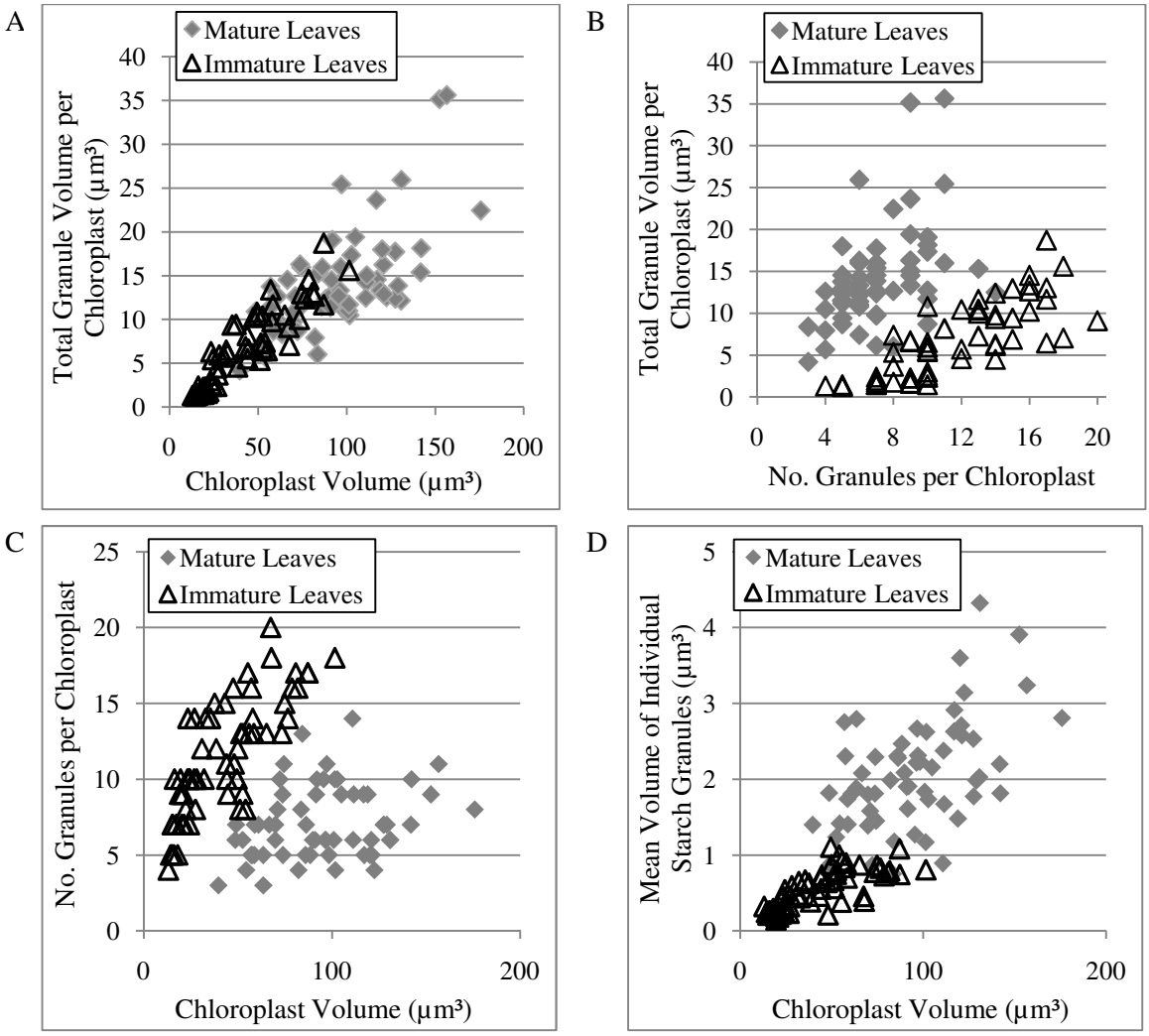

Figure 3.6: Data from the FIB-SEM analysis. A comparison of chloroplasts in mature and immature leaves. (A) The total granule volume per chloroplast plotted against the chloroplast volume. (B) The total granule volume per chloroplast plotted against the number of granules per chloroplast. (C) The number of starch granules in a chloroplast plotted against the chloroplast volume. (D) The mean volume of a starch granule in a chloroplast plotted against the chloroplast volume. For each graph; sixty chloroplasts (20 chloroplasts from 3 leaves) for each time of day or leaf age were measured.

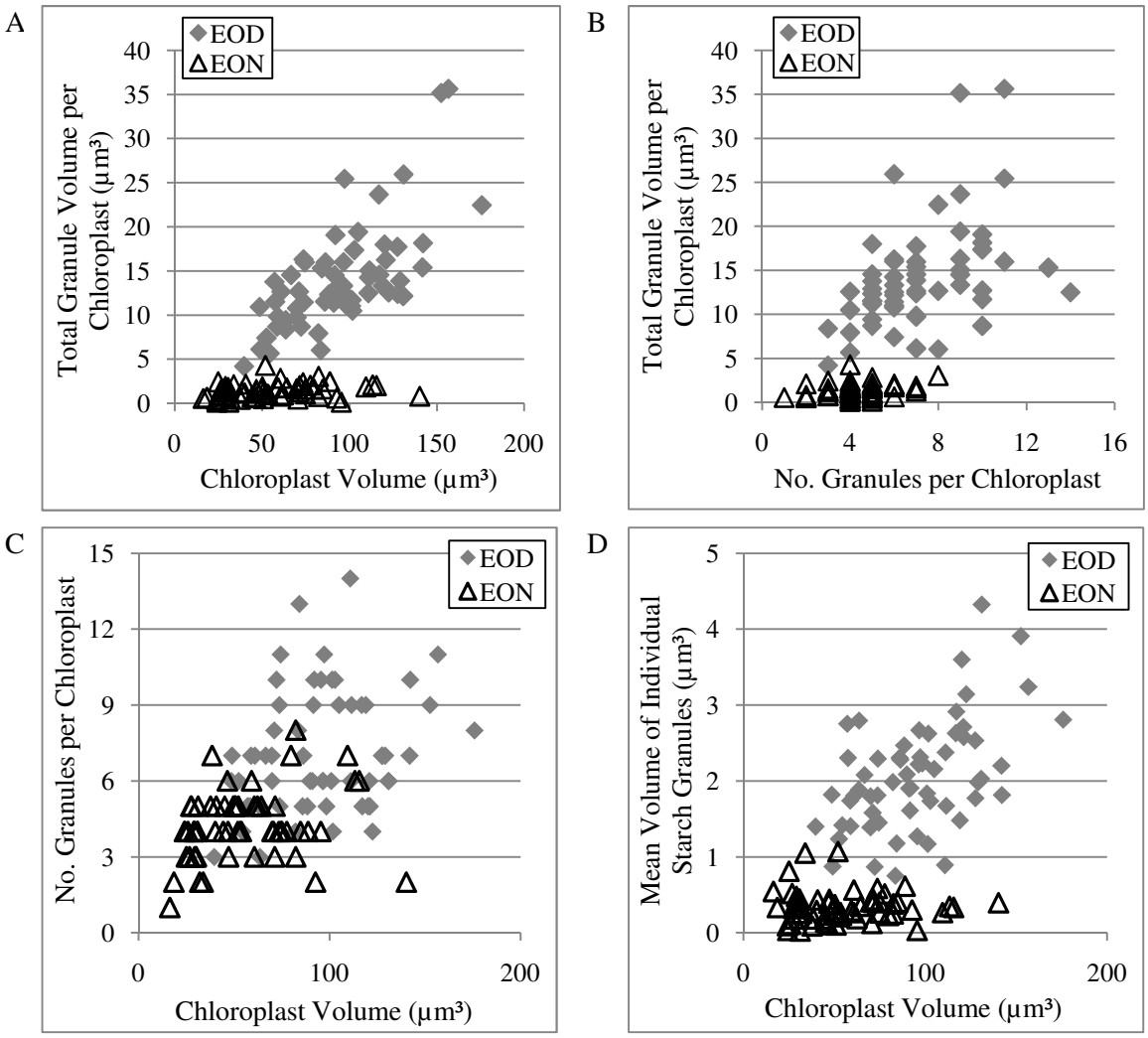

Figure 3.7: Data from the FIB-SEM analysis. A comparison of chloroplasts from mature leaves at the end of the day (EOD) and the end of the night (EON). (A) The total granule volume per chloroplast plotted against the chloroplast volume. (B) The total granule volume per chloroplast plotted against the number of granules per chloroplast. (C) The number of starch granules in a chloroplast plotted against the chloroplast volume. (D) The mean volume of a starch granule in a chloroplast plotted against the chloroplast volume. For each graph; Sixty chloroplasts (20 chloroplasts from 3 leaves) per time of day or leaf age are measured. Note: The EOD data presented here are the same as for mature leaves in Figure 3.4; the data are presented in separate graphs for clarity.

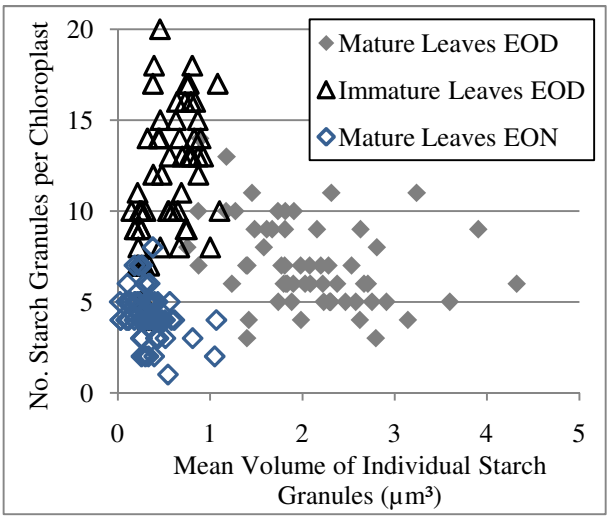

Figure 3.8: Data from the FIB-SEM analysis. A comparison of chloroplasts from mature leaves (at the end of the day (EOD) and the end of the night (EON)) and immature leaves. The mean volume of starch granules in a chloroplast is plotted against the number of starch granules in a chloroplast. Sixty chloroplasts (20 chloroplasts from 3 leaves) for each time of day or leaf age were measured.

3.3 Discussion

In this section, I first discuss separately the insights provided by two very different methods of measurement of granule numbers per chloroplast, GCAM and FIB-SEM microscopy. I then present a critical comparison of the various methods for measuring granule size and number. Finally I use the data as a whole to propose a new view of how starch granule number per chloroplast may be controlled.

3.3.1 Interpreting the Granule per Chloroplast Approximation Method (GCAM) Data

The results from the GCAM indicate that the mean granule number per chloroplast remains constant over a wide range of variation in leaf starch content, amount of starch per chloroplast and granule volume. This implies that there is a control over the number of granules initiated per chloroplast. In particular, the results indicate that the number of granules per chloroplast does not change over the day and night cycle. At the end of the night none of the starch granules is completely degraded, so as the leaf starch content increases during the following day the same granules must increase in size, rather than new granules initiating and growing. This contrasts with the results of Grange *et al.* (1989b), who concluded that in the leaves of mature pepper plants, new granules are initiated during the first part of the day and the number plateaus as the day progresses. Granule initiation may differ between pepper and *Arabidopsis* plants. Alternatively, the methodology used by Grange *et al.* (1989b) may not be accurate. For example, as noted in their discussion, starch granules may be lost during extraction or be too small to measure using SEM. In addition all starch content and granule number measurements were made on a leaf area basis, rather than a more accurate leaf weight basis.

Application of GCAM showed that when plants were grown at a higher light intensity, leaves contained less starch and smaller granules, but there was no change in the number of granules per chloroplast. The reduction in starch content and granule size appear to represent a longer term acclimation to higher light, because they are observed in plants grown at the higher light level from germination but not in plants grown at the higher light level for only 24 hours prior to harvest. Acclimation to higher light in a variety of species, including *Fagus sylvaytica* (Common Beech), sugar beet and *Aesculus hippocastanum* (Horse chestnut), is known to involve changes in chloroplast

size and number, without affecting the total chloroplast volume (Butterfass 1979; Possingham and Lawrence 1983). The fact that the number of granules per chloroplast remains constant despite changes in chloroplast size as a whole again suggests the existence of a mechanism that controls the number of granules per chloroplast, rather than a control over the number of granules initiated in a given stromal volume.

When plants were grown in long day conditions, the GCAM results show a reduction in the starch granule volume, but no change in starch content or granule number per chloroplast. One interpretation of these data is that under long day conditions there is a greater number of smaller chloroplasts in *Arabidopsis* leaves. My results show that while granule number per chloroplast is maintained under long days, there is no increase in leaf starch content. This helps explain the reduced granule size under long days, because the photosynthate destined for starch is distributed between a greater number of granules throughout the leaf. In contrast, Grange *et al.* (1989b), found that there were fewer and larger granules in the leaves of mature pepper plants when they were grown under long day conditions. It is important to note that in the study by Grange *et al.* (1989b) starch numbers are calculated on a leaf area basis, which is also found to increase under longer days. Therefore the leaves of pepper plants grown under long days may still contain the same total number of granules as those plants grown under short days, but the granule density per unit area may be reduced.

Thus far the GCAM has shown remarkable constancy of granule number per chloroplast in all conditions tried. It would be valuable to examine the response of granule number per chloroplast to other conditions known to affect starch content, such as enhanced CO_2, reduced nitrogen or water stress (Pritchard *et al.,* 1997; Sun *et al.,* 2002; Teng *et al.,* 2009), to discover whether this relationship can be broken down. If variation can be found, this would provide a basis for experiments to discover control mechanisms. Further discussion of the value and potential drawbacks of the GCAM is presented and discussed in section 3.3.3.2.

3.3.2 Analysis of the FIB-SEM method

The results from the FIB-SEM provide a somewhat different set of conclusions from results from the GCAM. In this section I discuss the FIB-SEM data only. I compare the two methods in section 3.3.3.2.

FIB-SEM is potentially the most detailed and accurate method available for counting the number of granules per chloroplast. A complete reconstruction of a chloroplast has not previously been attempted and is only now possible using the FIB-SEM technique. No method has previously been reported that can accurately count the large numbers of starch granules in a specific tissue and cell type. The results clearly demonstrate that the widely cited "five starch granules per chloroplast" (Zeeman *et al.,* 2007b) is an underestimate. At the end of a 12 hour light period chloroplasts in mature leaves contain a mean of 6.8 (± SE 0.2) granules, while chloroplasts in immature leaves contain 11.4 (± SE 0.3) granules. This reinforces the arguments against the use of TEM images of sections through embedded material for determining the number of granules per chloroplast. Data from the FIB-SEM also highlight the huge variability in chloroplast size in wild-type leaves, even among one cell type in the same leaf. This variety in chloroplast size in wild-type *Arabidopsis* leaves is not evident from previous measurements of chloroplasts from cross sectional areas (Marrison *et al.,* 1999; Pyke and Leech 1992; Pyke and Leech 1994).

A potentially important finding from the FIB-SEM analysis is that the volume of stroma per granule is approximately the same at the end of the day and at the end of the night in mesophyll cells of mature leaves. This suggests that there may be some control over the number of granules that are initiated in a given volume of stroma.

FIB SEM shows that immature leaves contain a greater number of smaller granules per chloroplast than mature leaves. As a result they have a smaller volume of stroma per granule. However, the percentage of the chloroplast volume that consists of starch remains the same as the leaf matures. At the end of the day starch accounts for approximately 15% of the chloroplast volume in both mature and immature wild-type leaves. Therefore, there appears to be a control over the total volume of starch accumulated per chloroplast, but how this starch is distributed between granules varies between mature and immature leaves. In both mature and immature leaves the size of

the chloroplast correlates with the magnitude of starch accumulation. A correlation between chloroplast size and starch accumulation has previously been reported in the needles of *Pinus palustris* (Pritchard *et al.,* 1997).

To the best of my knowledge this is the first report that the chloroplasts of immature leaves contain more, smaller granules than the chloroplasts of mature leaves. If there is a control over the number of granules that initiate in a given volume of stroma, as suggested above based on data from mature leaves, then in the chloroplasts of immature leaves, the control must allow for a greater number of initiations in a set volume of stroma than in the mature leaves.

It is also worth bearing in mind that the chloroplasts of immature leaves still have to divide. In wild-type plants, controls may be in place to limit starch accumulation per chloroplast and partition starch between the granules in order to allow correct division and maturation of chloroplasts. Work by Heitz (1922 referenced in Butterfass, 1979; the original reference is a PhD thesis from a German University and was unobtainable) on detached moss leaflets, suggested that while a lack of starch or excess starch ("chloroplasts crammed with starch") inhibited chloroplast division, a moderate amount of starch promoted chloroplast division. A large starch granule may directly inhibit the correct division of a chloroplast (Figure 5B in Lopez-Juez and Pyke 2005).

FIB SEM analysis showed that in both mature and immature *Arabidopsis* wild-type leaves, at the end of the day starch constitutes on average 15% of the chloroplast volume. The only previous measurements of starch in individual chloroplasts that are sufficiently detailed to compare with my FIB-SEM data are those of Winter *et al.* (1993; 1994). These authors examined sections through embedded barley and spinach leaves and found broadly similar results to *Arabidopsis* in terms of the percentage of the chloroplast that consists of starch. For example, nine hours into a fifteen hour light period, starch accounts for on average 10% of the chloroplast volume in barley leaves (Winter *et al.,* 1993), while in spinach leaves, at the end of a nine hour light period, starch accounts for on average 11% of the chloroplast volume (Winter *et al.,* 1994). However, in both cases detailed examination of the chloroplasts was conducted on only 25 cells (one section through each cell) (Winter *et al.,* 1993; Winter *et al.,* 1994).

The FIB-SEM analyses suggest that both the starch granule size and the number of granules per chloroplast decreases during the night. This indicates that some granules are completely degraded during the night and new granules are initiated during the following day. However, it is entirely possible that the granules do not completely degrade, but instead decrease in size to such an extent that they are not visible using FIB-SEM. The mean chloroplast volume at the end of the night is almost half the volume at the end of the day and the mean volume of starch per chloroplast is reduced by more than 90% over the night. However, the volume of stroma per granule does not vary between the end of the day and end of the night. This implies that as the granules degrade during the night, the chloroplast retracts.

3.3.3 Comparison of granule measurement methods

3.3.3.1 Granule size variation

The results presented in section 3.2.1 described the use of three different methods to examine granule size variation. Method one involved the measurement of isolated starch granules photographed using SEM; in method two, starch granules were measured from light microscopy images of single sections through embedded leaf material and in method three, starch granules were measured from FIB-SEM serial section images through blocks of embedded material. All three methods show an increase in granule size during the light period and a decrease during the dark period, representing starch synthesis during the day and degradation at night.

The range of granule sizes present throughout the 24 hour photoperiod clearly shows that starch granule initiation and/or growth is not synchronised across chloroplasts and cells. Given that during the day starch accumulation occurs at a linear rate (Gibon *et al.,* 2009) and the smaller the granule the larger the increase in diameter when a given mass is added to it, the average granule diameter is expected to increase at a faster rate at the beginning of the day than towards the end, if granule number remains constant. This is exactly what is observed from measurements of granules in light microscopy images of sections through embedded leaf material. However, this is not the picture that emerges from measurements of isolated granules, where granule diameter increases at a faster rate towards the end of the day than at the start of the day (Figure 3.1). It is feasible, that

at the beginning of the light period new granules are being initiated, so the average diameter does not alter and only when all granules are initiated does the diameter rapidly increase as all the glucans produced are channelled into these granules. Alternatively, at the beginning of the day, tiny granules may be present, initially undetectable in SEM images of isolated granules because of their small size, but then becoming detectable in the first few hours of light as their size increases. So in these first few hours of light the average diameter does not appear to increase rapidly, because measurements are skewed by the now visible smaller granules. Alternatively, the starch granule extraction method used to obtain isolated granules may be skewed against small granules. For example, the centrifugal speed used to pellet the starch (for method see section 2.14.1), may be insufficient to pellet the smallest granules which become stuck to the unpelleted cell debris.

The range of granule sizes measured at the end of both the day and the night varies depending upon which of the three different methods is used. At the end of the day granules measured from light microscopy images of sections through embedded leaves present the narrowest range of granule sizes of the three granule measurement methods. This suggests that either the true size of the granules is obscured in the sections, i.e. size extremes (the largest and smallest granules) are not distinguishable, or it is not possible to visualise the smallest granules using light microscopy, or the full range of granule sizes measured in the isolated granule population is not present in the chloroplasts of mature mesophyll cells. However, granules measured from sequential FIB-SEM images through mesophyll cells present the broadest range of granule sizes at the end of the day. This demonstrates that a wide range of granule sizes are present in the chloroplasts of mature mesophyll cells at the end of the day. Thus it appears that measurement of granules in individual sections underestimates the number of smaller granules and the full size of larger granules, reinforcing the argument against the use of light microscopy or TEM images of single sections through embedded material for determining the number of granules per chloroplast. Although the range in granule sizes observed by light microscopy on sections and FIB-SEM on blocks of embedded mesophyll cells is different, there is no significant difference in the mean granule diameter of end of day samples (Table 3.1). This indicates that the use of images of mesophyll sections to compare mean granule sizes between different plants may be an acceptable method.

At the end of the night isolated starch granules have a much larger range of diameters than granules measured by light microscopy on sections through embedded mesophyll cells or FIB-SEM on blocks of embedded mesophyll cells. This is likely to be because the isolated granule population is derived from a mixture of different leaf ages and cell types. In contrast, when granules from sections and blocks are measured by light microscopy or FIB-SEM respectively, only the chloroplasts of mature mesophyll cells are examined. FIB-SEM images show that the mesophyll cells of immature leaves contain smaller granules than mature leaves, and this potentially explains the greater proportion of smaller granules measured in the isolated granule population.

The mean granule diameter of the isolated granules might also be skewed by the measurement of large granules isolated from the guard cells or bundle sheath cells. In C_3 species like *Arabidopsis,* starch is predominantly stored in the mesophyll cells, but starch also accumulates in the guard cells, which border stomata, and in bundle sheath cells which surround the leaf vein (Streb *et al.,* 2008; Tipping and Murray 1999). The starch within these cell types is thought to vary from that within the chloroplasts of mesophyll cells (Miyake and Maeda 1975; Miyake and Maeda 1978). For example, the guard cells in a large number of plant species are known to retain their starch during the night (Pallas 1964). The plastids in the guard cells of the coffee plant resemble amyloplasts rather than chloroplasts, containing starch which is more permanent and resembles storage starch more than transitory starch (Badenhuizen 1966). Additional evidence that the starch in the guard cells and bundle sheath cells differs from mesophyll cell starch comes from the *pgi* mutant and the albino *ispH* mutant. The *ispH* mutant has no chlorophyll in its plastids to support photosynthesis, while the *pgi* mutant is unable to catalyse the reversible isomerisation of fructose-6-P and glucose 6-P, so normal starch synthesis cannot take place in photosynthetic cells (Neuhaus *et al.,* 1989; Yu *et al.,* 2000). As a result starch is absent from the mesophyll cells of both the *pgi* and the *ispH* mutant; but starch is still present in the guard cells and bundle sheath cells (Tsai *et al.,* 2009). This indicates that although bundle sheath cells are capable of producing starch via photosynthesis (Williams *et al.,* 1989), they are also capable of producing starch heterotrophically, probably through the uptake of glucose-6-P from the cytosol (Tsai *et al.,* 2009). In *Arabidopsis,* bundle sheath cells constitute 15% of chloroplast-containing cells in the leaf, although the chloroplasts are smaller and there are fewer per cell compared to mesophyll cells (Kinsman and Pyke 1998). In conclusion

the starch from the guard cells and bundle sheath cells potentially constitutes a significant proportion of the starch isolated from a whole rosette and may skew the granule diameter calculations towards larger granules in isolated granule samples, particularly at the end of the night. If the granules within guard and bundle sheath cells are not degraded, then at the end of the night, when the majority of starch granules in the mesophyll cells are very small or have been fully degraded, large granules could easily skew the average.

The measurement of chloroplasts and starch granules from images of embedded material is unlikely to be entirely accurate because shrinkage of the cellular components may well have taken place during the fixing and embedding process. For example Winter *et al.* (1993) recorded a cell volume reduction of 63% during fixation and embedded of barley leaves as a result of dehydration. However, Winter *et al.* (1993) found that there is not equal shrinkage of all the cell components and that loss of volume from the vacuole is mainly responsible for the shrinkage, while the reduction in chloroplast volume is much lower. More detailed analysis by Winter *et al.* (1994) showed a 54% reduction in the cell volume of spinach leaves during fixation and embedding, but only an approximate 29% reduction in chloroplast volume. Any shrinkage in chloroplast or starch volumes that do occur during fixation will probably be relative and equal across samples and therefore measurements of granule dimensions are probably reliable for comparative purposes. An alternative technique that would achieve the same image resolution as FIB-SEM and TEM without the problems of dehydration is freeze-fracture SEM. Freeze-fracture or freeze-etch SEM involves the rapid freezing of fresh tissue, which is then fractured while maintaining the freezing temperature (-100^{o}C or lower). Samples are then coated in a conductive coating such as platinum and viewed in an electron microscope. While freeze-fracture SEM avoids the problems of shrinkage during fixation, there is no control over the plane of fracture, and quite often the fracture goes over the top of the chloroplast envelope rather than through the chloroplast, so the internal structure cannot be seen (Chaly *et al.,* 1980). In addition, freeze-fracture SEM does not permit serial-sectioning, and therefore, like single sections, only permits a snapshot of the chloroplast rather than an accurate count of the number of starch granules present.

In summary, the measurement of granules from FIB-SEM serial section images through blocks of embedded material is likely to provide the most accurate picture of starch granule size over a 24-hour photoperiod. As described above, unlike the light microscopy method, the FIB-SEM method will always measure the true size of starch granules, and unlike the measurement of isolated granules, will only record the size of transitory starch granules in leaf tissue of the selected type and age.

My results on starch granule size distribution contrast with those of Howitt *et al.* (2006) who reported that the distribution of starch granule sizes was the same at the end of the day and end of the night in *Arabidopsis* leaves. This led them to suggest that rather than starch granule degradation taking place slowly over the night, once a granule begins to degrade, it is completely degraded very quickly, otherwise the granule size distribution would be skewed towards smaller granules at the end of the night. However, the data presented in this thesis from three different granule measurement methods show a far greater range in granule diameter at the end of the day than at the end of the night, and a large increase in smaller granules at the end of the night. Howitt *et al*. (2006) did not present data on diurnal variation in starch content in their plants and it is possible that starch turnover was different from that in plants used in my studies. In addition the method used by Howitt *et al.* (2006) for measuring the granule size may be inaccurate. For example, they used the Malvern MasterSizer 2000 (Malvern instruments, Malvern, Worcestershire, UK); a machine capable of measuring down to 0.02 µm, but the smallest granule size they recorded was 0.4 µm. Their measurement method did not take into account the clumping of isolated granules that may occur in a suspension; if clumping occurs it would give inaccurate readings, because it would suggest larger granules are present than actually are.

The smallest granules, measured are 0.11 µm and 0.13 µm in diameter, using SEM of isolated granules and FIB-SEM on blocks of embedded mesophyll cells respectively. Either granules below this size are not distinguishable using the microscopy methods employed in this study or do not exist. It has been suggested that the core of the starch granule is less organised than the outer layers (Ziegler *et al.,* 2005). If this is the case, the cycle of phosphorylation and dephosphorylation required for the degradation of organised crystalline layers of the granule (section 1.2.3) may no longer be as necessary when granules reach a very small size during the night. It may be that once the less

organised core of the granule is exposed the degradation rate can no longer be controlled and the granule is completely and quickly degraded by BAM and ISA3, or indeed by AMY3. If this were the case, it is entirely possible that granules smaller than 0.11 µm do not occur in the chloroplast during the night. Interestingly, if some granules are completely degraded at night, it would suggest that new granules are initiated during the following light period.

3.3.3.2 GCAM versus FIB-SEM

GCAM and FIB-SEM results differ in two major and important ways. First, the results as a whole support different views of how starch granule numbers may be controlled. Second, the estimates of the numbers of granules per chloroplast differ. The GCAM method supports the theory that there is a control over the number of granules initiated per chloroplast and that this number is maintained throughout the 24 h photoperiod. However, analysis of the FIB-SEM data supports the theory that there is a control over the number of granules that initiate in a given stromal volume rather than the number of granules that initiate per chloroplast. The GCAM estimates the mean granule number per chloroplast at the end of the day to be 5.5 (± SE 0.3) compared to the FIB-SEM measurements of 6.8 (± SE 0.2) granules in mature leaves and 11.4 (± SE 0.3) granules in immature leaves. In contrast, at the end of the night the GCAM estimates there to be 5.8 (± SE 0.3) granules per chloroplast, while the FIB-SEM measurements estimates 4.0 (± SE 0.1) granules per chloroplast in mature leaves.

The FIB-SEM method can potentially present a true picture of granule number and size in the chloroplasts of a specific cell type and leaf age, at least at the end of the day; whereas the GCAM averages the results across the entire rosette. It is possible that at the whole rosette level the GCAM estimate of an average of 5.5 granules per chloroplast at the end of the day is correct. However, this is unlikely given that both mature and immature leaves have been shown to have a higher mean number of granules per chloroplast using the FIB-SEM method. Thus it appears that the GCAM underestimates the number of granules per chloroplast at the end of the light period.

The results of GCAM are dependent upon the phenotype of the isolated intact chloroplasts harvested during the extraction process and may skew the final result by

favouring smaller chloroplasts which contain fewer granules. Thus the lower granule number per chloroplast at the end of the day estimated by the GCAM compared to FIB-SEM may be because smaller chloroplasts containing fewer granules are more likely to remain intact during the isolation process. In contrast, at the end of the night there is less likely to be any preference in chloroplast survival during isolation, because all chloroplasts contain low levels of starch. An underestimate of the number of granules per chloroplast may also arise because of the difficulty in obtaining intact chloroplasts. It is virtually impossible to obtain a suspension of 100% intact chloroplasts, so some of the chloroplasts counted within a suspension, during the GCAM process will have ruptured and lost their starch granules. Therefore, within a suspension the number of intact chloroplasts will be overestimated relative to the number of starch granules, resulting in an underestimation of the number of granules per chloroplast. Alternatively, an underestimation of granule number per chloroplast using the GCAM could be caused by an overestimation of the mean granule volume. This situation may occur if smaller starch granules are preferentially lost during extraction and measuring (as discussed previously). However, the SEM was able to resolve granules down to 0.11 µm in diameter and the supernatants were apparently free of starch granules.

While the GCAM estimate of granules per chloroplast at the end of the night is larger than the FIB-SEM estimate (5.8 and 4.0 granules respectively), it is important to note that the FIB-SEM estimate is based only on mature leaves. FIB-SEM data are not available for immature leaves at the end of the night, but if the chloroplasts of immature leaves experienced a similar reduction in granule number to those in mature leaves (approximately 41%) they would be expected to contain an average of 6.7 granules. Therefore, the GCAM calculation of granule number per chloroplast at the end of the night may be a realistic average across mature and immature leaves of the rosette. Another explanation for the difference in granule number per chloroplast estimated by the GCAM and FIB-SEM, is the sensitivity of FIB-SEM. The apparent reduction in granule number per chloroplast during the night observed via FIB-SEM may simply be because the smallest granules are not visible using this technique. If this were the case, granule number per chloroplast may remain constant.

Because it averages data across the whole rosette, the GCAM fails to demonstrate the large variations that occur in the number of granules per chloroplast and chloroplast

volume at any time of the day or leaf age. The mechanical chloroplast extraction method requires a minimum weight of leaf tissue, meaning that individual plants can not be compared. It is also difficult to compare leaves of different ages and impossible to compare different cell types using this method, because whole rosettes must be harvested. As a result, chloroplasts from cells at different developmental stages are grouped together, ranging from immature leaves that have mitotic cells in the basal region and expanding cells in the tip, to mature leaves that contain fully expanded and developed cells (Pyke *et al.,* 1991). Some evidence suggests that it is acceptable to average the starch phenotype across different cell types of the leaf. For example, the chloroplasts from palisade and spongy mesophyll cells of *Phaseolus vulgaris* varied in size, but the relative partial volumes of chloroplast structural parts (thylakoid membranes, stroma, starch and plastoglobules) were similar (Kutík 1989). In contrast, other studies emphasise the difference in starch accumulation between different leaf cell types. For example, Carmi and Shomer (1979) found that the chloroplasts of *P. vulgaris* spongy mesophyll cells accumulated proportionally more starch than palisade cells.

An argument against the use of FIB-SEM for the measurement of granule number per chloroplast is the relatively small sample size that can be analysed. This may fail to capture the variation across a leaf or the rosette and a lot of work is required to obtain representative data that is not skewed by very local variation. I attempted to overcome this problem by analysing one leaf from three separate plants for each data point. However, further investigation of the extent to which this method is representative is required.

In conclusion, FIB-SEM arguably produces better results than GCAM for calculating the number of granules per chloroplast, in terms of accuracy and detail of information obtained. The GCAM results may not be strictly accurate, but the relative changes in different samples can be easily detected. In addition, the GCAM is much less labour intensive and yields quicker results than FIB-SEM and it can be applied in any lab, without specialist equipment. Therefore depending upon the questions asked the GCAM may well provide robust data of adequate quality. If time and resources were available there are many more experiments which would ideally be conducted using FIB-SEM. For example, no data have been collected from FIB-SEM to date about how the granule number per chloroplast changes under different day lengths or light conditions.

3.3.4 Insights into the control of granule number per chloroplast

Initial results from GCAM that I developed suggested that on a whole rosette level there is a control over the mean number of granules per chloroplast in the leaves of *Arabidopsis,* such that this number is constant over the day/night cycle and during growth under a range of light conditions. However, analysis of mature mesophyll cells by FIB-SEM indicates that in *Arabidopsis* leaves the granule number per chloroplast varies over the diurnal cycle. The number and size of granules appears to increase during the day as transitory starch accumulates and then decrease at night, although a number of granules remain in each chloroplast at the end of the night. If the FIB-SEM estimate of a reduction in granule number over the night is correct, there is maintenance of the stromal volume per granule over the day/night cycle. This may be the basis for the control over the number of granules initiated per chloroplast. However, the mechanism for such a control is completely unknown. If the control over how many granules are initiated per chloroplast is indeed at the level of stromal volume per granule, then the volume of stroma required per granule changes as the leaf matures.

The use of the FIB-SEM technique to reconstruct chloroplasts and accurately count the number of granules has shown clearly for the first time that the average number of granules per chloroplast and the size of the granules changes dramatically as the leaf ages. Despite the average chloroplast volume in an immature leaf being less than half the volume of a chloroplast in a mature leaf, the chloroplasts contain more than 1.5 times more granules, which are on average three times smaller. Calculation of the exact number of granules per chloroplast at the end of the day has not previously been possible. While examination of individual sections through embedded material might allow the conclusion that starch granules in immature leaves are on average smaller, it would not have permitted the counting of all the granules present in the chloroplast.

The possibility exists that there is no direct control mechanism over the number of granules that are initiated per chloroplast. For example, new granules may simply initiate when the amount of material available for assimilation into starch exceeds the amount that can be incorporated onto the existing granules. In other words, if the rate at which new starch is produced by the starch synthase enzymes exceeds the amount that

can be incorporated onto the existing granule surfaces, then new granules will be initiated. This could provide an explanation for the difference in starch granule number per chloroplast between the immature and mature leaves. The proplastids in non-photosynthetic organs that will eventually develop into amyloplasts, in a variety of species, contain starch (Reibach and Benedict 1982; Sagisaka *et al.,* 1999; Sakai *et al.,* 1992; Thomson *et al.,* 1972). However, both proplastids destined to develop into chloroplasts and developing chloroplasts in the peripheral regions of the *Arabidopsis* shoot meristem and basal regions of young leaves do not appear to contain starch granules (Sakamoto *et al.,* 2009). Therefore, when a chloroplast first accumulates starch, there will be no pre-existing granules and many small granules may initiate. Initially the numerous small granules which form in the chloroplasts of immature leaves may be completely degraded by the end of the night. However, as the day/night cycles progress the growth of a few granules may exceed the degradation rate and slowly granules increase in size. In the chloroplasts of mature leaves granules are not completely degraded by the end of the night, so at dawn newly synthesised glucans may be preferentially added to the existing granules, with only a few new granules initiating during the day.

One theory on how the number of granules is controlled was proposed by Grange *et al.* (1989b) who suggested that new granules may initiate when the older granules reach a maximum size. However, this proposal is based on reference to the work by Giesy and Geiger (unpublished, cited in Geiger and Batey 1967) who concluded, from studies of electron microscopy images, that in sugar beet leaves, a point is reached when starch granules stopped growing in size and new granules were initiated. This seems an unlikely control mechanism in *Arabidopsis* leaves, as the size of granules varies across the rosette, with chloroplasts in the immature leaves containing larger numbers of smaller granules compared to the chloroplasts of mature leaves.

My results show that even within the mesophyll cells of a single leaf there is a large range of chloroplast sizes. The larger the chloroplast the more starch it contains, in the form of a greater number of larger granules. Chloroplast size may be affected by the starch content. The intrinsic size and contents (excluding the starch granules) of each chloroplast may be the same, and the amount of starch it accumulates may be responsible for the alterations in size, i.e. the greater amount of starch a chloroplast

accumulates the greater the size of the chloroplast, as the chloroplast expands to accommodate the granules. However, if all chloroplasts have the same amount of metabolic machinery, one would expect them all to accumulate approximately the same amount of starch. In order to resolve this issue, detailed measurements of the stromal (excluding the starch granules) and thylakoid volumes of each chloroplast would be required. Alternatively, this hypothesis could be tested by measuring the chloroplasts from a starchless *Arabidopsis* mutant, such as the *pgm* mutant, to see if in the absence of starch chloroplasts are similar sizes.

4 The Role of Starch Synthase 4 in Starch Granule Initiation and Growth

4.1 Introduction

A major aim of my project was to investigate how starch granule initiation and starch granule number per chloroplast are controlled. The starch synthases are responsible for the elongation of glucan polymers and are essential for the synthesis of the starch granule (Ball and Morell 2003). In this study I focussed specifically on the role of STARCH SYNTHASE4 (SS4), because as discussed in the introduction (section 1.3.1.4), recent evidence suggests that SS4 may play a central role in granule initiation. The *ss4* mutant of *Arabidopsis* has fewer, larger starch granules per chloroplast, suggesting that SS4 is required for the establishment of the initial structure of the starch granule and hence control of granule numbers. SS4 is a minor SS, in the sense that it makes up a small percentage of starch synthase activity in *Arabidopsis* leaves (no difference in total soluble SS activity was observed between extracts of *ss4* and wild-type leaves: Roldan *et al.,* 2007, and Szydlowski *et al.,* 2009), yet its loss has a massive effect on starch granule numbers that is not seen when any other individual SS isoform is lost.

Additional evidence that suggests a critical role for SS4 in starch granule initiation comes from the unicellular chlorophyte *O. taurii* (discussed in more detail in section 1.3.3), which never fully degrades its one central starch granule and during cell division selectively degrades the granule in the middle so that it is divided between the two daughter cells (Ral *et al.,* 2004). Interestingly, *O. taurii* does not contain an *SS4* gene (Leterrier *et al.,* 2008). This raises the possibility that because the organism never needs to initiate a new granule it does not require the unique function of SS4 to do so. An alternative perspective is that, because the *SS4* gene has been lost, the organism is no longer able to initiate new granules, resulting in strong selective pressure for acquisition of a new means of perpetuating its starch.

The reduced number of granules in the *ss4* mutant suggests a key role of SS4 in granule initiation. SS4 may be involved specifically in processes that allow the initiation of the semi-crystalline starch granule. In the *ss4* mutant these processes are restricted, so fewer

granules initiate. Alternatively SS4 may be involved in the initiation of synthesis of glucan polymers, which then self-assemble to initiate a starch granule. In the *ss4* mutant these initiating molecules are less abundant and/or inappropriate in structure, so self-assembly to form the nucleus of a granule is a less frequent event.

Although SS4 is clearly important for the initiation of starch granules, characterisation of the *Arabidopsis ss4* mutant thus far has been rather superficial and does not provide the information to allow the above ideas about how SS4 functions in granule initiation to be tested (Roldan *et al.,* 2007; Szydlowski *et al.,* 2009). In addition, interpretation of the *ss4* mutant phenotype is difficult because of complex pleiotropic effects. *ss4* mutant plants are slow growing, have a delayed flowering time, the leaves are paler and there is an altered diurnal pattern of starch turnover in the leaves compared to wild-type (Roldan *et al.,* 2007); this makes it difficult to deduce the primary effect of loss of SS4 on starch. To date there has been no analysis of the role SS4 plays in any species or organ other than *Arabidopsis* leaves. Roldan *et al.* (2007) found that SS4 was expressed throughout wild-type *Arabidopsis* plants, but did not examine starch in the *ss4* mutant in any organ other than the leaves. They did, however, note that while there was a reduced growth rate and delayed flowering time in the *ss4* mutant, fruit size, germination rate and the number of seeds per silique were unaltered. While SS4 was found to be expressed in both the leaves and endosperm of rice plants, no mutant plants were examined and a role for SS4 was not established (Dian *et al.,* 2005).

Prior to the start of my project, measurements of adenosine 5'-diphosphate glucose (ADPG) were made on *ss1*, *ss2*, *ss3*, *ss4*, Col wild-type, and Ws wild-type (*ss1* is in the *Arabidopsis* ecotype Ws background) plants (plants harvested 6h into a 12h day at JIC, analyses by John Lunn and Regina Feil at the Max Planck Institute for Molecular Plant Physiology, Golm, Germany). Both *ss2* and *ss3* have approximately wild-type levels of ADPG; *ss2* had 0.9 times and *ss3* had 1.1 times wild-type ADPG levels. The *ss1* mutant has ADPG levels approximately double that of the wild-type (x1.7), whereas *ss4* has levels approximately 59 times greater than the control (124.2 nmol g^{-1} FWT versus 2.1 nmol g^{-1} FWT; M. Pike, A. Smith, J. Lunn and R. Feil unpublished data). This suggests that something unique is occurring in *ss4* which does not occur in the other starch synthase mutants and which causes a build-up of ADPG. Thus although SS4 appears to be responsible for very little of the total starch synthase activity (Szydlowski *et al.,*

2009), the accumulation of ADPG suggests that SS4 plays a unique and essential role in converting ADPG into starch. For example, SS4 may play a role in amylopectin molecule initiation. SS4 may use ADPG to make a glucan primer molecule which is required by the other starch synthases as a substrate. In the absence of SS4, glucan chains initiate only very rarely and the concentration is low, making crystallisation to form a starch granule a much rarer event than in wild-type chloroplasts. With fewer initiations occurring in the *ss4* mutant this leads to a build up of ADPG, because there are fewer glucan chains present for the other SSs to act upon.

In this chapter I describe two new approaches to discover the role and importance of SS4 in granule initiation; production of a double mutant lacking both SS4 and ISA1 and production of lines in which loss of SS4 could be triggered in mature rosettes by induction of expression of RNAi.

A mutant which lacks both SS4 and ISA1 will provide information about the point at which SS4 acts during granule synthesis. It will reveal whether SS4 is required specifically for normal granule initiation, or whether it is also necessary for the initiation of glucan polymers. ISA1 has an important role in, but is not essential for, starch biosynthesis (Burton *et al.,* 2002; Delatte *et al.,* 2005; James *et al.,* 1995; Mouille *et al.,* 1996; Posewitz *et al.,* 2004; Streb *et al.,* 2008; Wattebled *et al.,* 2005). In the absence of ISA1 there is a reduction in the amount of glucan stored as semi-crystalline starch granules and instead glucans accumulate as a highly branched, soluble glucan called phytoglycogen (Delatte *et al.,* 2005; Streb *et al.,* 2008). It has been proposed that the role of ISA1 during normal starch biosynthesis is to promote amylopectin crystallisation by removal of misplaced branch points from newly-synthesised amylopectin molecules (Streb *et al.,* 2008) (see section 1.3.1.1 for further details). If SS4 is required specifically for the initiation of the starch granule I would expect that loss of SS4 would still allow phytoglycogen accumulation in an *isa1* background. If SS4 is important for the initiation of each glucan chain then I would expect either no phytoglycogen accumulation or - considering that the *ss4* mutant can eventually produce one starch granule - a strong reduction in phytoglycogen accumulation.

Use of a dexamethasone (dex) inducible RNA interference (RNAi) line that targets SS4 will allow a reduction in the expression of SS4 at specific times during development. This will allow me to dissect the complex pleiotropic phenotypes of the *ss4* mutant. The inducible RNAi technology is based upon the mechanism that exists in plants to defend against foreign mRNA e.g. viral mRNA introduced by plant viruses (Hamilton and Baulcombe 1999). Single stranded RNA forms a hairpin which is then processed into short interfering RNA (siRNA) molecules of 21 nucleotides. The siRNAs bind the RNA-induced silencing complex (RISC), which subsequently binds to and cleaves the foreign mRNAs which match the siRNA that is bound to it.

In inducible RNAi lines, the DNA fragment inserted into the construct is transcribed only when dex is present (Wielopolska *et al.,* 2005), therefore a plant harbouring an inducible RNAi construct will exhibit a wild-type phenotype unless treated with dex. The plant can be allowed to reach a suitable stage for analysis, and then sprayed with dex to eliminate or reduce expression of the target gene. An inducible RNAi line that targets SS4 will enable me to distinguish between an immediate requirement for SS4 for normal starch metabolism in mature leaves and a longer term requirement for establishment of granule numbers through leaf development. Any phenotype that does develop in the dex inducible RNAi line can be compared directly with wild-type plants and with the original *ss4* mutant. This allows direct observation of the primary effects of loss of expression. If following a reduction in SS4 the starch granules are unaltered in the mature leaves, this may be an indication that the starch granule number per chloroplast is established in the immature leaves.

There is no guarantee that an RNAi construct targeted to the *SS4* gene would result in a reduction in protein levels. The degree of reduction in transcript accumulation achieved in RNAi lines has been shown to vary from one target gene to another. For example, some genes show little or no reduction in transcript levels, whereas others have no detectable residual target RNA (Kerschen *et al.,* 2004). Factors that could affect the effectiveness of RNAi include; gene expression levels and patterns, target gene RNA turnover rate and sequence composition (Kerschen *et al.,* 2004).

In this chapter I describe my analysis of the *ss4* mutant and explore the role of SS4 in starch granule initiation. First I describe characterisation of the *ss4* mutant, including a

detailed analysis of starch accumulation and the importance of SS4 for starch metabolism through leaf development. I then present my results on the involvement of SS4 in granule initiation, including the genetic interaction of SS4 with ISA1. I then describe experiments to test the hypothesis that altering the level of SS4 will alter numbers of starch granules, including the production of a dexamethasone inducible RNAi line that targets SS4. Finally I discuss my results and describe how they build upon our existing knowledge of granule initiation.

4.2 Results

4.2.1 Characterizing the phenotype of the *starch synthase 4* (*ss4*) mutant of *Arabidopsis thaliana*

In this section I will describe analysis of the phenotypic alterations produced by the specific loss of SS4 from *Arabidopsis.* These observations provide a more rigorous and detailed characterisation of the effects of loss of SS4 than those already published (Roldan *et al.,* 2007).

The *AtSS4* (At4g18240) gene is located on chromosome 4 and consists of 16 exons separated by 15 introns. The *SS4* gene encodes a 1040 amino acid protein with a predicted mass of 117 747 Da (Roldan *et al.,* 2007). The first 42 amino acids comprise a chloroplast-targeting signal, rendering a mature protein of 112 997 Da (Roldan *et al.,* 2007). An *Arabidopsis* line with a potential T-DNA insertion in the *SS4* gene (SALK_096130) was acquired and a line homozygous for the insertion isolated by Chris Hylton (John Innes Centre, Norwich, UK). The T-DNA insertion is located in intron 4 (position +2186 with respect to the start codon Figure 4.1). Western blot analysis was performed to check for the absence of SS4 protein in the mutant *Atss4-3*, hereafter referred to as *ss4*. *Atss4-3* is an independent mutant allele from *Atss4-1* and *Atss4-2* used by Roldan *et al.* (2007). In *Atss4-1* and *Atss4-2* T-DNA insertions are located in introns 11 and 2 (position +3763 and +227 bp with respect to the start codon for *Atss4-1* and *Atss4-2*, respectively; Figure 4.1).

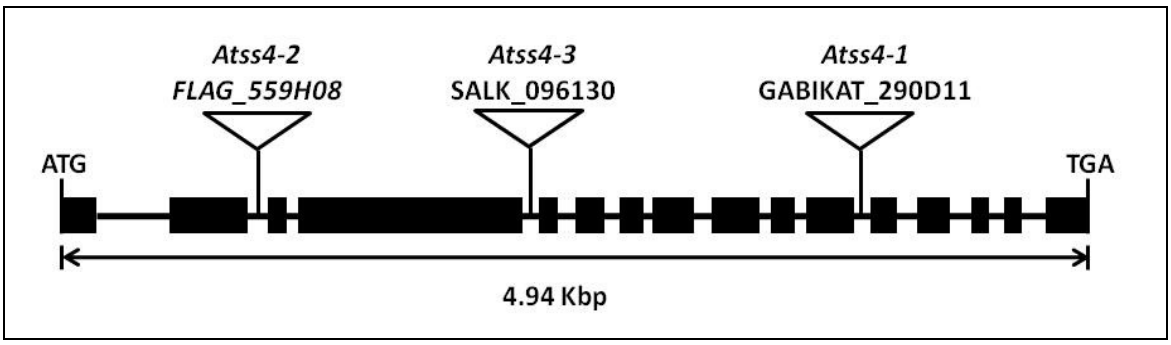

Figure 4.1: T-DNA insertions in locus *AtSS4*. Exons and introns are indicated as thick and thin black bars, respectively. Insertion sites of T-DNA in mutant lines *Atss4-1, Atss4-2* and SALK_096130 at introns 11 (+3763bp from start codon), 2 (+227bp) and 4 (+2186bp) respectively are indicated by triangles. *Atss4-1* and *Atss4-2* are the T-DNA insertion mutants identified and used by Roldan *et al.* (2007)

4.2.1.1 Starch and sugar accumulation in *ss4*

The *ss4* mutant has an unusual pattern of starch accumulation compared to wild-type plants. The *ss4* mutant has no starch in its immature leaves at either the end of the day or the end of the night (Dr Marilyn Pike, JIC; unpublished, Figure 4.2). Even the first true leaves that form are free from starch when immature (Figure 4.3), but this is not true of the cotyledons, which have a starch excess phenotype at the end of the night. In mature *ss4* leaves there is a starch excess phenotype compared to wild-type (Figure 4.2), with significant amounts of starch still present at the end of the night.

	End of Day	End of Night
wild-type		
ss4		

Figure 4.2: Wild-type and *ss4* rosettes decolourised in 80% ethanol and stained with iodine solution. Scale bar = 1 cm.

	End of Day	End of Night
wild-type		
ss4		

Figure 4.3: Wild-type and *ss4* seedlings decolourised in 80% ethanol and stained with iodine solution. Scale bar = 1mm

Roldan *et al*. (2007) reported that *ss4* mutants have a reduced rate of starch synthesis and degradation, based on analyses of whole rosettes. To quantify starch levels in the *ss4* mutant used in this study, leaves were harvested at the end of the 12 h light period and then again at the end of the 12 h dark period. The *ss4* rosette as a whole appears to have a reduced rate of starch turnover (Figure 4.4A). Starch content at the end of the illuminated period was reduced compared to the wild-type rosette: a 45.5% decrease. However, starch content at the end of the dark period was increased compared to wild-type: a 56.2% increase. Thus on a whole rosette basis there is a reduction in both synthesis and degradation rates in the ss4 mutant.

A more detailed analysis of starch accumulation across the rosette was carried out. Each plant was divided into five samples, each containing progressively older leaves (Figure 4.4C and D). Sample one contained the youngest leaves and sample five the oldest leaves. The starch content at the end of the day of the leaves in the oldest two fractions of the *ss4* mutant was similar to the wild-type, but all younger *ss4* fractions contained significantly less starch than the wild-type fractions (Figure 4.4C). Conversely, the starch content at the end of the night of the leaves in the youngest two fractions of the *ss4* mutant was similar to the wild-type, but all older *ss4* fractions contained significantly more starch than the wild-type fractions (Figure 4.4D).

Based on these measurements, there are two striking differences between the wild-type and *ss4* mutant in terms of starch turnover. Firstly, *ss4* has extremely restricted starch metabolism in the young leaves (Figure 4.4B). Secondly, whereas the starch turnover peaks in newly-expanded leaves (fractions 2 and 3) in wild-type, then declines somewhat as leaves age, the opposite is true in *ss4*. In *ss4* starch turnover increases as the leaves age and almost reaches wild-type levels in the oldest leaves (Figure 4.4B), demonstrating that the starch excess phenotype at the end of the night develops progressively as the leaves age. The above evidence clearly shows that SS4 is necessary in younger leaves for the accumulation of starch, but is also required for normal starch turnover as the leaf matures.

Roldan *et al.* (2007) found the sucrose, glucose and fructose levels in the *ss4* rosette to be higher than wild-type at midday, but did not analyse these metabolites at other times of the day. In this study sugar levels in the *ss4* mutant and wild-type were analysed at

both the end of the 12 h light period and at the end of the 12 h dark period (Figure 4.5). At the end of the day *ss4* rosettes contain significantly more sucrose and glucose, but significantly less fructose than wild-type (Figure 4.5A). At the end of the night the two genotypes are more similar. There was no significant difference between the sucrose levels, but *ss4* had significantly more glucose and fructose. Sugar levels across the rosette were also analysed (Figure 4.5B-D). In general, sugar contents of *ss4* and wild-type are similar in the older leaves (fractions 4 and 5) and the major differences between the genotypes are generally seen in the youngest leaves (fractions 1 and 2).

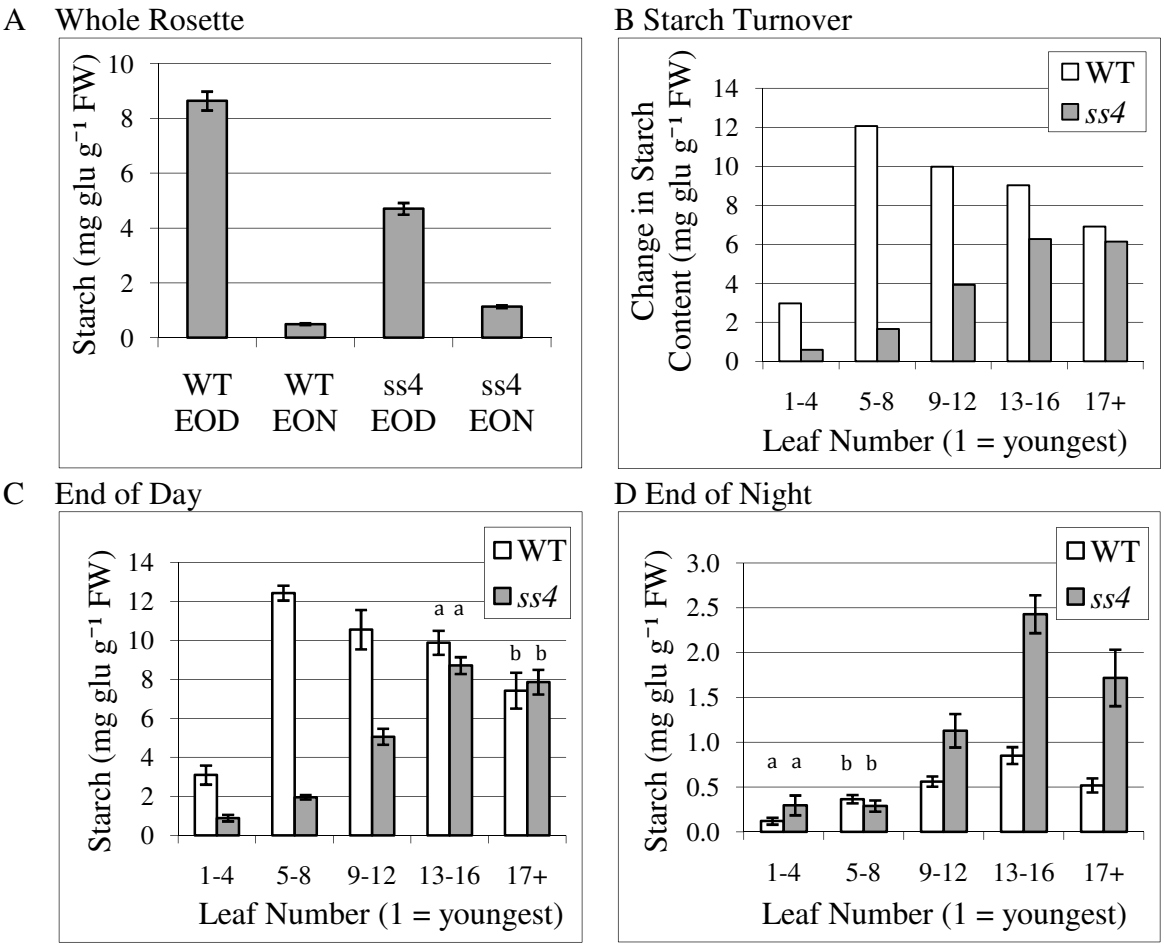

Figure 4.4: Starch levels in wild-type (WT) and the *ss4* mutant 25-day-old rosettes. (A) Starch in the whole rosette. (B) Starch turnover across the rosette. Data are differences in starch levels at the end of the day and end of the night taken from values in C and D. (C and D) Starch levels across the rosette at the end of the day and end of the night. Each bar is the mean (±SE) of at least seven replicate samples (except EOD leaves 17+, WT = 3 replicates). Bars with the same letter are not significantly different from each other.

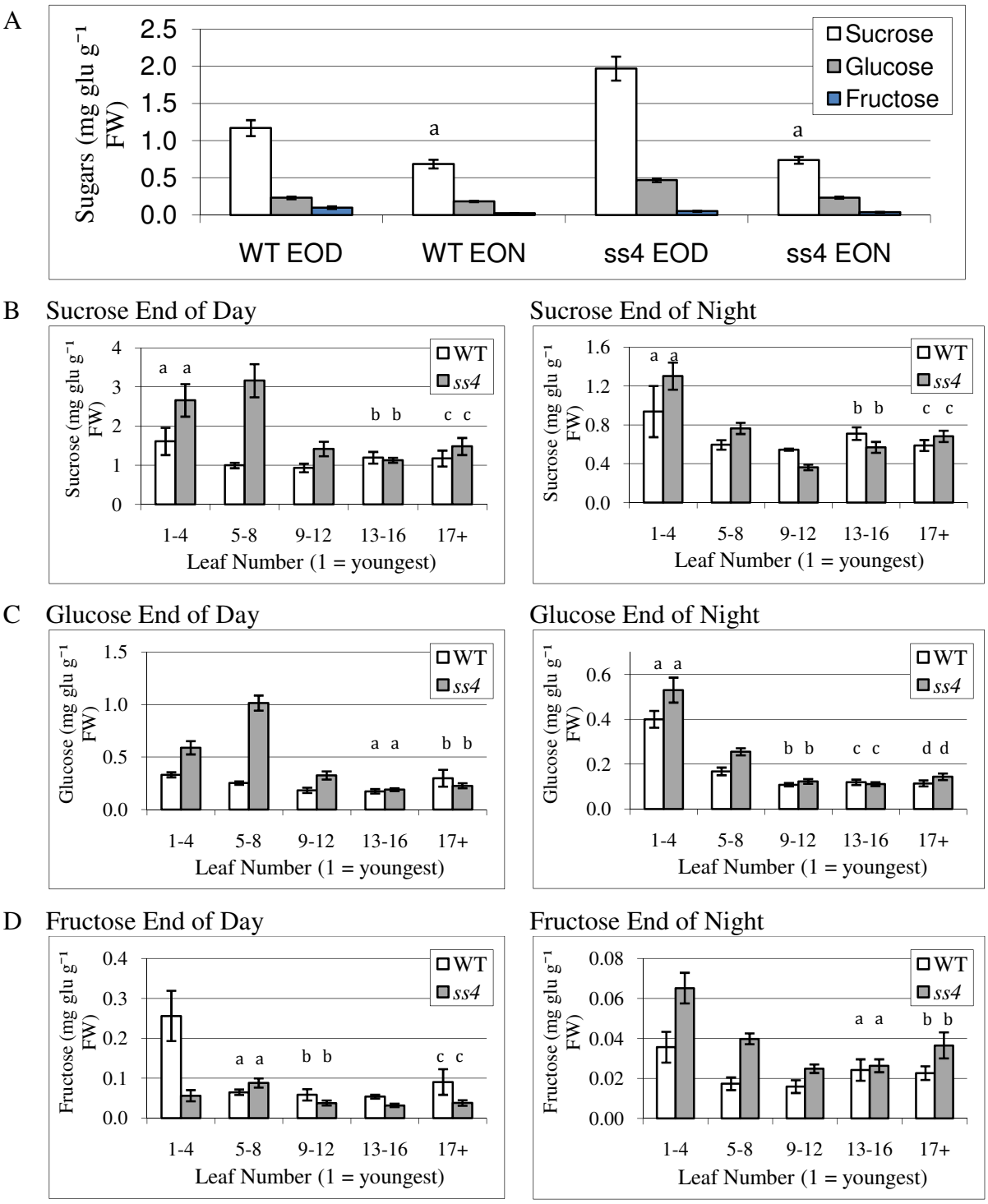

Figure 4.5: Sugar levels in wild-type (WT) and the *ss4* mutant. (A) Whole rosette. (B-D) Sugar levels across the rosette. (B) Sucrose (C) Glucose. (D) Fructose. EOD = End of day. EON = End of night. Each bar is the mean (±SE) of at least seven replicate samples (except: EOD, leaves 17+, WT = 3 replicates and EON sucrose, leaves 1-4, WT = 5 replicates). Bars with the same letter are not significantly different from each other. Note: all scale bars are different.

	End of Day	End of Night
Whole rosette	t (14) = -9.74, p <0.001	t (14) = 10.68, p <0.001
Leaf Number 1 to 4	t (14) = 4.28, p = 0.002	t (14) = 1.50, p = 0.170
Leaf Number 5 to 8	t (14) = 26.41, p <0.001	t (14) = 1.45, p = 0.170
Leaf Number 9 to 12	t (14) = 5.11, p <0.001	t (14) = 2.91, p = 0.019
Leaf Number 13 to 16	t (14) = 0.66, p = 0.518	t (14) = 6.81, p <0.001
Leaf Number 17+	t (8) = 0.38, p = 0.712	t (13) = 3.69, p = 0.008

Table 4.1: Statistical analysis (*t*-test) performed on the starch content data from the wild-type and *ss4* rosettes displayed in Figure 4.4. Test of the null hypothesis that the mean starch contents of the two datasets are not different. The degrees of freedom (listed in brackets), test statistic and statistical significance are displayed.

	Sucrose		Glucose		Fructose	
	End of Day	End of Night	End of Day	End of Night	End of Day	End of Night
Whole rosette	t (14) = 4.14 p = 0.001	t (14) = 0.70 p = 0.495	t (14) = 7.80 p <0.001	t (14) = 3.18 p = 0.007	t (14) = -2.65 p = 0.026	t (14) = 3.67 p = 0.002
Leaf Number 1 to 4	t (13) = 1.90 p = 0.080	t (11) = 0.66 p = 0.525	t (12) = 3.82 p = 0.004	t (14) = 1.94 p = 0.073	t (13) =-3.10 p = 0.019	t (13) = 2.71 p = 0.018
Leaf Number 5 to 8	t (14) = 5.05 p = 0.001	t (14) = 2.25 p = 0.041	t (14) =10.25 p <0.001	t (14) = 3.75 p = 0.002	t (14) = 1.74 p = 0.104	t (14) = 5.41 p < 0.001
Leaf Number 9 to 12	t (14) = 2.26 p = 0.041	t (14) = -6.05 p < 0.001	t (14) = 3.06 p = 0.008	t (14) = 1.16 p = 0.265	t (14) = -1.34 p = 0.210	t (14) = 2.32 p = 0.036
Leaf Number 13 to 16	t (13) = -0.41 p = 0.687	t (14) = -1.64 p = 0.123	t (14) = 0.64 p = 0.529	t (14) = -0.58 p = 0.571	t (13) = -3.47 p = 0.004	t (14) = 0.34 p = 0.740
Leaf Number 17+	t (10) = 0.89 p = 0.392	t (14) = 1.18 p = 0.259	t (9) = -1.21 p = 0.257	t (14) = 1.51 p = 0.153	t (9)= -1.60 p = 0.240	t (14) = 1.89 p = 0.080

Table 4.2: Statistical analysis (*t* test) performed on the sugar (sucrose, glucose and fructose) measurements across rosettes of wild-type and *ss4* plants displayed in Figure 4.5. Test of the null hypothesis that the mean sugar contents of the two datasets are not different. The degrees of freedom (listed in brackets), test statistic and statistical significance are displayed.

4.2.1.2 Starch degradation in *ss4*

My results showed that starch turnover is reduced in leaves of *ss4* plants (Figure 4.4B). To investigate further the capacity for starch degradation, I examined the effect on starch content of a prolonged period of darkness. The starch content of the *ss4* rosette is still higher than in wild-type, even after 72 hours of darkness (Figure 4.6). After 24 hours of darkness wild-type plants are almost completely depleted of starch, with only 0.4% of the starch present at the beginning of the experiment remaining. However, after 24 hours of darkness starch levels in *ss4* rosettes are almost ten times higher than wild-type levels, with 6.5% of the starch present at the beginning of the experiment remaining. The level of starch in the *ss4* mutant remains approximately the same over the next 24 hours (48 h dark), before being degraded further over the final 24 hours of the experiment (72 h dark), till only 1.6% of the starch present at the beginning of the experiment remains. However, even after 72 hours of darkness *ss4* rosettes contain almost three times more starch than wild-type rosettes and starch levels are still significantly higher than wild-type levels. This indicates that a proportion of the starch in *ss4* is more resistant to degradation, or alternatively that the overall metabolism of the *ss4* mutant alters during an extended night, reducing the demand for carbon, and as a result carbohydrate stores are preserved for a longer period of time.

A

	0 hours dark	12 hours dark	36 hours dark	72 hours dark
Wild -type				
ss4				

B

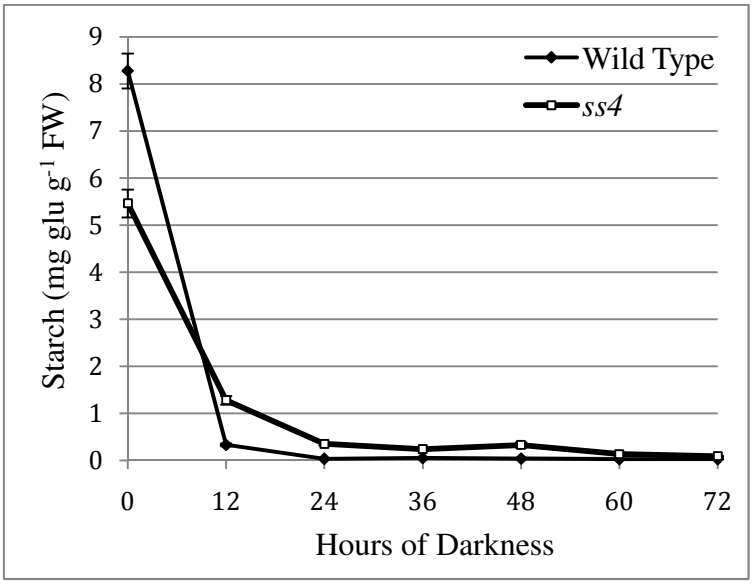

C

	Hours of Darkness						
	0	12	24	36	48	60	72
t	5.93	-9.91	-10.92	-6.48	-5.35	-5.6	-5.2
d.f.	10	10	10	10	9	10	10
p	< 0.001	< 0.001	< 0.001	< 0.001	0.002	< 0.001	0.003

Figure 4.6: Starch in the whole rosette of wild-type and *ss4* after transfer to continuous darkness. Prior to transfer to continuous darkness plants grown for 25 days in 12h light/12h dark conditions. Experiment begins at the end of a 12 h light period. (A) Rosettes decolourised with ethanol and stained with iodine solution. Scale bar = 1cm. (B) Starch levels in the rosettes of WT and *ss4* plants. n = 6 ± SE. Where error bars are not visible the SE is smaller than the symbols. (C) Statistical analysis (*t*-test) performed on the starch levels in wild-type and *ss4* rosettes data displayed in B. Test of the null hypothesis that the mean starch contents of the two datasets are not different. The test statistic, degrees of freedom (d.f.) and statistical significance are displayed.

4.2.1.3 Starvation in *ss4*

In wild-type plants starch degradation provides sufficient sugars to prevent starvation. Starvation symptoms are seen only if the night is artificially extended (see section 1.2.3). The inner leaves of the *ss4* mutant lack starch and the outer leaves have a reduced rate of starch degradation compared to wild-type. The sugars released from the starch granules of the mature leaves may be sufficient to compensate for the lack of starch in the immature leaves, but it seems possible that the inner leaves starve during the normal 12 h dark period.

To determine whether the altered starch turnover pattern of the *ss4* mutant causes starvation across the rosette, I used a starvation reporter line, harbouring the promoter of the sugar-repressed or "carbohydrate starvation-marker" gene *At*1g10700, fused to luciferase (*pAt1g10070::LUC*, developed and described in Graf *et al.* (2009; 2010)). The fusion of a starvation responsive promoter fragment and the luciferase (LUC) reporter gene should allow determination of the onset of carbon starvation in intact plants through measurements of bioluminescence. Characterisation of the *pAt1g10070::LUC* line by Graf *et al.* (2009; 2010) showed that LUC activity is induced strongly and rapidly in response to carbon starvation during extended night periods, but under normal day-night cycles there is no detectable luciferase expression (Graf *et al.,* 2010). Bioluminescence or photon emission is the result of a reaction catalysed by the LUC enzyme on its substrate luciferin. Photon emission is proportional to the LUC activity of the sample and therefore quantification of the photon emission from the rosette leaves allows an indirect estimate of the transcription of the "starvation reporter" gene. LUC expression was measured and analysed using the NightOwl imaging system with WinLight software. Examples of typical images produced by the NightOwl imaging system with WinLight software from wild-type and *ss4* mutant plants, along with an illustration of how the photon emission from the inner and outer leaves is segregated, are displayed in Figure 4.7.

The *At1g10070* gene was selected by Graf (2009) as the "starvation reporter" because there is a strong and fast induction of expression under growth conditions expected to cause carbon starvation in plants. Analysis of microarray data showed *At1g10070* to have a stronger than 4-fold induction in response to sucrose and glucose starvation, low atmospheric carbon dioxide and an extended night (6 h into an extended night) (Graf

2009). Importantly, there are very low expression levels throughout the normal diurnal cycle and changes in expression level over the diurnal cycle are small, thereby avoiding high levels of background signal. Characterisation of the *pAt1g10070::LUC* reporter line by Graf (2009) showed that in response to an extended night LUC activity increases with a delay of approximately one hour compared to rise in *At1g10070* transcript level.

To introduce the starvation reporter gene into the mutant backgrounds, I crossed the *ss4* mutant with the *pAt1g10070::LUC* reporter line. In the F2 population I obtained plants homozygous for the *ss4* mutation (using PCR to genotype plants), and containing a copy of the *pAt1g10070::LUC* insert. Because only one copy of the *pAt1g10070::LUC* insert is required for bioluminescence, it is unknown whether plants which display bioluminescence after exposure to an extended night are heterozygous or homozygous for the *pAt1g10070::LUC* insert. Therefore, the F3 population was screened for segregation of bioluminescence. Lines in which all plants displayed bioluminescence (after exposure to an extended night) were confirmed as homozygous for both the *pAt1g10070::LUC* insert and the *ss4* mutation, and were used in the following experiments.

To observe the LUC expression and hence the starvation pattern in whole rosettes during the normal night, wild-type plants were grown under normal 12 h light-12 h dark conditions for 21 days and *ss4* plants for 28 days, and then transferred to the NightOwl at the end of a normal 12 h day. Wild-type and *ss4* plants of different ages were used in order to compare plants of approximately the same size, because *ss4* has a slower growth rate than wild-type. It should be noted that there is a five to ten minute delay between removal of the plants from the growth cabinet and the first image being taking in the NightOwl. Using the WinLight software the bioluminescence expressed by the whole rosette can be measured or the outer/mature and inner/immature leaves can be measured separately, as illustrated in Figure 4.7A. As previously observed (Graf *et al.,* 2010), wild-type plants do not express LUC during the normal 12 h night, and LUC expression (visualised by bioluminescence) only begins to occur an hour into the extended night (Figure 4.8). In contrast, both the inner and outer leaves of the *ss4* mutant express LUC and therefore appear to be experiencing carbohydrate starvation at the beginning of the night (Figure 4.8). The immature leaves of the *ss4* mutant display

higher levels of LUC expression than the mature leaves. The LUC expression peaks in *ss4* two hours into the night, before decreasing as the night proceeds (Figure 4.8).

To observe the LUC expression and hence the starvation pattern in whole rosettes during an extended night, a separate batch of plants was grown under normal 12 h light-12 h dark conditions for 21 days for both wild-type and *ss4* plants, transferred to the NightOwl 8 h into a normal night, then held in darkness for the remainder of the normal night and a further extended night period. The pattern of LUC expression in *ss4* and wild-type rosettes is displayed in Figure 4.9. The bioluminescence of the whole rosette was measured (Figure 4.9B), and the outer/mature (Figure 4.9C) and inner/immature (Figure 4.9D) leaves were measured separately.

Both the inner and outer leaves of the wild-type rosette begin to show bioluminescence and therefore exhibit symptoms of starvation about an hour into the extended night (13 h dark). After a short lag phase, bioluminescence increased exponentially, implying that the carbohydrate starvation was worsening. This is the same pattern observed by Graf *et al.* (2010). The outer and inner leaves of the *ss4* mutant vary in their bioluminescence emission and therefore in their degree of carbohydrate starvation. The inner leaves of *ss4* have a low level of LUC expression at the start of the experiment, 8 hours into a normal night, indicating that the immature leaves, which contain very low levels of starch at the end of the day, are undergoing carbohydrate starvation during the normal night. In contrast the outer, starch-containing leaves of *ss4* do not begin to display bioluminescence until approximately three hours into the extended night (15 h dark), two hours later than the wild-type rosettes display bioluminescence (Figure 4.9C). This could indicate that the slower starch degradation rate in the *ss4* mutant (Figure 4.4 and 4.6), is potentially delaying the onset of LUC expression caused by carbohydrate starvation in the mature leaves. The level of starch degradation in these mature leaves appears to be unable to maintain adequate sugar levels in the immature leaves, which express LUC long before it is expressed in the mature leaves. The level of LUC expression remains low in the immature leaves of *ss4* until four hours into the extended night (16 h dark), when, an hour after the mature leaves begin to display bioluminescence, LUC expression begins to increase (Figure 4.9D).

There was a difference between the two NightOwl experiments in the level of LUC expression in *ss4* plants after eight hours of night (compare Figure 4.8 and Figure 4.9). In the first experiment mature leaves were expressing LUC during a normal night whereas in the second experiments there was no LUC expression in these leaves during a normal night; expression was seen only in the extended night. This difference may arise from the fact that *ss4* plants were seven days older in the first than the second experiment. Further experiments would be required to confirm that this is a developmental difference and to investigate its causes.

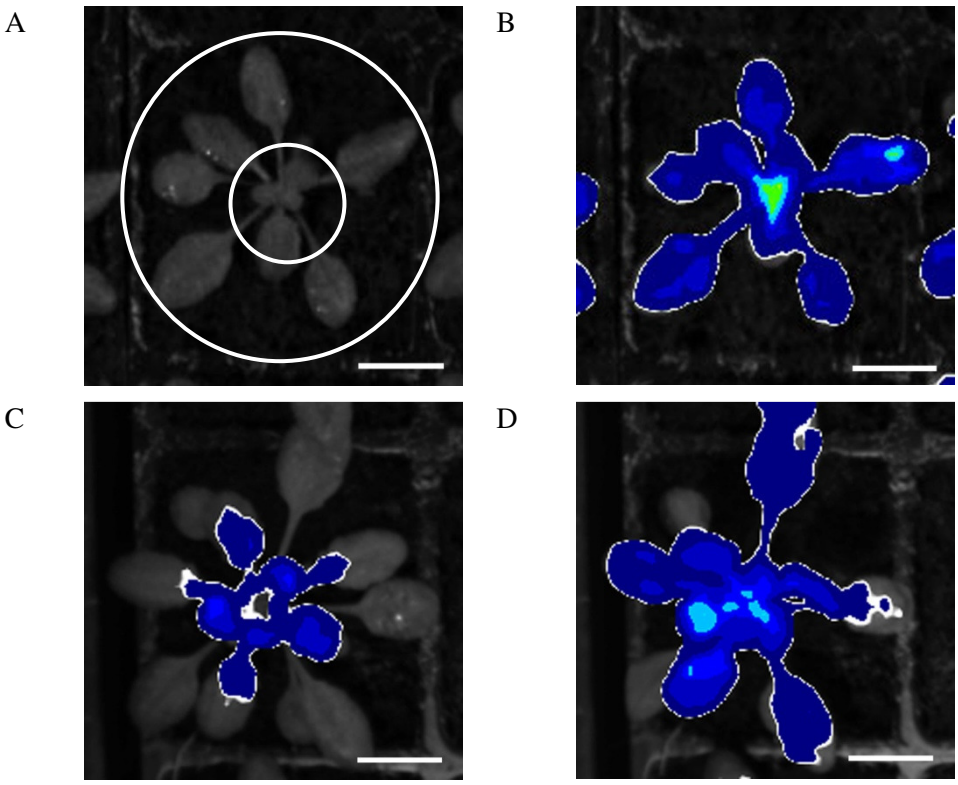

Figure 4.7: Typical images produced by the NightOwl imaging system with WinLight software. The true image and the bioluminescence image are overlaid in order to view which areas of the rosette are expressing the *pAt1g10070::*LUC reporter. (A) Wild-type rosette at the end of the day, after 0 hours dark. Using the WinLight imaging software specific areas can be selected from which the luminescence is measured. For example, the smaller circle encompasses the inner leaves and the larger circle the whole rosette. Shapes other than a circle can be drawn to specify regions of interest, for example areas can be drawn freehand. In any one experiment the same sized region of interest was used for all rosettes for the inner leaves. (B) Wild-type rosette after 24 hours dark. (C) *ss4* rosette at the end of the day, after 0 hours dark. (D) *ss4* rosette after 24 hours dark. In this experiment the wild-type plants were 21 days old and the *ss4* plants were 28 days old, in order to compare plants of similar sizes. Scale bar = 1 cm.

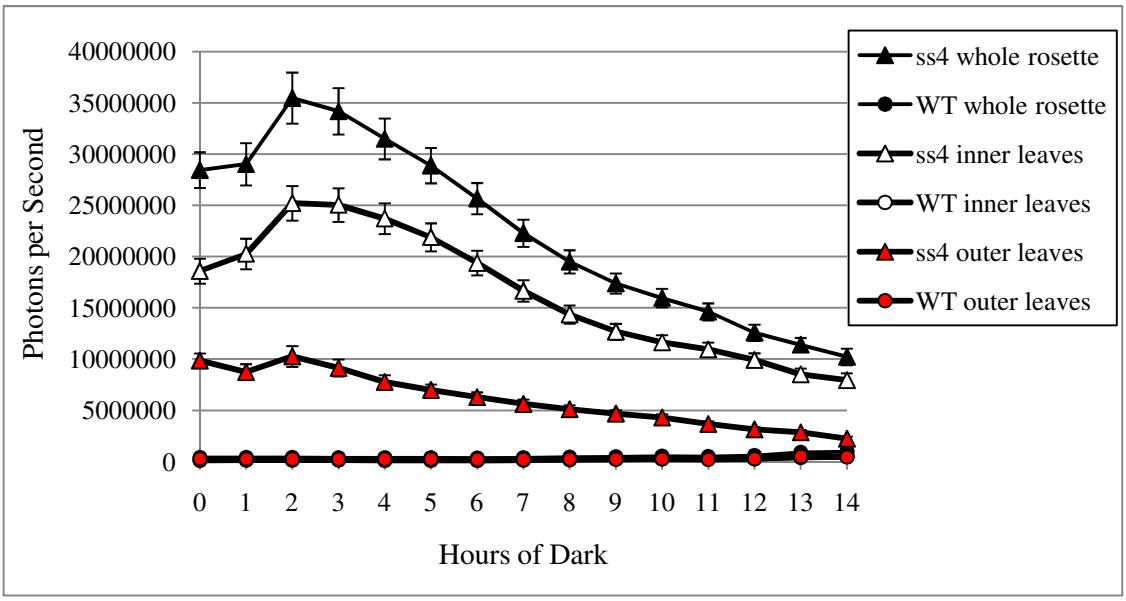

Figure 4.8: Emission of bioluminescence by wild-type (WT) and *ss4* mutant rosettes expressing LUC from the promoter of the "starvation reporter" gene At1g10070 (*pAt1g10070::*LUC) during a normal night. Plants transformed with the starvation reporter (*pAt1g10070::*LUC) construct were grown under 12 h day-12 h night conditions. Experiment began at the start of the normal night (0 h), after a normal day of 12 h light. Normal night ends after 12 h dark. In order to compare plants of approximately similar sizes, the wild-type plants were 21 days old and the *ss4* plants were 28 days old. n = 54 plants (18 plants from 3 independent experiments). Where error bars are not visible they are smaller than the symbols.

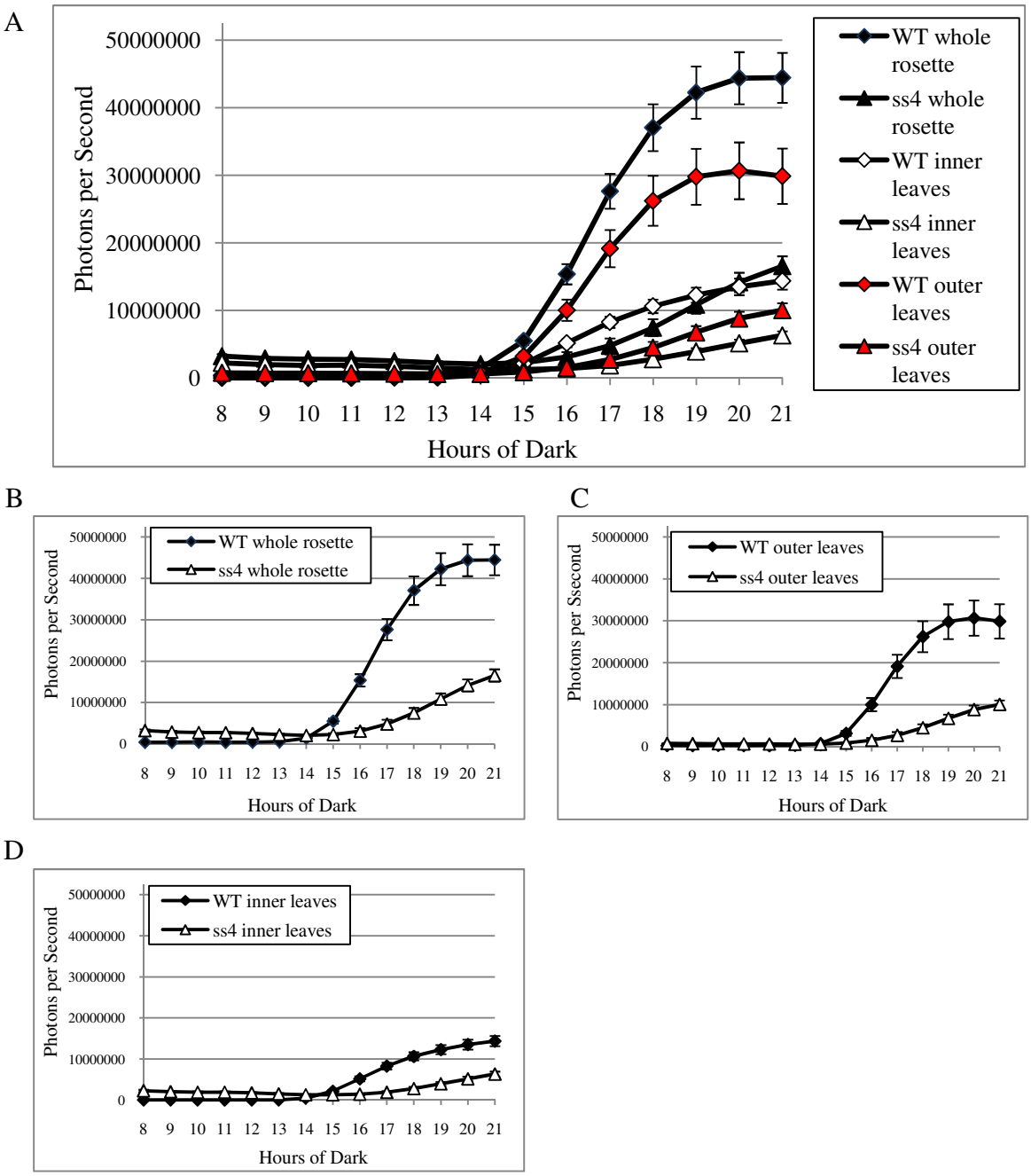

Figure 4.9: Emission of bioluminescence by wild-type (WT) and *ss4* mutant plants expressing LUC from the promoter of the "starvation reporter" gene At1g10070 (*pAt1g10070::*LUC) during an extended night. (A) All data (B) Whole rosette. (C) Outer leaves. (D) Inner leaves. Plants transformed with the starvation reporter (*pAt1g10070::*LUC) construct were grown under 12 h day-12 h night conditions for 21 days. Experiment began 8 h into the normal night. Normal night ends after 12 h dark. n = 27 plants ± SE (9 plants from 3 independent experiments). WT = wild-type. Where error bars are not visible they are smaller than the symbols.

4.2.2 Involvement of SS4 during development

The experiments above reveal very different effects of loss of SS4 in young and old leaves. To discover whether this reflected differences in levels of SS4 protein across the rosette in WT leaves, I investigated changes in the protein through leaf development.

An antibody raised against an SS4 peptide (Chris Hylton, JIC) was used to compare SS4 levels in immature and mature leaves of wild-type and *ss4* mutant plants (Figure 4.10). Immature and mature leaves of wild-type plants contain approximately equal quantities of SS4 protein on a fresh weight basis (Figure 4.10). Western blots using the SS4 antiserum always show the presence of two bands. This was also noted for the antibody used by Roldan *et al.* (2007). These bands approximately match the expected size of the mature SS4 protein and are absent from the mutant line (Figure 4.10A). The mature leaves appear to have a greater amount of the SS4 protein as the lower band than the immature leaves (Figure 4.10A and B), but while there is a small difference, there is a low number of replicates and the standard errors are large. A western blot is not fully quantitative, and I cannot draw any conclusions on the difference in activity from such a small difference.

A

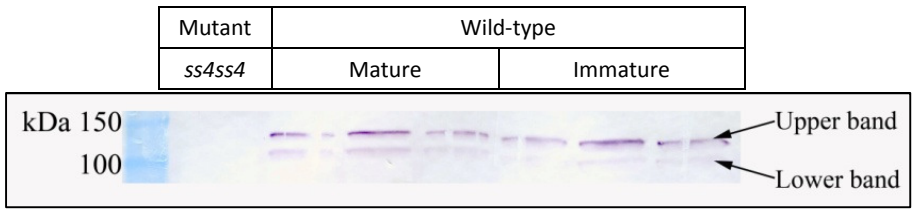

B

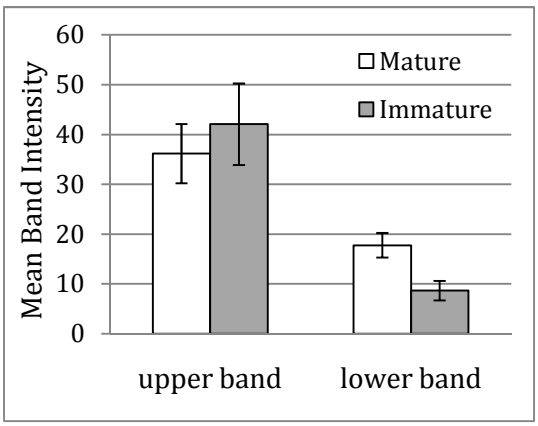

	Mature		Immature	
	Band Intensity	SE	Band Intensity	SE
Upper Band	36.2	8.3	42.1	10.5
Lower Band	17.8	5.3	8.7	4.2

Figure 4.10: Comparison of SS4 protein levels in mature and immature leaves of wild-type plants. (A) Western blot of wild-type leaves. (B) Western blot band intensities (mean pixel intensity) for the blot pictured in (A) ± SE (n = three bands for each leaf age from the same western blot). Each lane on the blot contains extract from a separate plant, with 40µl of protein extract loaded in each lane. All extracts contain the same mg tissue per ml extraction buffer. To check the equal loading a gel was run at the same time, using the same extracts as used for the western blot, and stained with Coomassie® InstantBlue™ stain (not shown). Using Adobe Photoshop software, images are converted to greyscale and mean pixel intensity of each band is measured (see section 2.15).

It is not known whether SS4 is important for starch metabolism in parts of the plant other than the leaves. To discover whether SS4 has different roles in starch metabolism in different parts of the plant, I examined the starch phenotype of root tips and siliques of *ss4*.

I observed that the gravitropic response of *ss4* roots is altered. Although many roots of vertically grown *ss4* seedlings grew downwards, a significant number deviated from the gravity vector (Figure 4.11). The roots of vertically grown wild-type plants were straighter than *ss4* roots and more uniformly oriented with respect to gravity. The distribution around and the extent of deviation from the gravity vector (vertically down) of roots in vertically orientated Petri dishes are shown in Figure 4.12. The mean angle from the vertical of wild-type roots was 9.3^{o} (± SE 0.5), whereas it was 20.7^{o} (± SE 1.1) for *ss4*. The largest variation in wild-type roots was 30^{o}, while some *ss4* roots deviated more than 90^{o} from the gravity vector (Figure 4.12B and 4.13E-G).

The columella cells and lateral root cap cells of different *ss4* plants vary in the amount of starch that they contain (Figure 4.13), which could explain the variation in gravitropic response among *ss4* roots. In fact, the amount of starch present in the root cap appears to correlate with the deviation of the root from vertical (Figure 4.13). The root cap shown in Figure 4.13A is a typical wild-type root. There was very little variation in the amount of starch present in wild-type root caps and the reduced levels seen in *ss4* (Figure 4.13D-G) were never observed. The starch content of the *ss4* developing siliques (Figure 4.14) also appears to be reduced compared to wild-type.

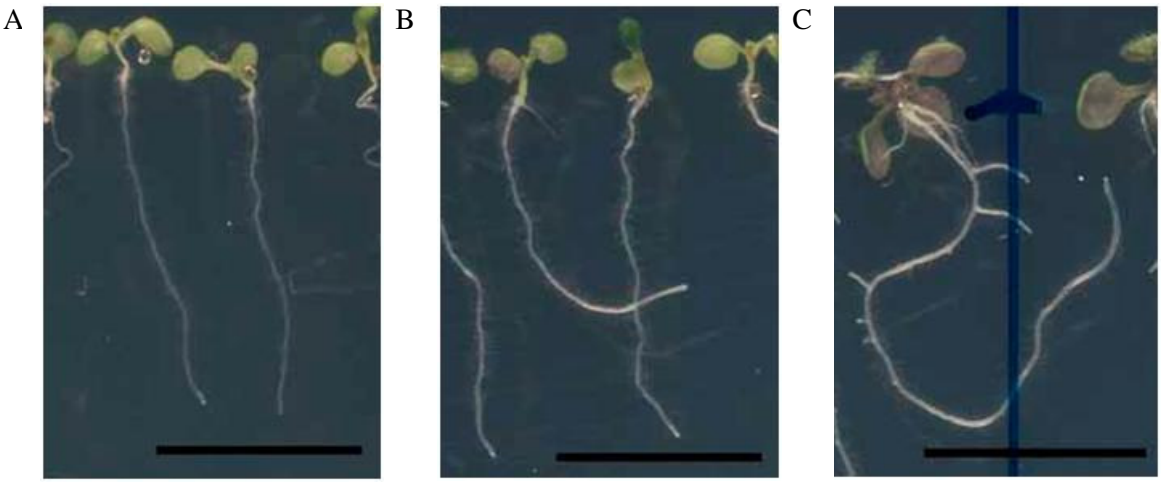

Figure 4.11: Wild-type and *ss4* seedlings grown vertically. (A) Wild-type. (B - C) *ss4*. A and B = 4 days after germination. C = 8 days after germination. Scale bar = 1 cm

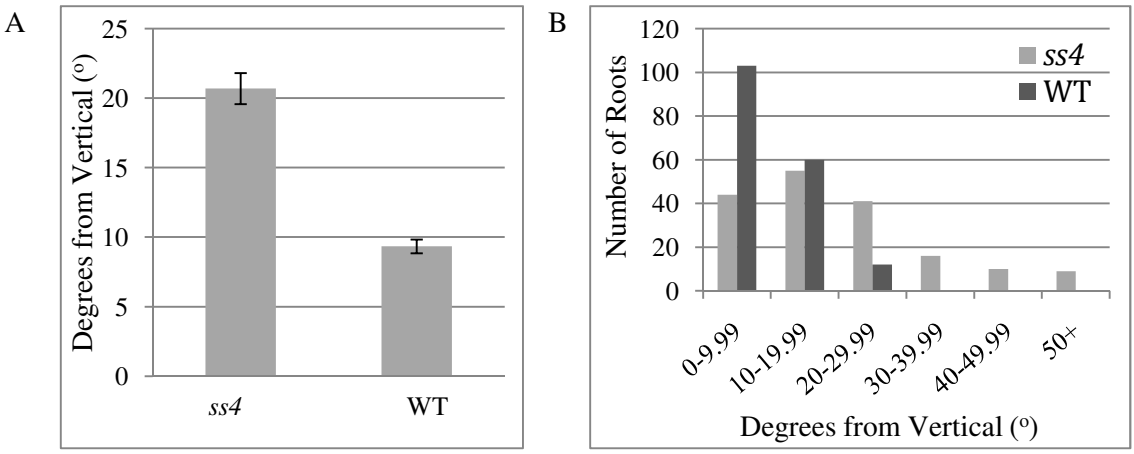

Figure 4.12: Deviation of the roots of vertically grown wild-type (WT) and *ss4* seedlings of Arabidopsis from the gravity vector. (A) Mean deviation from gravity vector ± SE. (B) Histogram of the deviation from gravity vector. Each bar represents a 10^{o} interval (except for 50^{o}+). Zero degrees represents the gravity vector. n = 175 plants per genotype. The above trend remains the same whether plants are grown under continuous light or 16 h light/8 h dark and on media with or without sucrose. For details of the growth conditions and measuring of the deviation from gravity vector, see section 2.13.

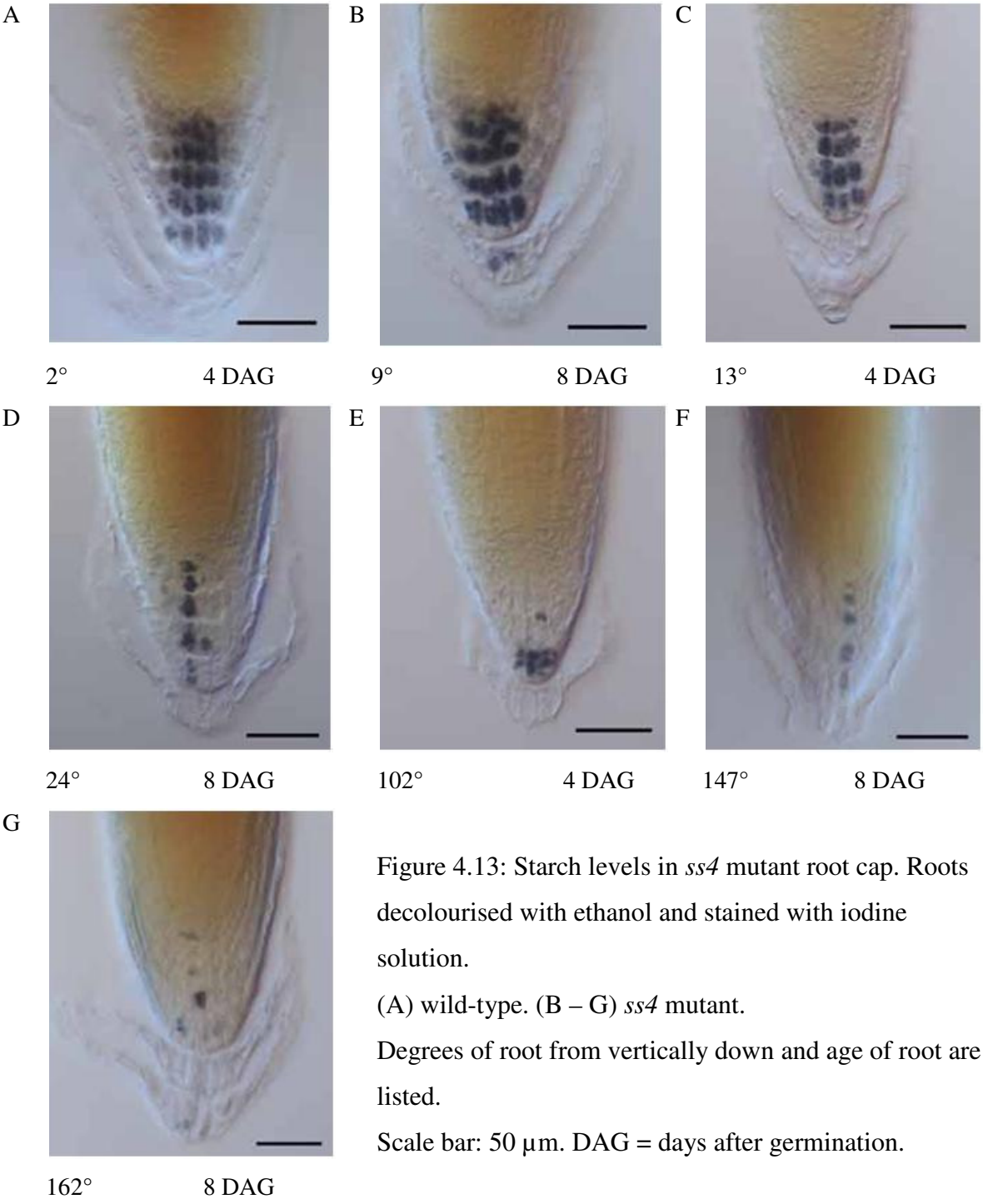

Figure 4.13: Starch levels in *ss4* mutant root cap. Roots decolourised with ethanol and stained with iodine solution.
(A) wild-type. (B – G) *ss4* mutant.
Degrees of root from vertically down and age of root are listed.
Scale bar: 50 µm. DAG = days after germination.

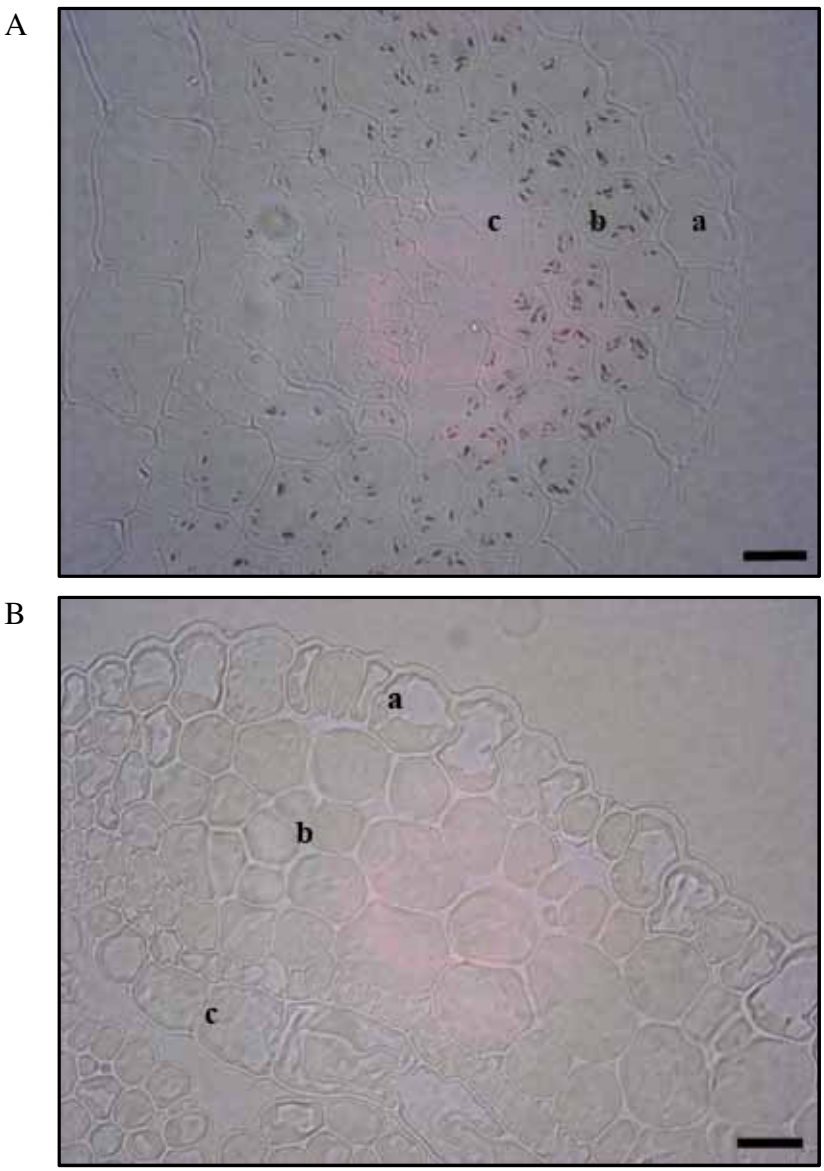

Figure 4.14: Starch in the silique walls. Sections through maturing siliques stained with iodine solution. (A) Wild-type. (B) *ss4*. a = exocarp b = mesocarp c = endocarp. Bar = 10 µm. Typical images of five plants examined.

4.2.3 The genetic interaction between *SS4* and *ISA1* during granule synthesis

To learn more about the role of SS4 in starch granule initiation I crossed the *ss4* mutant to an *Arabidopsis* line homozygous for a T-DNA insertion in the *ISA1* gene At2g39930 (SALK_042704; *Atisa1-1*), hereafter referred to as *isa1*. Double mutants homozygous for both the *ss4* and *isa1* mutations were identified from the F2 population via PCR (Figure 4.15). Both the *ss4* and *isa1ss4* mutant appear paler than the wild-type and *isa1* plants.

Both the SALK_042704 T-DNA insertion mutant (exon 13; position +4591 bp with respect to the start codon) and the SALK_029442 T-DNA insertion mutant (exon 13; position +4566 bp with respect to the start codon) have been referred to as *Atisa1-1* (Delatte *et al.,* 2005; Wattebled *et al.,* 2005). The *isa1* mutant used in my study was a gift from Prof. Sam Zeeman (ETH, Zurich) and was described in Delatte *et al.* (2005). The *isa1* mutants lack a functioning ISA1 protein and as a result have reduced synthesis of starch granules and increased production of a highly branched, soluble glucan called phytoglycogen (see section 1.3.1.1).

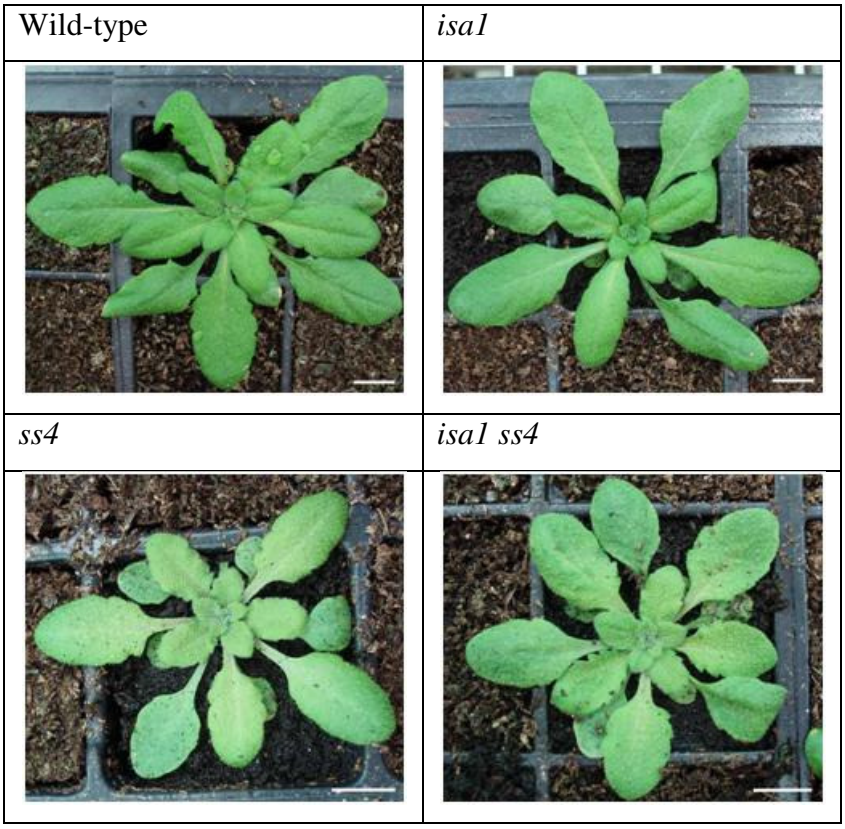

Figure 4.15: Twenty-five-day-old rosettes of wild-type, *isa1*, *ss4* and *isa1 ss4*. Scale bar = 1 cm

4.2.3.1 Glucan accumulation in the *isa1* and *isa1 ss4* mutants

Staining leaves with iodine revealed that the *isa1ss4* mutant has a distinct starch phenotype, different from either of its parents (Figure 4.16). Both *isa1* and *isa1ss4* stain a red colour with iodine solution, indicating the presence of phytoglycogen, whereas the *ss4* mutant and wild-type stain a purple colour with iodine solution. While the whole of the mature leaf of the *isa1ss4* mutant stains a red colour, indicating phytoglycogen throughout, the younger leaves of the *isa1ss4* mutant have low levels of glucans, similar to the *ss4* mutant (Figure 4.16).

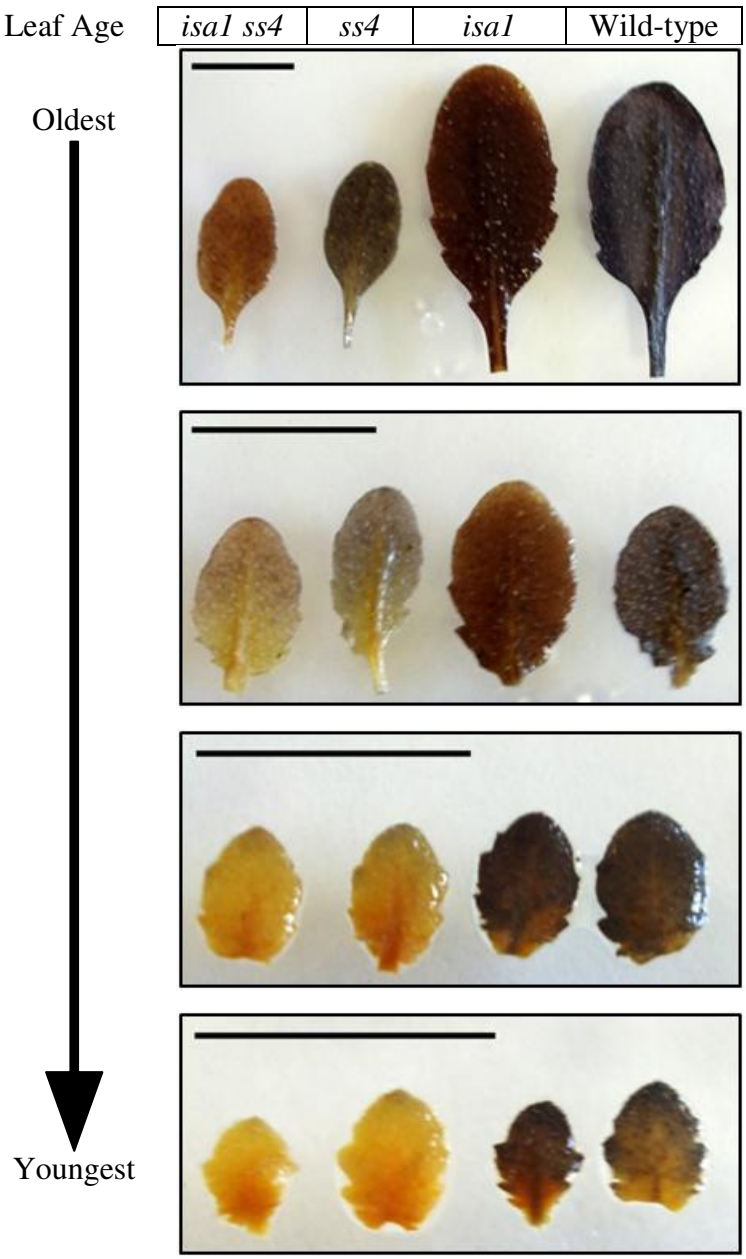

Figure 4.16: Leaves dissected from twenty-five-day-old wild-type, *isa1, ss4* and *isa1 ss4* rosettes harvested at the end of the light period, decolourised in 80% ethanol and stained with iodine solution. Scale bar = 1 cm.

The pattern of glucan accumulation in the *isa1ss4* mutant can be seen more clearly in Transmission Electron Microscopy (TEM) sections of mesophyll cells (Figure 4.17). The chloroplasts in mature leaves of the *ss4* mutant contained on average one (mean 1.1 ± SE 0.04 of 40 random chloroplasts from four sections) large starch granule relative to wild-type granules. This contrasts with wild-type mature leaves, where an average of 3.4 (± SE 0.2, of 40 random chloroplasts from four sections) clearly defined granules can be seen per chloroplast in section. In *isa1* and *isa1ss4* mature leaves there are no distinct starch granules and rather a diffuse material forms inside the chloroplasts, which is assumed to be phytoglycogen. In immature leaves the chloroplasts of *ss4* and *isa1ss4* appear to lack either starch granules or the putative phytoglycogen. Immature leaves of wild-type plants contain clearly defined starch granules, while those of *isa1* contain a mix of starch granules and phytoglycogen.

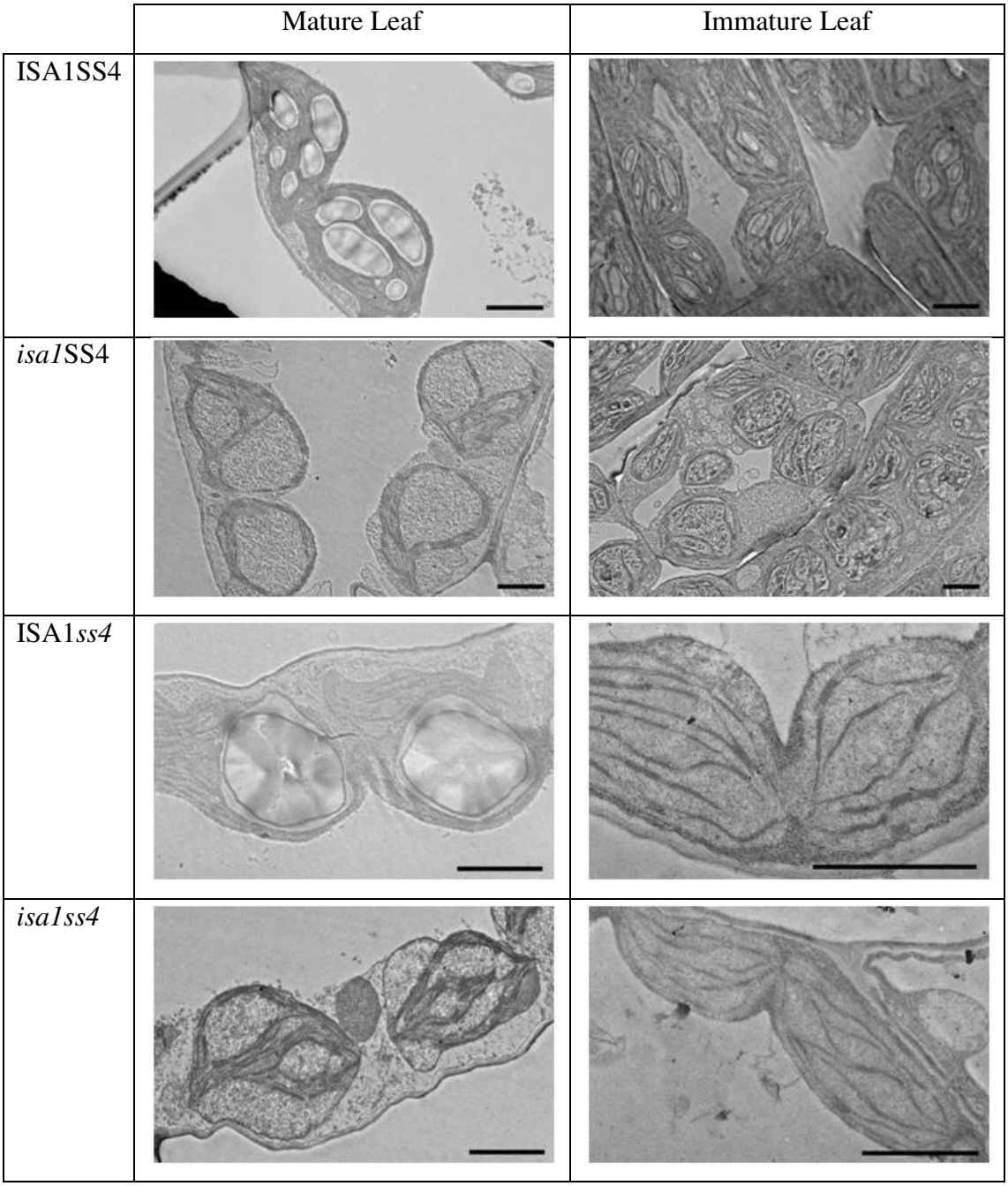

Figure 4.17: TEM sections of mesophyll cells from 25-day-old rosettes. The four youngest leaves (greater than 1 mm long) on a 25-day-old rosette are harvested as the immature leaves. Images taken by Sue Bunnewell (JIC). Scale bar = 2 μm.

To quantify starch, phytoglycogen and sugar levels in wild-type, *isa1*, *ss4* and *isa1ss4,* leaves were harvested at the end of the 12 h light period and then again at the end of the 12 h dark period (Figure 4.18 and 4.19). Each plant was divided into five samples, each containing progressively older leaves (Figures 4.18 and 4.19). The mean starch contents at the end of the day, when all the leaves of each plant were considered together, were 4.7 ± 0.2, 3.1 ±0.2, 4.1 ± 0.2 and 1.5 ± 0.1 mg g^{-1} FW for wild-type, *isa1*, *ss4* and *isa1ss4* respectively (means ± SE of measurements on six different plants; Figure 4.18A). The mean phytoglycogen contents at the end of the day when all the leaves of each plant were considered together were 0.4 ± 0.1, 2.0 ± 0.2, 0.4 ± 0.02 and 1.2 ± 0.1 mg g^{-1} FW for wild-type, *isa1*, *ss4* and *isa1ss4* respectively (means ± SE of measurements on six different plants; Figure 4.18A). Therefore, at the end of the day wild-type and *isa1* rosettes contain approximately equal amounts of total glucan (as previously shown by Delatte *et al.,* 2005), but the *isa1* mutant has much less of its glucans stored as starch and a greater proportion stored as phytoglycogen. As in *ss4*, the total glucans at the end of the day in the *isa1ss4* mutant are reduced compared to wild-type, but like *isa1* approximately equal proportions are stored as starch and phytoglycogen (Figure 4.18A). By the end of the night, the *isa1* and *isa1ss4* rosettes contained significantly less starch and phytoglycogen than wild-type or *ss4* plants (Figure 4.18A; Table 4.3 and Table 4.4).

As I showed previously (Figure 4.4), at the end of the day in the *ss4* mutant the younger leaves (fractions1 and 2; leaves 1 to 8) contain very little starch, while the older leaves (fractions 4 and 5; leaves 13 to 17) contain similar quantities or a greater amount of starch than wild-type leaves (Figure 4.18B). In the youngest leaves (1 to 4), at the end of the day, there is no significant difference between the genotypes in phytoglycogen levels (Figure 4.18C and Table 4.6). However, all *isa1ss4* leaves beyond the second fraction, contained significantly more glucans as phytoglycogen than the wild-type leaves (Table 4.6). In *isa1* at the end of the day all the leaves except the youngest fraction had less starch than the wild-type (Figure 4.18B; Table 4.5), while in *isa1ss4* all the leaves had less starch than the wild-type (Figure 4.18B; Table 4.5). By the end of the night all leaf fractions from *isa1* and *isa1ss4* rosettes contain low levels of starch; approximately the same as, or significantly less than wild-type leaves (Figure 4.18B; Table 4.5). In contrast, by the end of the night all leaf fractions from *ss4* rosettes contain relatively high levels of starch; approximately the same as, or significantly more than

wild-type leaves (Figure 4.18B; Table 4.5). By the end of the night all plants contain low levels of phytoglycogen and few significant differences are seen between the genotypes across the rosette (Figure 4.18C; Table 4.6).

In summary, preventing expression of the *ISA1* gene in the *ss4* mutant and thereby removing the capacity to produce normal starch granules made no difference to the overall pattern of glucan accumulation. Only very low levels of glucans accumulate in the immature leaves of both the *ss4* and *isa1ss4* mutant. The glucan levels in the *isa1ss4* mutant also illustrate that the reduced starch degradation rate at night and the resulting starch excess in mature leaves of the *ss4* mutant is primarily due to the abnormal starch granules, because no excess is present in the *isa1ss4* mutant.

Sugar levels in *ss4*, *isa1, isa1ss4* and wild-type were analysed across the rosette at both the end of the day and night (Figure 4.19; Tables 4.7 - 4.12). The pattern of sugar accumulation in *ss4*, *isa1, isa1ss4* and wild-type is not straight forward, with levels fluctuating across the rosette in all genotypes at both times of the day (Figure 4.19B-D). However, a few trends do emerge. The *isa1*, *ss4* and *isa1ss4* rosettes all contain significantly more sucrose, glucose and fructose at the end of the day compared to wild-type rosettes (Figure 4.19A and Tables 4.7 – 4.9). This is due to the differences, compared to wild-type, in the quantity of sugars in the first four leaf fractions, because the sucrose, glucose and fructose levels at the end of the day in the most mature leaves (Figure 4.19B-D; fraction 5 containing leaves 17+) do not vary between genotypes (Tables 4.10 - 4.12).

At the end of the night there is no difference in fructose levels in the most mature leaves of the four genotypes (Figure 4.19D; fraction 5 containing leaves 17+; Table 4.12). In general, less variation occurs in sucrose and glucose levels in the immature leaves between the four genotypes (Figure 4.19B and C; fraction 1 containing leaves 1-4) than in the expanding and mature leaves (Figure 4.19B and C; fractions 2 to 5 containing leaves 5+; Table 4.10 and 4.11).

The sugar levels in the *isa1ss4* rosette vary in several respects from wild-type levels and often to the same extent as one of the parental single mutants, but not always the same one. For example, the glucose levels at both the end of the day and night of the *isa1ss4*

rosette are similar to *ss4*, whereas the fructose levels at both the end of the day and end of the night are similar to *isa1* (Figure 4.19A; Table 4.8 and 4.9). As stated above, at the end of the day *isa1* and *isa1ss4* rosettes both contain significantly more sucrose, glucose and fructose than wild-type (Tables 4.7 – 4.9). However, at the end of the night *isa1* rosettes have significantly less sucrose and fructose, but similar quantities of glucose to wild-type rosettes. In contrast, *isa1ss4* rosettes have wild-type sucrose levels, but significantly more glucose and significantly less fructose than wild-type rosettes (Tables 4.7 – 4.9).

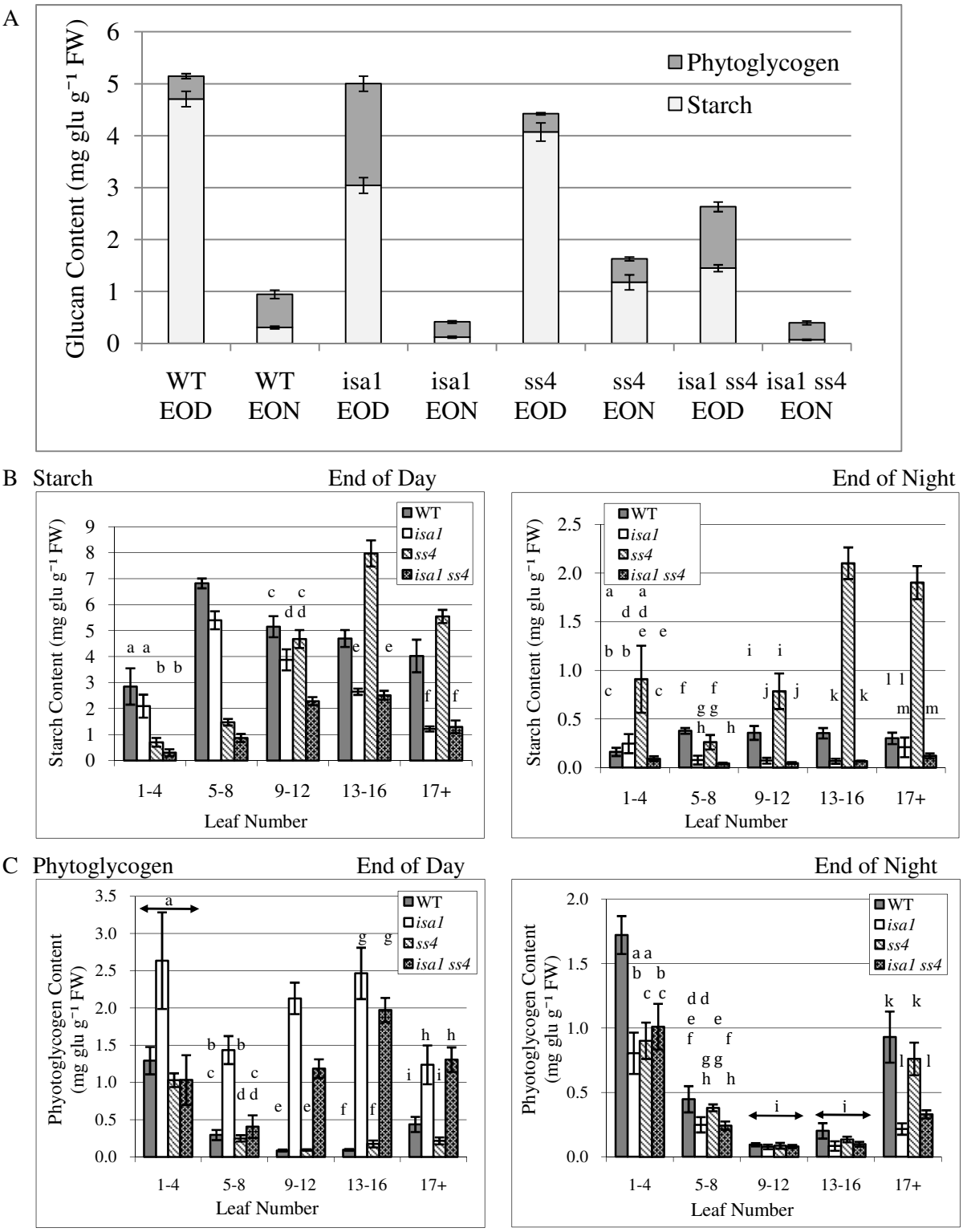

Figure 4.18: Starch and phytoglycogen levels in wild-type (WT), *ss4, isa1* and *isa1ss4*. Each bar is the mean (±SE) of at least five replicate samples. Leaf Number 1 = youngest. Bars with the same letter are not significantly different from each other. EOD = End of Day. EON = End of night. (A) Starch and phytoglycogen content in the whole rosette. (B) Starch across the rosette. (C) Phytoglycogen across the rosette.

	End of Day		
	Wild-type	*isa1*	*ss4*
isa1	t (10) = -7.84 p <0.001		
ss4	t (10) = -2.75 p = 0.02	t (10) = -4.44 p = 0.001	
isa1ss4	t (10) = -20.02 p <0.001	t (10) = 9.73 p <0.001	t (10) = -13.99 p <0.001
	End of Night		
	Wild-type	*isa1*	*ss4*
isa1	**t (10) = -5.89** **p <0.001**		
ss4	t (10) = 5.90 p = 0.002	**t (10) = -7.22** **p <0.001**	
isa1ss4	**t (10) = -8.46** **p <0.001**	t (10) = 2.26 p = 0.047	**t (10) = -7.61** **p <0.001**

Table 4.3: Statistical analysis (t test) of the starch measurements in wild-type, *isa1, ss4* and *isa1 ss4* rosettes displayed in Figure 4.18A. Test of the null hypothesis that the mean starch contents of the two datasets are not different. The degrees of freedom (listed in brackets), test statistic and statistical significance are displayed.

	End of Day		
	Wild-type	*isa1*	*ss4*
isa1	t (10) = 9.91 p <0.001		
ss4	t (10) = -1.71 p = 0.119	t (10) = 10.89 p <0.001	
isa1ss4	t (10) = 7.15 p <0.001	t (10) = 4.51 p = 0.001	t (10) = 8.74 p <0.001
	End of Night		
	Wild-type	*isa1*	*ss4*
isa1	**t (10) = -3.99** **p = 0.007**		
ss4	t (10) = -2.05 p = 0.068	**t (10) = -3.55** **p = 0.005**	
isa1ss4	**t (10) = -3.46** **p = 0.006**	t (10) = -0.70 p = 0.503	**t (10) = -2.44** **p = 0.035**

Table 4.4: Statistical analysis (t test) of the phytoglycogen measurements in wild-type, *isa1, ss4* and *isa1 ss4* rosettes displayed in Figure 4.18A. Test of the null hypothesis that the mean phytoglycogen contents of the two datasets are not different. The degrees of freedom (listed in brackets), test statistic and statistical significance are displayed.

	End of Day			End of Night		
Leaf Number 1 to 4						
	Wild-type	*isa1*	*ss4*	Wild-type	*isa1*	*ss4*
isa1	***t* (10) = -0.91 *p* = 0.382**			*t* (9) = 1.7 *p* = 0.124		
ss4	*t* (10) = -2.99 *p* = 0.027	*t* (10) = 2.95 *p* = 0.015		*t* (10) = 2.15 *p* = 0.082	*t* (9) = -1.71 *p* = 0.142	
isa1ss4	***t* (10) = -3.58 *p* = 0.014**	*t* (10) = 3.89 *p* = 0.008	*t* (10) = -1.90 *p* = 0.087	*t* (9) = -1.35 *p* = 0.21	*t* (8) = 2.61 *p* = 0.031	*t* (9) = -2.37 *p* = 0.064
Leaf Number 5 to 8						
	Wild-type	*isa1*	*ss4*	Wild-type	*isa1*	*ss4*
isa1	***t* (10) = -3.60 *p* = 0.005**			*t* (8) = -5.83 *p* < 0.001		
ss4	*t* (10) = -23.57 *p* <0.001	*t* (10) = 10.63 *p* <0.001		*t* (10) = -1.46 *p* = 0.175	*t* (8) = -1.85 *p* = 0.102	
isa1ss4	***t* (10) = -24.28 *p* <0.001**	*t* (10) = 11.91 *p* <0.001	*t* (10) = -3.03 *p* = 0.013	*t* (10) = -10.99 *p* < 0.001	*t* (8) = 0.76 *p* = 0.501	*t* (10) = -2.93 *p* = 0.032
Leaf Number 9 to 12						
	Wild-type	*isa1*	*ss4*	Wild-type	*isa1*	*ss4*
isa1	***t* (10) = -2.23 *p* = 0.040**			*t* (10) = -3.72 *p* = 0.004		
ss4	*t* (10) = -0.90 *p* = 0.390	*t* (10) = -1.50 *p* = 0.164		*t* (10) = 2.18 *p* = 0.054	*t* (10) = -3.85 *p* = 0.011	
isa1ss4	***t* (10) = -6.63 *p* <0.001**	*t* (10) = 3.65 *p* = 0.004	*t* (10) = -6.31 *p* <0.001	*t* (10) = -4.33 *p* = 0.007	*t* (10) = 0.79 *p* = 0.461	*t* (10) = -4.03 *p* = 0.010
Leaf Number 13 to 16						
	Wild-type	*isa1*	*ss4*	Wild-type	*isa1*	*ss4*
isa1	***t* (10) = -5.89 *p* <0.001**			*t* (10) = -4.82 *p* < 0.001		
ss4	*t* (10) = 5.44 *p* <0.001	*t* (10) = -10.22 *p* <0.001		*t* (10) =10.22 *p* < 0.001	*t* (10) = -12.38 *p* < 0.001	
isa1ss4	***t* (10) = -5.93 *p* <0.001**	*t* (10) = 0.64 *p* = 0.537	*t* (10) = -10.22 *p* <0.001	*t* (10) = -5.33 *p* = 0.003	*t* (10) = 0.01 *p* = 0.992	*t* (10) = -12.53 *p* < 0.001
Leaf Number 17+						
	Wild-type	*isa1*	*ss4*	Wild-type	*isa1*	*ss4*
isa1	***t* (10) = -4.42 *p* = 0.006**			*t* (8) = -0.86 *p* = 0.417		
ss4	*t* (10) = 2.24 *p* = 0.049	*t* (10) = -15.82 *p* <0.001		*t* (9) = 8.19 *p* < 0.001	*t* (7) = -7.39 *p* < 0.001	
isa1ss4	***t* (10) = -4.04 *p* = 0.002**	*t* (10) = -1.31 *p* = 0.764	*t* (10) = -11.97 *p* = <0.001	*t* (10) = -2.81 *p* = 0.018	*t* (8) = 0.84 *p* = 0.457	*t* (9) = -9.46 *p* < 0.001

Table 4.5: Statistical analysis (*t* test) of the starch measurements across the rosette of wild-type, *isa1, ss4* and *isa1 ss4* plants displayed in Figure 4.18B. Test of the null hypothesis that the mean starch contents of the datasets are not different. The degrees of freedom (listed in brackets), test statistic and statistical significance are displayed.

	End of Day			End of Night		
Leaf Number 1 to 4						
	Wild-type	*isa1*	*ss4*	Wild-type	*isa1*	*ss4*
isa1	***t* (9) = 2.11** ***p* = 0.064**			*t* (9) = -4.00 *p* = 0.003		
ss4	***t* (10) = -1.09** ***p* = 0.301**	***t* (9) = 2.45** ***p* = 0.068**		*t* (9) = -3.86 *p* = 0.004	*t* (10) = -0.45 *p* = 0.660	
isa1ss4	***t* (9) = -0.67** ***p* = 0.52**	***t* (8) = 2.2** ***p* = 0.059**	***t* (9) = 0.11** ***p* = 0.997**	*t* (8) = -2.97 *p* = 0.018	*t* (9) = -0.86 *p* = 0.411	*t* (9) = 0.49 *p* = 0.636
Leaf Number 5 to 8						
	Wild-type	*isa1*	*ss4*	Wild-type	*isa1*	*ss4*
isa1	*t* (10) = 5.75 *p* = 0.001			*t* (10) = -1.68 *p* = 0.124		
ss4	*t* (10) = -0.61 *p* = 0.556	*t* (10) = 6.14 *p* = 0.001		*t* (10) = -0.63 *p* = 0.552	*t* (10) = -2.02 *p* = 0.071	
isa1ss4	*t* (10) = 0.68 *p* = 0.513	*t* (10) = 4.24 *p* = 0.002	*t* (10) = 0.99 *p* = 0.360	*t* (10) = -1.92 *p* = 0.103	*t* (10) = 0.11 *p* = 0.911	*t* (10) = -3.28 *p* = 0.008
Leaf Number 9 to 12						
	Wild-type	*isa1*	*ss4*	Wild-type	*isa1*	*ss4*
isa1	*t* (10) = 9.66 *p* < 0.001			*t* (10) = -0.83 *p* = 0.428		
ss4	*t* (10) = 0.33 *p* = 0.748	*t* (10) = 9.65 *p* < 0.001		*t* (9) = 0.46 *p* = 0.658	*t* (9) = -1.11 *p* = 0.297	
isa1ss4	***t* (10) = 8.7** ***p* <0.001**	*t* (10) = 3.85 *p* = 0.003	***t* (10) = 8.7** ***p* <0.001**	*t* (10) = -0.83 *p* = 0.425	*t* (10) = -0.16 *p* = 0.878	*t* (9) = -1.19 *p* = 0.266
Leaf Number 13 to 16						
	Wild-type	*isa1*	*ss4*	Wild-type	*isa1*	*ss4*
isa1	*t* (10) = 6.86 *p* < 0.001			*t* (9) = -1.32 *p* = 0.221		
ss4	*t* (10) = 1.69 *p* = 0.148	*t* (10) = 6.57 *p* = 0.001		*t* (10) = -1.05 *p* = 0.332	*t* (9) = -0.75 *p* = 0.475	
isa1ss4	***t* (10) = 11.52** ***p* <0.001**	*t* (10) = 1.29 *p* = 0.226	***t* (10) = 10.62** ***p* <0.001**	*t* (10) = -1.64 *p* = 0.152	*t* (9) = 0.13 *p* = 0.902	*t* (10) = -1.26 *p* = 0.235
Leaf Number 17+						
	Wild-type	*isa1*	*ss4*	Wild-type	*isa1*	*ss4*
isa1	*t* (10) = 2.90 *p* = 0.026			*t* (9) = -3.50 *p* = 0.015		
ss4	*t* (10) = -2.17 *p* = 0.055	*t* (10) = 3.86 *p* = 0.011		*t* (10) = -0.72 *p* = 0.489	*t* (9) = -4.07 *p* = 0.006	
isa1ss4	***t* (10) = 4.61** ***p* <0.001**	*t* (10) = -0.23 *p* = 0.824	***t* (10) = 6.37** ***p* <0.001**	*t* (10) = -2.98 *p* = 0.029	*t* (9) = -2.16 *p* = 0.059	*t* (10) = -3.31 *p* = 0.018

Table 4.6: Statistical analysis (*t* test) of the phytoglycogen measurements across the rosette of wild-type, *isa1, ss4* and *isa1 ss4* plants displayed in Figure 4.18C. Test of the null hypothesis that the mean phytoglycogen contents of the datasets are not different. The degrees of freedom (listed in brackets), test statistic and statistical significance are displayed.

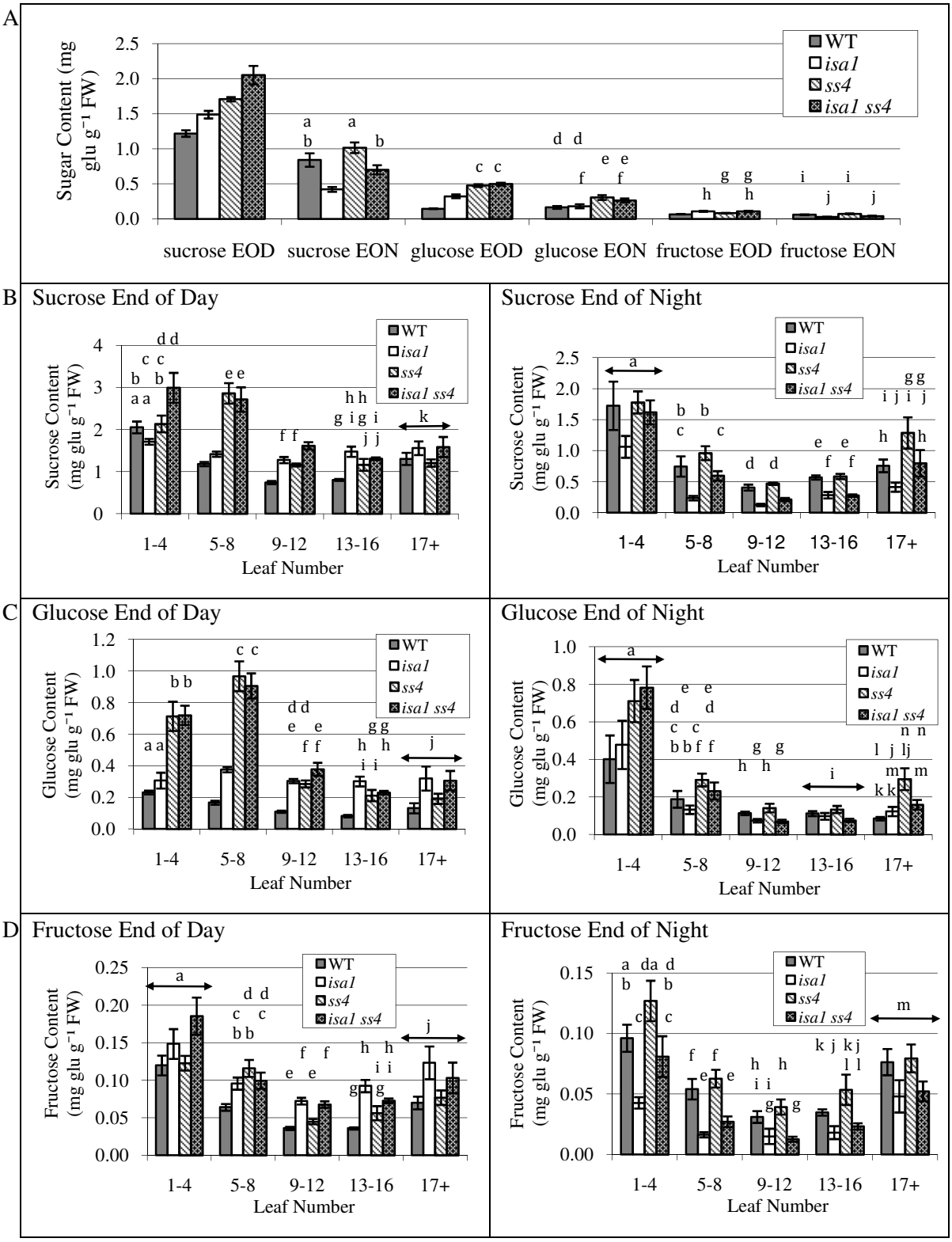

Figure 4.19: Sucrose, glucose and fructose in wild-type, *ss4, isa1* and *isa1ss4* rosettes. EOD = End of Day. EON = End of Night. Each bar is the mean (±SE) of at least six replicate samples. Leaf Number 1 = youngest. Bars with the same letter are not significantly different from each other. (A) Sugars in whole rosettes. (B) Sucrose across the rosette. (C) Glucose across the rosette (D) Fructose across the rosette.

	End of Day		
	Wild-type	*isa1*	*ss4*
isa1	***t* (10) = 3.80, *p* = 0.003**		
ss4	***t* (10) = 8.95, *p* <0.001**	*t* (10) = -3.58, *p* = 0.005	
isa1ss4	***t* (10) = 5.92, *p* <0.001**	*t* (10) = -3.93, *p* = 0.003	*t* (10) = 2.53, *p* = 0.049
	End of Night		
	Wild-type	*isa1*	*ss4*
isa1	***t* (10) = -4.11, *p* = 0.006**		
ss4	*t* (10) = 1.44, *p* = 0.180	*t* (10) = -7.15, *p* <0.001	
isa1ss4	***t* (10) = -1.21, *p* = 0.255**	*t* (10) = -3.78, *p* = 0.004	*t* (10) = -3.17, *p* = 0.010

Table 4.7: Statistical analysis (*t* test) of the sucrose measurements in the rosettes of wild-type, *isa1, ss4* and *isa1 ss4* plants displayed in Figure 4.19A. Test of the null hypothesis that the mean sucrose contents of the datasets are not different. The degrees of freedom (listed in brackets), test statistic and statistical significance are displayed.

	End of Day		
	Wild-type	*isa1*	*ss4*
isa1	***t* (10) = 6.62, *p* <0.001**		
ss4	***t* (10) = 16.17, *p* <0.001**	*t* (10) = -4.66, *p* <0.001	
isa1ss4	***t* (10) = 17.27, *p* <0.001**	*t* (10) = -5.32, *p* <0.001	***t* (10) = 0.77, *p* = 0.458**
	End of Night		
	Wild-type	*isa1*	*ss4*
isa1	***t* (10) = 0.47, *p* = 0.650**		
ss4	*t* (10) = 3.53, *p* = 0.005	*t* (10) = -2.73, *p* = 0.021	
isa1ss4	***t* (10) = 3.02, *p* = 0.013**	*t* (10) = -2.09, *p* = 0.063	***t* (10) = -0.91, *p* = 0.382**

Table 4.8: Statistical analysis (*t* test) of the glucose measurements in the rosettes of wild-type, *isa1, ss4* and *isa1 ss4* plants displayed in Figure 4.19A. Test of the null hypothesis that the mean glucose contents of the datasets are not different. The degrees of freedom (listed in brackets), test statistic and statistical significance are displayed.

	End of Day		
	Wild-type	*isa1*	*ss4*
isa1	***t* (10) = 6.13, *p* <0.001**		
ss4	***t* (10) = 4.17, *p* = 0.002**	*t* (10) = 3.26, *p* = 0.009	
isa1ss4	***t* (10) = 4.04, *p* = 0.009**	***t* (10) = 0.05, *p* = 0.959**	*t* (10) = 2.24, *p* = 0.064
	End of Night		
	Wild-type	*isa1*	*ss4*
isa1	***t* (10) = -5.71, *p* <0.001**		
ss4	*t* (10) = 2.12, *p* = 0.060	*t* (10) = -7.23, *p* <0.001	
isa1ss4	***t* (10) = -3.07, *p* = 0.012**	***t* (10) = -1.97, *p* = 0.077**	*t* (10) = -4.77, *p* <0.001

Table 4.9: Statistical analysis (*t* test) of the fructose measurements in the rosettes of wild-type, *isa1, ss4* and *isa1 ss4* plants displayed in Figure 4.19A. Test of the null hypothesis that the mean fructose contents of the datasets are not different. The degrees of freedom (listed in brackets), test statistic and statistical significance are displayed.

	End of Day			End of Night		
Leaf Number 1 to 4						
	Wild-type	*isa1*	*ss4*	Wild-type	*isa1*	*ss4*
isa1	t (10) = -2.18 p = 0.054			**F (3, 20) = 1.719, p = 0.195**		
ss4	t (10) = 0.33 p = 0.745	t (10) = -2.01 p = 0.090				
isa1ss4	t (9) = 2.62 p = 0.028	t (9) = -3.52 p = 0.022	t (9) = 2.20 p = 0.056			
Leaf Number 5 to 8						
	Wild-type	*isa1*	*ss4*	Wild-type	*isa1*	*ss4*
isa1	t (10) = 2.95 p = 0.015			t (10) = -3.05 p = 0.025		
ss4	t (10) = 6.73 p <0.001	t (10) = -5.73 p = 0.002		t (10) = 1.09 p = 0.303	t (10) = -6.14 p <0.001	
isa1ss4	t (9) = 5.22 p = 0.003	t (10) = -4.39 p = 0.006	t (10) = -0.39 p = 0.708	t (10) = -0.84 p = 0.422	t (10) = -4.27 p = 0.002	t (10) = -2.70 p = 0.022
Leaf Number 9 to 12						
	Wild-type	*isa1*	*ss4*	Wild-type	*isa1*	*ss4*
isa1	t (10) = 6.47 p <0.001			t (10) = -5.47 p <0.001		
ss4	t (10) = 8.30 p <0.001	t (10) = 1.39 p = 0.196		t (10) = 1.21 p = 0.254	t (10) = -11.99 p <0.001	
isa1ss4	t (10) = 9.16 p <0.001	t (10) = -2.95 p = 0.015	t (10) = 4.77 p <0.001	t (10) = -3.58 p = 0.005	t (10) = -2.63 p = 0.025	t (10) = -7.67 p <0.001
Leaf Number 13 to 16						
	Wild-type	*isa1*	*ss4*	Wild-type	*isa1*	*ss4*
isa1	t (10) = 5.43 p = 0.002			t (10) = -4.52 p = 0.001		
ss4	t (10) = 2.52 p = 0.051	t (10) = 1.67 p = 0.126		t (10) = 0.28 p = 0.783	t (10) = -4.41 p = 0.001	
isa1ss4	t (10) = 12.36 p <0.001	t (10) = 1.33 p = 0.234	t (10) = 0.99 p = 0.364	t (10) = -.32 p = <0.001	t (10) = 0.09 p = 0.929	t (10) = -6.49 p <0.001
Leaf Number 17+						
	Wild-type	*isa1*	*ss4*	Wild-type	*isa1*	*ss4*
isa1	**F (3, 18) = 1.400, p = 0.275**			t (10) = -2.65 p = 0.027		
ss4				t (10) = 1.95 p = 0.080	t (10) = -3.33 p = 0.017	
isa1ss4				t (10) = 0.17 p = 0.865	t (10) = -1.70 p = 0.139	t (10) = -1.48 p = 0.171

Table 4.10: Statistical analysis (t test and ANOVA) of the sucrose measurements across the rosettes of wild-type, *isa1, ss4* and *isa1 ss4* plants at the end of the day and end of the night displayed in Figure 4.19B. Test of the null hypothesis that the mean sucrose contents of the datasets are not different. The degrees of freedom (listed in brackets), test statistic and statistical significance are displayed.

	End of Day			End of Night		
Leaf Number 1 to 4						
	Wild-type	*isa1*	*ss4*	Wild-type	*isa1*	*ss4*
isa1	t (10) = 1.46 p = 0.199			**F (3, 18) = 2.151, p = 0.129**		
ss4	t (10) = 5.15 p = 0.003	t (10) = -3.85 p = 0.003				
isa1ss4	t (10) = 7.88 p <0.001	t (10) = -5.24 p <0.001	t (10) = 0.06 p = 0.953			
Leaf Number 5 to 8						
	Wild-type	*isa1*	*ss4*	Wild-type	*isa1*	*ss4*
isa1	t (10) = 10.29 p <0.001			t (10) = -1.11 p = 0.295		
ss4	t (10) = 8.41 p <0.001	t (10) = -6.19 p = 0.001		t (10) = 1.83 p = 0.097	t (10) = -3.86 p = 0.003	
isa1ss4	t (9) = 9.17 p <0.001	t (9) = -6.54 p = 0.002	t (9) = -0.49 p = 0.638	t (10) = 0.70 p = 0.501	t (10) = -1.97 p = 0.077	t (10) = -1.03 p = 0.326
Leaf Number 9 to 12						
	Wild-type	*isa1*	*ss4*	Wild-type	*isa1*	*ss4*
isa1	t (10) = 12.82 p <0.001			t (10) = -3.14 p = 0.011		
ss4	t (10) = 7.69 p <0.001	t (10) = 0.70 p = 0.501		t (10) = 1.13 p = 0.284	t (10) = -2.71 p = 0.022	
isa1ss4	t (10) = 6.49 p = 0.001	t (10) = -1.74 p = 0.131	t (10) = 2.00 p = 0.073	t (10) = -3.28 p = 0.008	t (10) = 0.30 p = 0.767	t (10) = -2.83 p = 0.018
Leaf Number 13 to 16						
	Wild-type	*isa1*	*ss4*	Wild-type	*isa1*	*ss4*
isa1	t (10) = 6.91 p <0.001			F (3, 20) = 2.652, p = 0.077		
ss4	t (10) = 3.60 p = 0.014	t (10) = 1.89 p = 0.088				
isa1ss4	t (10) = 11.35 p <0.001	t (10) = 2.15 p = 0.073	t (10) = 0.49 p = 0.640			
Leaf Number 17+						
	Wild-type	*isa1*	*ss4*	Wild-type	*isa1*	*ss4*
isa1	**F (3, 20) = 2.868, p = 0.062**			t (9) = 1.54 p = 0.159		
ss4				t (10) = 2.28 p = 0.069	t (9) = -1.67 p = 0.145	
isa1ss4				t (10) = 2.68 p = 0.034	t (9) = -1.00 p = 0.344	t (10) = -1.18 p = 0.282

Table 4.11: Statistical analysis (t test and ANOVA) of the glucose measurements across the rosettes of wild-type, *isa1, ss4* and *isa1 ss4* plants at the end of the day and end of the night displayed in Figure 4.19C. Test of the null hypothesis that the mean glucose contents of the datasets are not different. The degrees of freedom (listed in brackets), test statistic and statistical significance are displayed.

	End of Day			End of Night		
Leaf Number 1 to 4						
	Wild-type	*isa1*	*ss4*	Wild-type	*isa1*	*ss4*
isa1	F (3, 19) = 2.749, p = 0.071			t (10) = -4.40 p = 0.001		
ss4				t (10) = 1.53 p = 0.156	t (10) = -4.87 p = 0.003	
isa1ss4				t (10) = -0.75 p = 0.469	t (10) = -2.20 p = 0.072	t (10) = -1.94 p = 0.080
Leaf Number 5 to 8						
	Wild-type	*isa1*	*ss4*	Wild-type	*isa1*	*ss4*
isa1	t (10) = 3.40 p = 0.007			t (10) = -4.33 p = 0.006		
ss4	t (10) = 4.28 p = 0.002	t (10) = -1.46 p = 0.175		t (10) = 0.78 p = 0.455	t (10) = -6.10 p = 0.001	
isa1ss4	t (10) = 3.02 p = 0.013	t (10) = -0.28 p = 0.784	t (10) = -1.05 p = 0.317	t (10) = -2.82 p = 0.018	t (10) = -2.18 p = 0.054	t (10) = -4.16 p = 0.002
Leaf Number 9 to 12						
	Wild-type	*isa1*	*ss4*	Wild-type	*isa1*	*ss4*
isa1	t (10) = 7.30 p <0.001			t (10) = -2.00 p = 0.073		
ss4	t (10) = 2.19 p = 0.054	t (10) = 4.80 p <0.001		t (10) = 1.03 p = 0.328	t (10) = -2.71 p = 0.022	
isa1ss4	t (10) = 6.64 p <0.001	t (10) = 0.73 p = 0.479	t (10) = 4.12 p = 0.002	t (10) = -3.45 p = 0.006	t (10) = 0.35 p = 0.738	t (10) = -3.99 p = 0.007
Leaf Number 13 to 16						
	Wild-type	*isa1*	*ss4*	Wild-type	*isa1*	*ss4*
isa1	t (10) = 6.76 p <0.001			t (10) = -2.81 p = 0.018		
ss4	t (10) = 2.13 p = 0.084	t (10) = 2.89 p = 0.016		t (10) = 1.46 p = 0.198	t (10) = -2.60 p = 0.027	
isa1ss4	t (10) = 10.49 p <0.001	t (10) = 2.22 p = 0.051	t (10) = 1.67 p = 0.145	t (10) = -3.16 p = 0.010	t (10) = -0.87 p = 0.405	t (10) = -2.37 p = 0.060
Leaf Number 17+						
	Wild-type	*isa1*	*ss4*	Wild-type	*isa1*	*ss4*
isa1	**F (3, 20) = 0.687, p = 0.570**			**F (3, 18) = 2.149, p = 0.130**		
ss4						
isa1ss4						

Table 4.12: Statistical analysis (t test and ANOVA) of the fructose measurements across the rosettes of wild-type, *isa1, ss4* and *isa1 ss4* plants at the end of the day and end of the night displayed in Figure 4.19D. Test of the null hypothesis that the mean fructose contents of the datasets are not different. The degrees of freedom (listed in brackets), test statistic and statistical significance are displayed.

4.2.3.2 Carbon starvation in the *isa1* and *isa1*ss4 mutants

In section 4.2.1.3 I showed that wild-type plants do not show symptoms of carbohydrate starvation during the normal 12 h night. Luciferase (LUC) expression (visualised by bioluminescence in *pAt1g10070::LUC* lines) only starts an hour into an extended night, after which bioluminescence increases exponentially (Figure 4.9). In contrast, in *ss4* mutant plants there is a low level of LUC expression throughout the night and after approximately three hours into the extended night (15 h dark) the bioluminescence increases steadily. For comparison, I examined carbohydrate starvation in the *isa1* and *isa1ss4* mutants, which store most of their glucans as phytoglycogen rather than starch. At night, phytoglycogen is broken down in an exponential manner, and reserves of this glucan are exhausted before dawn (Delatte *et al.,* 2005; Streb *et al.,* 2008; Zeeman *et al.,* 1998b), therefore I would expect the *isa1* mutant to exhibit symptoms of carbohydrate starvation prior to the end of the night. To introduce the starvation reporter gene into the mutant backgrounds, I crossed the *isa1* and *isa1ss4* mutants with the carbohydrate starvation reporter line *pAt1g10070::LUC* and obtained plants homozygous for both the starvation reporter insert and the *isa1* or *isa1ss4* mutations (as described for the *ss4* mutant in section 4.2.1.3).

To observe the starvation pattern in whole rosettes, plants were grown under normal 12 h light-12 h dark conditions for 21 days, transferred to the NightOwl, 8 h into a normal night, then held in darkness for the remainder of the normal night and a further extended night period. The pattern of LUC expression (visualised by bioluminescence and measured using the WinLight software), in *isa1* and *isa1ss4* is displayed in Figure 4.20. The *isa1* and *isa1ss4* rosettes begin to express LUC, and hence exhibit symptoms of starvation, about 2 h before the end of the normal night (10 h dark). After this, bioluminescence increases at a slower and more linear rate than in wild-type.

A

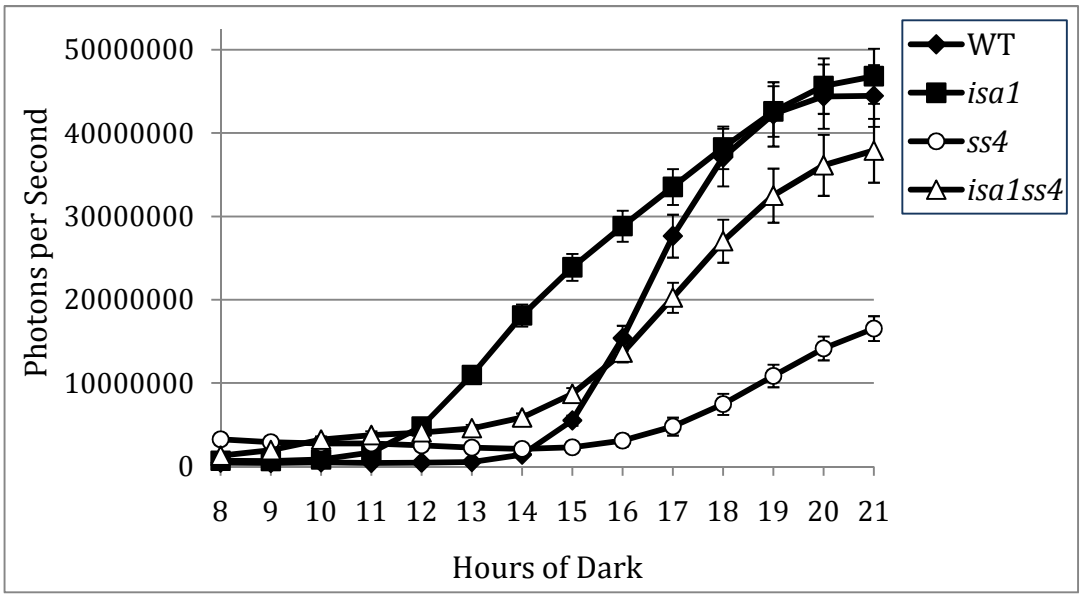

Figure 4.20: Emission of bioluminescence by wild-type and *isa1, isa1ss4* and *ss4* mutant plants expressing LUC from the promoter of the "starvation reporter" gene At1g10070 (*pAt1g10070::*LUC). Plants transformed with the starvation reporter (*pAt1g10070::*LUC) construct were grown under 12 h day-12 h night conditions for 21 days and the experiment began 8 h into the normal night. Normal night ends after 12 h dark. N = 27 plants ± SE (9 plants from 3 independent experiments). WT = wild-type. Where error bars are not visible they are smaller than the symbols. Note: The wild-type and *ss4* data displayed here are the same as those shown in Figure 4.8; experiments were performed at the same time.

4.2.4 Dosage effects of the *ss4* mutant allele

In the next section I describe experiments to test the hypothesis that altering the level of SS4 within the plant will alter numbers of starch granules. If SS4 does indeed regulate the number of starch granules that can be initiated, one might simplistically expect there to be fewer granules in plants with reduced SS4 and more in plants over-expressing SS4. The following section describes plants with reduced levels of SS4 protein and the effect of these reductions on plant growth and starch accumulation.

4.2.4.1 Analysis of the SS4*ss4* heterozygous plant

Given that the loss of SS4 results in such a striking starch phenotype (one granule per chloroplast, see section 4.2.3), I wanted to know at what level a reduction in SS4 protein would result in an alteration in the number of granules initiated per chloroplast. A cross between a wild-type (SS4SS4) plant and an *ss4* mutant (*ss4ss4*) was performed to obtain an F1 generation with plants heterozygous for the *ss4* mutation (SS4*ss4*).

A western blot using an antibody raised against an SS4 peptide confirmed that the SS4 protein levels are reduced by approximately half, relative to wild-type levels, in both the mature and immature leaves of plants heterozygous for the *ss4* mutation (Figure 4.21 and Figure 2.2). As seen in wild-type plants (Figure 4.10), the immature and mature leaves of heterozygous plants contain approximately equal quantities of the SS4 protein on a fresh weight basis (Figure 4.22).

To discover whether this level of reduction in SS4 affects starch metabolism and plant performance, heterozygous F1 plants from a cross between a wild-type (SS4SS4) plant and an *ss4* mutant (*ss4ss4*) were allowed to self. The seed was sown out and measurements of rosette weight and diameter were taken. The genotype of the plant was then determined via DNA extraction and PCR. The relationship between the diameter and weight was approximately linear and was the same across all three genotypes (Figure 4.23A). While the *ss4* mutants were uniformly smaller than the other genotypes, the wild-type and heterozygous plants were indistinguishable in terms of size or weight (Figure 4.23A). There was no difference in rosette weight or rosette diameter between wild-type and heterozygous plants, which were both heavier and larger than *ss4* (Figure 4.23B and C).

A

Mutant	Heterozygote	Wild-type
ss4ss4	SS4*ss4*	SS4SS4

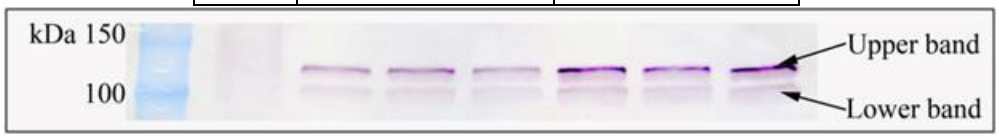

B

	Heterozygote		Wild-type	
	Band Intensity	SE	Band Intensity	SE
Upper Band	28.9	5.9	62.8	8.2
Lower Band	9.1	2.5	18.6	2.0

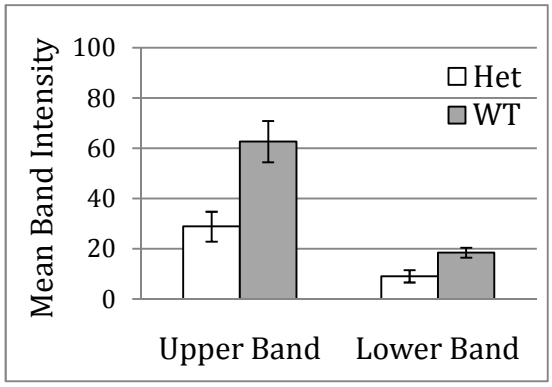

C

Mutant	Heterozygote	Wild-type
ss4ss4	SS4*ss4*	SS4SS4

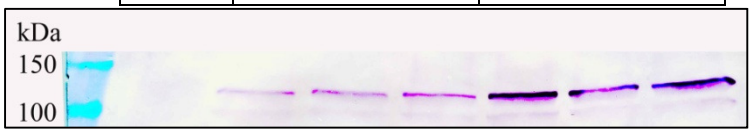

D

	Heterozygote		Wild-type	
	Band Intensity	SE	Band Intensity	SE
Upper Band	26.8	6.7	76.3	12.2
Lower Band	9.6	1.2	11.0	2.4

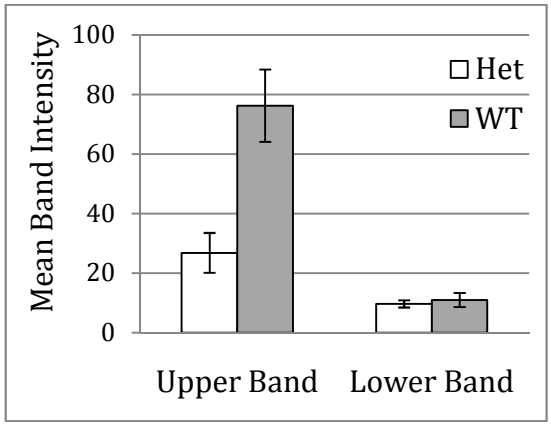

Figure 4.21: Comparison of SS4 protein levels in wild-type (WT), heterozygote and *ss4* plants. (A) Western blot of mature leaves. (B) Table of western blot band intensities for the blot pictured in (A) ± SE (n = three bands for each genotype from the same western blot). (C) Western blot of immature leaves. (D) Table of western blot band intensities for the blot pictured in (C). Each lane on the blot contains extract from a separate plant, with 40µl of protein extract loaded in each lane. All extracts contain the same mg tissue per ml extraction buffer. To check the equal loading a gel was run at the same time, using the same extracts as used for the western blot and stained with Coomassie® InstantBlue™ stain (not shown). Using Adobe Photoshop software, images are converted to greyscale and mean pixel intensity of each band is measured (see section 2.15).

A

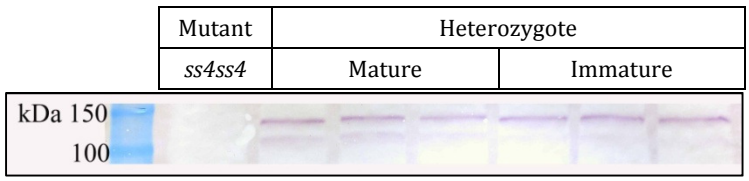

B

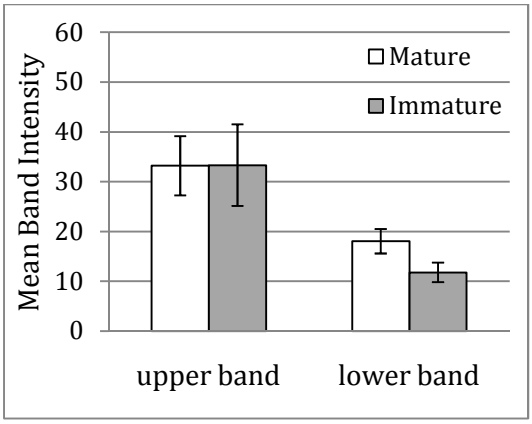

	Mature		Immature	
	Band Intensity	SE	Band Intensity	SE
Upper Band	33.2	6.9	33.3	4.2
Lower Band	18.1	8.0	11.8	4.4

Figure 4.22: Comparison of SS4 protein levels in mature and immature leaves of heterozygote (SS4*ss4*) plants. (A) Western blot of heterozygote leaves (SS4*ss4*). (B) Western blot band intensities for the blot pictured in (A) ± SE (n = three bands for each leaf age from the same western blot). Each lane on the blot contains extract from a separate plant, with 40µl of protein extract loaded in each lane. All extracts contain the same mg tissue per ml extraction buffer. To check the equal loading a gel was run at the same time, using the same extracts as used for the western blot and stained with Coomassie® InstantBlue™ stain. Using Adobe Photoshop software, images are converted to greyscale and mean pixel intensity of each band is measured (see section 2.15).

A

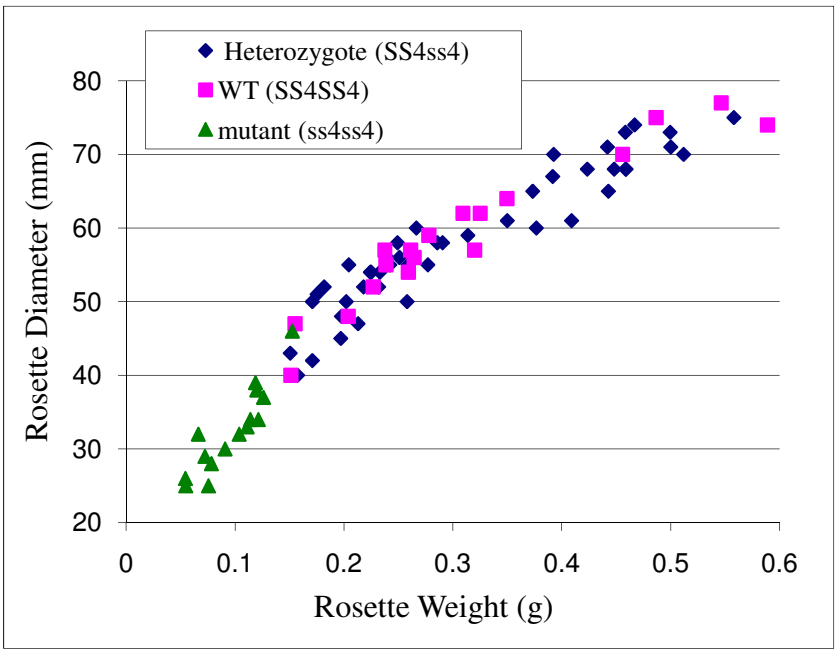

B

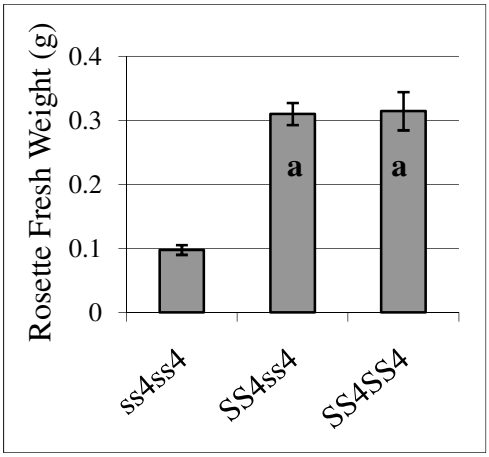

C

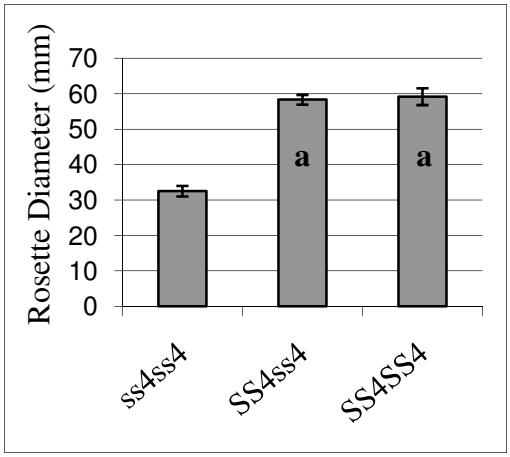

D

	SS4SS4	SS4*ss4*
SS4*ss4*	*t* (62) = -0.14 *p* = 0.891	
ss4ss4	*t* (31) = -7.03 *p* <0.001	*t* (59) = -11.25 *p* <0.001

E

	SS4SS4	SS4*ss4*
SS4*ss4*	*t* (62) = -0.32 *p* = 0.749	
ss4ss4	*t* (31) = -9.54 *p* <0.001	*t* (59) = -10.03 *p* <0.001

Figure 4.23: Comparison of wild-type, *ss4* and SS4*ss4* rosette size and weight. F2 plants from a cross between SS4SS4 and *ss4ss4* plants were grown for 25 days in 12 h light/12 h dark conditions. (A) Rosette diameter vs. rosette fresh weight (B) Rosette fresh weight. (C) Rosette diameter. Genotype was determined following harvesting and measurements. Bars with the same letter are not significantly different from each other. Statistical analysis (*t* test) for rosette fresh weight (D) displayed in B and rosette diameter (E) displayed in C. Test of the null hypothesis that the mean rosette fresh weights or mean rosette diameters of the two datasets are not different. The degrees of freedom (listed in brackets), test statistic and statistical significance are displayed.

Plants heterozygous for the SS4 mutation (SS4*ss4*) have the same starch accumulation pattern as wild-type (SS4SS4) plants (Figure 4.24A). Starch is present throughout the wild-type and heterozygote rosette at the end of the light period. The chloroplasts of heterozygous plants appear to contain the same number and size of granules as wild-type plants, in contrast to the *ss4* mutant, which on average only has one starch granule per chloroplast (Figure 4.24B and C). The morphology and size of the starch granules were analysed using both SEM of isolated granules and light microscopy of sections through embedded material. The profile of granule size distribution of wild-type and heterozygous plants are very similar and contrast with the profile of *ss4,* which has a shift to larger granules (Figure 4.25A). There is no difference in the volume of starch granules from wild-type and heterozygous plants (Figure 4.25B) and no difference in the stromal area per granule (the chloroplast cross-sectional area divided by the number of granules present; Figure 4.25C). However, both wild-type and heterozygous plants contain smaller granules (Figure 4.25B) and have less stromal area per granule than *ss4* (Figure 4.25C).

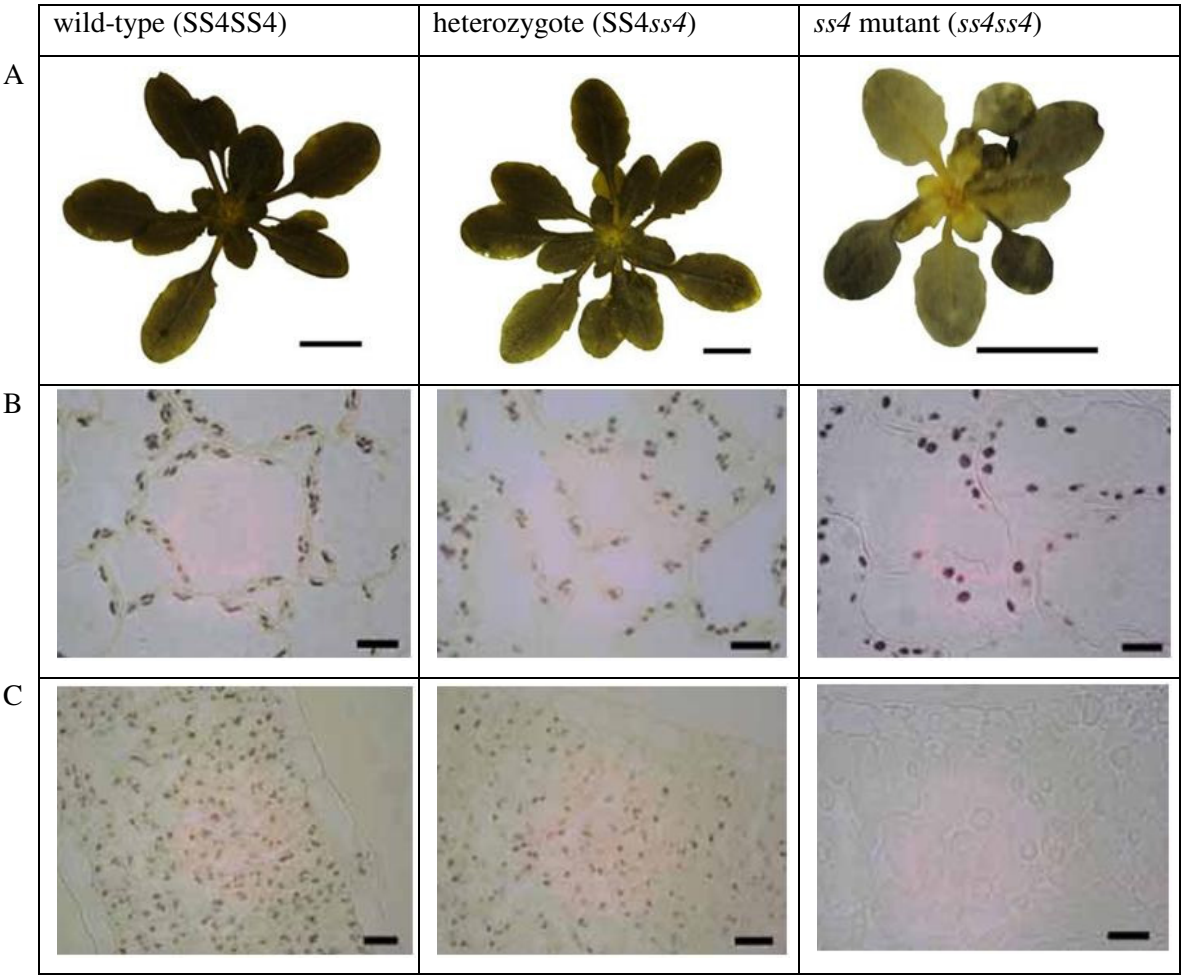

Figure 4.24: Starch in WT, SS4*ss4* and *ss4* leaves. (A) Rosettes harvested at the end of the light period, decolourised with ethanol and stained with iodine solution. Plants were grown for 25 days in 12 h light - 12 h dark conditions. Scale bar = 1 cm. (B and C) 1 µm thick sections through embedded leaves, stained with iodine solution. Leaves harvested 9 h into the light period. (B) Mature leaves. (C) Immature leaves. Scale bar = 10 µm

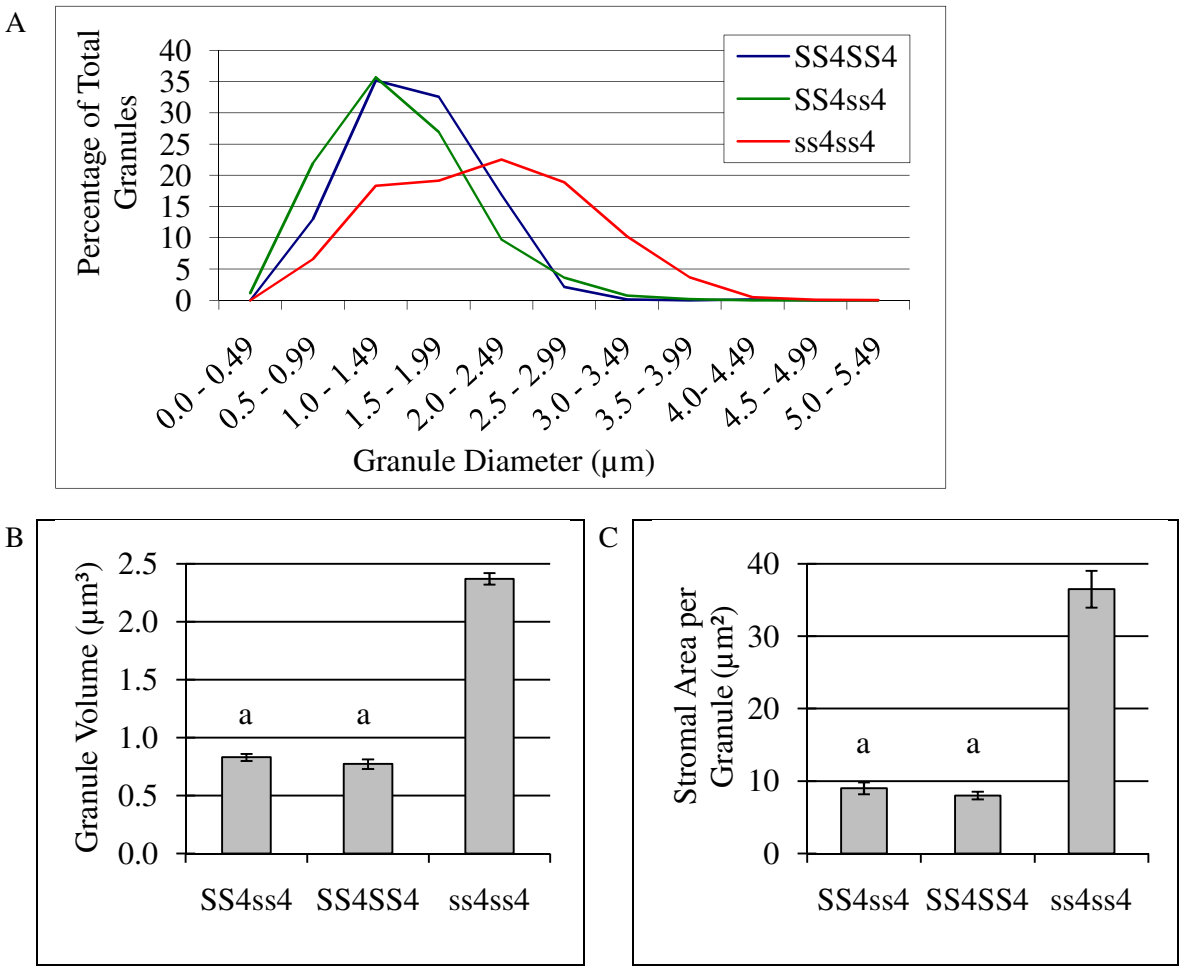

Figure 4.25: Comparison of starch granule number, size and distribution in wild-type, *ss4* and SS4*ss4*. (A) Size distribution of isolated granules from wild-type, *ss4* and SS4*ss4* (divided into 0.5 µm size intervals). Measurements taken using imaging software on SEM images of isolated granules. For each genotype the value is the mean of measurements on between 523 and 2270 granules. (B) Average starch granule volume. Measurements taken using imaging software on SEM images of isolated granules. Volume calculated using the equation derived by Scott Grandison (JIC and University of East Anglia) to calculate the volume of a starch granule from its radius (section 2.14.4). For each genotype the value is the mean of measurements on between 523 and 2270 granules ± SE. (C) The stromal cross sectional area per granule (chloroplast cross sectional area divided by the number of starch granules per chloroplast in cross section). For each genotype an average of 52 chloroplasts was measured from 5 random sections. Two mature leaves from two rosettes per genotype were harvested 9 h into a 12 h light period. Measurements taken using imaging software on photos of mesophyll cell sections stained with iodine solution. Bars with the same letter are not significantly different from each other. Statistics for data are in Table 4.13.

A

	SS4SS4	SS4*ss4*
SS4*ss4*	*t* (1320) = -1.13 *p* = 0.26	
ss4ss4	*t* (3067) = 26.52 *p* <0.001	*t*(2791) = -24.77 *p* = <0.001

B

	SS4SS4	SS4*ss4*
SS4*ss4*	*t* (115) = 1.29 *p* = 0.199	
ss4ss4	*t* (78) = 11.00 *p* <0.001	*t* (115) = -10.46 *p* <0.001

Table 4.13: Statistical analysis (*t* test) of the granule volume (A) and stromal area per granule (B) measurements of wild-type, heterozygous and *ss4* plants displayed in Figure 4.25B and 4.25C. Test of the null hypothesis that the mean granule volumes or stromal areas per granule of the datasets are not different. The degrees of freedom (listed in brackets), test statistic and statistical significance are displayed.

To quantify starch in wild-type, heterozygous (SS4*ss4*) and *ss4* rosettes, leaves were harvested at the end of the 12 h light period and then again at the end of the 12 h dark period (Figure 4.26). Each plant was divided into five samples, each containing progressively older leaves; sample 1 contained the youngest leaves and sample 5 the oldest leaves. There was no significant difference in the amount of starch at the end of the day or night between the wild-type and heterozygous rosettes (Figure 4.26A). The *ss4* mutant contained significantly less starch at the end of the day than wild-type and heterozygous rosettes, but a greater amount at the end of the night (Figure 4.26A).

A more detailed analysis of starch accumulation across the rosette was carried out. Wild-type leaves contained between 3.4 and 9.4 mg glu g^{-1} fresh weight (FW) at the end of the day, while heterozygote leaves between 5.9 and 8.4 mg glu g^{-1} FW. As observed previously (Figure 4.4 and 4.18), in the *ss4* mutant the youngest leaves contain very little starch (0.8 mg glu g^{-1} FW), while the oldest leaves contain a greater amount of starch than the wild-type and heterozygote leaves (Figure 4.26B, fraction 5, containing leaves 17+). As previously observed, in wild-type the leaf fraction containing the most recently expanded leaves (fraction 2, leaves 5-8), contains more starch than the youngest leaves (fraction 1, leaves 1-4) and the very oldest leaves (fraction 5; leaves 17+) and the same is true in heterozygote plants (Figure 4.26B). The end of night starch levels show a similar trend to the end of the day (Figure 4.26C), with the younger *ss4* leaves containing less starch (0.2 mg glu g^{-1} FW) than the mature leaves (3.0 mg glu g^{-1} FW). There is no significant difference in starch levels between the wild-type and heterozygous plants at any leaf age at the end of the night (Figure 4.26C).

In summary, despite the reduction in SS4 protein levels, plants heterozygous for the *ss4* mutation are essentially identical to wild-type plants in terms of their starch phenotype and growth rate.

A

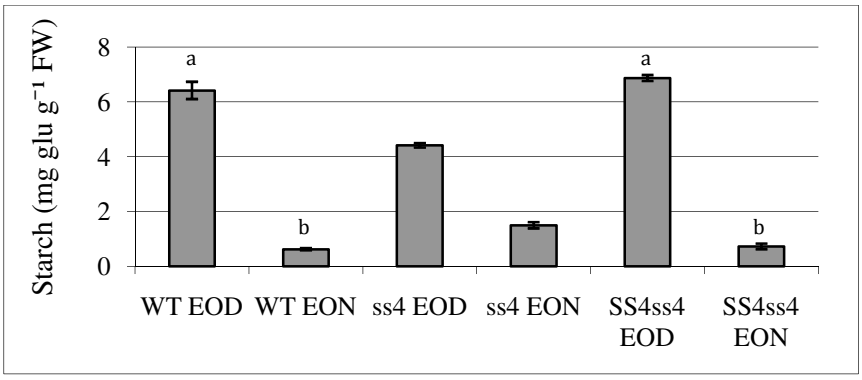

B End of Day

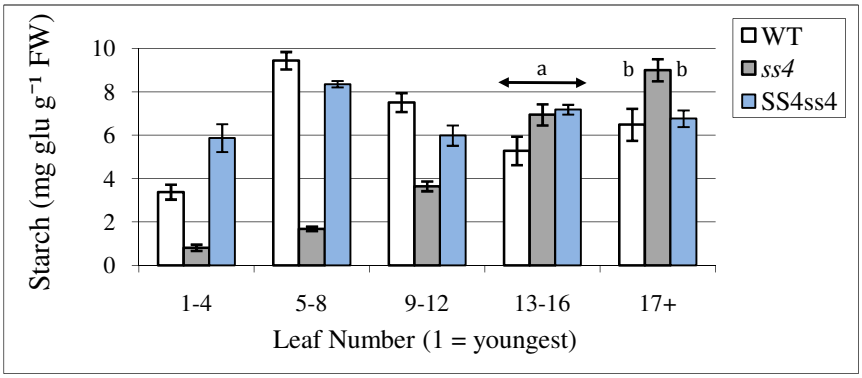

C End of Night

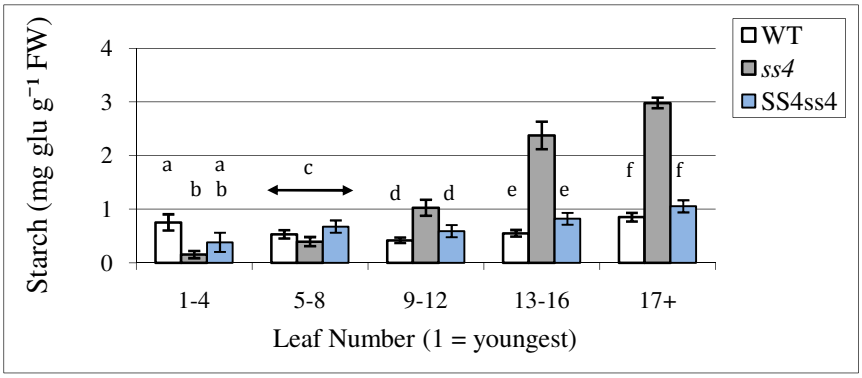

Figure 4.26: Starch levels in wild-type, *ss4* and SS4*ss4*. (A) Whole rosette. (B) End of day (EOD) across the rosette. (C) End of night (EON) across the rosette. Each bar is the mean (±SE) of at least six replicate samples each from a different plant. Leaf Number 1 = youngest. Bars with the same letter are not significantly different from each other.

	End of Day	
	SS4SS4	SS4*ss4*
SS4*ss4*	*t* (10) = 1.36, *p* = 0.223	
ss4ss4	*t* (10) = -6.14, *p* = 0.001	*t* (10) = 18.42, *p* <0.001
	End of Night	
	SS4SS4	SS4*ss4*
SS4*ss4*	*t* (10) = 0.96, *p* = 0.375	
ss4ss4	*t* (10) = 7.24, *p* <0.001	*t* (10) = -4.95, *p* <0.001

Table 4.14: Statistical analysis (*t*-test) performed on the starch levels in wild-type, heterozygous and *ss4* rosettes, data displayed in Figure 4.26A. Test of the null hypothesis that the mean starch contents of the datasets are not different. The test statistic, degrees of freedom (d.f.) and statistical significance are displayed.

	End of Day		End of Night	
Leaf Number 1 to 4				
	SS4SS4	SS4*ss4*	SS4SS4	SS4*ss4*
SS4*ss4*	*t* (10) = -3.60 *p* = 0.006		***t* (8) = 1.59** ***p* = 0.151**	
ss4ss4	*t* (9) = 6.90 *p* = 0.001	*t* (9) = -7.72 *p* = 0.001	*t* (8) = 3.08 *p* = 0.015	*t* (6) = -1.18 *p* = 0.281
Leaf Number 5 to 8				
	SS4SS4	SS4*ss4*	SS4SS4	SS4*ss4*
SS4*ss4*	*t* (10) = 2.53 *p* = 0.043		***t* (9) = -1.08** ***p* = 0.308**	
ss4ss4	*t* (10) = 18.74 *p* <0.001	*t* (10) = -38.01 *p* <0.001	*t* (10) = 1.17 *p* = 0.269	*t* (9) = -2.00 *p* = 0.076
Leaf Number 9 to 12				
	SS4SS4	SS4*ss4*	SS4SS4	SS4*ss4*
SS4*ss4*	*t* (10) = 2.38 *p* = 0.039		***t* (10) = -1.38** ***p* = 0.199**	
ss4ss4	*t* (10) = 7.92 *p* <0.001	*t* (10) = -4.47 *p* = 0.001	*t* (10) = -3.86 *p* = 0.008	*t* (10) = -2.32 *p* = 0.043
Leaf Number 13 to 16				
	SS4SS4	SS4*ss4*	SS4SS4	SS4*ss4*
SS4*ss4*	*t* (10) = -2.73 *p* = 0.33		***t* (10) = -2.15** ***p* = 0.057**	
ss4ss4	*t* (10) = -2.03 *p* = 0.07	*t* (10) = -0.45 *p* = 0.662	*t* (10) = -6.89 *p* <0.001	*t* (10) = 5.54 *p* <0.001
Leaf Number 17+				
	SS4SS4	SS4*ss4*	SS4SS4	SS4*ss4*
SS4*ss4*	*t* (10) = -0.34 *p* = 0.744		***t* (8) = -1.50** ***p* = 0.172**	
ss4ss4	***t* (10) = -2.80** ***p* = 0.019**	***t* (10) = 3.50** ***p* = 0.006**	*t* (10) = -16.74 *p* <0.001	*t* (10) = 12.66 *p* <0.001

Table 4.15: Statistical analysis (*t*-test) performed on the starch levels across rosettes of wild-type, heterozygous and *ss4* plants, data displayed in Figure 4.26B and C. Test of the null hypothesis that the mean starch contents of the datasets are not different. The test statistic, degrees of freedom (d.f.) and statistical significance are displayed.

4.2.4.2 Dexamethasone inducible *SS4* RNAi lines

The *ss4* mutant has a complex pleiotropic phenotype. It is not clear from analysis of this phenotype whether SS4 has a specific and essential role in starch synthesis in older as well as younger leaves, or whether the problems in the older leaves (reduced granule number per chloroplast and starch excess at the end of the night) in *ss4* plants are all downstream consequences of loss of an essential function of SS4 in younger leaves. To test the effect of down regulating SS4 during development and to learn more about the role of SS4 in granule initiation and growth, dexamethasone-inducible RNAi lines were produced using the pOpOff2(hyg) vector system (Figure 4.27; Wielopolska *et al.,* 2005).

Regions of the SS4 coding sequence that were selected to be targeted by RNAi were amplified using PCR. The position of these regions within the *SS4* coding sequence is shown in Figure 4.28. PCR products were cloned into the GATEWAY-ready pCR8/GW/TOPO TA entry plasmid, before transfer into the destination plasmid pOpOff2(hyg). Subsequently *E. coli* and then *A. tumefaciens* cells were transformed with the destination plasmid (containing the selected PCR fragments) and plasmid DNA respectively. At all stages correct sequence amplification, cloning or recombination was confirmed by PCR or colony PCR and sequencing. The four different dexamethasone inducible RNAi constructs (pOpOff2(hyg)::*SS4*A, pOpOff2(hyg)::*SS4*B, pOpOff2(hyg)::*SS4*C and pOpOff2(hyg)::*SS4*D), targeted to different regions of the *SS4* transcript, were then transformed separately into wild-type plants. Four different constructs were created because the degree of reduction in SS4 mRNA accumulation achieved in RNAi lines may vary from one to another and a construct targeting a particular region may be more effective than another.

T1 plants containing a pOpOff2(hyg)::*SS4* construct were selected by their survival on media containing hygromycin (hyg). Surviving plants were grown to maturity and seed collected. To select for plants that contained only a single pOpOff2(hyg)::*SS4* construct, the T2 seed was screened for survival rates on hyg containing media. If a T1 plant contains the desired single copy of the construct, ¼ of the T2 seed it produces will be homozygous for the construct, $^{2}/_{4}$ will be heterozygous and ¼ will not contain the construct. Therefore, if the survival rate of T2 plants varied from ¾, the parental plant and T2 seed it produced were rejected. Selected surviving plants were transferred to

soil. Ten-day-old plants were sprayed with a 30 µM dexamethasone solution, once a day for 10 days, and harvested at the end of the light period.

The SS4 protein level and mRNA levels were reduced in all four lines containing the pOpOff2(hyg)::*SS4* construct (note: results from only two lines shown). Plants with the greatest reduction in protein and mRNA levels, containing constructs pOpOff2(hyg)::*SS4*A and pOpOff2(hyg)::*SS4*B, were selected for further investigation. To select lines homozygous for a pOpOff2(hyg)::*SS4* construct, T3 seed were screened for their survival rate on hyg containing media; lines in which all plants survived were confirmed as homozygous. All subsequent experiments were performed on T3 plants, homozygous for a pOpOff2(hyg)::*SS4* construct. Plants of a wild-type (Col) line containing an empty pOpOff2(hyg) construct (produced by Alexander Graf, JIC) were used as a control in all experiments.

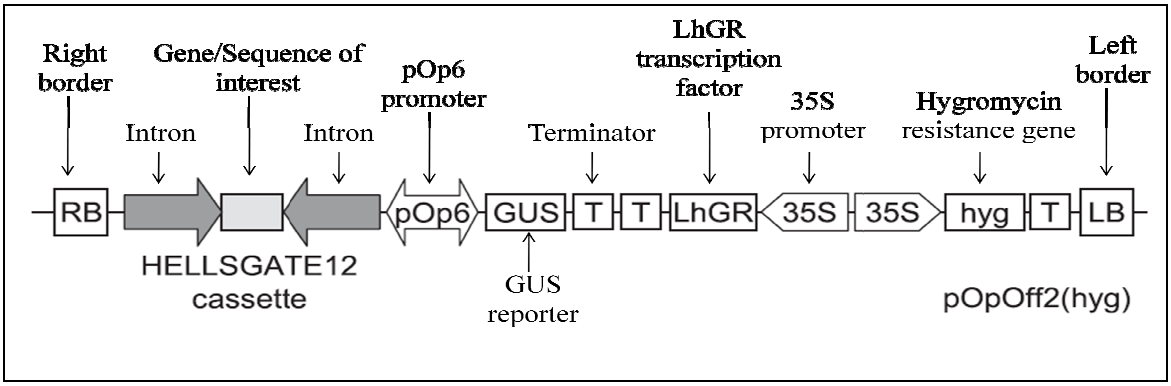

Figure 4.27: pOpOff2(hyg) vector system for the production of dexamethasone-inducible RNAi lines (Wielopolska *et al.,* 2005). The LhGR transcription factor is constitutively expressed from the 35S promoter but activates transcription from the pOp6 promoter only when dexamethasone is present. The pOp6 promoter drives expression of a hairpin RNA (hpRNA) cassette (HELLSGATE12 cassette). The pOp6 promoter is bidirectional, driving expression of both the gene of interest and the GUS reporter. The hygromycin resistance gene acts as a selectable marker.

ATGACGACGAAGCTATCGAGCTTCTGTTTCTT[AACCCATGGATTAGCAGGAATCTCCTGCGAGAGAGAACATGGAAGTTCTCGTCGA
TTTTTCTATCTCCCTTCTCGTCGATTAGTTTCTACTTCGTGTAAGATGCGACAACAACGTGGTTTCGACTCTAGTAAAAGACAAGAGG
TCAAGAAAGGCTCCC](C)CTAAACCGATCCTATCTATAAATTCAGGTCTTCAGAGCAACAATGATGAGGAATCTGATCTGGAGAATG
GTTCTGCGGACAGTGTCCCGAGTCTTAAGTCAGATGCTGAAAAGGGTAGTAGTATTCATGGCAGCATAGATATGAATCATGCTGATGA
GAATCTTGAAAAGAAAGATGATATACAAACAACTGAAGTTACTCGGCGCAAGAGTAAAACTGCAAAGAAGAAAGGGGAGAGTATTCAT
GCTACGATTGATATTGGACATGATGATGGGAAGAATTTAGATAATATTACTGTGCCTGAGGTTGCAAAAGCTTTGTCCCTTAACAAAA
GTGAAGGCGAGCAGATTTCAGATGGACAGTTTGGGGAACTAATGACAATGATAAGAAGTGCAGAAAAAAATATTCTTCGGCTTGATGA
AGCACGGGCCACTGCTCTTGACGACCTTAACAAGATTCTTAGTGATAAGGAAGCGTTGCAGGGAGAAATCAATGTCTTGGAAATGAAA
TTGTCTGAGACTGATGAAAGGATTAAAACTGCTGCTCAAGAGAAAGCACATGTAGAGCTTCTGGAAGAACAGTTAGAGAAGCTTCGTC
ATGAAATGATCTCCCCTATAGAAAGTGATGGTTATGTTCTAGCTCTTAGCAAAGAGCTTGAAACATTGAAGCTGGAGAATCTATCTTT
GAGAAACGATATAGAAATGCTTAAGTCAGAACTTGACAGTGTTAAAGATACCGGTGAACGTGTGGTTGTGTTGGAAAAGGAGTGCTCC
GGTTTGGAATCTTCTGTAAAGGATTTGGAATCTAAGTTATCGGTTTCTCAGGAAGATGTCTCGCAGCTTTCTACTCTTAAAATCGAAT
GCACTGATCTATGGGCGAAGGTAGAGACTCTACAGCTGTTGTTAGATAGAGCTACCAAACAAGCAGAGCAAGCAGTTATAGTGTTACA
ACAGAACCAAGATCTAAGAAATAAGGTCGACAAAATTGAGGAATCACTTAAAGAAGCCAACGTTTATAAAGAATCTTCAGAGAAAATT
CAACAGTACAATGAGCTAATGCAACATAAGGTGACATTACTTGAGGAGCGGCTCGAAAAGTCTGATGCAGAGATATTCTCATATGTTC
AGTTATATCAAGAATCGATAAAAGAATTCCAGGAAACACTTGAAAGTTTGAAGGAAGAAAGCAAGAAAAAATCAAGAGATGAACCGGT
TGATGATATGCCTTGGGATTATTGGAGTCGGTTACTTTTAACTGTTGATGGATGGCTGCTTGAAAAGAAAATAGCAAGCAACGATGCT
GACTTACTGAGAGACATGGTATGGAAGAAAGATCGAAGAATTCATGATACCTATATTGACGTCAAAGATAAGAATGAACGTGATGCCA
TCTCTGCATTTCTCAAGCTTGTCTCATCTCCAACAAGTTCAGGATTGTATGTCGTTCACATTGCAGCTGAGATGGCACCTGTAGCTAA
GGTGGGAGGTTTGGGAGATGTTGTGGCAGGTCTTGGTAAGGCATTGCAAAGAAAAGGTCATCTGGTGGAGATTATTCTTCCCAAATAT
GACTGTATGCAGTATGATCGCGTGCGTGACTTAAGGGCTTTGGATACTGTTGTGGAGTCATATTTTGATGGGAAGTTATATAAAAACA
AAATCT[GGATTGGCACTGTTGAAGGTTTACCTGTACATTTCATTGAACCTCAACATCCAAGCAAATTCTTCTGGAGAGGACAGTTTT
ATGGAGAGCAAGATGATTTCAGACGCTTCTCGTATTTTAGCCGAGCTGCACTAGAGTTGCTTCTTCAGTCCGG](A)CAAAAAACCCG
ACATCATACATTGTCATGACTGGCAAACAGCTTTTGTTGCGCCGCTGTATTGGGATCTGTATGCTCCAAAGGGATTAGATTCTGCAAG
AATATGCTTTACATGTCATAATTTTGAGTATCAAGGTACCGCGTCTGCTTCAGAATTGGGATCTTGCGGGCTTGATGTTAACCAGTTA
AATAGACCAGACAGAATGCAGGATCACTCGTCTGGAGATAGAGTCAATCCTGTTAAGGGCGCTATAATTTTCTCAAACATTGTAACAA
CCGTGTCCCCTACTTATGCACAAGAAGTTCGAACAGCTGAGGGAGGAAAAGGACTCCATTCAACACTCAATTTTCACTCCAAGAAATT
CATTGGAATCCTCAACGGCATTGACACAGATTCATGGAATCCTGCCACCGACCCCTTCCTCAAGGCTCAGTTCAACGCTAAAGATCTA
CAAGGGAAAGAAGAAAACAAACACGCCCTTAGAAAGCAGCT[TGGACTTTCTTCAGCGGAGTCAAGACGGCCTTTGGTTGGTTGCATA
ACAAGATTAGTACCACAGAAAGGAGTTCATCTAATCAGACATGCCATATACAGAACATTAGAGTTAGGTGGACAATTTGTACTTCTTG
GTTCTAGCCCGGTTCCACATATTC](D)AGAGGGAATTTGAAGGTATTGAACAACAGTTTAAAAGCCATGATCATGTCCGGTTGTTAC
TGAAGTACGATGAAGCTCTGTCTCATACGATTTACGCAGCCTCCGATTTGTTCATCATTCCGTCAATTTTTGAGCCTTGTGGACTTAC
ACAGATGATCGCTATGAGATATGGCTCCATTCCAATTGCGCGAAAAACTGGAGGCTTAAATGACAGTGTCTTCGACATTGATGATGAT
ACAATACCAACACAGTTTCAAAATGGATTTACATTTCAAACCGCGGACGAACAGGGTTTCAATTATGCG[TTGGAGCGAGCATTTAAT
CACTACAAGAAAGATGAAGAGAAATGGATGAGACTTGTAGAGAAAGTGATGAGTATAGATTTCAGCTGGGGATCATCAGCTACACAAT
ACGAAGAACTCTACACGAGATCAGTGTCCAGAGCAAGAGCTGTTCCTAATCGCACGTGAG](B)

Figure 4.28: SS4 coding sequence with the regions of the SS4 mRNA targeted by RNAi. Primer regions are highlighted in red and the rest of the sequence in blue. The letter in brackets indicates the letter assigned to that region, i.e. pOpOff2(hyg)::*SS4*A targets region 'A'.

Ten-day-old plants were sprayed with 30 µM dexamethasone solution once a day for 10 days, 10 h into the 12 h light period. For experiments monitoring the decline in SS4 protein and mRNA levels, plants were harvested every day for 11 days, 10 h into the 12 h light period, immediately prior to that day's dexamethasone spraying. The first harvest (Day 0) was performed immediately prior to the first dexamethasone spraying. The final harvest (Day 10) was performed 24 h after the last dexamethasone treatment. For all other experiments, end of night samples were harvested 14 h after the final dexamethasone treatment, at the end of a normal 12 h night, and end of day samples were harvested 26 h after final dexamethasone treatment, at the end of a normal 12 h light period.

Compared to control plants, the SS4 mRNA levels are strongly reduced in the pOpOff2(hyg)::*SS4*A and pOpOff2(hyg)::*SS4*B lines (Figure 4.29). At the beginning of the experiment there is no evidence of SS4 silencing in the absence of dexamethasone, since plants containing the pOpOff2(hyg)::*SS4* construct have the same levels of *SS4* mRNA as control plants (Figure 4.29). Upon dexamethasone application, the lowest levels of *SS4* mRNA are achieved after 24 h, as was achieved in the original vector development by Wielopolska *et al.* (2005).

Western blots using an antibody raised against an SS4 peptide confirmed that the SS4 protein level in pOpOff2(hyg)::*SS4* lines is reduced after dexamethasone treatment (Figure 4.30). At the beginning of the experiment there is no evidence of SS4 silencing in the absence of dexamethasone, since plants containing the pOpOff2(hyg)::*SS4* construct have the same levels of the SS4 protein as control plants (Figure 4.30). The level of the SS4 protein in the dexamethasone treated pOpOff2(hyg)::*SS4* lines begins to fall after the second day of dexamethasone treatment and reaches its lowest level after seven days. Following 10 days of dexamethasone treatment the SS4 protein in pOpOff2(hyg)::*SS4* lines is often below the level of detection (Figure 4.30).

A

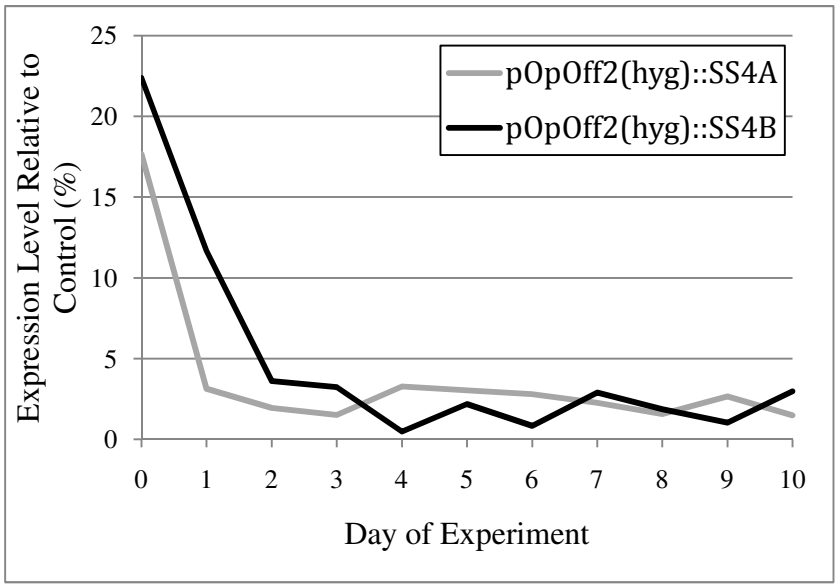

B

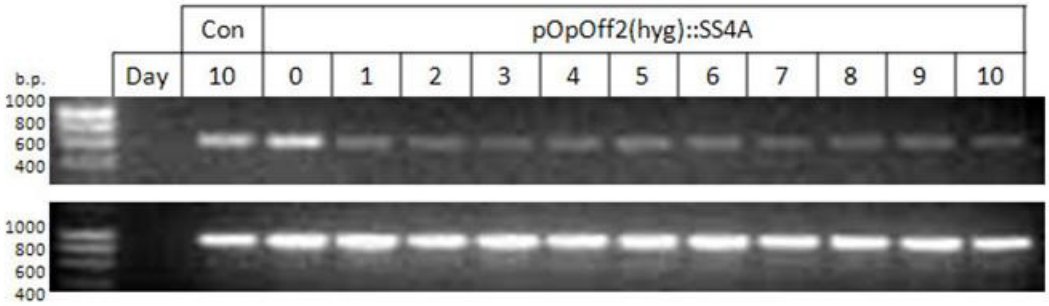

Figure 4.29: SS4 RNA levels in the rosette leaves of pOpOff2(hyg)::*SS4* lines. (A) Transcript levels of the *SS4* gene relative to TUBULIN control levels. Created from single repetitions at each time point. (B) Example of a typical semi-quantitative RT-PCR gel. Upper row = *SS4*; lower row = *TUBULIN* control. Using imaging software images are converted to greyscale and mean pixel intensity of each band is measured to create the graph in (A). Plants sprayed with 30 µM dexamethasone solution once a day for 10 days. Plants harvested 10 h into light period, immediately prior to dexamethasone spraying. First harvest (Day 0) immediately prior to first spraying. Final harvest (Day 10) 24 h after last dexamethasone treatment.

A

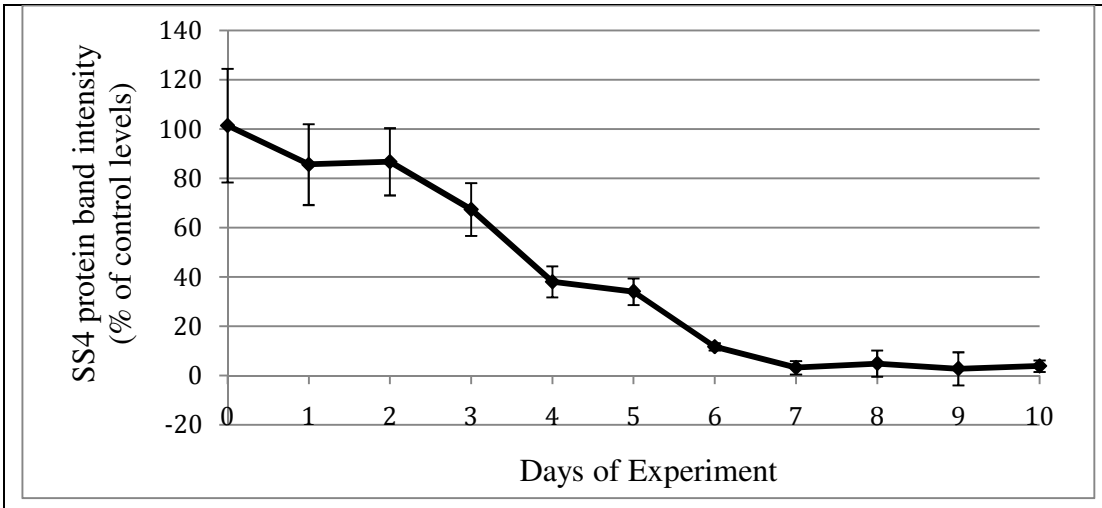

B

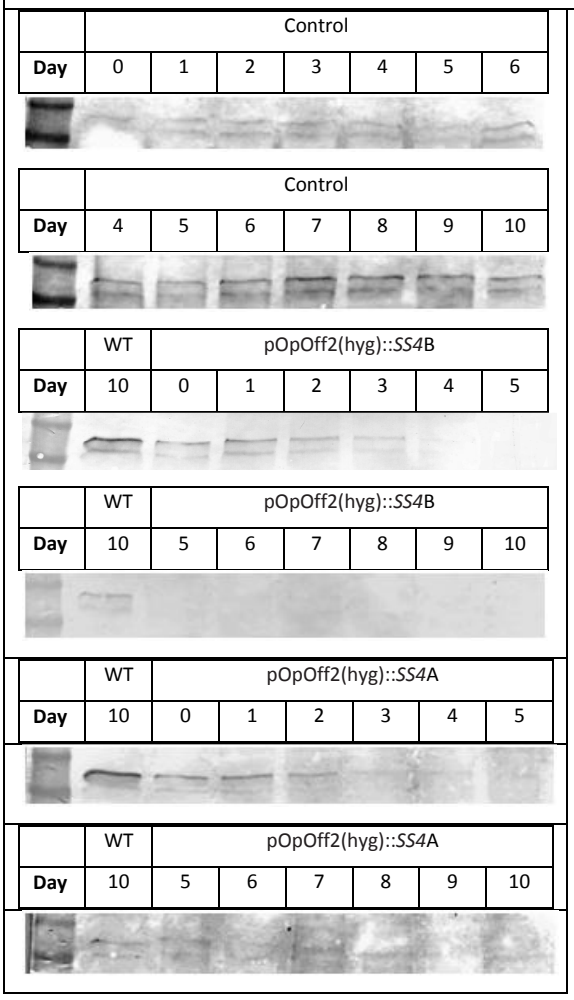

Figure 4.30: SS4 protein levels in whole rosettes of pOpOff2(hyg)::*SS4* lines. Plants were sprayed with dexamethasone once a day for 10 days. Plants were harvested immediately prior to dexamethasone spraying. First harvest (Day 0) was immediately prior to first spraying. Final harvest (Day 10) was 24 h after last dexamethasone treatment.

(A) Levels of the SS4 protein relative to control plants. Note: the western blots shown in B are for presentation only; for the measurement of relative protein levels, six plants harvested at the same time point are run on the same blot. Each time point in A is an average of six measurements (6 plants; 3 from line pOpOff2(hyg)::*SS4*A and 3 from line pOpOff2(hyg)::*SS4*B) ± SE, taken from the same western blot (see section 2.15 for method).

(B) Representative western blots of wild-type and pOpOff2(hyg)::*SS4* leaves, showing the decline in protein levels. Each lane on the blot contains extract from a separate plant, with 40µl of protein extract loaded in each lane. All extracts contain the same mg tissue per ml extract.

Following the 10 day dexamethasone treatment described above, rosettes were harvested at the end of the day and night, decolourised with ethanol and stained with iodine solution to test for the presence of starch (Figure 4.31). At the end of the day the whole rosettes of control plants stain a purple/black colour indicating the presence of starch, whereas *ss4* immature leaves, which contain very low levels of starch, remain colourless. All leaves of the pOpOff2(hyg)::*SS4* lines, at the end of the day, stained a purple/ black colour, indicating the presence of starch. At the end of the night control plant rosettes treated with iodine solution remain colourless, consistent with very low levels of starch, whereas *ss4* mature leaves, which have a starch excess at the end of the night, stain a faint purple/black colour. Although iodine staining is not as strong as in the *ss4* mutant, the outer leaves of the pOpOff2(hyg)::*SS4* lines stain a faint purple/black colour, indicating they contain a starch excess compared to wild-type plants (Figure 4.31). Therefore, while the pOpOff2(hyg)::*SS4* lines appear to have a wild-type starch accumulation pattern in all leaves at the end of the day, they differ from control plants in an apparent starch excess in older leaves at the end of the night, similar to *ss4* plants.

To quantify starch levels in dexamethasone treated pOpOff2(hyg)::*SS4* rosettes after ten days of dexamethasone treatment, leaves were harvested at the end of the 12 h light period and then again at the end of the 12 h dark period (Figure 4.32). As reported above the *ss4* rosette has a reduced rate of starch turnover, with less starch than the control at the end of the day, but more starch at the end of the night. Compared to wild-type plants the pOpOff2(hyg)::*SS4* plants have a reduced rate of starch turnover and this results in a starch excess at the end of the night. However, these differences are very mild compared with the strong reductions in starch turnover and the starch excess phenotype in the *ss4* mutant. If we assume starch degradation rates are constant during the night, control plants degrade 0.75 mg glu g^{-1} FW h^{-1}, whereas *ss4* plants degrade 0.32 mg glu g^{-1} FW h^{-1}. However, the dexamethasone treated pOpOff2(hyg)::*SS4* lines have only a slightly reduced rate of starch turnover compared to the control (0.70 mg glu g^{-1} FW h^{-1} and 0.71 mg glu g^{-1} FW h^{-1}).

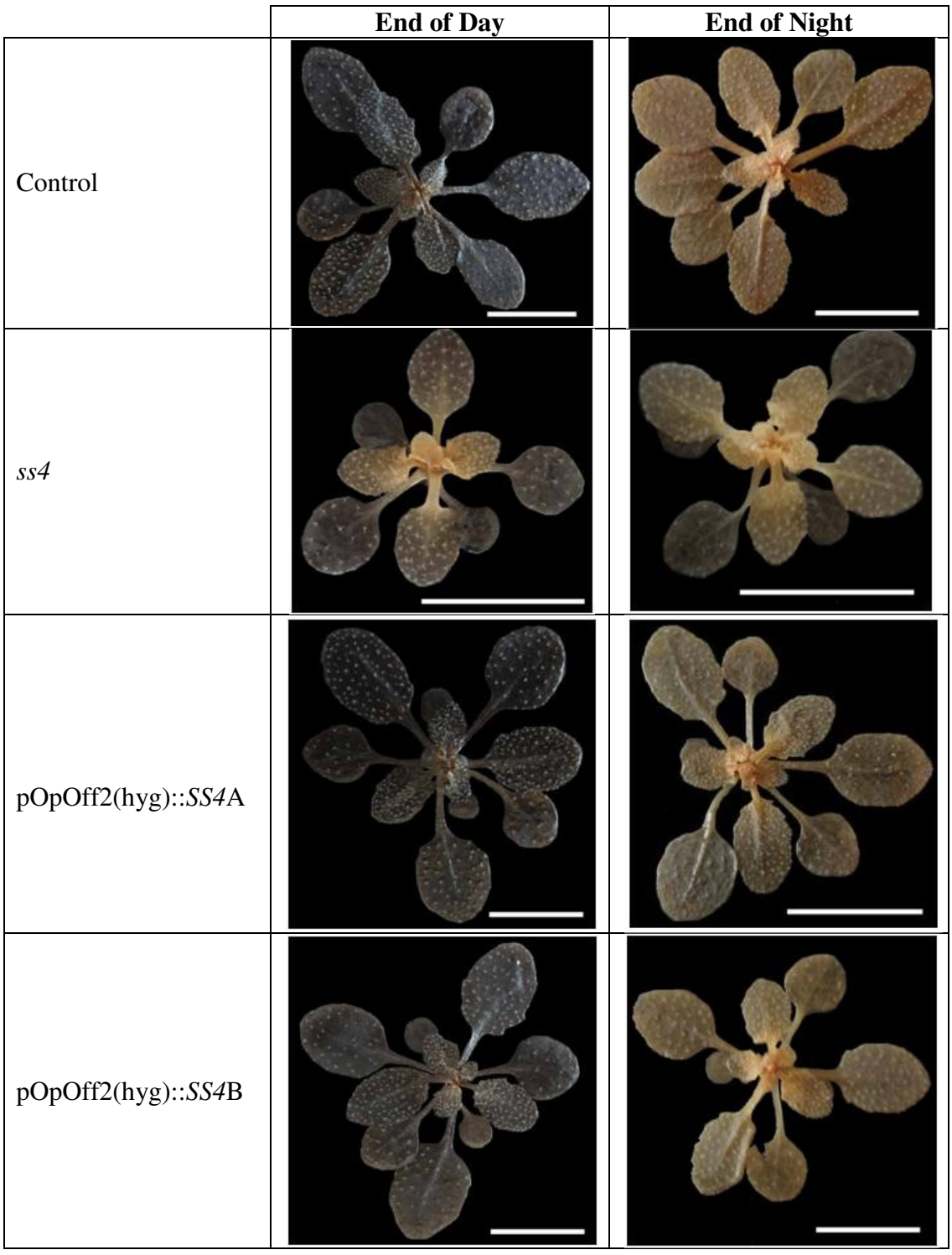

Figure 4.31: Whole rosettes harvested at the end of the light and end of the dark period, decolourised with ethanol and stained with iodine solution. Plants grown for 21 days in 12 h light/12 h dark conditions. Plants sprayed with 30 µM dexamethasone solution once a day, for 10 days prior to harvest. End of night samples harvested 12 h after final dexamethasone treatment. End of day samples harvested 24 h after final dexamethasone treatment. Scale bar = 1 cm.

A

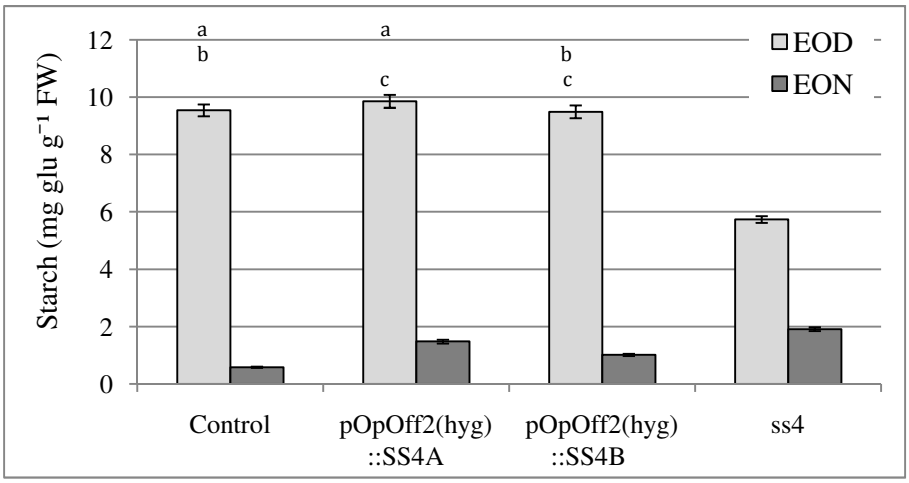

B

End of Day

	Control	pOpOff2(hyg)::*SS4*A	pOpOff2(hyg)::*SS4*B
pOpOff2(hyg)::*SS4*A	*t* (14) = 1.04 *p* = 0.318		
pOpOff2(hyg)::*SS4*B	*t* (14) = -0.17 *p* = 0.871	*t* (14) = 1.16 *p* = 0.267	
ss4	*t* (14) = -16.10 *p* <0.001	*t* (14) = 16.14 *p* <0.001	*t* (14) = 14.98 *p* <0.001

End of Night

	Control	pOpOff2(hyg)::*SS4*A	pOpOff2(hyg)::*SS4*B
pOpOff2(hyg)::*SS4*A	*t* (14) =12.39 *p* <0.001		
pOpOff2(hyg)::*SS4*B	*t* (14) = 9.43 *p* <0.001	*t* (14) = 5.92 *p* <0.001	
ss4	*t* (14) = 19.53 *p* <0.001	*t* (14) = -4.61 *p* <0.001	*t* (14) = -12.01 *p* <0.001

Figure 4.32: (A) Starch levels in control, pOpOff2(hyg)::*SS4* lines and *ss4*. EOD = End of Day. EON = End of Night. Each bar is the mean (±SE) of eight replicate samples. Bars with the same letter are not significantly different from each other. (B) Statistical analysis (*t*-test) performed on the starch levels in control pOpOff2(hyg)::*SS4* lines and *ss4* mutant rosettes displayed in A. Test of the null hypothesis that the mean starch contents of the datasets are not different. The test statistic, degrees of freedom (d.f.) and statistical significance are displayed.

The pattern of starch granule accumulation in the pOpOff2(hyg)::*SS4* lines following dexamethasone treatment is shown in iodine stained sections of embedded leaf material viewed under a light microscope and TEM sections of mesophyll cells (Figure 4.33). Chloroplasts in the mature leaves of the *ss4* mutant contain on average one large starch granule, while chloroplasts in the immature leaves of the *ss4* mutant lack visible starch granules. The chloroplasts in the immature leaves of both pOpOff2(hyg)::*SS4* lines appear to have fewer starch granules than equivalent chloroplasts in wild-type plants, but the chloroplasts in the mature leaves look like those of wild-type plants in the number and size of starch granules they contain.

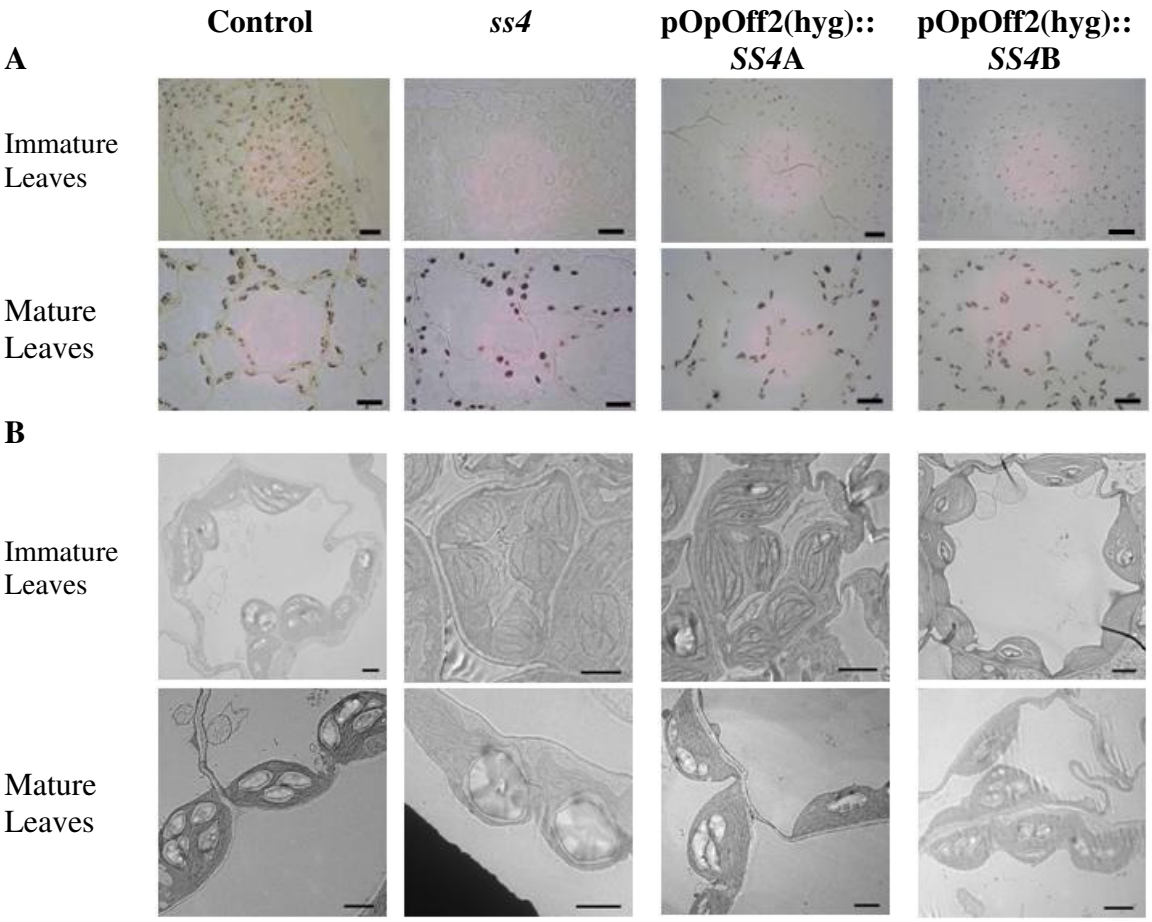

Figure 4.33: Starch in the leaves of control, *ss4* and pOpOff2(hyg)::*SS4* lines. (A) 1 µm thick sections through embedded leaves, stained with iodine solution and viewed under a light microscope. (B) TEM images of chloroplasts from spongy mesophyll cells. Plants sprayed with 30 µM dexamethasone solution once a day, for 10 days prior to harvest. A scale bar = 10 µM. B scale bar = 2 µM.

Measurement of granule number and chloroplast size from sections through mesophyll cells confirms that the chloroplasts in mature leaves of dexamethasone treated pOpOff2(hyg)::*SS4* lines contain the same number of starch granules as control plants (Figure 4.34). In mature leaves there was no difference in the stromal area per granule (the chloroplast cross-sectional area divided by the number of granules) between control and pOpOff2(hyg)::*SS4* lines (Figure 4.34A). The stromal area per granule of the control and pOpOff2(hyg)::*SS4* lines is smaller than that of the *ss4* mutant (Figure 4.34A) because *ss4* only contains one starch granule on average per chloroplast. However, in the immature leaves of dexamethasone treated pOpOff2(hyg)::*SS4* lines there is a greater stromal area per granule than control plants (an average of 48% and 52% more stroma per granule than control; Figure 4.34B) indicating that the chloroplasts contain fewer granules than control plants.

The morphology and size of the starch granules in dexamethasone treated pOpOff2(hyg)::*SS4* lines was analysed using SEM. The profile of granule size distribution of dexamethasone treated control and pOpOff2(hyg)::*SS4* plants are very similar and contrast with the profile of *ss4,* which has a shift to larger granules (Figure 4.35A). There was no difference in the radius of starch granules from control and pOpOff2(hyg)::*SS4* plants (Figure 4.35B). The starch granule radius of both the control and pOpOff2(hyg)::*SS4* lines is smaller than that of the *ss4* mutant (Figure 4.35B). Typical SEM pictures of starch granules from control plants, dexamethasone treated pOpOff2(hyg)::*SS4* lines and the *ss4* mutant are shown in Figure 4.36 (A-D).

A Mature Leaves

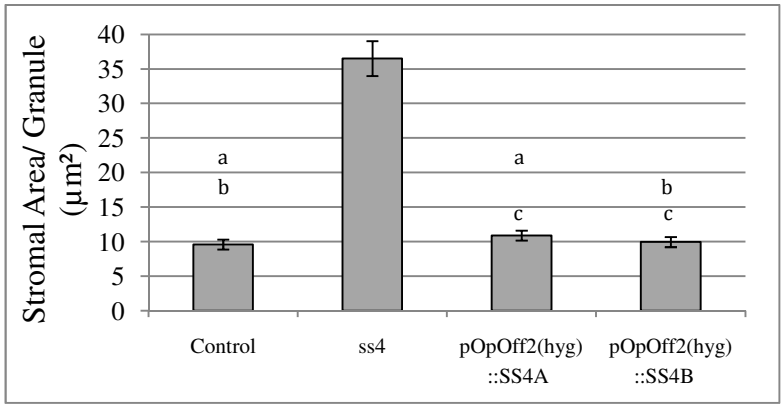

B Immature Leaves

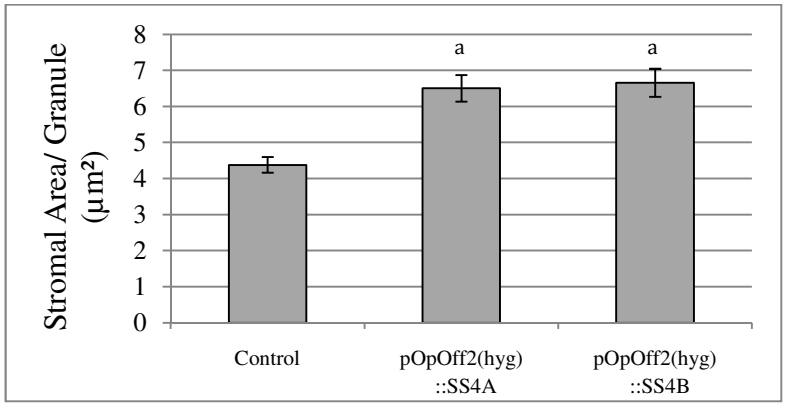

Figure 4.34: The stromal area per granule (the chloroplast cross sectional area divided by the number of starch granules per chloroplast section) in control, *ss4* and the pOpOff2(hyg)::*SS4* lines. (A) Mature leaves (B) Immature leaves (the four youngest leaves (greater than 1 mm long) on 25-day-old rosettes). Measurements were taken using imaging software on photos of mesophyll cell sections stained with iodine solution. Data are means of measurements on 40 chloroplasts (± SE) measured from 7 sections. Plants were grown for 21 days in 12 h light/12 h dark conditions. Plants were sprayed with 30 µM dexamethasone solution once a day, for 10 days prior to harvest. Leaves from two rosettes per genotype were harvested 10 h into a 12 h light period. The *ss4* mutant is not included in immature leaf data because immature *ss4* leaves lack starch. Bars with the same letter are not significantly different from each other. Statistics in Table 4.16.

A Mature Leaves

	Control	pOpOff2(hyg)::*SS4*A	pOpOff2(hyg)::*SS4*B
pOpOff2(hyg):: *SS4*A	t (78) = 1.27, p = 0.208		
pOpOff2(hyg):: *SS4*B	t (78) = 0.36, p = 0.716	t (78) = 0.90, p = 0.371	
ss4	t (78) = 10.20, p <0.001	t (78) = -9.71, p <0.001	t (78) = -10.05, p <0.001

B Immature Leaves

	Control	pOpOff2(hyg)::*SS4*A
pOpOff2(hyg)::*SS4*A	t (78) = 4.97, p <0.001	
pOpOff2(hyg)::*SS4*B	t (78) = 5.09, p <0.001	t (78) = -0.28, p = 0.777

Table 4.16: Statistical analysis (*t*-test) performed on the stromal area per granule in control, pOpOff2(hyg)::*SS4* lines and *ss4* chloroplasts from mesophyll cells in mature leaves (A) and immature leaves (B), data displayed in Figure 4.34. Test of the null hypothesis that the mean stromal area per granule of the datasets are not different. The test statistic, degrees of freedom (d.f.) and statistical significance are displayed.

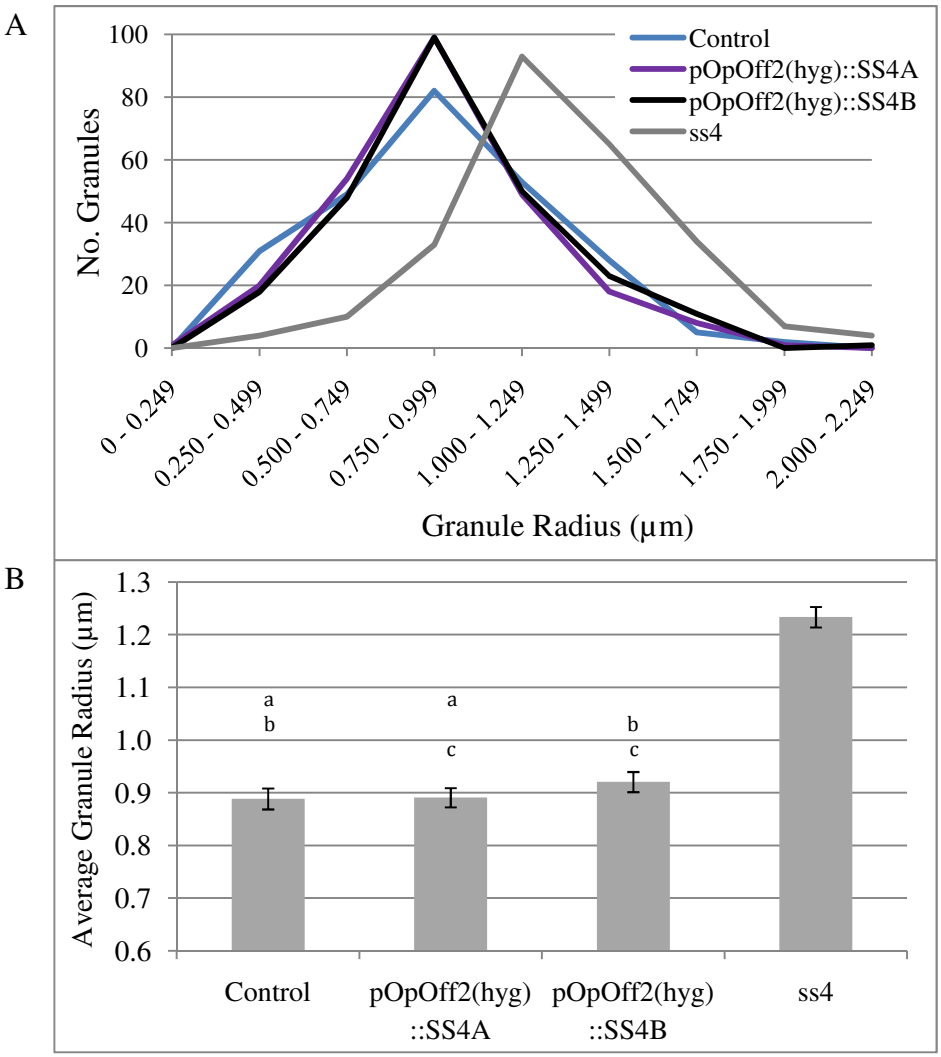

C	Control	pOpOff2(hyg)::*SS4*A	pOpOff2(hyg)::*SS4*B
pOpOff2(hyg)::*SS4*A	t (498) = 0.09, p = 0.927		
pOpOff2(hyg)::*SS4*B	t (498) = 1.16, p = 0.246	t (498) = -1.12, p = 0.264	
ss4	t (498) = 12.36, p <0.001	t (498) = -12.80, p <0.001	t (498) = -11.45, p <0.001

Figure 4.35: Granule size and distribution. (A) Average granule radius. n = 250 ±SE. Bars with the same letter are not significantly different from each other. (B) Granule radius distribution. Total of 250 granules. (C) Statistical analysis (*t*-test) performed on the mean granule radius in control, pOpOff2(hyg)::*SS4* lines and *ss4* plants, data displayed in B. Test of the null hypothesis that the mean granule radius of the datasets are not different. The test statistic, degrees of freedom (d.f.) and statistical significance are displayed.

A 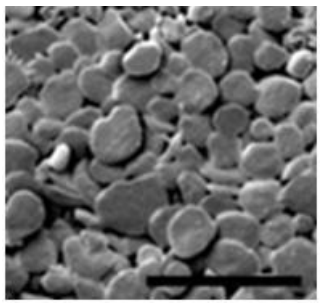 B 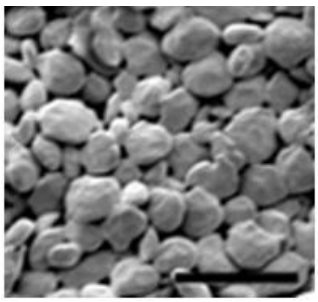 C 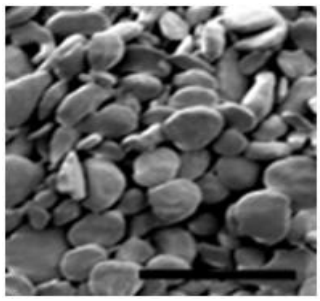

D 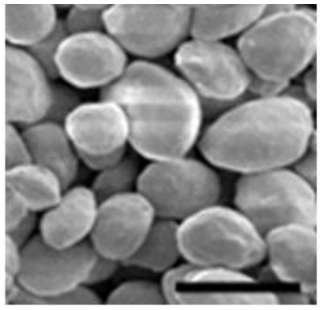

Figure 4.36: Typical SEM images of isolated starch granules. Scale bar = 5 µm. (A) Control. (B) pOpOff2(hyg)::*SS4*A. (C) pOpOff2(hyg)::*SS4*B. (D) *ss4*.

4.3 Discussion

The original aim of this thesis/chapter was to find out what determines the number and size of starch granules in *Arabidopsis* chloroplasts. Results of studies of the *ss4* mutant provide a wealth of new information and hypotheses about the determination of starch granule number. They also provide new insights into numerous other aspects of leaf carbohydrate turnover and its relationship to growth. In this discussion, I present first my major conclusions about the role of SS4 in the determination of starch granule numbers in chloroplasts. I then discuss other new information about carbohydrate metabolism and growth that arises from my experiments. pOpOff2(hyg)::SS4.

4.3.1 New insights into the determination of granule number

4.3.1.1 SS4 is necessary for normal starch granule initiation in chloroplasts of developing leaves and root columella cells.

The reduced number of starch granules that initiates in the *ss4* mutant indicates that SS4 clearly has an essential role during starch granule initiation. The *ss4* mutant has a reduced rate of both starch synthesis and degradation in all of its rosette leaves, leading to a reduced amount of starch at the end of the day and a starch excess at the end of the night compared to wild-type plants. My results and earlier results by Marilyn Pike (JIC) show that the immature leaves of the *ss4* mutant contain very low levels of starch at both the end of the day and night, with few chloroplasts containing starch granules. While Roldan *et al.* (2007) noted that *ss4* only had a single starch granule per chloroplast, they failed to note the low levels of starch in the chloroplasts of immature leaves.

The results from the dexamethasone treated pOpOff2(hyg)::*SS4* lines support and highlight the importance of SS4 in granule initiation in the immature leaves and the influence of this process on the starch phenotype of the whole plant. SS4 mRNA and protein levels are reduced in dexamethasone treated pOpOff2(hyg)::*SS4* plants, however low levels do remain and appear to be sufficient to allow granule initiation in the immature leaves to continue, albeit at a reduced rate.

My results suggest that SS4 has a similar role in granule initiation in other organs of the *Arabidopsis* plant, as loss of SS4 affects starch accumulation in the root cap and developing siliques. The starch present in the root cap of the primary root of *Arabidopsis ss4* mutants varies from wild-type levels in some plants, to occurrence within just a few cells in other plants (Figure 4.13). The amount of starch that accumulates appears to correlate with the deviation of the root from vertical (Figure 4.13), which fits with previous studies on starchless and reduced starch *Arabidopsis* mutants (Kiss and Edelmann 1999). In all cases studied, mutants with reduced starch in the root cap and starch deficient mutants show reduced gravitropism compared to their respective wild-type organs (Caspar and Pickard 1989; Kiss *et al.,* 1989; Kiss and Sack 1990; Saether and Iversen 1991). Gravitropism is the directed growth of plant organs in response to gravity. The majority of evidence supports the starch statolith hypothesis of gravity sensing, which proposes that plants perceive the force of gravity by sedimentation of dense, starch-filled amyloplasts that function as statoliths (dense, movable intracellular particles) in the root cap (Caspar and Pickard 1989; Kiss *et al.,* 1998b; Molas and Kiss 2009; Sack 1997). If the plants are reorientated, the amyloplasts settle to the new lower cell wall (Blancaflor *et al.,* 1998). This provides signals that allow the roots to grow in the correct direction in response to gravity. In *Arabidopsis* roots the inner, central columella cells have the highest amyloplast sedimentation velocities and provide the greatest contribution to gravity sensing, while the peripheral and tip cells have no role in graviresponse (Blancaflor *et al.,* 1998). In roots, starch is not absolutely required for gravity perception, but is necessary for full gravitropic sensitivity (Kiss *et al.,* 1989). Despite the reduced levels of starch within the *ss4* mutant roots, the roots are often orientated correctly and the mean angle from vertical is only 11% greater in the *ss4* mutant than wild-type plants. This is explained by the fact that only 51-60% of wild-type starch levels are required for full gravitropic response (Kiss *et al.,* 1998a). Therefore, if the *ss4* root contains greater than 51% of wild-type starch levels it will respond as if it were a wild-type root and grow down vertically.

4.3.1.2 SS4 does not directly control the number of granules in wild-type leaves.

If levels of SS4 protein do indeed regulate the number of starch granules that can be initiated, one might simplistically expect to find fewer granules in plants with reduced SS4 and more in plants over-expressing SS4. However, examination of plants

heterozygous for the *ss4* mutation indicate that the effects of SS4 are not linearly dosage dependent, because halving the SS4 protein content does not detectably reduce the number of granules initiated per chloroplast. This contrasts with glycogenin (see Chapter 1, section 1.3.1.3), the effects of which appear to be dosage dependent in rats. The overexpression of glycogenin in rat fibroblasts does not alter the overall rate of glycogen synthesis but causes the production of more, smaller glycogen molecules (Skurat *et al.,* 1997). In summary, analysis of *Arabidopsis* plants heterozygous for the *ss4* mutation reveals that while SS4 is required for normal granule initiation, it exerts very little or no control over the numbers of granules that initiate in wild-type plants. It is likely that control of granule numbers in wild-type plants is partitioned in a complex way between enzymes of glucan synthesis and factors that control background stromal conditions promoting crystallisation.

4.3.1.3 The action of SS4 is probably to make a primer that other starch synthases can use.

SS4 is necessary for the initiation of glucans that then form granules and appears to act upstream of ISA1 during starch granule initiation and growth. The chloroplasts in the young leaves of the *isa1ss4* double mutant not only fail to produce starch granules, they are unable to synthesise any glucan polymers. The production of phytoglycogen in the mature leaves of the *isa1ss4* double mutant shows that as the leaf matures, something is able to compensate for the loss of SS4 by allowing the initiation of glucan chains.

When SS4 is absent from young leaves, the other starch synthases are unable to make the appropriate structure or quantity of glucans required to initiate a granule and high levels of the starch synthase substrate, ADPG, accumulate. Therefore, the young leaves of the *ss4* mutant contain the capacity to make the starch synthase substrate ADPG and to polymerise glucose (the other SSs), indicating that something is missing that allows the SSs to make ADPG into polymers. I suggest that SS4 may be responsible for the production of a small malto-oligosaccharide (MOS) that is required as a primer for the polymerising activity of the other starch synthases.

Recombinant SS4 has been shown to have some affinity for maltose and a high affinity for maltotriose, whereas SS3 has no or very low affinity for these substrates

(Szydlowski *et al.,* 2009). This is consistent with the idea that SS4 can make very small MOS into longer, but still small MOS, which the other starch synthases can elongate further. Maltotriose could be the substrate that SS4 elongates and the other starch synthases then act upon the elongated maltotriose product.

There are however arguments against maltotriose or maltose being the key substrates for SS4. In plants there is no known pathway for the production of maltose or maltotriose de novo in the chloroplast, rather than from the degradative action of DPE1 and BAM3 on starch (Critchley *et al.,* 2001; Lao *et al.,* 1999; Scheidig *et al.,* 2002). In bacteria maltose is known to be formed by the action of maltose phosphorylase (EC 2.1.1.8), from β-D-glucose-1-phosphate and free glucose (Decker *et al.,* 1993; Fitting and Doudoroff 1952). In plants there are reports of maltose being synthesised de novo in the chloroplasts in the light. For example, the rapid appearance of [^{14}C]maltose and [^{14}C]maltotriose in chloroplast feeding experiments and intact leaves, led Schilling and Kandler (1975), Linden *et al.* (1975) and Herold *et al.* (1981) to suggest that maltose phosphorylase may function in a synthetic role in plants. Kruger and ap Rees (1983) also found that a maltose phosphorylase like activity was responsible for the synthesis of maltose, from glucose-1-phosphate, in isolated pea chloroplasts, although their work focussed upon maltose production during starch degradation. It has also been reported that maltose synthase (EC 2.4.1.139) activity in spinach chloroplasts can make maltose and maltotriose from α-D-glucose-1-phosphate molecules (Linden and Schilling 1984; Schilling 1982). In addition, Witt and Sauter (1994) detected maltose synthase and maltose phosphorylase activity in protein extracts of poplar wood ray cells. However, there are no recent reports of maltose synthase or maltose phosphorylase activity in plants. There are no genes in the *Arabidopsis* genome that resemble bacterial maltose phosphorylase and to my knowledge no reports of a gene encoding maltose synthase in any organism.

The predicted coiled coil regions within the N-terminal region of SS4 indicates that it may participate in multiple coiled coil interactions with other proteins (Leterrier *et al.,* 2008; Lohmeier-Vogel *et al.,* 2008). A coiled coil domain is a three-dimensional structure consisting of a repeating heptad pattern of alternating hydrophobic and hydrophilic residues, resulting in an α-helical coil (Lupas and Gruber 2005; Mason and Arndt 2004). Coiled coil domains are involved in attaching protein complexes to larger

cellular structures (Rose *et al.,* 2004). Leterrier *et al.* (2008) detected, using bioinformatics, two coiled-coil domains and a 14-3-3-protein recognition site in the N-terminal region of the wheat *SSIVb* gene. Lohmeier-Vogel *et al.* (2008) noted the exceptionally long predicted coiled coil region of *At*SS4, which they predicted to be more than 200 residues long. Szydlowski *et al.* (2009) speculated that SS4 may form a complex through its coiled coil domains which allows the formation of a specific glucan, which would serve as a nucleation centre required for normal granule initiation.

4.3.1.4 Synthesis of a granule in the absence of SS4 may be a function of SS3.

In the absence of SS4, the chloroplasts of immature leaves lack starch granules, but at a certain point during leaf development one or multiple starch synthases may begin to compensate for the loss of SS4 resulting in the production of a starch granule. Evidence suggests that SS4 is partially redundant with respect to SS3, because the removal of SS3 from the *ss4* mutant background, results in no detectable starch being produced (Szydlowski *et al.,* 2009). Therefore, in the *ss4* mutant, SS3 can eventually and inefficiently produce either the substrate normally produced by SS4 or a substitute for it. An additional piece of evidence that suggests SS3 could have a role in starch granule initiation comes from Busi *et al*. (2008), who described the complementation of an *Agrobacterium tumefaciens* glycogen synthase mutant with *Arabidopsis* SS3 and proposed that SS3 played a role in initiating glycogen synthesis.

Potentially, as the leaf matures, the concentration of glucans or malto-oligosaccharides (MOS) necessary for a starch granule to initiate may reach a critical concentration within the stroma at which a granule spontaneously crystallises out from the soluble phase. In the absence of SS4 it takes longer for this event to occur. Szydlowski *et al*. (2009) proposed that SS3 is unable to form the same sort of granule initiating structure ("nucleation point") as SS4 and so granules form at a much lower rate; one granule per chloroplast, compared to an average of six granules per chloroplast in wild-type. The core of *ss4* mutant granules has been reported to be less electron-dense compared to wild-type granules, potentially indicating the presence of a cavity in the hilum (Roldan *et al.,* 2007). This could support the theory that the nucleation point of the granule is altered in structure in the *ss4* mutant.

Plastidic α-glucan phosphorylase may be involved in starch granule initiation in the *ss4* mutant. This has been suggested because of the observed increase in levels of plastidic (and cytosolic) α-glucan phosphorylase (*At*PHS) (see section 1.3.1.2) activity in the *ss4* mutant (Roldan *et al.,* 2007). Evidence from wheat endosperm, rice endosperm, potato tubers and green algae (*Chlamydomonas reinhardtii*) suggests that Pho1 is potentially involved in starch synthesis; either directly synthesising glucans or indirectly by shortening long unbranched side chains of pre-amylopectin molecules (Albrecht *et al.,* 2001; Dauvillee *et al.,* 2006; Fettke *et al.,* 2010; Satoh *et al.,* 2008; Schupp and Ziegler 2004). So while loss of plastidial 1,4-glucan phosphorylase has no effect on starch synthesis in *Arabidopsis* and potato leaves (Sonnewald *et al.,* 1995; Zeeman *et al.,* 2004), in the *ss4* mutant it may play a role in granule initiation. The absence of starch from the *ss3ss4* double mutant (Szydlowski *et al.,* 2009) casts doubt on the involvement of α-glucan phosphorylase in granule initiation. If α-glucan phosphorylase were involved in granule initiation in the *ss4* mutant, then granules would still be expected to occur in the *ss3ss4* double mutant.

4.3.2 Other information gained from the study of the *ss4* mutant

4.3.2.1 Starch phenotypes of mature SS4 leaves are largely, but not entirely determined in younger leaves.

Wild-type immature and mature *Arabidopsis* leaves contain equal quantities of SS4 protein on a fresh weight basis (Figure 4.10), which would suggest SS4 is equally active throughout leaf development; although post translational control cannot be ruled out.

The starch phenotype observed in the mature leaves of *ss4* mutants (i.e. a reduced number of granules per chloroplast compared to wild-type plants, an abnormal pattern of starch turnover and an accumulation of ADPG); are largely, but not entirely, determined in younger leaves. Reducing the amount of the SS4 protein to below 10% of the control levels in pOpOff2(hyg)::*SS4* lines, reduces the number of granules that are initiated, but only in leaves that developed after the reduction in SS4 protein levels occurs and not in the chloroplasts of older leaves. In the mature leaves of dexamethasone treated pOpOff2(hyg)::*SS4* lines, wild-type granule number per chloroplast and granule size is maintained. Therefore, the single enlarged granule that

occurs in the mature leaf chloroplasts of the *ss4* mutant is a result of granule initiation problems that occur in the immature leaves. The fact that a reduction in SS4 had no effect on starch granule number in mature leaves suggests that few or no granules are initiated in these leaves. This is consistent with the idea that once granules are initiated in the chloroplasts of immature leaves they grow and shrink over the day/night cycle. However, there is a starch excess in the dexamethasone treated pOpOff2(hyg)::*SS4* lines at the end of the night compared to the control. This suggests that the reduction in SS4 levels does have some minor effect on granule turnover later in development in the mature leaves.

The granules that form in the *ss4* mutant are larger and rounder than granules in wild-type plants. The small numbers of granules that initiate in the *ss4* mutant appear to be structurally normal. It has previously been reported that *ss4* starch has both a normal amylose to amylopectin ratio and only minor alterations in the amylopectin structure (Roldan *et al.,* 2007). Therefore, once a starch granule is initiated the other SSs, SBEs and DBEs are able to act as they normally would. It is reasonable to assume that the *ss4* granules are larger because the newly synthesised glucans that would usually be distributed between a number of granules in the chloroplasts of wild-type leaves is only delivered onto one granule. However, it is not clear why the granules that form in *ss4* are rounder than those of wild-type plants. As previously discussed, a change in granule size does not always result in an alteration in granule shape (Section 1.4). For example, the granules from the starch excess mutant *sex4* are not only larger, but also more spherical than wild-type granules (Sokolov *et al.,* 2006; Zeeman *et al.,* 2002b), and resemble those formed in *ss4*. This contrasts with the granules from another starch excess mutant, *gwd1,* which are larger but remain disc shaped and resemble wild-type granule shape (Zeeman *et al.,* 2002b). Therefore, under the *ss4* mutant conditions the plant is unable to maintain normal control over granule shape. This suggests that potentially SS4 is involved throughout wild-type granule growth.

4.3.2.2 The reduction in granule growth in the *ss4* mutant may be a direct or indirect consequence of loss of SS4.

Within the mature leaves of the *ss4* mutant the single large granule that is produced has a reduced surface area compared to the multiple smaller granules which form in the chloroplasts of wild-type plants. Thus in addition to the ADPG accumulation caused by

reduced amylopectin molecule initiations, ADPG may further accumulate because of the reduced rate of its incorporation onto the starch granule surface. Roldan *et al.* (2007) suggested that the reduced granule surface area available for both starch synthesis and degradation was responsible for the reduced rates of starch turnover, as the enzymes responsible have a reduced surface area upon which to act. However, while this may partly explain the reduced starch turnover, I do not feel this provides a satisfactory answer for the extent of the reduced degradation rate in the *ss4* mutant. My hypotheses are discussed below. There are no changes in the activities of a number of starch metabolising enzymes in *ss4* (Roldan *et al.,* 2007), for example there was no reduction in AGPase, SBE, D-enzyme or phosphorylase in the *ss4* mutant. On this basis there is no reason to suspect that reductions in starch synthesis or degradation enzymes are responsible for the reduced rate of starch turnover. However, Roldan *et al.* (2007) did not measure all enzymes involved in starch metabolism and others may be affected in the *ss4* mutant.

The reduced granule surface area in the *ss4* mutant may not be the only explanation for the reduced rate of starch synthesis in mature leaves. If, as the results suggest, SS4 is responsible for the production of a unique primer molecule acted upon by the other SSs to produce amylopectin molecules, then SS4 potentially plays a role throughout granule growth and not just during initiation. However, this would depend upon the method by which starch granules grow, for which there is no direct evidence. If starch granules grow solely by the addition of ADPG directly to glucan chains projecting from the surface of the granule (Nakamura 2002; Nielsen *et al.,* 2002), then the major role for SS4 would be during the initial granule formation. However, if throughout granule growth amylopectin molecules form in the stroma and then spontaneously crystallise onto the granule surface (section 1.3.2), then the *ss4* mutant will be compromised in its ability to produced starch throughout granule growth.

To date most evidence suggests that granules grow by the addition of ADPG at the surface, with elongation, branching and debranching all happening together at the surface (Nakamura 2002; Nielsen *et al.,* 2002). Nielsen *et al.* (2002) used radioactive-labelling experiments to show that leaf starch grows by elongation of the outer chains of the granule to twelve or more glucoses in length. A six-glucose long chain is then cleaved off by a SBE, and transferred elsewhere on the granule surface to make a new

glucan chain. Nielsen *et al.* (2002) found that any highly branched intermediary glucan structure that forms, upon which a debranching enzyme (ISA) may act, is bound to the granule, rather than occurring as separate pre-amylopectin molecules. However, Nielsen *et al.* (2002) did not rule out the occurrence of a short-lived intermediate glucan in the form of small soluble branched glucans (pre-amylopectin), which may occur at undetectable levels free in the stroma. Therefore, the possibility remains that granule growth may also occur via spontaneously crystallisation of amylopectin molecules onto the granule surface; in which case SS4 would be involved throughout starch granule growth. The chloroplasts of the triple mutant lacking SS1, SS2 and SS3 (*ss1 ss2* ss3) contain a wild-type number of starch granules (Szydlowski *et al.,* 2009), indicating that SS4 can synthesis amylopectin throughout granule growth, and is not just involved in initiation. However, the extent to which SS4 contributes to amylopectin synthesis in mature leaves of a wild-type plant is unknown.

4.3.2.3 The reduced growth rate of the *ss4* mutant may be due to a combination of disrupted adenylate metabolism and reduced carbohydrate availability.

The reduced growth rate of the *ss4* mutant plant may be the result of impaired photosynthesis. For example, the exceptionally high ADPG levels are likely to be an important factor in the overall *ss4* phenotype. The failure to regenerate ADP through conversion of ADPG to starch is likely to compromise photophosphorylation and hence the light reactions of photosynthesis and carbon assimilation.

The balance between the rate of starch synthesis during the day and the rate of degradation at night is disrupted within the *ss4* mutant. As discussed previously (section 1.2.2), the starch accumulated in leaves during the day is essential for normal metabolism and growth at night (Naegele *et al.,* 2010) and control of the starch turnover, i.e. control of the rate of starch synthesis during the day and of the rate of degradation at night, is considered critical for normal plant growth and development (Caspar *et al.,* 1985; Corbesier *et al.,* 1998; Geiger *et al.,* 2000; Schulze *et al.,* 1994). In a model of plant growth and carbohydrate turnover proposed by Rasse and Tocquin (2006), the maximum growth rate was very sensitive to the level of starch accumulated during the day, since this was essential for maintenance of the growth rate at night. In other words, plants need to maintain a steady supply of soluble sugar to maintain normal plant growth. If the carbon supply is depleted then growth and development of

the plant is inhibited. For example, during a normal day-night cycle wild-type plants maintain a steady rate of root growth. However, when wild-type plants are exposed to an extended night, root extension slows and then stops (Brouquisse *et al.,* 1998; Gibon *et al.,* 2004). Under normal conditions there is a fine balance between carbon reserves and growth (Paul and Foyer 2001; Smith and Stitt 2007). The disruption of this balance in the *ss4* mutant is a possible cause of the reduced growth rate of the plant.

In the maturing leaves of *ss4,* transitory starch is not completely degraded during the night, and as a result gradually accumulates to higher levels with age, a phenotype often seen in starch degradation mutants. However, there is no evidence that SS4 is involved in starch degradation. The starch degradation phenotype of the *ss4* mutant may be a result of the problems in starch synthesis, such as the formation of only a single large granule in each chloroplast and the large pool of ADPG that accumulates. It is possible that ADPG, which normally disappears at the onset of the night, inhibits one or more enzymes of starch degradation. Thus, its disappearance may be part of the mechanism that normally switches on starch degradation at the starch of the night.

The single, rounded granule that forms in each chloroplast of the *ss4* mutant will have a reduced surface area compared to the six or so disc shaped granules that form in each chloroplast of wild-type plants. The reduced granule surface area available for degradative enzymes to act upon could be responsible for the reduced rate of starch degradation in the *ss4* mutant (Roldan *et al.,* 2007). However, while the limited surface area might be partially responsible, it is unlikely to fully explain the reduced degradation rate. A steady rate of starch degradation is maintained throughout the night in wild-type plants (Graf *et al.,* 2010), even at the end of the night, when the granules are very small and surface area might be expected to become limiting. Therefore, in addition to the reduced surface area, there are likely to be additional reasons for the reduced degradation rate in *ss4.*

Mutants classified as starch degradation mutants because they retain high levels of starch in their leaves at the end of the night include *sex4, lsf1* and *gwd1*. As described in Chapter 1, *sex4, gwd1* and possibly *lsf1* are involved in a cycle of glucan phosphorylation and dephosphorylation that facilitates the attack on the starch granule by β-amylase and ISA3 and is essential for normal starch degradation (Edner *et al.,*

2007; Hejazi *et al.,* 2008; Kötting *et al.,* 2009). The starch degradation mutants listed above are inhibited in their degradation to a much greater extent than *ss4*. For example, the *gwd1* mutant only degrades 30% of its starch even after 84 h of continuous darkness (Caspar *et al.,* 1991) compared to 98% in *ss4* after 72 h. *lsf1* degrades only 51% of its starch during a normal night (Comparot-Moss *et al.,* 2010), compared to 76% in *ss4*. Interestingly, while *sex4* and *lsf1* have reduced starch degradation rates, they maintain sufficient rates of starch degradation through the night to avoid the onset of a starvation response (Graf *et al.,* 2010). It is possible that an altered structure of the *ss4* starch granule, such as misplaced or an increased frequency of branch points, could affect the subsequent phosphorylation and dephosphorylation necessary for normal starch degradation. However, although the size and shape of the *ss4* mutant granule is altered, only minor alterations in the amylopectin structure have been observed (Roldan *et al.,* 2007), and it therefore seems unlikely that impaired phosphorylation or dephosphorylation is responsible for the altered degradation rate.

The *ss4* mutant takes more than 60 hours in continuous darkness to degrade the starch in its rosette leaves to negligible levels; unlike wild-type plants, which degrade more than 99.5% of their starch within 24 hours of continuous darkness. This fits with a previous study that found when wild-type plants, grown under long day conditions, were transferred to continuous darkness, by 16 hours into the period of darkness they had degraded their starch to negligible levels (Lu *et al.,* 2005). It is worth noting that in wild-type plants, 15 hours into a period of continuous darkness, the transcript levels of starch degradative enzymes have declined, and protein levels are reduced (Lu *et al.,* 2005). If levels of starch degradative enzymes were also reduced in the *ss4* mutant after 15 hours of continuous darkness, then beyond this point the mutant's ability to further degrade its starch would be reduced, which could partly explain the extended period of time taken for the starch in *ss4* to be completely degraded under conditions of continuous darkness. Alternatively, there may be unknown structural differences in the starch granule or metabolic differences in the *ss4* mutant compared to wild-type that delay starch degradation and cause the mutant to retain its starch.

The fact that the *ss4* mutant apparently experiences reduced carbohydrate availability during the normal night is a likely cause of its reduced growth rate. Unlike wild-type plants that have no detectable luciferase (LUC) expression during the normal 12 hour

night (promoter of the sugar-repressed or "carbohydrate starvation" gene *At*1g10700, fused to a luciferase reporter (*pAt1g10070::LUC*)), the *ss4* mutant expresses LUC in at least some leaves throughout the normal 12 hour night. Even though the *ss4* mutant contains starch, it appears that because of the low overall rate of starch mobilisation, carbohydrate availability falls below the normal levels in a wild-type plant, hence the *ss4* mutant expresses a higher level of At1g10070 than wild-type plants.

Despite this clear indication of starvation in the *ss4* mutant at night, my measurements show that sugar levels across the rosette in *ss4* are higher or equal to wild-type levels at both the end of the day and end of the night. It is difficult to reconcile these high sugar levels with the starvation phenotype. However, it is unknown exactly what the "starvation reporter" responds to. At1g10070 is known to be expressed in conditions when the plant is expected to experience a fall in available carbohydrate below "normal" levels (Graf *et al.,* 2010), but it is not known what is actually sensed in order to activate this gene. It may not be low levels of sucrose, glucose or fructose that activate the "starvation" response, but instead, for example, low levels of a molecule released during the degradation of starch such as maltose. Thus "starvation" signals could be produced by low rates of starch degradation, regardless of sucrose and glucose levels. Alternatively, in the *ss4* mutant a defect in sugar-signalling could be causing abnormal activation of the starvation reporter, independent of the actual carbon availability.

Another consideration in interpreting "starvation reporter" results is the nature of sugar measurements made on leaves. When sugar levels in a leaf are measured, they are averaged across the whole leaf and incorporate all components, including for example the apoplast, phloem and vacuole. Therefore, the sugar content of the compartment in which changes in carbohydrate levels are sensed is unknown. For example, while sugar levels in the *ss4* mutant leaf are recorded as being high, the sugar content in the chloroplast or cytosol may be low and this may be the location at which sugar levels are perceived by the "starvation response" pathway.

It is unknown whether a plant is actually experiencing carbohydrate starvation, in the sense that growth has become limited directly by low carbohydrate availability, when "starvation reporter" genes such as At1g10070 are expressed. If the gene is being

expressed in response to a fall in carbohydrate availability (rather than actual starvation), then it could in fact form part of an "early warning system" that precedes carbon limitation and alters metabolism and growth so that the plant can subsequently cope better if the problem of limited carbohydrate persists or worsens.

The high sugar levels produced during the day in *ss4* could potentially have a knock on effect, reducing the starch degradation rate at night. For example, high sucrose levels were found to suppress the accumulation of α-amylase in rice, by repressing gene expression (Sheu *et al.,* 1994). Although, as previously discussed, under normal wild-type conditions α-amylase activity is not required for starch degradation in *Arabidopsis* leaves (section 1.2.3), other degradation enzymes may be repressed by high sugar levels. If high sugar levels in the *ss4* mutant do repress expression of starch degradation enzymes, then there should be lower assayable activities of starch degradation enzymes. However, Roldan *et al.* (2007) found no change in the activity of the starch degradation enzyme a-1,4-glucanotransferase (D-enzyme/DPE1) in *ss4* relative to wild-type plants, and an increase in the gene expression and activity of plastidial and cytosolic α-glucan phosphorylase (*At*PHS1 and *At*PHS2).

4.3.3 Testing theories on how SS4 promotes granule initiation

Given that the majority of evidence suggests SS4 is necessary for normal granule initiation, a principal theory to test is that SS4 is unique among the starch synthases in its ability to initiate a glucan chain from maltose or maltotriose. This chain would then act as a primer for the other starch synthases to elongate. I suggest that the starch phenotype of an *ss4 dpe1* double mutant may reveal if SS4 is uniquely able to use maltotriose as a primer for amylopectin initiation. In *dpe1* maltotriose accumulates at night and rapidly disappears at the start of the day, accompanied by transient accumulations of longer malto-oligosaccharides (MOS) (Critchley *et al.,* 2001). It is assumed that maltotriose is being used as a substrate by the starch synthases once ADPG is available again during the day. If SS4 alone is able to use the accumulated maltotriose, then the disappearance of maltotriose seen in the *dpe1* mutant should be blocked in the older leaves of the *ss4 dpe1* double mutant.

Another test of this theory would be to introduce a different enzyme that is capable of elongating maltose into longer MOS, into the *ss4* mutant so that it is expressed in the chloroplasts. If the normal role of SS4 is to elongate maltose, then normal granule initiation would be expected to be restored and wild-type granule numbers obtained. A suitable enzyme would be the bacterial enzyme amylomaltase (MalQ).

MalQ (EC 2.4.1.25) catalyzes an inter-molecular glucan transfer reaction from one 1,4-α-glucan molecule to another, or to glucose. In *E. coli* maltose is known to act as an acceptor for amylomaltase (Kitahata *et al.,* 1989). *Arabidopsis* has two enzymes capable of catalysing an intermolecular transfer (disproportionating) reaction, in the form of DPE1 and DPE2. DPE1 is located in the chloroplast, but is unable to act upon maltose (Takaha *et al.,* 1993). DPE2 is active in the cytosol, not in the chloroplast, where it acts on maltose to transfer a soluble heteroglycan (SHG) onto the maltose and release a glucose; a key step in the conversion of starch to sucrose (Chia *et al.,* 2004; Lu and Sharkey 2004; Lu *et al.,* 2006). However, while DPE2 is an ortholog of bacterial amylomaltase (MalQ), there are differences in their functions in maltose metabolism (Lu *et al.,* 2006). For example, DPE2 and MalQ have a difference in substrate preference. In addition to maltose, DPE2 prefers the use of branched glucans e.g. SHG, as one of its substrates (Lu *et al.,* 2006) and cannot use maltose as the sole substrate (Christian Ruzanski (JIC); personal communication). In contrast, MalQ prefers short MOS (maltotriose to maltoheptaose) as substrates, in addition to maltose (Lu *et al.,* 2006).

It has previously been claimed that maltose cannot be used by MalQ as the sole substrate, i.e. MalQ cannot transfer a glucose from maltose to maltose, producing maltotriose and glucose (Palmer *et al.,* 1976). If this is the case, maltose phosphorylase (discussed above) would initially be required. In theory, maltose phosphorylase could produce maltose and a little maltotriose from glucose and glucose-1-phosphate and then MalQ would use these, and subsequent MOS products, as substrates on which to perform chain lengthening glucosyltransfer reactions, thereby potentially producing a spectrum of MOS. However, more recent results (Christian Ruzanski (JIC); personal communication) show that recombinant MalQ can disproportionate from maltose alone, and therefore the proposed maltose phosphorylase step would be irrelevant. Therefore, the bacterial amylomaltase, MalQ, would have a unique role in the *Arabidopsis*

chloroplast. If MalQ were able to compensate for the loss of SS4 and restore wild-type granule numbers, it would indicate that SS4 uniquely is able to use maltose and maltotriose to produce a MOS that the other starch synthases can then act upon.

4.3.4 Summary

My results support the idea that the main role of SS4 occurs in the immature leaves of *Arabidopsis,* where it is required to initiate starch granules. It appears from the accumulation of high levels of ADPG and the phenotype of the *isa1ss4* mutant that SS4 is acting earlier in the pathway from the Calvin cycle to starch than other parts of the starch synthesising apparatus. This is consistent with SS4 producing a "primer" on which the other starch synthase, starch branching and debranching enzymes then act.

5 The Impact of Mutations Affecting Chloroplast Division on Starch Granule Initiation and Growth

5.1 Introduction

5.1.1 Aim

The question remains as to how the amount of starch accumulated during the day is measured or monitored. As I described in Chapter 1, recent work established that correct timing of the degradation of starch during the night is required for optimal growth and productivity in *Arabidopsis* plants (Graf *et al.,* 2010). The setting of the degradation rate that will consume most of the starch reserves almost precisely by dawn requires the use of information about the amount of starch present at the onset of darkness. It seems highly likely that the size, shape and number of granules in the chloroplast may be important in this respect.

In the preceding chapters, I showed that the initiation of starch granules may be directly related to the volume of the chloroplast stroma (Chapter 3). I also showed that although the starch synthase SS4 is necessary for granule initiation, it is not responsible for determining how many granules initiate in a given volume of stroma in a wild-type plant (Chapter 4). In this chapter I describe use of the *accumulation and regulation of chloroplast* (*arc*) mutants of *Arabidopsis* to shed light on both of these issues. The *arc* mutants are deficient in elements of the chloroplast division apparatus (described further below), so have abnormal numbers of abnormally-sized chloroplasts in leaf cells. Their use will enable me to probe further the relationship between stromal volume and the frequency of granule initiation, and to test hypotheses about the relationship between starch granules and the chloroplast 'plastoskeleton', a filamentous network of proteins within plastids that may be formed by elements of the division apparatus. My rationale is described further below.

5.1.2 The 'Plastoskeleton'

5.1.2.1 Why the plastoskeleton structure is important for my work

A hypothetical plastoskeleton and the chloroplast division apparatus might be important in starch metabolism in three respects. Firstly, the plastoskeleton might form part of mechanism that provides information on starch granule size and shape in order to set the appropriate rate of starch degradation at night. Starch itself is considered inert, but it is possible that changes in granule volume are directly measured by mechanosensitive receptors in the internal chloroplast envelope (Haswell and Meyerowitz 2006; Pyke 2006), perhaps acting together with components of a chloroplast "plastoskeleton". Secondly, plastoskeletal components might play a role in granule initiation. As I showed in Chapter 3, there is a remarkable conservation in the number of granules per chloroplast over the day night/cycle and under different day lengths. This might be explained if granules initiated at and are anchored to specific nodes in a plastoskeleton. It has been suggested that the 'plastoskeleton' may provide a framework which organises the enzymes involved in starch synthesis, although there is no direct evidence for this (reviewed in Reski 2002). Thirdly, the fate of granules during chloroplast division is unknown. In bacteria some low-copy-number cellular structures such as large plasmids are segregated between daughter cells by association with elements of the cytoskeleton (Graumann 2007; Pogliano 2008). A similar mechanism might ensure even distribution of starch granules between daughter chloroplasts. It is known that during chloroplast division, nucleoids (a protein-plastid DNA complex) become filamentous and form a network structure, which is important in the equal partitioning of nucleoids between the daughter chloroplasts (Terasawa and Sato 2005).

5.1.2.2 Existing knowledge about the plastoskeleton

'Plastoskeleton' is a term coined by Kiessling *et al*. (2000) to describe the scaffold of microtubule like filaments made from Filamentary temperature-sensitive (FtsZ) protein molecules, within the chloroplasts of the moss, *Physcomitrella patens* (Gremillon *et al.,* 2007). Although FtsZ occurs in higher plants it is important to note that the existence of a plastoskeleton in plants other than moss has not been established. The FtsZ proteins found in plants are orthologues of the bacterial cytoskeletal element FtsZ (Stokes and Osteryoung 2003). FtsZ is involved in bacterial cell division and is thought to be the

prokaryotic orthologue of tubulin, due to structural and functional similarities (Romberg and Levin 2003; van den Ent *et al.,* 2001). The bacterial cytoskeleton also contains numerous other proteins necessary for shape and for correct cell division (Graumann 2007; Pogliano 2008). Orthologues of many of these proteins are found in plant chloroplasts and mutational analysis shows them to be important for correct division (Glynn *et al.,* 2007). Their roles during division are described in more detail in section 5.1.4.

The FtsZ proteins may have functions beyond the chloroplast. There is good evidence for this in the moss *P. patens.* While most higher plants contain two FtsZ families *P. patens* has three families and a total of five FtsZ genes, which have roles not only in chloroplast division, but also in chloroplast shaping, cell patterning, plant development and gravity sensing; leading Martin *et al.* (2009) to propose that the plastoskeleton in *P. patens* is functionally integrated into the cytoskeleton.

Microtubule-like structures (MTLS), described as forming connecting and intersecting grid-like networks, have been observed in the chloroplasts of several species (Reski 2009). The composition of these MTLS has not been established and their relationship to the more recently discovered FtsZ and related proteins is unknown. Work on MTLS was entirely at the level of electron microscopy and the question of their nature and importance has not been re-examined in recent years.

The presence of MTLS has been noted in the plastids of *Hordeum vulgare* (barley) (Jhamb and Zalik 1975; Sprey 1968), *Vicia faba* (broad bean) (Allaway and Setterfield 1972), green algae (Hoffman 1967; Pickett-Heaps 1968; Ueda *et al.,* 1994), *Triticum aestivum* (wheat) (Artus *et al.,* 1990), the moss *Timmiella barbuloides* (Gambardella and Alfano 1991), the cactus *Echinomastus intertextus* (Rivera and Arnott 1982), *Sedum* sp. (Brandao and Salema 1974), *Hypoestes sanguinolenta* (polka-dot plant) (Vaughn and Wilson 1981), *Brassica rapa* var. *rapa* (turnip) and *Spinacia oleracea* (spinach) (Lawrence and Possingham 1984; Oross and Possingham 1991). The MTLS described in these papers, vary considerably between species in diameter, location within the plastid and number of tubules per plastid. The MTLS were proposed to occur in clusters, attached to the inner chloroplast membrane and thylakoids and thought to have roles in plastid development and division (Gambardella and Alfano 1991; Lawrence and

Possingham 1984; Pickett-Heaps 1968; Sprey 1968), orientating the thylakoid lamella system (Artus *et al.,* 1990; Jhamb and Zalik 1975) and structural support of the chloroplast (Ueda *et al.,* 1994; Vaughn and Wilson 1981). Vaughn and Wilson (1981) showed MTLS widely distributed throughout the chloroplasts in mature leaves of the *H. sanguinolenta* plant. They proposed that these MTLS are always present within plastids, but are not normally visible in electron micrographs due to substances in the traditional fixation techniques interfering with their visibility. The occurrence of MTLS in mature chloroplasts implies that they may have roles in addition to those of division and development (Gambardella and Alfano 1991; Hoffman 1967; Rivera and Arnott 1982; Vaughn and Wilson 1981). This led Vaughn and Wilson (1981) to propose a more structural role for the MTLS in chloroplasts. Although these studies were inconclusive in determining the functional significance of the MTLS and no such structures have been described in the chloroplasts of *Arabidopsis,* there is still the possibility that MTLS form a network within the chloroplast. Indeed, MTLS may be formed from the more recently described proteins known to be necessary for chloroplast division.

The opportunity to study the relationship between the division and potential "plastoskeleton" apparatus and starch metabolism is provided by the *accumulation and regulation of chloroplast* (*arc*) mutants. These mutants lack components of the division apparatus. They were first identified in a screen for chloroplast division mutants by Pyke and Leech (1991). The *arc* mutants contain a severely reduced number of larger and irregularly shaped chloroplasts. For example, while wild-type (*Arabidopsis* ecotype Wassilewskija (Ws)) leaf mesophyll cells usually contain around 83 chloroplasts, mesophyll cells of the *arc6* mutant contain only one to two chloroplasts, which are 20-fold larger (in sectional area) than wild-type (Pyke *et al.,* 1994). The *AtFtsZ1-1* mutant is classified among the *arc* mutants, because it has fewer, larger chloroplasts (Yoder *et al.,* 2007). The role of a number of the *ARC* genes in plastid division has been well studied (reviewed in Glynn *et al.,* 2007; Maple and Møller 2007c). However, the impact of chloroplast size and number on the composition and quantity of starch has not been examined. Examination of the *arc* mutants would provide information about the involvement of chloroplast division apparatus in starch metabolism, including granule size, shape, number, distribution and rate of degradation at night.

The idea of a possible link between starch metabolism and elements of the chloroplast division apparatus is supported by examination of genes co-expressed with those encoding enzymes of starch metabolism. Transcript levels of *Arabidopsis* enzymes involved in starch metabolism generally show strong correlation with the levels of transcripts of *Arabidopsis* orthologues of bacterial plastid division proteins such as FtsZ and MinE. For example, entering *ACCUMULATION AND REGULATION OF CHLOROPLAST3* (*ARC3*), a gene necessary for chloroplast division, into a co-regulation search on ATTED-II (http://atted.jp/top_search.shtml#coexsearch), reveals *ISA1* to be the second most co-regulated gene with *ARC3* (according to the Mutual Rank).

5.1.3 The *accumulation and regulation of chloroplast* (*arc*) mutants

Table 5.1 summaries the *arc* mutants used in my work. A number of the *arc* mutations originally identified by Pyke and Leech (1991) were later discovered to lie in genes independently identified as plastid division components, including *arc10* in *AtFtsZ1-1* (Yoder *et al*., 2007), *arc11* in *AtMinD1* (Fujiwara *et al.,* 2004) and *arc12* in *AtMinE1* (Glynn *et al.,* 2007). To maximise the opportunity to uncover any relationships between division apparatus and starch, I selected for study mutants affected at various points during the plastid division cycle and occurring at different locations in, and around, the chloroplast. I also chose mutations affecting genes of both prokaryotic and eukaryotic ancestral origin. For a recent review of the evolution of plastid division machinery see Maple and Moller (2010). Below is a brief summary of the *arc* mutants I selected for study, a full description of their known roles in chloroplast division follows.

Gene	Name	Alternative name	References	Chloroplasts
Unknown	ARC1	None	(Marrison *et al.,* 1999; Pyke and Leech 1994)	94[*3]
AT1G75010	ARC3	None	(Austin and Webber 2005; Maple *et al.,* 2007; Shimada *et al.,* 2004)	13-18
AT3G19720	ARC5	None	(Austin and Webber 2005; Gao *et al.,* 2003; Marrison *et al.,* 1999; Pyke and Leech 1994; Robertson *et al.,* 1996)	3-15
AT5G42480	ARC6	None	(Austin and Webber 2005; Glynn *et al.,* 2008; Koniger *et al.,* 2008; Maple *et al.,* 2005; Pyke *et al.,* 1994; Vitha *et al.,* 2003)	1-2
AT5G55280	ARC10	*At*FtsZ1-1	(McAndrew *et al.,* 2001; Yoder *et al.,* 2007)	23*[1]
AT5G24020	ARC11	*At*MinD1	(Aldridge and Møller 2005; Colletti *et al.,* 2000; Fujiwara *et al.,* 2004; Marrison *et al.,* 1999)	29-33*[2]
AT1G69390	ARC12	*At*MinE1	(Glynn *et al.,* 2007; Itoh *et al.,* 2001; Maple *et al.,* 2002)	1-2

Table 5.1: Summary of plastid division mutants in *Arabidopsis* used in this study. The *arc1, arc3, arc5, arc10, arc11* and *arc12* mutants are in the Landsberg *erecta* (L*er*) background which has an average of 121 chloroplasts per cell. The *arc6* mutant is in the Wassilewskija (Ws) background, which has an average of 83 chloroplasts per cell. *[1]One greatly enlarged chloroplast and some smaller chloroplasts. *[2] Heterogeneous population of chloroplasts, 40-50% wild-type size, 50-60% larger than wild-type (Marrison *et al.,* 1999). *[3] Smaller chloroplasts compared to wild-type (*arc1* = 31 µm² average chloroplast cross sectional area; wild-type = 50 µm²) (Pyke and Leech 1994).

The identity of ARC1 is unknown, and the *arc1* mutant is complex, with a variety of phenotypes affecting mesophyll cell size as well as chloroplast division and expansion (Marrison *et al.,* 1999; Pyke and Leech 1994). The *arc1* mutant differs from the other *arc* mutants studied here, in that it has more chloroplasts per cell plan area (32/1000 μm^2) than wild-type L*er* (25/1000 μm^2), but the cells are smaller than wild-type (2910 μm^2 versus 4778 μm^2) and in fact contain a reduced number (*arc1* = 94; wild-type = 121) of smaller chloroplasts than wild-type (Pyke and Leech 1994).

The *ARC3* gene is a fusion of the prokaryotic *FtsZ* gene and part of the eukaryotic phosphatidylinositol-4-phosphate 5-kinase (*PIP5K*) gene (Shimada *et al.,* 2004) and only occurs in higher plants (Maple and Moller 2010). ARC3 is a plastid division protein, which has been shown through yeast two hybrid interactions and bimolecular fluorescence complementation (BiFC) assays, (which allow visualisation of protein–protein interactions in planta), to interact with *At*FtsZ1-1, *At*MinE1 and *At*MinD1 in the stroma (Maple *et al.,* 2007). It has been speculated that ARC3 plays a role in regulating the expansion of chloroplasts before division (Shimada *et al.,* 2004).

ARC5 has no bacterial orthologues and is thought to be derived from the dynamin involved in eukaryotic cytokinesis. ARC5 is located in the cytosol and is involved in the final stages of division (Gao *et al.,* 2003; Miyagishima *et al.,* 2008). In the *arc5* mutant chloroplasts appear to enter division, but arrest after central constriction begins, so that the mature chloroplasts appear dumbbell shaped (Robertson *et al.,* 1996).

ARC6 shows homology to and is thought to be a descendant of the cyanobacterial cell division protein Ftn2 (Koksharova and Wolk 2002; Vitha *et al.,* 2003). ARC6 is important during the early stages of chloroplast division, acting upstream of *At*MinD1, ARC3 and ARC5 (Marrison *et al.,* 1999). ARC6 is a J-domain containing protein that spans the chloroplast inner envelope membrane at the chloroplast division site, with the N-terminal region, including the J-domain, extending into the stroma (Vitha *et al.,* 2003). A J-domain is a highly conserved region, approximately 73 amino acids long (Hennessy *et al.,* 2000). The presence of a J-domain defines ARC6 as a member of the extremely diverse DnaJ/Hsp40 (heat shock protein 40) family, which are co-chaperone proteins expressed in a wide variety of organisms from bacteria to humans (Cheetham and Caplan 1998; Qiu *et al.,* 2006). DnaJ/Hsp40 proteins determine the activity of

Hsp70 chaperone proteins by stimulating their ATPase activity and stabilising their interaction with substrate proteins (reviewed in Cheetham and Caplan 1998; Qiu *et al.,* 2006).

ARC10 (*At*FtsZ1-1) is of bacterial origin, located in the stroma and is involved early on in the plastid division process (McAndrew *et al.,* 2001; Osteryoung and Nunnari 2003; Stokes and Osteryoung 2003). The *Arabidopsis* genome contains two FtsZ families; *At*FtsZ1 (consisting of the gene *AtFtsZ1-1*) and *At*FtsZ2 (which consists of the genes *AtFtsZ2-1* and *AtFtsZ2-2* (Fujiwara and Yoshida 2001)). *At*FtsZ1-1, *At*FtsZ2-1 and *At*FtsZ2-2 have all been shown to interact in the stroma and play a role in chloroplast division (Gremillon *et al.,* 2007; Schmitz *et al.,* 2009). While *At*FtsZ2-1 and *At*FtsZ2-2 are functionally redundant, the two *At*FtsZ families, *At*FtsZ1 and *At*FtsZ2, are functionally non-redundant in chloroplast division (Osteryoung *et al.,* 1998; Schmitz *et al.,* 2009). Changes in the levels of *At*FtsZ1-1, *At*FtsZ2-1 or *At*FtsZ2-2 cause dose-dependent defects in plastid division and knock-out mutations in *At*FtsZ1-1, *At*FtsZ2-1 or *At*FtsZ2-2 result in fewer and larger chloroplasts compared to wild-type (McAndrew *et al.,* 2008; Schmitz *et al.,* 2009; Yoder *et al.,* 2007). AtFtsZ2-1 and AtFtsZ2-2 are able to substitute for one another in vivo (Schmitz *et al.,* 2009). Expression of *At*FtsZ2-1 in an *AtftsZ2-2* null mutant can fully rescue the chloroplast division defects and restore wild-type chloroplast numbers (Schmitz *et al.,* 2009). However, *At*FtsZ1-1 was not able to rescue chloroplast division in the *AtftsZ2-2* null mutant (Schmitz *et al.,* 2009).

ARC11 (*At*MinD) is a homolog of the bacterial MinD. *At*MinD is a Ca^{2+}-dependent ATPase that acts within the chloroplast, early on in plastid division, to help correctly position the division site (Aldridge and Møller 2005; Colletti *et al.,* 2000; Fujiwara *et al.,* 2004). Mutations in the *AtMinD* gene result in asymmetric chloroplast division and mesophyll cells of the *At*MinD1 mutant *arc11* contain a reduced number of chloroplasts, some wild-type in size and others enlarged (Marrison *et al.,* 1999). ARC12 (*At*MinE) is a homologue of MinE, a component of the bacterial division apparatus (Itoh *et al.,* 2001), which interacts with *At*MinD to help correctly place the plastid division site (Fujiwara *et al.,* 2008; Maple *et al.,* 2002; Maple and Møller 2007a).

The use of the *arc* mutants is preferable to the use of chemical inhibitors of plastid division for studying the effects of plastid division defects on starch, because plants

homozygous for an *arc* mutation have no known mutant phenotypes other than chloroplast size and number. Known inhibitors of plastid division include cytidine deoxyriboside, cycloheximide and β-lactam antibiotics. Although these inhibitors could be applied to *Arabidopsis* plants to examine the effects of plastid division defects on starch, unlike the *arc* mutants they often cause additional phenotypes. For example, although cytidine deoxyriboside causes a 50% reduction in plastid number in *Lemna minor* fronds, with no effect on the growth rate or cell size, plastid differentiation is also affected and the cell area covered by the plastids is reduced by approximately 90% compared to untreated plants (Pizzolato and Frick 1979). Cycloheximide inhibits chloroplast division in cultured spinach leaves, but cell size is also reduced after only 24 hours of treatment (Leonard and Rose 1979). Cycloheximide is not considered a specific inhibitor of plastid division in plants, because it also inhibits protein synthesis and affects respiration and ion uptake (Ellis and Macdonald 1970; Macdonald and Ellis 1969). β-lactam antibiotics, such as ampicillin, cefotaxime and penicillin, have been found to inhibit plastid division in the moss *Physcomitrella patens,* but had no effect in tomato (*Lycopersicon esculentum*), suggesting they have no effect upon plastid division in higher plants (Kasten and Reski 1997).

Photosynthetic capacity is unaffected in the *arc* mutants under normal light conditions (Austin and Webber 2005; El-Kafafi *et al.,* 2008). A large scale screen of *Arabidopsis* mutants for assorted traits such as chlorophyll fluorescence, amino acid content and metabolite accumulation showed that *arc10* and *arc12* do not vary significantly from wild-type (Lu *et al.,* 2008). However, *arc10* did have significantly increased levels of tryptophan in its seeds, and both *arc10* and *arc12* had a significantly altered carbon: nitrogen ratio in their seeds compared to wild-type (Lu *et al.,* 2008).

Although there is a decrease in chloroplast numbers in the *arc* mutants, there is an increase in the size of the chloroplasts and as a result chloroplast plan area is fairly similar between wild-type plants and the plastid division mutants (Pyke and Leech 1992; Pyke and Leech 1994). The variation in chloroplast size and number that occurs in the *arc* mutants to some extent replicates natural variation in chloroplast number that occurs under varying environmental conditions; for example, under different light intensities and day lengths. The total chloroplast volume per cell in all species studied, including *Betula pendula* (silver birch)*, Aesculus hippocastanum* (horse chestnut) and

Cleome spinosa (spiny spider flower), remains more or less unchanged in sun and shade conditions (Butterfass 1979). However, plants grown at higher light intensities have a greater number of smaller chloroplasts per cell (Butterfass 1979).

Before I present my results, I will first describe the process of chloroplast division, including the involvement of the ARC proteins, and speculate how alterations in chloroplast division might lead to changes in starch granules.

5.1.4 Chloroplast division

Chloroplasts arose from an endosymbiotic event between a protoeukaryote and a photosynthetic prokaryote (reviewed in Gould *et al.,* 2008; Gray 1999; McFadden 2001; Reski 2009) and as a result the division machinery of chloroplasts is a mixture of components originating from both prokaryotic and eukaryotic ancestors (Miyagishima *et al.,* 2008). Chloroplasts develop from undifferentiated, small, colourless proplastids found in dividing meristematic cells. As a leaf grows and expands the number of chloroplasts per cell increases. For example, measurements of spinach leaves showed a five-fold increase in the number of chloroplasts per cell over a ten day growth period (Possingham and Saurer 1969) and in alfalfa if the cell volume is doubled the number of chloroplasts per cell doubles (Molin *et al.,* 1982). In wild-type *Arabidopsis* (ecotype Landsberg *erecta* (L*er*)) meristematic mesophyll cells contain around fifteen proplastids, destined to become chloroplasts, while mature mesophyll cells contain around 120 chloroplasts, therefore three rounds of division must take place (Marrison *et al.,* 1999).

In leaves, chloroplasts divide by binary fission, summarised in Figure 5.1 and described below. A diagrammatic representation of the sequence of plastid division is shown in Figure 5.1A, and a summary of the locations and interactions of the chloroplast division machinery is shown in Figure 5.1C. In mesophyll cells, chloroplasts expand and a central constriction forms. This constriction becomes increasingly narrow and the chloroplasts appear dumbbell shaped (Figure 5.1B), with two regions of approximately equal size either side of the constriction. Constriction continues until two daughter chloroplasts of approximately equal size are completely separated.

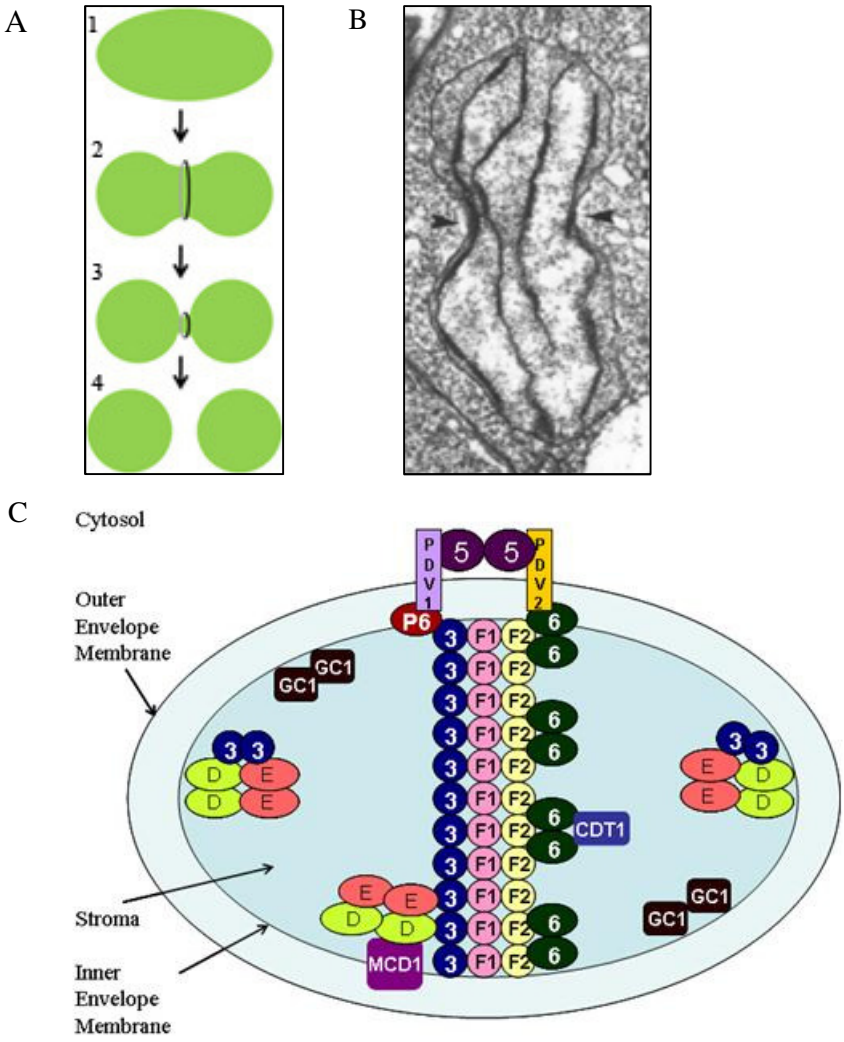

Figure 5.1: Chloroplast division. (A) A diagram of the sequence of chloroplast division. The ring in the diagram represents the position of constriction and division. (1) Plastids increase in size and appear to elongate. (2) Constriction occurs at the central point along the long axis. (3) Further constriction occurs and the chloroplasts appear dumbbell shaped, with two chloroplast regions of approximately equal size either side of the constriction. (4) The division ring completely constricts and division is completed when the two daughter chloroplasts are completely separated. (B) Electron micrograph of a dumbbell shaped dividing chloroplast in the leaf primordia of a 10 day old *Arabidopsis* wild-type seedling, Figure 5 from Robertson *et al.* (1996). Arrowheads indicate the position of constriction. (C). Summary of chloroplast division machinery locations and interactions, see text for details. *At*FtsZ1-1 (F1); *At*FtsZ2-1 and *At*FtsZ2-2 (F2); *At*MinD1 (D); *At*MinE1 (E); ARC6 (6); Paralogue of ARC6 - PARC6 (P6); ARC3 (3); Giant Chloroplast 1 (GC1); ARC5 (5); PLASTID DIVISION1 (PDV1); PLASTID DIVISION2 (PDV2); Multiple Chloroplast Division Site1 (MCD1); *Arabidopsis* Cdc10-dependent transcript 1 (CDT1). Adapted from Figure 1 in Maple and Møller (2007b).

Early electron microscopic examinations of dividing chloroplasts in a number of higher plants noted concentric ring-like structures that occurred on both the stromal side of the chloroplast inner membrane and on the cytoplasm side of the chloroplast outer membrane at the constricting region (Hashimoto 1986; Modrusan and Wrischer 1990; Oross and Possingham 1989). It was later determined that FtsZ1 and FtsZ2 filaments form a "Z-ring" on the stromal side of the chloroplast envelope at the plastid division site (McAndrew *et al.,* 2001; Mori *et al.,* 2001; Schmitz *et al.,* 2009; Vitha *et al.,* 2001) and ARC5 that forms a dynamin-like ring structure on the cytosolic surface at the plastid division site (Gao *et al.,* 2003). A number of components are required for correct formation and positioning of the Z-ring at the mid-plastid site including correct levels of the plastid chaperonin proteins ptCpn60α (ARC2) and ptCpn60β (BR04) (Suzuki *et al.,* 2009). The known interactions between the chloroplast division components are summarised in Figure 5.1C.

In the green alga *Chlamydomonas reinhardtii*, the maximum expression levels of *FtsZ1*, *FtsZ2*, *MinD* and *MinE* correlate with the onset of chloroplast division, suggesting that chloroplast division could be regulated by the expression levels of the *FtsZ* and *MIN* genes (Hu *et al.,* 2008). *At*MinD1 is recruited to the mid-chloroplast constriction site by *At*MinE1-stimulated ATP hydrolysis (Aldridge and Møller 2005; Fujiwara *et al.,* 2009; Maple *et al.,* 2005; Maple and Møller 2007a). *At*MinE1 and *At*MinD1 act together to limit *At*FtsZ ring formation to the chloroplast division site (Fujiwara *et al.,* 2008). *At*MinD1 also interacts with the Multiple Chloroplast Division Site1 (MCD1) protein which spans the inner envelope membrane and localises at the division site as a continuous ring (Nakanishi *et al.,* 2009). Nakanishi *et al.* (2009) suggested that MCD1 and *At*MinD1 may act in a complex with *At*MinE1 to limit FtsZ ring formation to the division site.

*At*FtsZ1, *At*FtsZ2, ARC6 and ARC3 associate in a complex, which is speculated to play a role in regulating *At*FtsZ polymer assembly and remodelling adjacent to the inner envelope membrane (McAndrew *et al.,* 2008). Using yeast two-hybrid analysis and confirmed in vivo with BiFC assays or fluorescence resonance energy transfer (FRET), ARC6 has been shown to interact with *At*FtsZ2-1 (Maple *et al.,* 2005) and *At*FtsZ2-2 (Schmitz *et al.,* 2009; yeast two-hybrid analysis only) but not *At*FtsZ1-1 (Maple *et al.,* 2005); while ARC3 interacts with *At*FtsZ1-1, *At*MinE1 and *At*MinD1 (Maple *et al.,*

2007). Yang *et al*. (2008) proposed a model in which ARC6 helps to stabilise *At*FtsZ2-1 polymers on the inner envelope membrane at the division site, promoting formation of the Z-ring.

The exact location of the ARC3-*At*MinD1-*At*MinE1 complex is unknown. Fluorescence microscopy (GFP-protein fusions in *Arabidopsis* leaves or YFP-protein fusions transiently expressed in tobacco leaf cells) has shown ARC3 to localise with *At*FtsZ1 as ring-like structures at the mid-chloroplast constriction site (Maple *et al.,* 2007; Shimada *et al.,* 2004), but ARC3 has also been shown to localise as one or two spots at the poles of chloroplasts with *At*MinD1 and *At*MinE1 (Maple *et al.,* 2002; Maple *et al.,* 2007).

In dividing chloroplasts ARC6 interacts with PLASTID DIVISION2 (PDV2) in the intermembrane space at the plastid division site, conferring information about the site of the Z-ring on the inner envelope membrane to the outer envelope membrane (Glynn *et al.,* 2008). Using both the yeast two-hybrid system and the BiFC technique, ARC6 has been found to interact with *Arabidopsis* Cdc10-dependent transcript 1 (*At*CDT1) (Raynaud *et al.,* 2005) a member of the pre-replicative complex (pre-RC) (Masuda *et al.,* 2004; Tsakraklides and Bell 2010). The pre-RC is a protein complex that binds to specific nucleotide sequences that mark sites where DNA replication can initiate (origins of replication) and is required for the initiation of DNA replication (Takisawa *et al.,* 2000; Tsakraklides and Bell 2010). *At*CDT1 was found to have a role in both nuclear DNA replication and plastid division (Raynaud *et al.,* 2005). *At*CDT1-RNAi lines with reduced mRNA abundance for *AtCDT1* had an increased frequency of endoreduplication and contained both cells which were wild-type in appearance and cells containing only three or four enlarged chloroplasts (Raynaud *et al.,* 2005).

Paralog of ARC6 (PARC6 - also referred to as *At*CDP1 or ARC6H), is a homologue of ARC6 (Glynn *et al.,* 2009; Zhang *et al.,* 2009) but contains two trans-membrane regions and lacks a J-domain (Ottesen *et al.,* 2010). Leaves of the *parc6* mutant contain on average seven enlarged chloroplasts per cell (Glynn *et al.,* 2009; Ottesen *et al.,* 2010). PARC6 is located in the inner envelope membrane at the division site, acting downstream of ARC6 to mediate PDV1 localisation, potentially via an interaction with ARC3 (Glynn *et al.,* 2009; Zhang *et al.,* 2009). PDV protein levels have been found to determine the chloroplast division rate (Okazaki *et al.,* 2009). PDV1 and PDV2 span the

chloroplast outer membrane and act together to recruit ARC5 to the division site (Miyagishima *et al.,* 2006).

ARC5 plays a role late in plastid division and is required to complete the separation process (Marrison *et al.,* 1999; Robertson *et al.,* 1996). ARC5 mediates division from outside the chloroplast, where it forms a dynamin-like ring structure on the cytosolic surface of the chloroplast outer envelope membrane at the chloroplast division site (Gao *et al.,* 2003). The stromal Z-ring then constricts, invaginating the chloroplast outer envelope membrane, and divides the plastid into two daughter chloroplasts. ARC5 acts to pinch off the membranes between the daughter chloroplasts (Yoshida *et al.,* 2006).

The *arc6* and Giant chloroplast1 (GC1) deficient phenotypes are very similar, therefore it is possible that these two proteins act in concert during plastid division (Aldridge *et al.,* 2005). However, GC1 is not thought to be directly involved in the FtsZ mediated plastid division pathway in *Arabidopsis* as it is unable to interact with the plastid division proteins *At*FtsZ1, *At*FtsZ2, *At*MinD1, *At*MinE1 or ARC6 (Maple *et al.,* 2004).

In the following section I will discuss existing evidence that suggests chloroplast division and starch metabolism are connected and how a putative plastoskeleton could be involved in starch granule distribution or initiation.

5.1.5 Chloroplast division and starch accumulation

There is some evidence for a correlation between chloroplast division and granule number or size, but it is important to note that the impact of chloroplast size and number on the composition and quantity of starch has not been examined beyond observations on microscope images. For example, TEM images suggested that immature leaves of the *arc3* mutant had chloroplasts of a similar size to wild-type, but with increased starch accumulation (Austin and Webber 2005). Over-expression of FtsZ in potato tubers resulted in smaller plastids apparently containing fewer, but larger starch granules (de Pater *et al.,* 2006). FtsZ1-overexpressing *Arabidopsis* plants had altered chloroplast morphology and thylakoid abnormalities, but despite maintaining wild-type levels of photosynthesis, were found to lack starch granules (El-Kafafi *et al.,* 2008). However, small granules could have been missed on TEM images of sections through embedded

material. Additionally, it was stated that the *At*FtsZ1 knockout mutant had an "increase in starch granule number" (El-Kafafi *et al.,* 2008), although there was no quantification and increased chloroplast size was not taken into account.

In non-photosynthetic storage organs, loss of an *ARC* gene can have a large effect on the starch produced. Yun and Kawagoe (2009) analysed the *arc5* mutant of rice and found the altered amyloplast division to have a significant effect on starch synthesis. Purified starch granules from amyloplasts were smaller and irregularly shaped compared to wild-type granules. The amylopectin was also structurally altered. Yun and Kawagoe (2009) even suggested that the starch granules themselves may influence the amyloplast division process. It is important to note that amyloplasts divide differently from chloroplasts. They may divide at multiple sites to produce a "beads on a string structure"; or alternatively budding-type division occurs from large amyloplasts (Yun and Kawagoe 2009). Interestingly the rice *arc5* mutant had reduced amounts of starch in the leaves; only 45% of wild-type levels (Yun and Kawagoe 2009).

As previously mentioned, in bacteria some low-copy-number cellular structures such as large plasmids are segregated between daughter cells by association with cytoskeletal components (Graumann 2007; Pogliano 2008). It is possible that a similar mechanism might ensure even distribution of starch granules between daughter chloroplasts. Bacterial cytoskeletal components include actin homologues such as ParM and AlfA (Graumann 2007; Pogliano 2008). Plasmid-segregating filaments, such as the ParA family of ATPases, are also involved in the distribution of protein complexes between bacterial daughter cells (Graumann 2007; Pogliano 2008). ParA is similar to MinD, both of which are ATPases and form filaments within cells or plastids (Graumann 2007; Pogliano 2008). Some of the altered chloroplast phenotypes in the *arc* mutants may arise because the wild-type protein is required for symmetrical division of plastids. For example, *arc5* chloroplasts have an unusual organisation of their thylakoid membranes (Robertson *et al.,* 1996), and it has been suggested that *At*FtsZ1 has a role in thylakoid membrane partitioning to daughter chloroplasts during division (El-Kafafi *et al.,* 2008). If components of the plastid division machinery are involved in segregation of starch granules between daughter chloroplasts then we might expect that in mutants with asymmetrical plastid division the distribution of starch granules between the dividing plastids is altered.

In the following section I present my results on the impact of the altered chloroplast number and size in the *arc* mutants on starch accumulation in *Arabidopsis* leaves, and discuss what the *arc* mutants tell us about both the relationship between stromal volume and the frequency of granule initiation, and the relationship between starch granules and the hypothetical chloroplast 'plastoskeleton'.

5.2 Results

5.2.1 Isolation of the *accumulation and regulation of chloroplast* (*arc*) mutants

In this section I will describe analysis of the phenotypic alterations produced by the specific loss of ARC1, ARC3, ARC5, ARC6, ARC10, ARC11 and ARC12 from *Arabidopsis.* The *arc* mutants *arc1*, *arc3*, *arc5*, *arc6*, *arc11* and *arc12* were kindly provided by Dr. Kevin Pyke (University of Nottingham, UK). With the exception of *arc6*, which is in the Ws background, all of the above mutations are in the L*er* background. I acquired *Arabidopsis* lines in the Col-0 background with potential T-DNA insertions in the *ARC3* gene (SALK_057144 and SALK_012892), *ARC5* gene (SAIL_71_D11), *ARC6* gene (SAIL_693_G04) and *ARC10* gene (SALK_073878) from NASC. A number of these T-DNA insertional lines had previously been identified (see below). I isolated a line homozygous for each insertion, using the oligonucleotides described in Table 2.5. For each homozygous line I confirmed the location of the T-DNA insertion by DNA sequencing, and the reduced chloroplast number was confirmed by extraction of protoplasts and observation under a light microscope.

For ARC3, the SALK_057144 T-DNA insertion is located in intron thirteen (position +4533bp with respect to the start codon; Figure 5.2) and SALK_012892 is located in intron ten (position +3402bp) of At1g75010. The T-DNA insertional line SALK_057144 was first identified and characterised by Shimada *et al.* (2004), and found to have the same abnormal chloroplast phenotype as the original *arc3* mutant resulting from the loss of the ARC3 protein. The *arc3* mutation (referred to as *arc3-1,* by Shimada *et al.,* 2004) is caused by an ethyl methanesulfonate (EMS)-induced single base pair mutation (Pyke and Leech 1992; Pyke and Leech 1994). In this study the mutant carrying the T-DNA insertion SALK_057144, is named *arc3-2*. The mutant carrying the SALK_012892 T-DNA insertion in the *ARC3* gene is, hereafter referred to as *arc3-3*. I confirmed that it had the same abnormal chloroplast phenotype as *arc3*.

For ARC5, the SAIL_71_D11 T-DNA insertion is located in intron nine (position +2698bp with respect to the start codon; Figure 5.3) of At3g19720. This mutant is hereafter referred to as *arc5-2* (as named by Miyagishima *et al.* (2006)). For ARC6, the SAIL_693_G04 T-DNA insertion is located in exon four (position +1359bp with

respect to the start codon) of At5g42480. This mutant is named *arc6-5*. A mutant containing the SAIL_693_G04 T-DNA insertion was characterised by Glynn *et al.* (2008), but was not named. The EMS-induced mutants *arc6-1, arc6-2* and *arc6-3* were identified and characterised by Pyke *et al.* (1994) and Vitha *et al.* (2003), while *arc6-4* was identified by Koniger *et al.* (2008). For ARC10, the SALK_073878 T-DNA insertion is located in exon one (position +138bp with respect to the start codon) of At5g55280. This mutant is hereafter referred to as *arc10-2*. A mutant containing the SALK_073878 T-DNA insertion was identified and characterised by Yoder *et al.* (2007), where it was referred to as *atfts*Z1-1-Δ1, while the EMS-induced mutant *arc10-1* was identified by Rutherford (1996).

During all analyses, the *arc* mutants are grouped with the appropriate wild-type control according to the genetic background from which they were isolated. For example, *arc1*, *arc3*, *arc5*, *arc11* and *arc12* are grouped with wild-type L*er*; *arc3-2, arc3-3, arc5-2, arc6-5* and *arc10-2* with wild-type Col and *arc6* with wild-type Ws.

The difference in chloroplast size and number per cell between wild-type plants and the *arc* mutants can clearly be seen in protoplasts (Figure 5.4A) and sections through mesophyll cells (Figure 5.4B). However, starch granules isolated from the *arc* mutants resemble wild-type granules in terms of size and shape (Figure 5.4C).

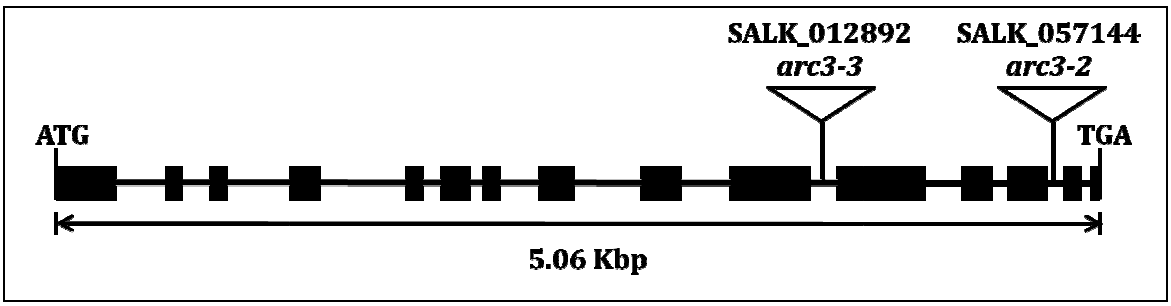

Figure 5.2: Analysis of lines carrying mutations in At1g75010 (ARC3). Exons and introns are indicated as thick and thin black bars, respectively. Insertion sites of T-DNA in mutant lines *arc3-2* and *arc3-3* at introns 13 (+4533bp from start codon) and 10 (+3402bp) respectively are indicated by triangles. SALK_057144 was identified and characterised by Shimada *et al.* (2004).

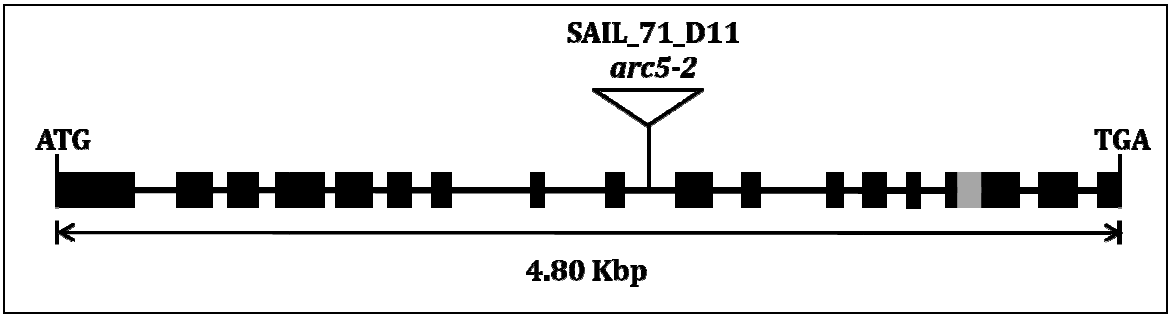

Figure 5.3: Analysis of a line carrying a mutation in At3g19720 (ARC5). Exons and introns are indicated as thick and thin black bars, respectively. Grey box indicates the alternatively spliced intron. Insertion site of T-DNA in mutant line *arc5-2* at intron 9 (+2698bp from start codon) is indicated by a triangle. SAIL_71_D11 was identified by Miyagishima *et al.* (2006). Note: the T-DNA in *arc5-2* was reported to be in intron 8 by Miyagishima *et al.* (2006) but the Tair website (http://www.arabidopsis.org) and my own sequencing shows the insert is in intron 9.

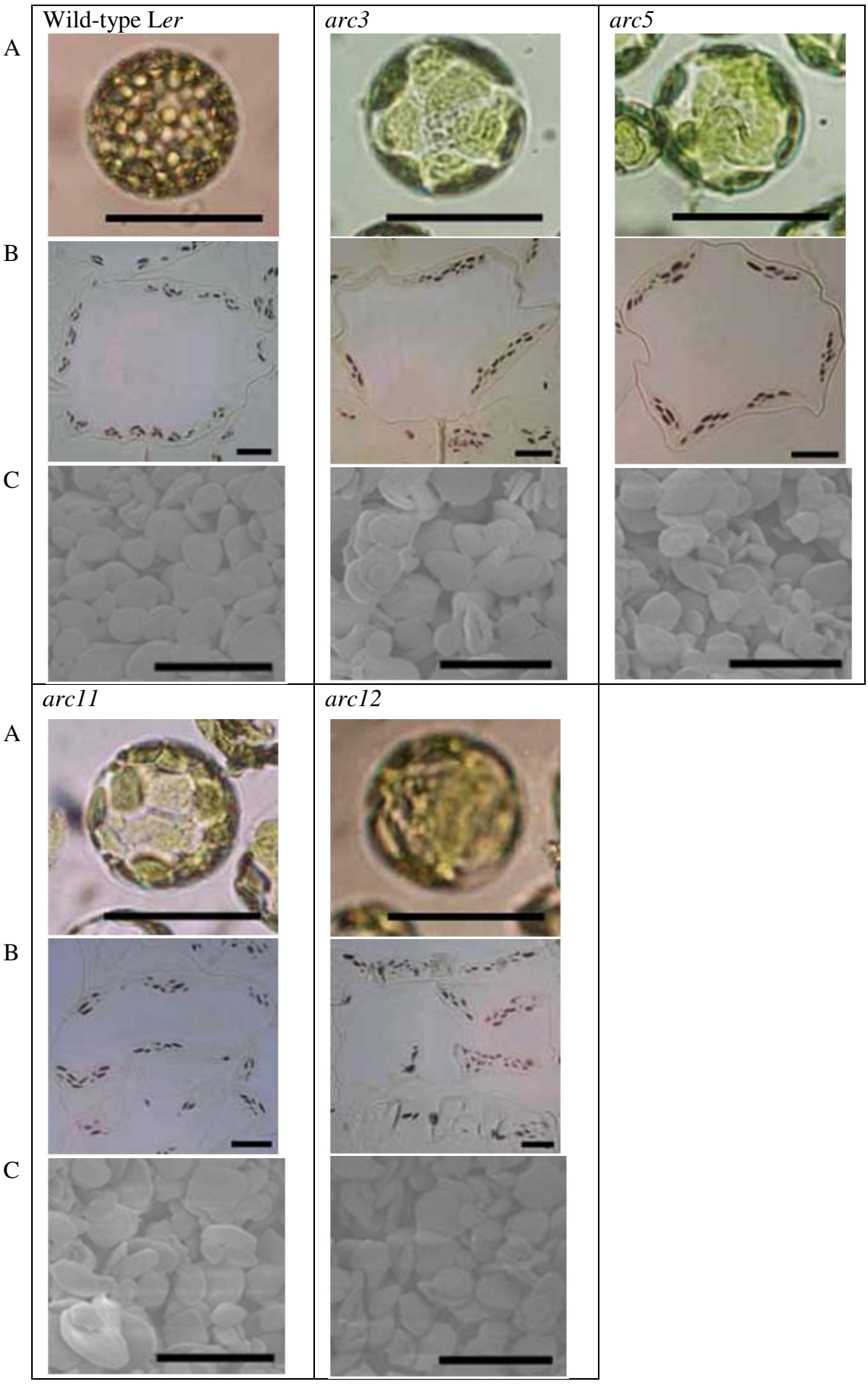
Wild-type Ler
arc3
arc5
A
B
C
arc11
arc12
A
B
C

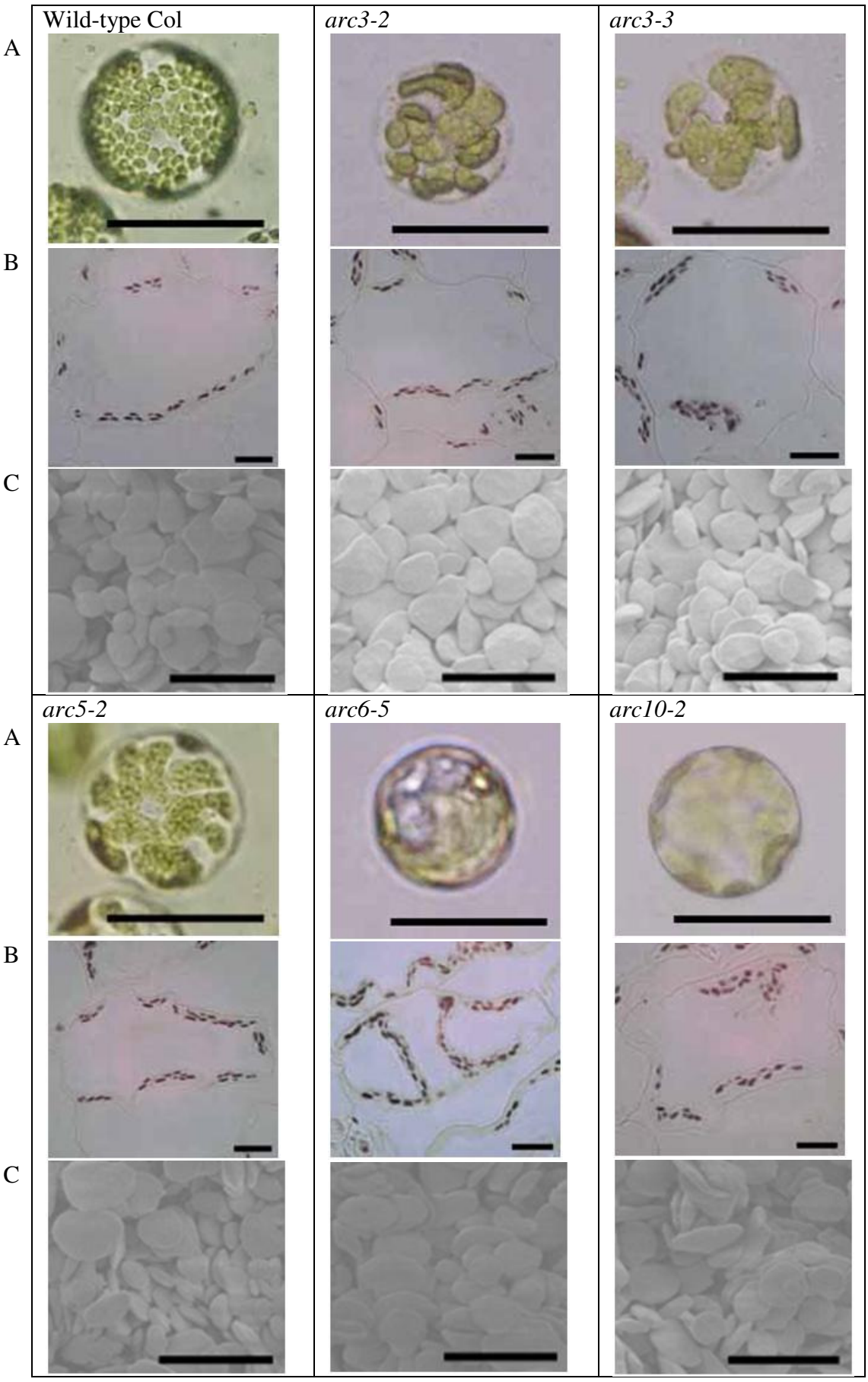
Wild-type Col
arc3-2
arc3-3
A
B
C
arc5-2
arc6-5
arc10-2
A
B
C

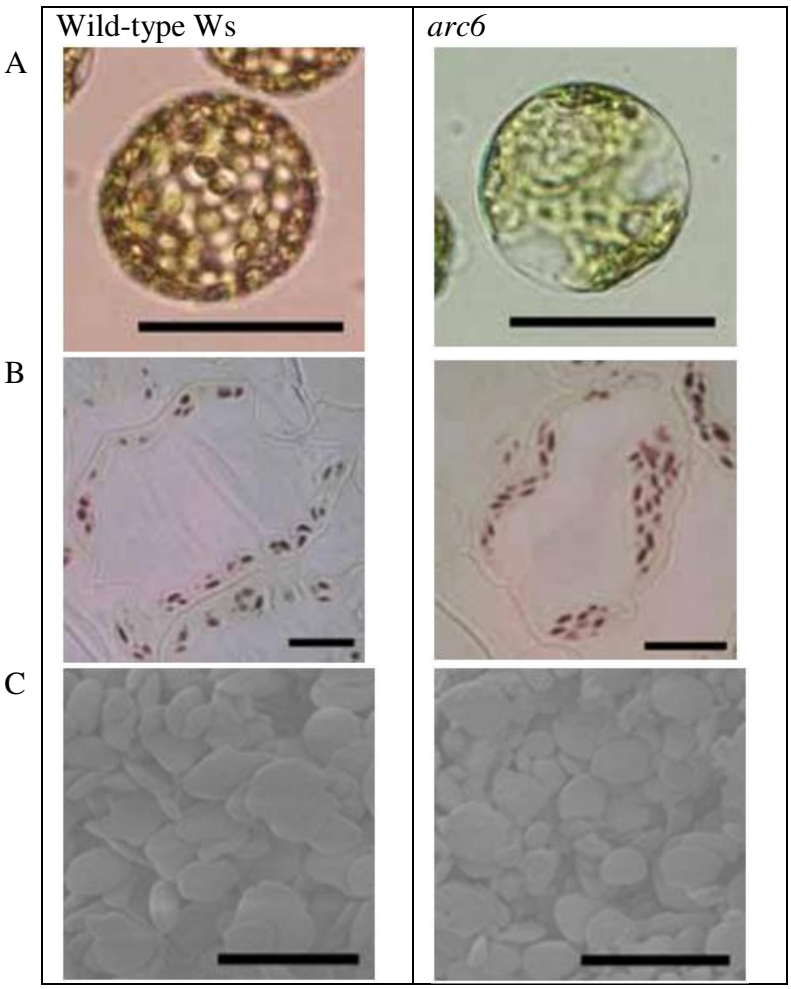

Figure 5.4: Phenotypes of the *arc* mutants and wild-type controls. (A) Protoplasts. (B) 1 µm thick sections of mesophyll cells stained with iodine solution. (C) SEM pictures of isolated starch granules. A scale bar = 50 µm. B scale bar = 10 µm; C scale bar = 5 µm.

To discover how the *arc* mutations affect starch metabolism, I measured starch content, starch granule size and the number of starch granules per chloroplast in cross-sectional area.

5.2.2 Starch turnover in *arc* mutants

Starch levels at the end of the light period and end of the dark period were measured in the *arc* mutants and wild-type controls (Figure 5.5). There is no difference in the starch content at the end of the light period between any of the *arc* mutants and the wild-type controls (Table 5.2). There are small, but significant differences, in the starch content of

the *arc* mutants and wild-type controls at the end of the dark period, but no one genotype is statistically significantly different from all the others and statistical differences are often dependent on the genetic background (Table 5.2). For example, while there is a highly significant difference in the end of night starch levels between *arc3* and L*er* wild-type, there is no significant difference between *arc3-2* and Col wild-type.

To detect whether the starch accumulation pattern across leaves of different ages was the same in *arc* mutant and wild-type rosettes, whole *arc* mutant and wild-type rosettes were harvested at both the end of the dark period and light period, decolourised in 80% ethanol and then stained in iodine solution (Figure 5.6; only shows the *arc* mutants in the Col background as an example). There were no differences in the staining pattern of the *arc* mutant and wild-type rosettes. Starch is distributed evenly throughout the rosettes in both the wild-type and *arc* mutants.

In summary, the overall pattern of starch accumulation and degradation is unaltered in the *arc* mutants.

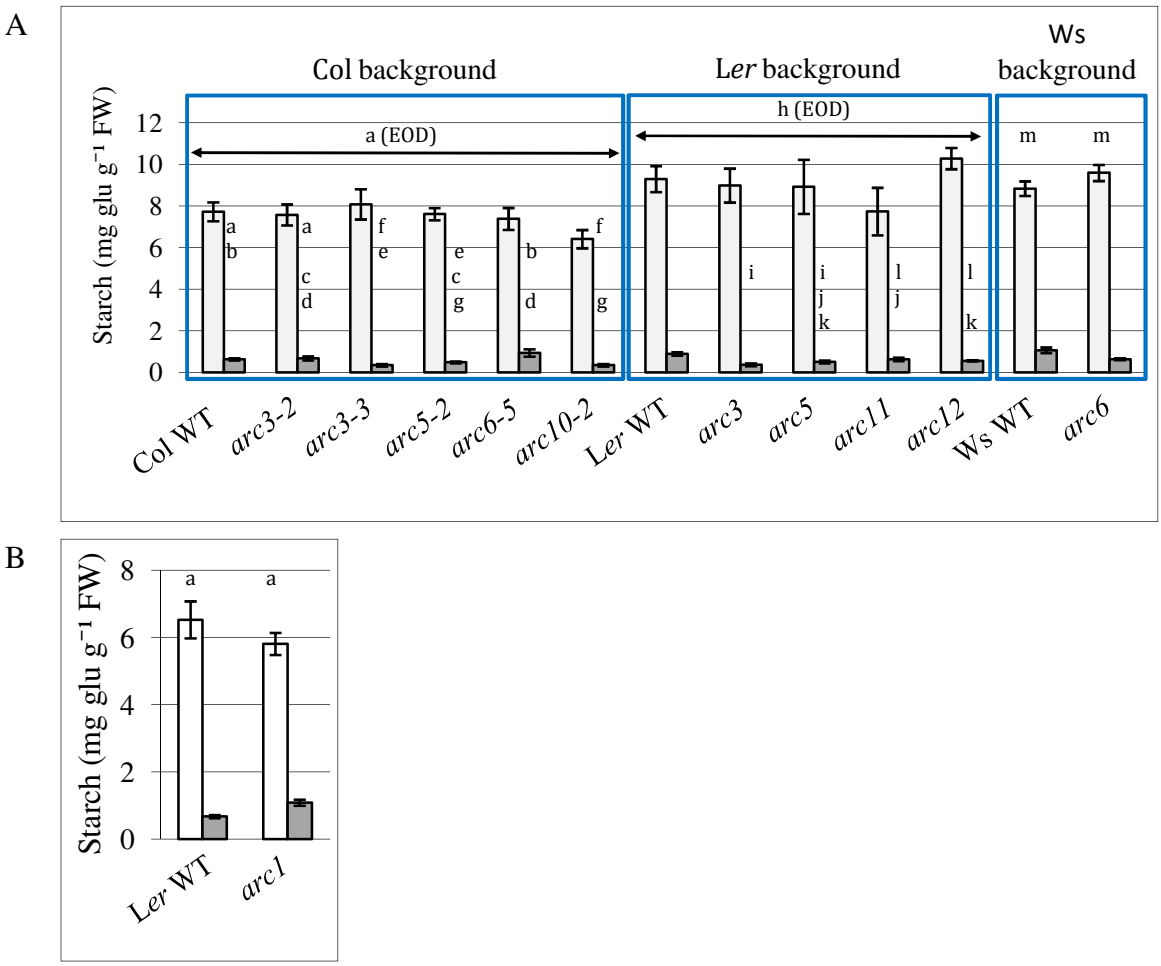

Figure 5.5: (A) Starch levels in the rosette leaves of *arc* mutants and wild-type (WT) controls. (B) The *arc1* mutant and L*er* wild-type control (measurements made on separate batch of plants from other starch measurements). Plants in the Col and L*er* background were grown for 25 days in 12 h light/12 h dark conditions. Due to earlier bolting, plants in the Ws background were harvested after 21 days. White bars = EOD; Grey bars = EON. n = 8 ±SE; where n = eight separate plants (except for *arc10-2* (EOD) where n = 7, *arc6-5* (EON) where n = 6 and *arc5* (EON) where n = 4). EON = end of night. EOD = end of day. Bars with the same letter are not significantly different from each other, see Table 5.2 for full statistical comparison.

Col Background					
End of Day	F (5,41) = 1.14, p = 0.355				
End of Night					
	Wild-type	*arc3-2*	*arc3-3*	*arc5-2*	*arc6-5*
arc3-2	t (14) = 0.43 p = 0.670				
arc3-3	t (14) = -3.61 p = 0.003	t (14) = -2.83 p = 0.013			
arc5-2	t (14) = -2.40 p = 0.031	t (14) = 1.83 p = 0.101	t (14) = -1.85 p = 0.085		
arc6-5	t (12) = 1.72 p = 0.138	t (12) = -1.42 p = 0.180	t (12) = -3.17 p = 0.018	t (14) = -2.53 p = 0.048	
arc10-2	t (14) = -3.93 p = 0.002	t (14) = -2.95 p = 0.010	t (14) = 0.05 p = 0.962	t (14) = -2.07 p = 0.057	t (12) = -3.22 p = 0.018
L*er* Background					
End of Day	F (4,30) = 1.26, p = 0.307				
	L*er* and *arc1*: t (13) = -1.08, p = 0.302				
End of Night					
	Wild-type	*arc3*	*arc5*	*arc11*	
arc1	t (14) = 4.81 p < 0.001				
arc3	t (14) = -4.81 p < 0.001				
arc5	t (10)= -3.05 p = 0.012	t (10) = -1.23 p = 0.248			
arc11	t (14) = -2.24 p = 0.042	t (14) = 2.32 p = 0.036	t (10) = 0.92 p = 0.378		
arc12	t (14) = -3.84 p = 0.004	t (14) = 2.44 p = 0.036	t (10)= 0.85 p = 0.417	t (14) = 0.77 p = 0.460	
Ws Background					
End of Day	t (14) = 1.44, p = 0.172				
End of Night	t (14) = -3.04, p = 0.015				

Table 5.2: Statistical analysis (ANOVA and *t* test) of the starch measurements in rosette leaves of *arc* mutants and wild-type controls displayed in Figure 5.5. Test of the null hypothesis that the mean starch contents of the datasets is not different. The degrees of freedom (listed in brackets), test statistic and statistical significance are displayed.

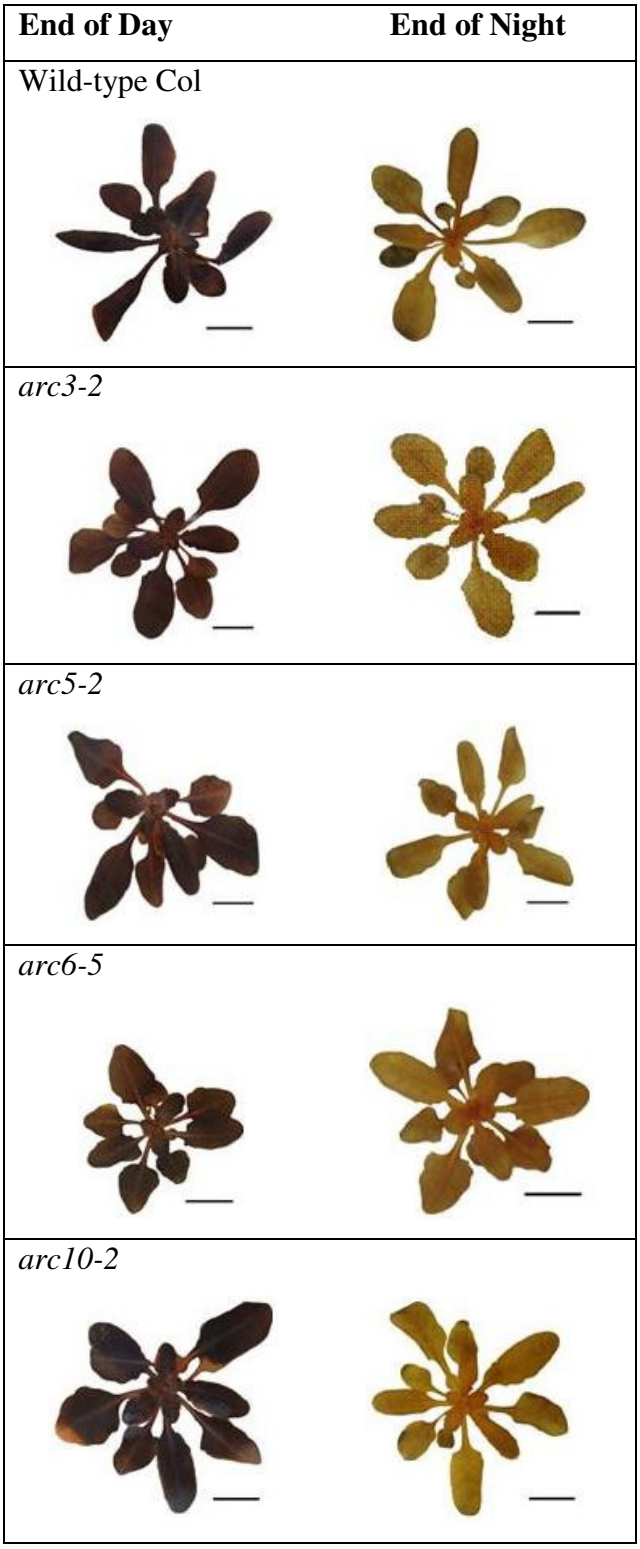

Figure 5.6: Whole rosettes of the *arc* mutants harvested at the end of the light and end of the dark period; decolourised with ethanol and stained with iodine solution. Plants grown for 25 days in 12 h light/12 h dark conditions. Scale bar = 1cm.

5.2.3 Granule initiation and distribution in the *arc* mutants

As described above, starch turnover in the *arc* mutants during the normal 12 h light/ 12 h dark day/night cycle is indistinguishable from that of wild-type plants. Thus, any variation I discover in granule size or number in the *arc* mutants is likely to be a direct result of the defects in chloroplast division and not due to impaired photosynthesis or pleiotropic effects on expression of genes involved in starch turnover. To explore the idea that components of the plastid division machinery might play a role in granule initiation, determining some aspect of granule size, shape or number per chloroplast, I examined the impact of the *arc* mutations on starch granule size and number.

The average granule radii for each *arc* mutant and appropriate wild-type control were obtained from SEM images of starch granules isolated from leaves harvested at the end of the light period. The mean and mode granule radius for each mutant, along with the distribution of granule sizes are displayed in Figure 5.7 (statistics Table 5.3). There was no significant difference in the mean granule radius between the *arc* mutants (excluding *arc1*) in the L*er* background. However, the mean granule radius of the *arc* mutants (excluding *arc1*) in the L*er* background was significantly smaller than the mean granule radius of the L*er* wild-type control. This may be due to differences in the L*er* genetic stock from which the *arc* mutants were derived and the wild-type L*er* used in this study. The mean granule radius of the *arc1* mutant was smaller than that of the other *arc* mutants. There were significant differences in granule radii between *arc* mutants in the Col and Ws backgrounds, but no one genotype was statistically significantly different from all the others and statistical differences were often dependent on the genetic background. For example, while there is a highly significant difference in granule radius between *arc6* and Ws wild-type, there is no significant difference between *arc6-5* and Col wild-type. The granule shape of all the *arc* mutants studied also appears the same as that of the wild-type controls (Figure 5.4C).

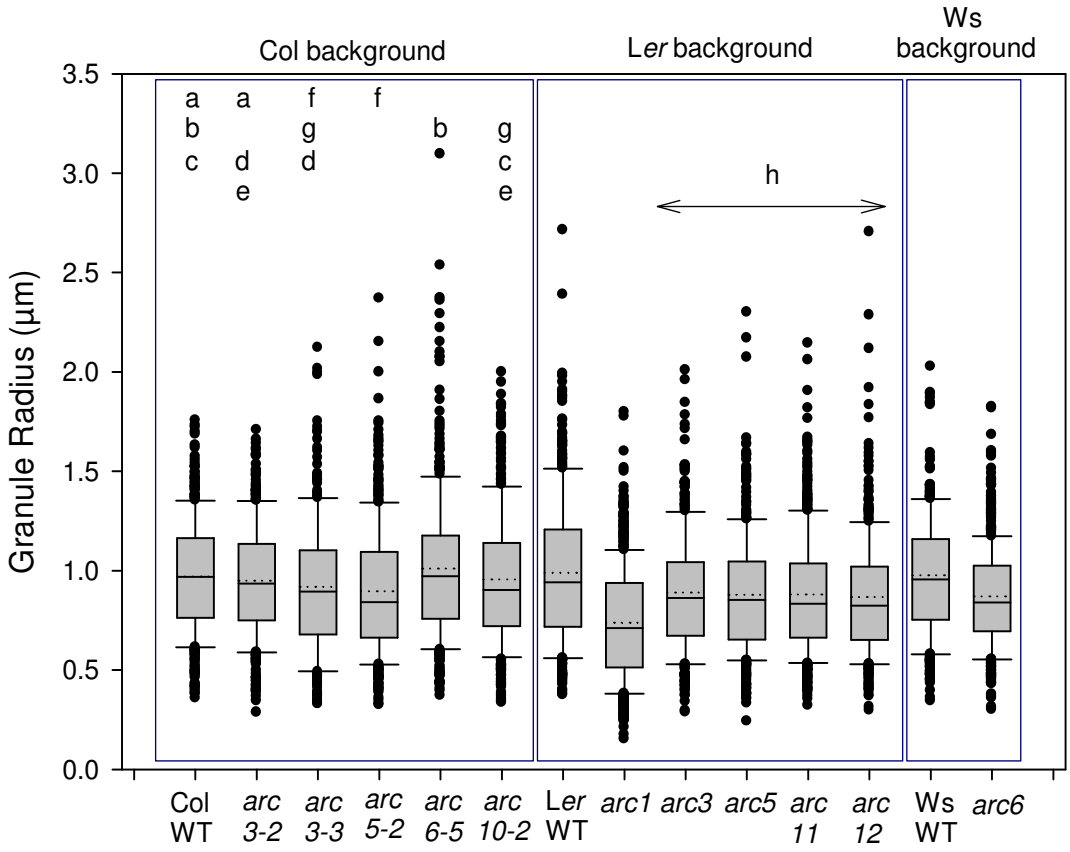

Figure 5.7: Box plot showing the range of granule radii for the *arc* mutants and wild-type controls. The band in the middle of the box is the median (50th percentile). The bottom and top of the box are the 25th and 75th percentiles. The upper and lower bars represent the 90th and 10th percentiles respectively. Outliers are represented as circles. WT = wild-type. The mean granule radii of genotypes labelled with the same letter are not statistically significantly different from each other (p >0.05). Mean shown as dotted line. Granules isolated from 25 day old plants (21 day old for wild-type Ws and *arc6*), 40 plants per genotype. Between 282 and 587 granules measured for each genotype, from ten SEM images taken at random. Full statistical comparisons are listed in Table 5.3.

Col Background					
	Wild-type	*arc3-2*	*arc3-3*	*arc5-2*	*arc6-5*
arc3-2	t (680) = -0.94 p = 0.348				
arc3-3	t (643) = -2.11 p = 0.036	t (599) = 1.26 p = 0.209			
arc5-2	t (750) = -3.35 p < 0.001	t (706) = 2.35 p = 0.019	t (669) = 0.83 p = 0.406		
arc6-5	t (747) = 1.66 p = 0.098	t (703) = -2.44 p = 0.015	t (666) = -3.30 p = 0.001	t (773) = -4.55 p < 0.001	
arc10-2	t (759) = -0.63 p = 0.527	t (715) = 0.27 p = 0.784	t (678) = 1.48 p = 0.139	t (785) = 2.57 p = 0.010	t (782) = -2.15 p = 0.032
L*er* Background					
ANOVA (*arc3*, *arc5*, *arc11* and *arc12*): F (3,1626) = 0.40, p = 0.750 ANOVA (wild-type L*er*, arc3, *arc5*, *arc11* and *arc12*): F (4,2022) = 10.18, p <0.001					
	Wild-type	*arc1*	*arc3*	*arc5*	*arc11*
arc1	t (978) = -11.51, p <0.001				
arc3	t (736) = -4.03 p < 0.001	t (930) = -7.72, p <0.001			
arc5	t (763) = -4.60 p < 0.001	t (957) = -7.31, p <0.001	t (715) = 0.52 p = 0.602		
arc11	t (860) = -4.75 p < 0.001	t (1054) = -7.94, p <0.001	t (812) = -0.47 p = 0.640	t (839) = 0.09 p = 0.930	
arc12	t (835) = -5.24 p < 0.001	t (1029) = -7.02, p <0.001	t (787) = -1.08 p = 0.282	t (814) = -0.55 p = 0.583	t (911) = 0.68 p = 0.498
Ws Background					
t (629) = -4.95, p < 0.001					

Table 5.3: Statistical analysis (ANOVA and *t* test) of the starch granule measurements of *arc* mutants and wild-type controls displayed in Figure 5.7. Test of the null hypothesis that the mean granule radii of the datasets are not different. The degrees of freedom (listed in brackets), test statistic and statistical significance are displayed.

Sections through mesophyll cells of the *arc* mutants and wild-type controls were stained with iodine solution and observed by light microscopy (Figure 5.4B). Measurements were taken using imaging software. Chloroplast area of the *arc* mutants varies as expected, with *arc* mutants which contain fewer chloroplasts per mesophyll cell having larger chloroplast cross-sectional areas (Figure 5.8A). A similar trend is seen in the number of starch granules per chloroplast in cross-section (Figure 5.8B). Mutants with fewer, larger chloroplasts have a greater number of starch granules per chloroplast, with the exception of *ss4,* which generally contains one granule per chloroplast (see Chapter

4). The *ss4* mutant is only included for comparison. However, dividing the chloroplast cross-sectional area by the granule number per chloroplast, I found a remarkable conservation in the stromal area per granule among the *arc* mutants and wild-type controls (Figure 5.8C; Table 5.4). The *arc* mutants have mean values, for the area of stroma per granule, 0.7 times (*arc*6-5) to 1.5 times (*arc12*) the wild-type control values, but most of these values are not significantly different (see below). This contrasts with the *ss4* mutant, which has approximately 4.5 times more stroma per granule than wild-type. Therefore any control over the number of granules initiated in a given volume of stroma is maintained in the *arc* mutants, but is lost in the *ss4* mutant. In the L*er* background there are no significant differences in the area of stroma per granule between L*er* wild-type, *arc3, arc5, arc11* and *arc12*. In contrast, *arc1* has significantly less stroma per granule than all other genotypes in the L*er* background. The average stromal area per granule in *arc6* is only 17% smaller than in Ws wild-type, however, this difference is statistically significant. In the Col background (excluding *ss4*), small differences do exist in the area of stroma per granule (1 times to 1.6 times difference), but no one genotype is statistically significantly different from all others.

In summary, with the exception of *arc1*, starch granule size, initiation and distribution in the *arc* mutants are similar to wild-type plants.

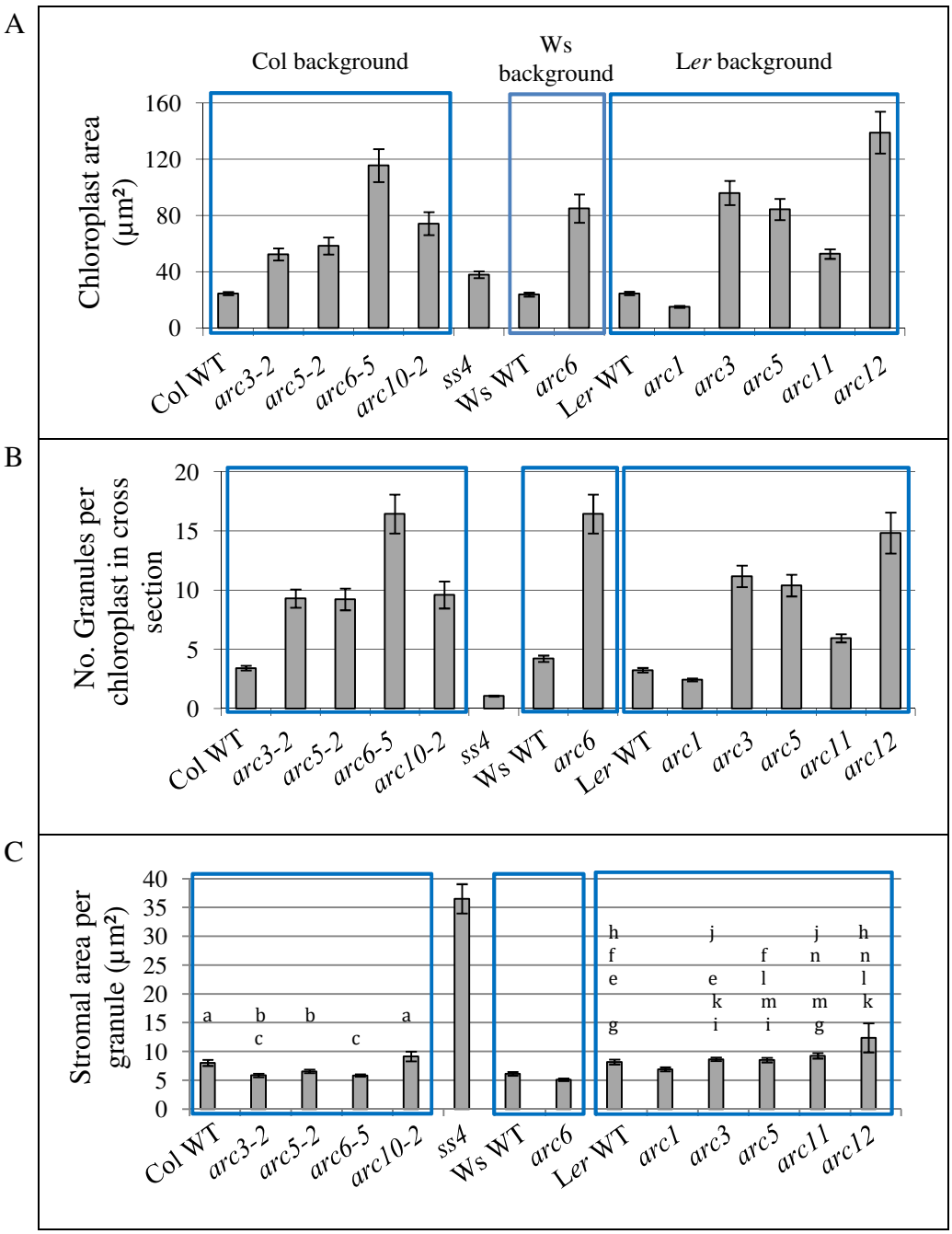

Figure 5.8: Comparison of chloroplast and starch granule number in the *arc* mutants. (A) Average chloroplast cross sectional area. (B) The average number of starch granules per chloroplast cross section. (C) Stromal area per granule [the chloroplast cross sectional area (A) divided by the number of starch granules per chloroplast section (B)]. Measurements taken using imaging software on photos of mesophyll cell sections stained with iodine solution. Values are means of measurements on an average of 40 chloroplasts measured from 5 sections per genotype. Sections from four mature leaves from two different rosettes per genotype (stage 3.90 (Boyes *et al.,* 2001)), were harvested 9 h into a 12 h light period. WT = wild-type. Bars with the same letter are not significantly different from each other. Statistics only performed on graph (C). For statistical analysis see Table 5.4.

Col Background				
	Wild-type	*arc3-2*	*arc5-2*	*arc6-5*
arc3-2	t (78) = -3.61 $p < 0.001$			
arc5-2	t (78) = -2.42 $p = 0.019$	t (78) = -1.65 $p = 0.103$		
arc6-5	t (78) = -3.93 $p < 0.001$	t (78) = 0.01 $p = 0.995$	t (78) = 1.98 $p = 0.052$	
arc10-2	t (78) = 1.12 $p = 0.265$	t (78) = 3.67 $p < 0.001$	t (78) = 2.87 $p = 0.006$	t (78) = 3.81 $p < 0.001$

L*er* Background					
	Wild-type	*arc1*	*arc3*	*arc5*	*arc11*
arc1	t (125) = -2.21 $p = 0.029$				
arc3	t (78) = 0.93 $p = 0.357$	t (125) = -3.78 $p < 0.001$			
arc5	t (78) = 0.60 $p = 0.553$	t (125) = -2.82 $p = 0.006$	t (78) = 0.27 $p = 0.790$		
arc11	t (78) = 1.71 $p = 0.092$	t (125) = -3.93 $p < 0.001$	t (78) = 1.05 $p = 0.300$	t (78) = 1.17 $p = 0.244$	
arc12	t (78) = 1.65 $p = 0.107$	t (125) = -2.16 $p = 0.037$	t (78) = 1.47 $p = 0.151$	t (78) = 1.51 $p = 0.138$	t (78) = -1.22 $p = 0.231$

Ws Background
T-test (Ws WT and *arc*6): t (78) = -2.80, $p = 0.007$

Table 5.4: Statistical analysis (t test) of the stromal area per granule measurements from *arc* mutants and wild-type controls displayed in Figure 5.8C. Test of the null hypothesis that the mean stromal area per granule of the datasets is not different. The degrees of freedom (listed in brackets), test statistic and statistical significance are displayed.

5.2.4 The *arc ss4* double mutants

To provide further information about the relationship between stromal volume and chloroplast number, I wished to discover the impact of radical alterations in chloroplast volume on starch granule size and number in the *ss4* mutant. As discussed in Chapter 3, there appears to be a control over the number of starch granules that are initiated in given volume of stroma and, as described in Chapter 4, in the *ss4* mutant this control is disrupted and on average only one starch granule initiates per chloroplast. It is unknown why only one granule forms per chloroplast. The phenotype may be because there is only one granule initiation point per chloroplast in the *ss4* mutant, regardless of

chloroplast size. Alternatively the relationship between stromal volume and granule initiation may be altered in the *ss4* mutant, so that a larger volume of stroma is required for each granule initiation. If this idea is correct, I would expect an increase in chloroplast volume in an *ss4* background to result in an increase in the number of starch granules per chloroplast.

Plants homozygous for the *ss4* mutation were crossed to the *arc3-2, arc5-2, arc6-5* and *arc10-2* mutants. Double mutants were identified from the F2 population, using PCR to confirm plants were homozygous for the T-DNA insertions in both the *SS4* gene and the appropriate *ARC* gene. For each cross a wild-type control was also identified, using PCR to screen the F2 population for plants that were wild-type for both the *SS4* gene and the appropriate *ARC* gene, and lacked T-DNA insertions in either the *SS4* gene or the appropriate *ARC* gene. The chloroplast number per cell in double-mutant lines was checked by protoplast extraction and light microscopy. This showed that double mutants have a reduced number of enlarged chloroplasts, similar to their *arc* parental line.

5.2.4.1 Starch turnover of the *arc ss4* mutants.

To quantify starch levels in the *arc ss4* double mutants, *arc* mutants, the *ss4* mutant and wild-type controls, leaves were harvested at the end of the 12 hour light period and then again at the end of the 12 hour dark period (Figure 5.9A). At the end of the day there are few significant differences in the starch content between the double mutants and the wild-type controls or the *arc* mutant parent (Table 5.5). However, all double mutants contain significantly more starch at the end of the day than *ss4* (Table 5.5).

All *arc* mutants and wild-type controls have significantly less starch than *ss4* at the end of the night (Table 5.6). In contrast, the *arc ss4* double mutants have significantly more starch at the end of the night than the *ss4* mutant, *arc* mutants and wild-type controls. The turnover of starch in the double mutants is different from both parents (Figure 5.9B). The amount of starch degraded at night (the difference in starch levels at the end of the day and end of the night), is less in the majority of the *arc ss4* double mutants than in the *arc* mutant parent and wild-type control, but is more than in the *ss4* mutant. Therefore, the starch excess at the end of the night in the double mutants is the result of

lower rates of starch degradation at night. However, the starch excess compared to the *ss4* mutant is related to the fact that mutations in both *SS4* and an *ARC* gene result in a higher overall starch content of the rosette than a mutation in the *SS4* gene alone.

All double mutants have a similar spatial pattern of starch accumulation to *ss4*. An example (*arc3-2ss4*) is shown in Figure 5.10. Iodine staining indicated that in both *ss4* and *arc3-2ss4 s*tarch may be absent from the youngest leaves, even at the end of the light period, and a starch excess is present in the mature leaves at the end of the night. This contrasts to the wild-type plant and *arc3-2* where starch is present throughout the rosette at the end of the day and undetectable by iodine staining at the end of the night.

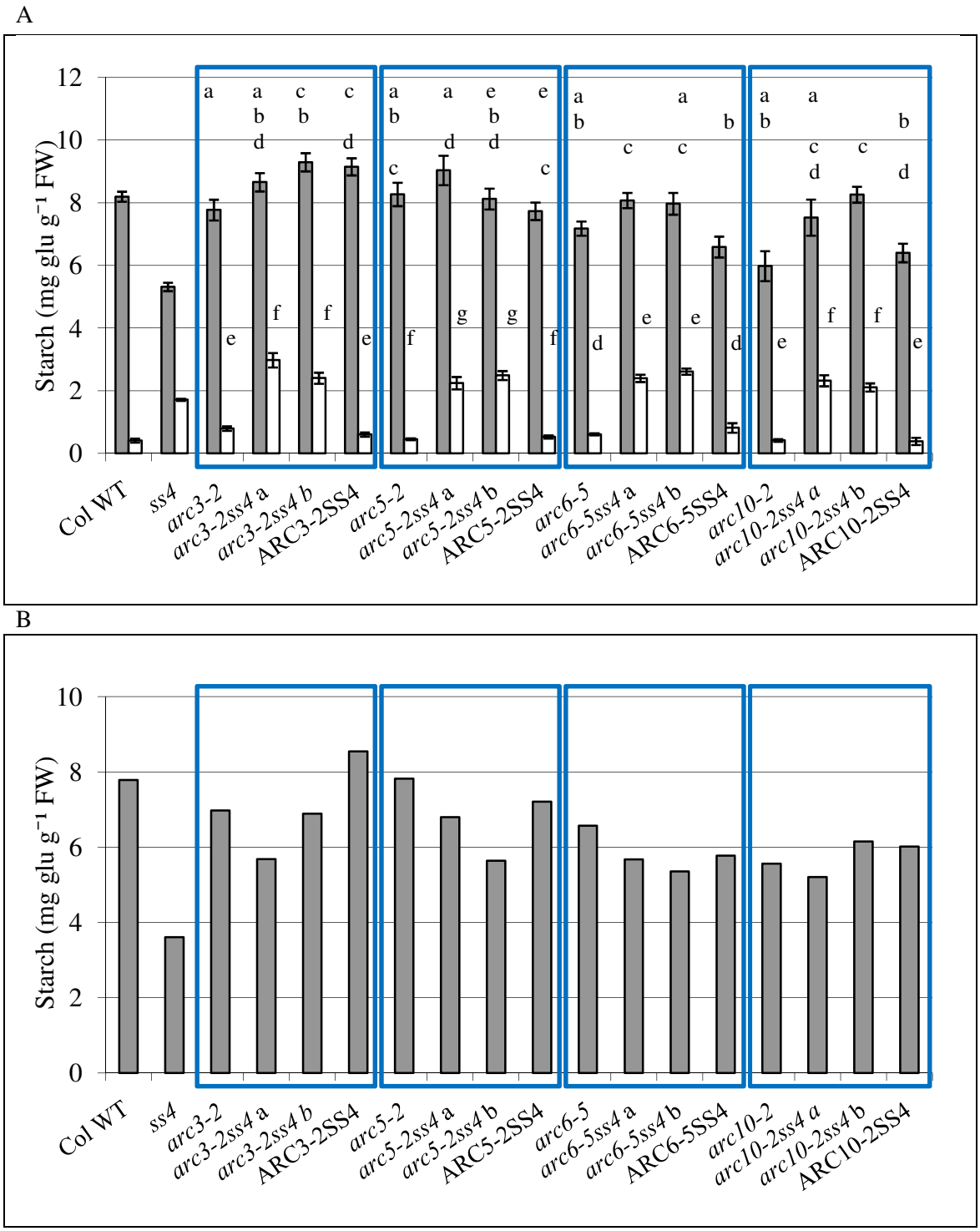

Figure 5.9: Starch levels in the rosette leaves of *ss4, arc* mutants, *arc ss4* double mutants and wild-type (WT) controls. Mutant plants are grouped with the appropriate wild-type control and *arc* parental line. (A) Starch levels at the end of day (EOD) and end of night (EON). (B) Starch turnover, derived from the difference in starch levels at the EOD and EON. Plants grown for 25 days in 12 h light/12 h dark conditions. n = 8 ± SE, where n = eight separate plants. Grey bars = EOD, White bars = EON. Mean values within each section labelled with the same letter are not statistically different from each other. For statistical analysis see Tables 5.5 and 5.6.

Starch Content - End of Day				
	arc3-2	*arc3-2ss4* a	*arc3-2ss4* b	ARC3-2SS4
arc3-2ss4 a	*t* (12) = -2.01 *p* = 0.068			
arc3-2ss4 b	*t* (13) = -3.48 *p* = 0.004	*t* (13) = -1.54 *p* = 0.147		
ARC3-2SS4	*t* (13) = -3.24 *p* = 0.006	*t* (13) = 1.23 *p* = 0.240	*t* (14) = -0.37 *p* = 0.720	
ss4	*t* (13) = 6.86 *p* < 0.001	*t* (13) = 10.81 *p* <0.001	*t* (14) = 12.43 *p* <0.001	*t* (14) = 12.57 *p* < 0.001
	arc5-2	*arc5-2ss4* a	*arc5-2ss4* b	ARC5-2SS4
arc5-2ss4 a	*t* (14) = -1.28 *p* = 0.222			
arc5-2ss4 b	*t* (14) = 0.29 *p* = 0.773	*t* (14) = -1.59 *p* = 0.134		
ARC5-2SS4	*t* (14) = 1.15 *p* = 0.269	*t* (14) = -2.39 *p* = 0.032	*t* (14) = 0.90 *p* = 0.384	
ss4	*t* (14) = 7.44 *p* <0.001	*t* (14) = 7.63 *p* <0.001	*t* (14) = 7.83 *p* <0.001	*t* (14) = 7.76 *p* < 0.001
	arc6-5	*arc6-5ss4* a	*arc6-5ss4* b	ARC6-5SS4
arc6-5ss4 a	*t* (14) = -2.70 *p* = 0.017			
arc6-5ss4 b	*t* (14) = -1.91 *p* = 0.076	*t* (14) = 0.25 *p* = 0.809		
ARC6-5SS4	*t* (14) = 1.46 *p* = 0.166	*t* (14) = -3.59 *p* = 0.003	*t* (14) = -2.87 *p* = 0.012	
ss4	*t* (14) = 7.09 *p* < 0.001	*t* (14) = 9.85 *p* <0.001	*t* (14) = 7.12 *p* <0.001	*t* (14) = 3.54 *p* = 0.006
	arc10-2	*arc10-2ss4* a	*arc10-2ss4* b	ARC10-2SS4
arc10-2ss4 a	*t* (14) = -1.16 *p* = 0.275			
arc10-2ss4 b	*t* (14) = -2.36 *p* 0.033	*t* (14) = -1.90 *p* = 0.079		
ARC10-2SS4	*t* (12)= -0.78 *p* = 0.448	*t* (14) = 1.74 *p* = 0.104	*t* (14) = 4.76 *p* < 0.001	
ss4	*t* (12) = 1.34 *p* = 0.231	*t* (14) = 3.73 *p* = 0.006	*t* (14) = 10.23 *p* <0.001	*t* (14) = 3.32 *p* = 0.005
	Wild-type Col			
ss4	*t* (14) = 13.76 *p* < 0.001			

Table 5.5: Statistical analysis (*t* test) of the starch measurements in rosette leaves at the end of the day, of the *ss4* mutant, *arc* mutants, *arc ss4* double mutants and wild-type controls displayed in Figure 5.9A. Test of the null hypothesis that the mean starch contents of the datasets are not different. The degrees of freedom (listed in brackets), test statistic and statistical significance are displayed.

Starch Content - End of Night				
	arc3-2	*arc3-2ss4* a	*arc3-2ss4* b	ARC3-2SS4
arc3-2ss4 a	t (14) = -9.09 p < 0.001			
arc3-2ss4 b	t (14) = -8.43 p < 0.001	t (14) = 1.97 p = 0.068		
ARC3-2SS4	t (14) = 1.93 p = 0.074	t (14) t = -9.95 p < 0.001	t (14) = -9.53 p < 0.001	
ss4	t (14) = -11.54 p <0.001	t (14) = 5.45 p <0.001	t (14) = 3.84 p = 0.006	t (14) = -15.02 p <0.001
	arc5-2	*arc5-2ss4* a	*arc5-2ss4* b	ARC5-2SS4
arc5-2ss4 a	t (14) = -8.94 p < 0.001			
arc5-2ss4 b	t (14) = -14.01 p < 0.001	t (14) = 1.00 p = 0.334		
ARC5-2SS4	t (14) = -1.24 p = 0.235	t (14) = -8.41 p < 0.001	t (14) = 13.01 p < 0.001	
ss4	t (14) = -27.97 p <0.001	t (14) = 2.64 p = 0.032	t (14) = 5.30 p <0.001	t (14) = -19.52 p <0.001
	arc6-5	*arc6-5ss4* a	*arc6-5ss4* b	ARC6-5SS4
arc6-5ss4 a	t (14) = -14.47 p < 0.001			
arc6-5ss4 b	t (14) = -19.32 p < 0.001	t (14) = -1.40 p = 0.183		
ARC6-5SS4	t (12) = -1.32 p = 0.240	t (12) = -8.34 p < 0.001	t (12) = -10.40 p < 0.001	
ss4	t (14) = -22.91 p <0.001	t (14) = 5.55 p <0.001	t (14) = 8.69 p <0.001	t (12) = -5.77 p = 0.002
	arc10-2	*arc10-2ss4* a	*arc10-2ss4* b	ARC10-2SS4
arc10-2ss4 a	t (13) = -10.37 p < 0.001			
arc10-2ss4 b	t (13) = -12.32 p < 0.001	t (14) = 0.96 p = 0.352		
ARC10-2SS4	t (11) = 0.26 p = 0.806	t (12) = 8.41 p < 0.001	t (12) = 9.53 p < 0.001	
ss4	t (13) = -23.88 p <0.001	t (14) = 3.35 p = 0.011	t (14) = 2.94 p = 0.019	t (12) = -11.10 p <0.001
	Wild-type Col			
ss4	t (14) = -18.33 p <0.001			

Table 5.6: Statistical analysis (t test) of the starch measurements in rosette leaves at the end of the night, of the *ss4* mutant, *arc* mutants, *arc ss4* double mutants and wild-type controls displayed in Figure 5.9A. Test of the null hypothesis that the mean starch contents of the datasets are not different. The degrees of freedom (listed in brackets), test statistic and statistical significance are displayed.

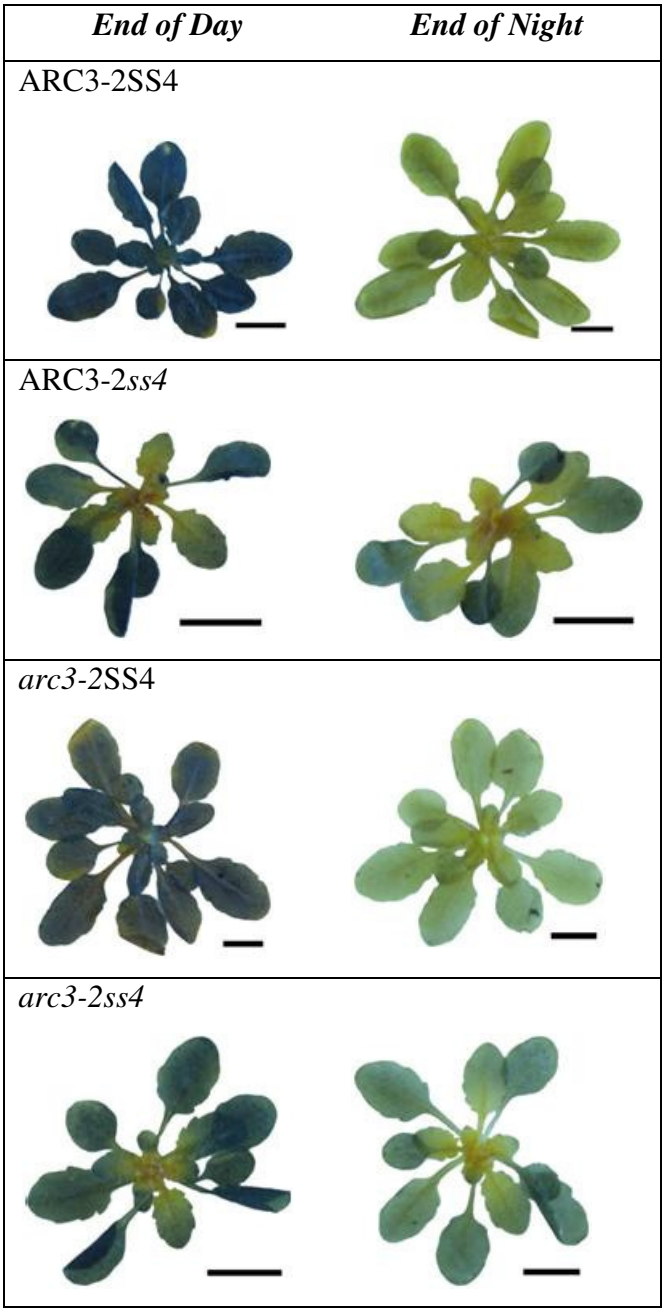

Figure 5.10: Whole rosettes of the *arc ss4* double mutants harvested at the end of the light and end of the night; decolourised with ethanol and stained with iodine solution. Plants grown for 25 days in 12 h light/12 h dark conditions. Scale bar = 1cm

5.2.4.1 Granule Size and Distribution in the *arc ss4* mutants.

The chloroplasts of the *arc ss4* double mutants contain granules with a much wider range of sizes than the parental lines (Figure 5.11). For example starch granules isolated from *arc3-2ss4* plants harvested at the end of the day (12 h light) range in diameter from 0.4 µm to 7.9 µm, while granules from the *ss4* mutant range from 0.6 µm to 5.0 µm in diameter and granules from *arc3-2* range from 0.6 µm to 3.4 µm in diameter. The average granule diameters of *arc3-2ss4* (2.0 ± SE 0.04, n = 785) and *arc5-2ss4* (2.5 ± SE 0.04, n = 806) are greater than that of *arc3-2* (1.9 ± SE 0.03, n = 319) and *arc5-2* (1.8 ± SE 0.03, n = 389) respectively (Table 5.7). However, the average granule diameter of *arc10-2ss4* (2.0 ± SE 0.04, n = 740) is not significantly different from the average granule diameter of *arc10-2* (1.9 ± SE 0.03, n = 398) and the average granule diameter of *arc6-5ss4* (1.7 ± SE 0.03, n = 778) is less than that of *arc6-5* (2.0 ± SE 0.04, n = 386). All of the double mutants have an average granule diameter different from that of *ss4* (Table 5.7). However, while *arc3-2ss4, arc6-5ss4* and *arc10-2ss4* have an average granule diameter less than *ss4*, *arc5-2ss4* has an average diameter greater than *ss4*. The variation in starch granule size in the double mutants can be seen in SEM images of isolated granules (Figure 5.12).

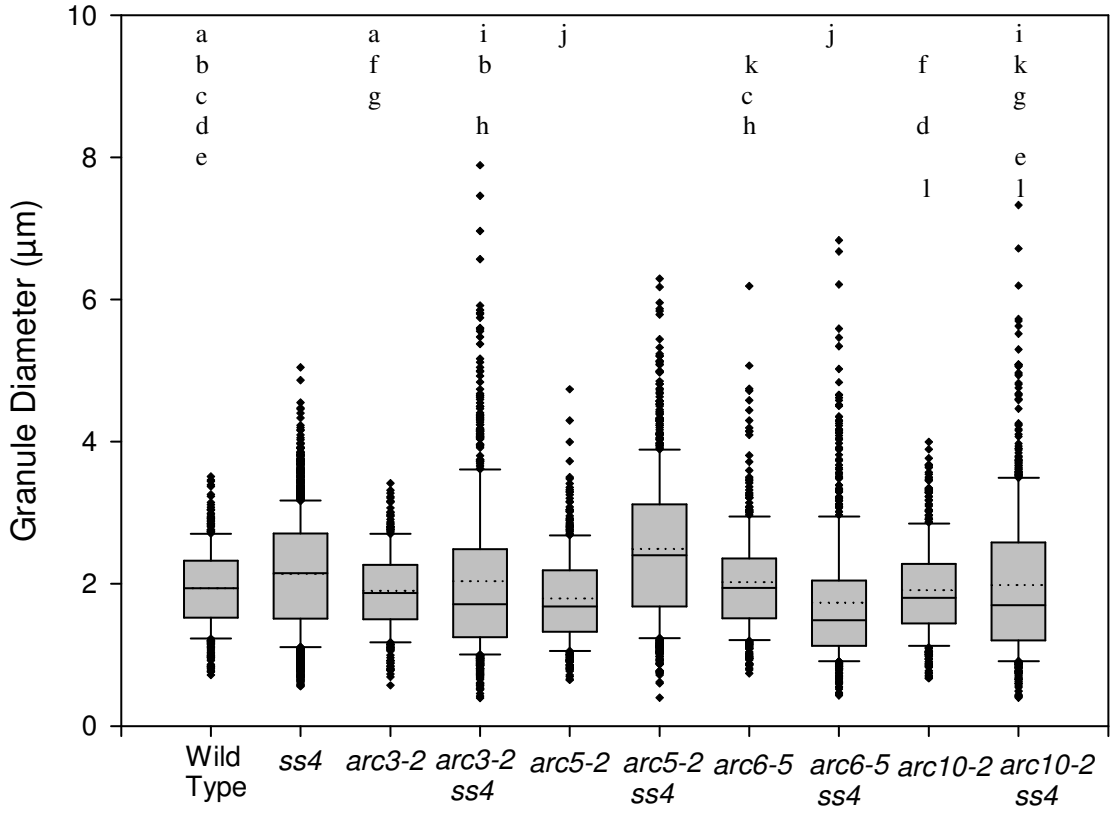

Figure 5.11: Starch granule size distribution. Box plot showing the range in granule diameters for *arc* and *ss4* mutants. The band in the middle of the box is the median (50th percentile). The bottom and top of the box are the 25th and 75th percentiles. The upper and lower bars represent the 90th and 10th percentiles respectively. Outliers are represented as diamonds. The mean granule diameters of genotypes labelled with the same letter are not significantly different from each other. Mean shown as dotted line. Between 319 and 2270 granules measured for each genotype, from eleven SEM images photographed at random. Granules isolated from 25 day old plants, 40 plants per genotype. For statistical analysis see Table 5.7.

	Wild-type	*arc3-2*	*arc5-2*	*arc6-5*	*arc10-2*	*arc3-2 ss4*	*arc5-2 ss4*	*arc6-5 ss4*	*arc10-2 ss4*
arc3-2	t (680) = -0.94 p = 0.348								
arc5-2	t (750) = -3.35 p <0.001	t (706) = 2.35 p = 0.019							
arc6-5	t (747) = 1.66 p = 0.098	t (703) = -2.44 p = 0.015	t (773) = -4.55 p <0.001						
arc10-2	t (759) = -0.63 p = 0.527	t (715) = 0.27 p = 0.784	t (785) = 2.57 p = 0.010	t (782) = -2.15 p = 0.032					
arc3-2 ss4	t (1146) = 1.89 p = 0.059	t (1102) = -2.66 p = 0.008	t (1172) = 4.72 p <0.001	t (1169) = 0.24 p = 0.807	t (1181) = -2.36 p = 0.018				
arc5-2 ss4	t (1167) = 11.64 p <0.001	t (1123) = -12.18 p <0.001	t (1193) = -14.22 p <0.001	t (1190) = 8.88 p <0.001	t (1202) = -11.68 p <0.001	t (1589) = -8.47 p <0.001			
arc6-5 ss4	t (1139) = -4.67 p <0.001	t (1095) = 3.64 p <0.001	t (1165) = 1.27 p = 0.204	t (1162) = 5.72 p <0.001	t (1174) = 3.82 p <0.001	t (1561) = 5.86 p <0.001	t (1582) = 15.42 p <0.001		
arc10-2 ss4	t (1101) = 0.86 p = 0.388	t (1057) = 1.66 p = 0.097	t (1057) = 3.75 p <0.001	t (1124) = -0.70 p = 0.486	t (1136) = -1.38 p = 0.168	t (1523) = -0.92 p = 0.355	t (1544) = -9.50 p <0.001	t (1516) = 4.90 p <0.001	
ss4	t (2633) = 5.89 p <0.001	t (2587) = -6.75 p <0.001	t (2657) = -9.54 p <0.001	t (2654) = -2.82 p = 0.005	t (2666) = -6.17 p <0.001	t (3053) = -2.49 p = 0.013	t (3074) = 8.72 p <0.001	t (3046) = -11.15 p <0.001	t (3008) = -3.74 p <0.001

Table 5.7: Statistical analysis (t test) of the starch granule diameters of isolated granules from the *ss4* mutant, *arc* mutants, *arc ss4* double mutants and wild-type controls displayed in Figure 5.11. Test of the null hypothesis that the mean granule diameters of the datasets are not different. The degrees of freedom (listed in brackets), test statistic and statistical significance are displayed.

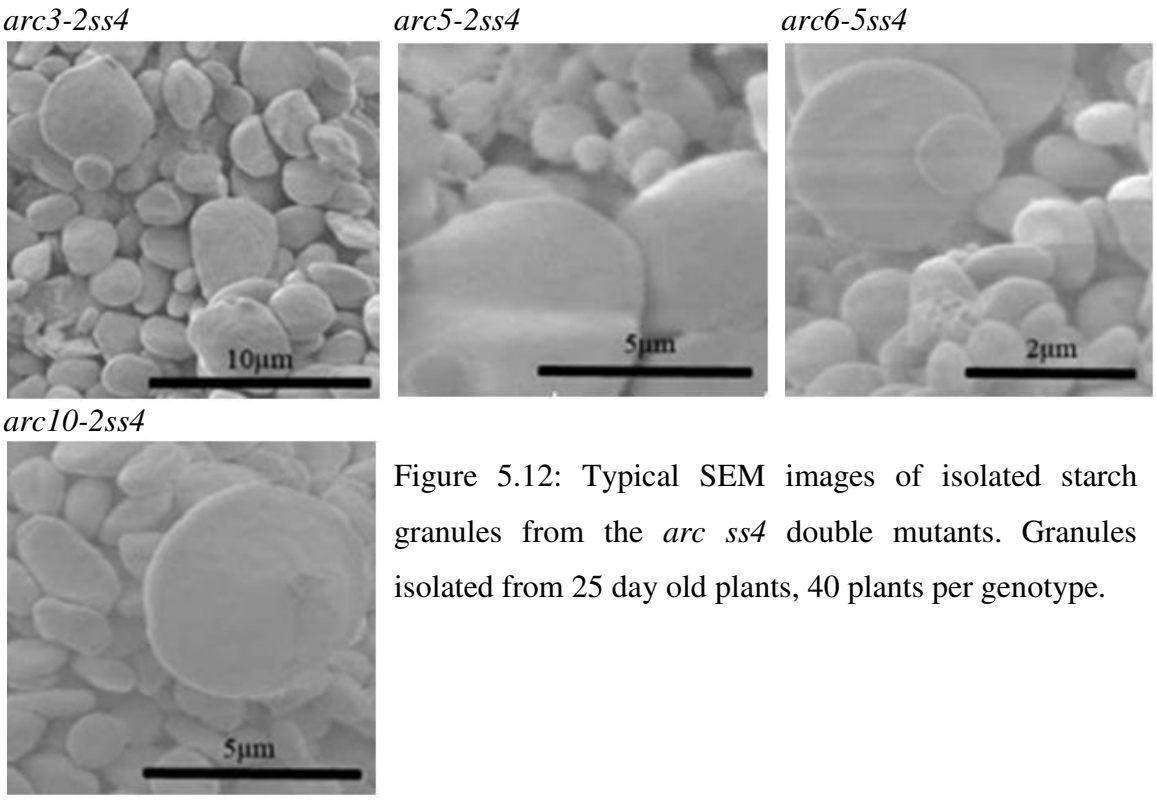

Figure 5.12: Typical SEM images of isolated starch granules from the *arc ss4* double mutants. Granules isolated from 25 day old plants, 40 plants per genotype.

Staining of sections through embedded leaves with iodine solution and observation under a light microscope confirms that the immature leaves of the *arc ss4* double mutants contain less starch than wild-type plants (Figure 5.13). Interestingly, while starch is present in all chloroplasts of the mature leaves, in the immature leaves starch granules are only present in a few chloroplasts.

The chloroplast cross-sectional areas of the *arc ss4* double mutants are larger than those of both parental lines (Figure 5.14A), including the *arc* mutant parent. While it appears from observations of protoplasts that chloroplast numbers in the *arc ss4* double mutants are similar to the *arc* mutant parents, the exact number of chloroplasts is not known. There may in fact be fewer, larger chloroplasts in the double mutants, rather than an equal number of larger chloroplasts. The *arc ss4* double mutants have more granules per chloroplast cross-section than *ss4* mutants, but fewer granules per chloroplast cross-section than the *arc* mutants (Figure 5.14B).

If the chloroplast cross-sectional area is divided by the granule number per chloroplast, there is remarkable conservation in the stromal area per granule between the *ss4* mutant

and the *arc ss4* double mutants (Figure 5.14C; test of the null hypothesis that the mean stromal area per granule of the datasets is not different; F (4,355) = 0.21, p = 0.933; Table 5.8), greater even than the conservation seen between the *arc* mutants and wild-type chloroplasts (Figure 5.8C; Table 5.4 and 5.14C; Table 5.8). The *ss4* mutant requires a greater area of stroma for a granule to initiate than in the *arc* mutants or wild-type plants (Figure 5.8C; Table 5.4 and Figure 5.14C; Table 5.8). This difference from *arc* mutants and wild-type plants, in the stromal area per granule is maintained in the *arc ss4* double mutants (Figure 5.14C).

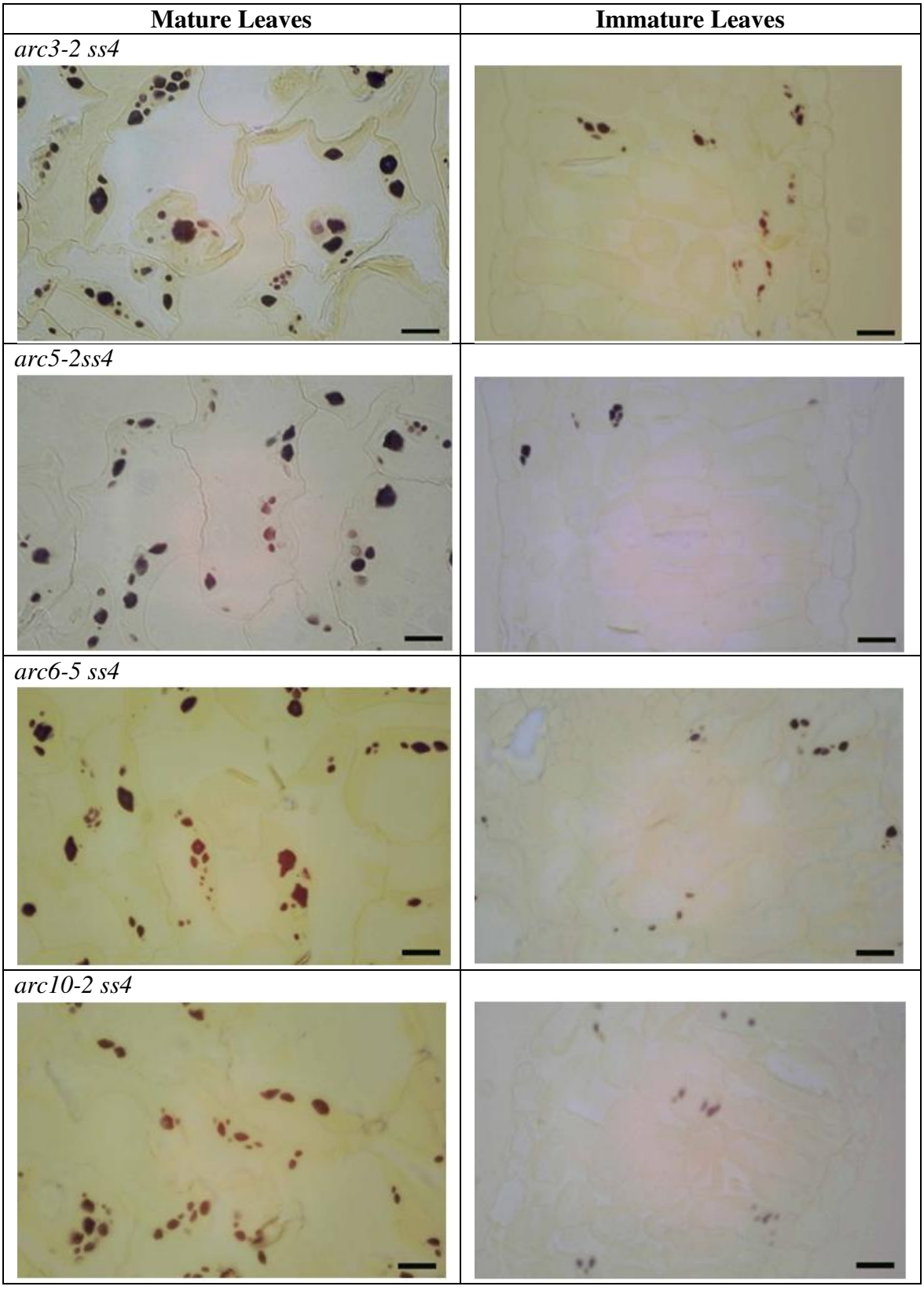

Figure 5.13: 1 µm thick sections through embedded leaves of the *arc ss4* double mutants; stained with iodine solution. Leaves harvested 9 h into the 12 h light period. scale bar = 10 µm

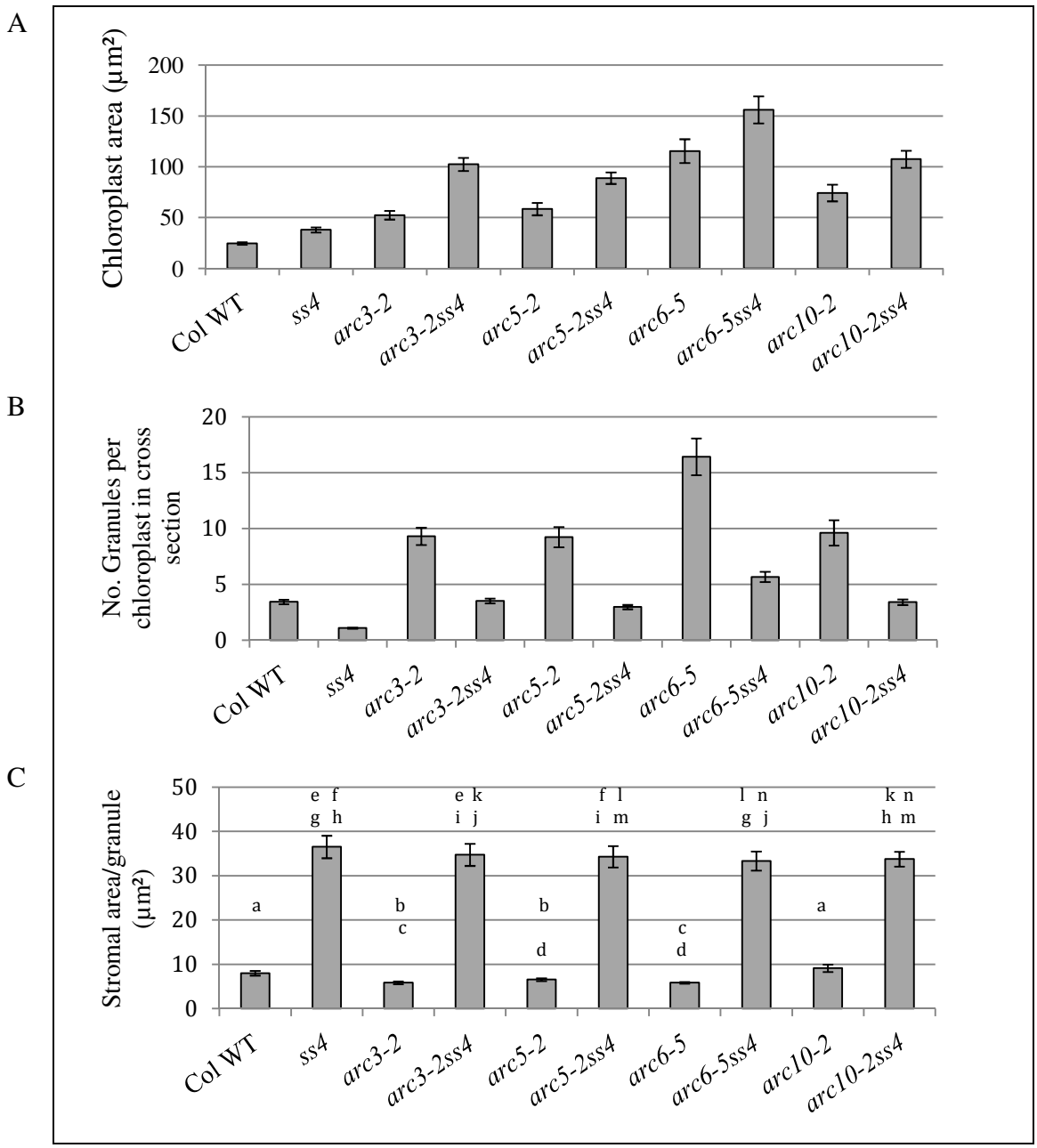

Figure 5.14: Comparison of chloroplast and starch granule number in the *arc* and *arc ss4* mutants. (A) Average chloroplast area. (B) The average number of starch granules per chloroplast cross-section. (C) Stromal area per granule [the chloroplast cross sectional area (A) divided by the number of starch granules per chloroplast section (B)]. Measurements taken using imaging software on photographs of mesophyll cell sections stained with iodine solution. Values are means of measurements on an average of 40 to 80 chloroplasts measured from 5 sections per genotype. Sections from four mature leaves from two different rosettes per genotype (stage 3.90 (Boyes *et al.,* 2001)), were harvested 9 h into a 12 h light period. WT = wild-type. Bars with the same letter are not statistically significantly different from each other (statistics performed only on data for stromal area per granule). For statistical analysis see Table 5.8.

	Wild-type	*arc3-2*	*arc5-2*	*arc6-5*	*arc10-2*	*ss4*	*arc3-2 ss4*	*arc5-2 ss4*	*arc6-5 ss4*
arc3-2	t (78) = -3.61 p <0.001								
arc5-2	t (78) = -2.42 p = 0.019	t (78) = -1.65 p = 0.103							
arc6-5	t (78) = -3.93 p <0.001	t (78) = 0.01 p = 0.995	t (78) = 1.98 p = 0.052						
arc10-2	t (78) = 1.12 p = 0.265	t (78) = 3.67 p <0.001	t (78) = 2.87 p = 0.006	t (78) = 3.81 p <0.001					
ss4	t (78) = 11 p <0.001	t (78) = -12 p <0.001	t (78) = -11.72 p <0.001	t (78) = -12.05 p <0.001	t (78) = -10.25 p <0.001				
arc3-2 ss4	t (118) = 10.51 p <0.001	t (118) = -11.52 p <0.001	t (118) = 11.24 p <0.001	t (118) = 11.57 p <0.001	t (118) = -9.75 p <0.001	t (118) = -0.5 p = 0.617			
arc5-2 ss4	t (118) = 10.67 p <0.001	t (118) = -11.72 p <0.001	t (118) = -11.43 p <0.001	t (118) = 11.78 p <0.001	t (118) = -9.87 p <0.001	t (118) = -0.63 p = 0.532	t (158) = 0.12 p = 0.905		
arc6-5 ss4	t () = 11.44 p <0.001	t (118) = -12.65 p <0.001	t (118) = -12.32 p <0.001	t (118) = -12.72 p <0.001	t (118) = -10.48 p <0.001	t (118) = -0.91 p = 0.367	t (158) = 0.43 p = 0.667	t (158) = 0.31 p = 0.757	
arc10-2 ss4	t (118) = 14.79 p <0.001	t (118) = 16.53 p <0.001	t (118) = 16.10 p <0.001	t (118) = 16.70 p <0.001	t (118) = -13.23 p <0.001	t (118) = 0.93 p = 0.353	t (158) = -0.33 p = 0.745	t (158) = -0.19 p = 0.849	t (158) = 0.16 p = 0.871

Table 5.8: Statistical analysis (*t* test) of the stromal area per granule measurements from the *ss4* mutant, *arc* mutants, *arc ss4* double mutants and wild-type control displayed in Figure 5.14. Test of the null hypothesis that the mean stromal area per granule of the datasets is not different. The degrees of freedom (listed in brackets), test statistic and statistical significance are displayed.

5.3 Discussion

In the introduction to this chapter, I suggested that components of the chloroplast division apparatus, and the hypothetical plastoskeleton they may form, could play an important role in starch metabolism in three respects. Firstly, the plastoskeleton might form part of the mechanism that provides information on starch granule size and shape in order to set the appropriate rate of starch degradation at night. Secondly, plastoskeletal components might play a role in granule initiation, perhaps providing an anchor at specific nodes in a plastoskeleton for initiation. Thirdly, the plastoskeleton or division apparatus might be involved in controlling the distribution of starch granules by interacting with the granules and ensuring their even segregation between daughter chloroplasts.

My results show that mutations in the chloroplast division components studied here do not affect starch accumulation or degradation, granule size or the number of granules that accumulate in a given area of stroma; indicating that ARC3, ARC5, ARC6, ARC10, ARC11 and ARC12 are not important and/or involved in starch metabolism. I explore the consequences of these observations in more detail below.

The starch accumulation and degradation in the *Arabidopsis arc* mutant leaves was the same as that of wild-type plants, indicating that the components of the chloroplast division apparatus studied here are unlikely to provide information about granule size and shape. This contrasts with the phenotype in the *arc5* rice mutant, where there is a 55% reduction in starch relative to wild-type (presented as % of fresh weight) content in the leaves at the end of the day (Yun and Kawagoe 2009). Yun and Kawagoe (2009) suggested that the reduction in leaf starch may be a result of impaired light responsive chloroplast movements, due to the unusual chloroplast morphology in the *arc5* mutant. The amyloplasts of the *arc5* rice mutant contained structurally altered starch granules that were irregular in shape compared to wild-type granules. ARC5 may thus play an additional role in rice compared to *Arabidopsis,* which results in reduced levels of starch in the leaves and altered granule morphology.

The granule size and number per unit stromal area is largely similar across the *arc* mutants and wild-type controls. Therefore, the components of chloroplast division

apparatus studied here are not likely to be responsible for providing an anchor point for initiation or for segregating the starch granules equally between daughter chloroplasts.

The remarkable conservation in the area of stroma per granule across the *arc* mutants and wild-type controls suggests the existence of controls over the number of granules that initiate in a given volume. An alternative hypothesis is that granule initiation is a random event that is dependent upon the concentration of suitable glucans or malto-oligosaccharides within the stroma. Once the glucans or malto-oligosaccharides become sufficiently concentrated and reach a critical mass per volume of stroma a new granule is initiated. Thus, when chloroplast size is increased, as in the *arc* mutants, the number of granules that initiate per chloroplast increases.

I was unable to examine all the known chloroplast division components in this study and therefore it remains possible that unexamined components of the chloroplast division apparatus may provide information about the granule size and shape in order to set the appropriate rate of starch degradation at night. Other components worthy of examination include the *Arabidopsis* proteins, MscS-like2 (MSL2) and MSL3, which localise to the plastid envelope, co-localising with the chloroplast division component *At*MinE1, and have been shown to be involved in the control of plastid size, shape and division (Haswell and Meyerowitz 2006). MscS is a bacterial mechanosensitive ion channel which protects against lysis during osmotic shock by opening in response to increased membrane tension. In Chapter 3 I showed that the mean chloroplast volume at the end of the night is almost half the volume at the end of the day. This change in chloroplast volume may partly be the result of the change in starch granule volume, which increases during the day and decreases at night. In other words, chloroplasts may expand during the day as the starch granules grow and retract at night as the granules are degraded. Changes in chloroplast volume may be detected via mechanosensitive ion channels in the internal chloroplast envelope (Haswell and Meyerowitz 2006; Pyke 2006) and the change in volume information fed into a signalling mechanism that controls the rate of starch degradation.

Further components of the division apparatus worthy of examination include FtsZ2-1, FtsZ2-2, PARC6, PDV1, PDV2 and MCD1 (discussed in section 5.1.4). It may also be worth investigating, a possible role in starch metabolism, for proteins that have roles in

multiple processes including plastid division. These include *At*CDT1, (discussed in section 5.1.4) that was found to have a role in both nuclear DNA replication and plastid division (Raynaud *et al.,* 2005). Mutants worthy of investigation are those with reduced chloroplast number per cell and reported increases in starch accumulation. For example the *chloroplast processing enzyme* (*cpe*) has 25% fewer chloroplasts per cell than wild-type plants and electron micrographs suggested they contain more starch (Wan *et al.,* 1998). However, CPE is a general stromal processing peptidase involved in the chloroplast import machinery with a critical role in chloroplast biogenesis. The *cpe* mutant has retarded growth with chlorotic leaves (Wan *et al.,* 1998). These additional phenotypic problems could have pleiotropic effects on starch accumulation.

5.3.1 Variation in granule initiation in the *arc1* mutant

As I discussed above, there is remarkable conservation in the area of stroma per granule across the *arc* mutants (with a reduced number of enlarged chloroplasts) and wild-type controls. However, this does not seem to apply to *arc1,* in which the stromal area per granule is less than that of wild-type L*er* and the other *arc* mutants. In addition the starch granules in *arc1* are significantly smaller than wild-type granules. The *arc1* mutant is clearly complex, with a variety of phenotypes affecting mesophyll cell size as well as chloroplast division and expansion. The identity of ARC1 has not been determined, but it is thought to act independently of the other ARC genes studied in this thesis (Marrison *et al.,* 1999) and might not be directly involved in the chloroplast division apparatus. Within the smaller chloroplasts of the *arc1* mutant, the mechanism that potentially controls the initiation of granules dependent upon stromal volume may be disrupted and as a result a greater number of granule initiation points arise. However, this does not mean that ARC1 is involved in this control mechanism.

5.3.2 The involvement of SS4 in granule initiation

When the *ss4* mutation is introduced into the *arc* background, multiple granules initiate in the enlarged chloroplasts. This contrasts with the *ss4* mutant where on average only one starch granule occurs per chloroplast. Thus the "single granule per chloroplast" phenotype observed in the *ss4* mutant is a result of the limited chloroplast size, and not because *ss4* chloroplasts can only ever initiate one granule.

The cause of the very wide range of granule sizes in the *arc ss4* mutants is not clear. One possible explanation is that because granule initiations occur less often in the *arc ss4* mutants than in the wild-type, granules may not all be initiated at the same time. The first granule to form in an *arc ss4* mutant chloroplast may grow to a significant size before subsequent granules are initiated.

The high level of starch remaining at the end of the night in the *arc ss4* mutants further supports the idea presented in Chapter 4 that the lower degradation rate of the *ss4* mutant is not simply a result of the reduced granule surface area available for the actions of degradative enzymes (proposed by Roldan *et al.* (2007)). The high starch levels in the *arc ss4* double mutants are not a consequence of large chloroplast size, because this phenotype is not seen in the single *arc* mutants. Even though more starch granules are initiated per chloroplast in the *arc ss4* double mutants than in *ss4*, it seems likely that the severe metabolic disturbances (e.g. high ADPG levels) seen in *ss4* are present and perhaps exacerbated in these double mutants.

D'Hulst and Merida (2010) recently proposed that SS4 may interact with FtsZ-like proteins in plants, in order to coordinate the initiation of starch granules with chloroplast division, and avoid aborted plastid division. The *Arabidopsis* genome contains three FtsZ genes, *AtFtsZ1-1, AtFtsZ2-1* and *AtFtsZ2-2*. I studied *arc10*, an *AtFtsZ1-1* mutant, but did not examine plants with mutations in the *AtFtsZ2-1* or *AtFtsZ2-2* genes. While no evidence is provided and no reference is made to the chloroplast division components being studied, D'Hulst and Merida (2010) state that preliminary results agree with the idea of an interaction between starch metabolism and plastid division. Evidence presented in this thesis does not support an interaction between the chloroplast division components and starch metabolism, because granule initiation and starch turnover are unaffected in the *arc* mutants studied. As discussed above, the introduction of the *ss4* mutation into the *arc* mutants does alter starch turnover compared to the wild-type control and parental lines, enhancing the starch excess phenotype observed in the *ss4* mutant at the end of the night. This evidence does not support a specific interaction between SS4 and FtsZ-like proteins, because starch turnover in the *arc ss4* double mutants is affected in the same way, regardless of what

division protein is missing. Further experimentation would be required to uncover any specific interactions that may be occurring.

Interestingly when the *ss4* mutation is introduced into the *arc* background, the number of granules initiated in an area of stroma is reduced compared to the *arc* parent line and the wild-type plant, but remains almost identical to the *ss4* mutant. This suggests that a control over the number of granules initiated in a given volume of stroma exists in the *ss4* mutant background, but that it is shifted so that a larger stromal volume is required for the initiation of each granule.

Starch granules are present within the immature leaves of the *arc ss4* double mutants, but only in a few chloroplasts. It is unknown why only certain chloroplasts in the immature leaf in the *arc ss4* mutants are capable of initiating starch granules and other chloroplasts are not, but this indicates that the trigger to produce starch granules in the mature leaves of *ss4* mutant is not related to a developmental switch, for example between sink and source leaves. Since all the chloroplasts in the mature leaf contain starch granules, at some point during cell maturation the conditions or requirements for granule initiation are fulfilled in all chloroplasts. Perhaps the critical concentration within the stroma of glucans or malto-oligosaccharides necessary for a starch granule to initiate is reached sooner in some chloroplasts than in others.

6 Summary

As described at the beginning of the thesis the principal aim of my work was to understand the variation in starch granule number and size in *Arabidopsis* leaves. I have developed new robust methods for assessing starch granule number per chloroplast and per unit stromal volume, something that has not been achieved previously. Each method has potential drawbacks, but nonetheless important new information has been obtained from their application. The degree of variation revealed by the methods in granule size and granule number per chloroplast that occurs within the leaves of a single rosette and even within a single cell at any one time is remarkable, and had not previously been documented. In this chapter I will summarise my conclusions and proposals on the two major themes of the thesis; firstly, how do starch granules initiate and secondly, what determines how many starch granules initiate.

6.1 How do starch granules initiate?

In the introduction to this thesis I described the three major suggestions for how granules may be initiated; by spontaneous crystallisation, via heterogeneous nucleation, or via a self-priming protein.

The crystallization of glucan polymers into starch granules could be a spontaneous event which does not require an initiating molecule. Granule initiation could occur when a critical concentration of appropriately sized and branched amylopectin molecules is achieved within the stroma. At this concentration phase separation would occur, followed by crystallisation. Another possibility is that a heterogeneous nucleation event could be responsible for the initial formation of the starch granule (Geddes and Greenwood 1969). During heterogeneous nucleation a foreign (non-glucan) particle would have a stabilising effect on polymer molecules, acting like a seed or nucleus for glucan crystallisation. In the chloroplast stroma there are many structures and proteins that could potentially act as stabilisers.

Alternatively, a self-priming protein or enzyme may be able to glucosylate one of its own amino acid residues using ADPG, then add glucosyl moieties from ADPG onto that glucose to make a glucan chain. This self-priming molecule would act in a similar

way to glycogenin, which is responsible in yeast and animals for priming glycogen synthesis. Glycogenin is a Mn^{2+}/Mg^{2+}-dependent UDPG-requiring glucosyltransferase (reviewed in Alonso *et al.,* 1995; Smythe and Cohen 1991), which glucosylates itself to create a chain of up to eight α-1,4-linked glucose residues that are covalently linked via a tyrosine residue to the glycogenin protein (Cheng *et al.,* 1995; Lomako *et al.,* 1992; Lomako *et al.,* 1993; Pitcher *et al.,* 1988; Whelan 1998). Glycogenin forms a complex with glycogen synthase (EC 2.4.1.11) (Pitcher *et al.,* 1987; Skurat *et al.,* 2006); allowing glycogen synthase to elongate the glucan chain attached to glycogenin. As described in the introduction (section 1.3.1.3), self-glycosylating proteins have been detected or purified from some plant tissues (Ardila and Tandecarz 1992; Langeveld *et al.,* 2002; Lavintman and Cardini 1973; Lavintman *et al.,* 1974; Quentmeier *et al.,* 1987; Rothschild and Tandecarz 1994; Singh *et al.,* 1995). However, evidence suggests that these proteins are involved in the synthesis of polysaccharide components of the cell wall rather than amylopectin (Delgado *et al.,* 1998; Dhugga *et al.,* 1997; Langeveld *et al.,* 2002), and to the best of my knowledge no self-glucosylating proteins have been discovered that are likely to be involved in the synthesis of amylopectin.

Taken as a whole my data strongly favour the idea that granules initiate via spontaneous crystallisation when the concentration of suitable glucans or malto-oligosaccharides within a volume of stroma reaches a critical level.

This idea can explain the following observations. Firstly, there is remarkable constancy in granule number in a certain volume of stroma, regardless of the chloroplast size. Secondly, the phenotype of the *ss4* mutant is consistent with the idea that when there is a reduction in the rate of production of suitable glucans for crystallization, there are fewer and more sporadic granule initiations. My results are consistent with SS4 acting earlier in the pathway from the Calvin cycle to starch than other parts of the starch synthesising apparatus. SS4 may elongate free small malto-oligosaccharides to produce a “primer” glucan molecule, upon which the other starch synthases and starch branching enzymes can then act. This suggestion is also compatible with data on the *ss4* mutant phenotype presented in Roldan *et al.* (2007) and Szydlowski *et al.* (2009). Experiments were proposed in Chapter 4 to explore the substrates upon which SS4 may act and further investigate the role of SS4 in glucan chain and granule initiation. Within the wild-type chloroplast, the combined actions of SS4 followed by the other SSs, SBEs

and DBEs may produce glucans that are sufficient in amount and appropriate in structure to crystallise into granules.

It seems unlikely that SS4 is a self-priming enzyme, as Szydlowski *et al.* (2009) were unable to find self-priming in a recombinant SS4 enzyme. The existence of a self-priming enzyme, the concentration or quantity of which would determine the number of glucan molecules initiated, cannot be ruled out. However, if SS4 does play a critical role in granule initiation, as described in the paragraph above, it is not clear how this would be compatible with the existence of a self-priming enzyme. For example, if a self-priming enzyme is responsible for the initiation of starch granules, it is difficult to explain why the absence of SS4 results in fewer granule initiations. One possibility is that a self-priming enzyme could be responsible for the initiation of very short glucan chains, rather than the starch granule itself, producing for example, maltotriose or maltotetraose. SS4 would still be required to further elongate these small malto-oligosaccharides to produce a glucan molecule, upon which the other starch synthases, starch branching and debranching enzymes can then act.

Granule initiation via heterogeneous nucleation can also not be ruled out. However, I have shown that major disruptions in plastoskeletal components do not affect granule initiation, so this structure is unlikely to be involved.

6.2 What determines how many starch granules initiate?

While SS4 is clearly essential for normal granule initiation, it exerts very little or no control over the numbers of granules that initiate in wild-type plants. The 'plastoskeletal' and plastid division components, or at least those studied here, are also not involved in controlling the number of starch granules in chloroplasts.

The successful initiation of a new granule is relatively rare, for example an average of 6.8 granules will form in the chloroplasts of wild-type mature leaves. If the idea about spontaneous initiation is correct, the numbers of granules that initiate are a simple reflection of the concentration of appropriate initiating glucans or malto-oligosaccharides in the stroma. Provided that the amount of synthetic machinery for these glucans, and background physiological-chemical factors that promote phase

separation that leads to crystallization, remain constant per volume of stroma, then the number of granules per given volume of stroma will be fixed within a statistical range. Therefore, as new chloroplasts are produced and expand, new granules will initiate. If the amount of crucial components of the synthetic machinery is altered, for example in the *ss4* mutant, then the time taken to accumulate the required concentration of glucans with an appropriate structure will increase and the probability of granule initiation will decrease.

If granules form by phase separation of glucans when a particular concentration is achieved in the stroma, followed by crystallization to form a core onto which further glucan deposition then occurs, a large number of factors will contribute to what determines the frequency with which granules initiate in the wild-type plant. These include the concentration and nature of stromal proteins and a host of other physiological-chemical factors required for phase separation and crystal stabilization, as well as glucan-synthesising machinery. Once a granule is present, it is reasonable to suppose that the starch synthesizing machinery will add new glucans to its surface rather than making more soluble glucans and initiating more granules. However, if the chloroplast volume increases, then the amount of starch synthesizing machinery may also increase. The existing granule surface area available for new glucans to be added to may then become limiting, leading to the accumulation of some soluble glucans and the initiation of new granules.

The work presented here does not address the issue of when starch granules first initiate in the leaves. As described in Chapter 3, in wild-type *Arabidopsis* (ecotype Landsberg *erecta* (L*er*)) meristematic mesophyll cells (young post-mitotic cells) contain around fifteen proplastids, destined to become chloroplasts, while fully expanded mature mesophyll cells contain around 120 chloroplasts, therefore three rounds of division must take place during cell maturation (Marrison *et al.,* 1999). The possibility remains that starch granules may all be initiated in the chloroplasts of the immature leaves or even proplastids in the meristematic mesophyll cells and then partitioned between the chloroplasts as they grow and divide. This would remove the requirement for new granules to be initiated later in leaf development. Although there is no direct evidence for this idea, it is supported by the fact that chloroplasts in mesophyll cells of immature *Arabidopsis* leaves contain on average a greater number of granules per chloroplast than

those in the mature leaves. However, if this theory of granule partitioning is correct, then the large variation in granule number per chloroplast in the mesophyll cells of mature *Arabidopsis* leaves suggests that unequal division of chloroplasts occurs. In other words during cell expansion, chloroplasts do not all grow and divide at an equal rate.

6.3 Implications in Other Species and Organs

It is reasonable to assume that the results and theories presented here, on initiation of starch granules in *Arabidopsis* leaves, may be generally applicable to transitory starch in other species. Starch granules from leaves undergoing diurnal starch turnover are flattened and disc-like and on average between 1 and 2 µm in diameter, regardless of species (Grange *et al.,* 1989a; Santacruz *et al.,* 2004; Steup *et al.,* 1983; Wildman *et al.,* 1980). The conservation in size and shape of granules in leaves suggests that the parameters controlling transitory leaf starch initiation and growth are similar regardless of species.

Less is known about the initiation of starch granules in other plant organs. As discussed in Chapter 1, storage starches show a huge variation in size (0.3 µm to over 100 µm, Lindeboom *et al.,* 2004), and shape from the smooth, oval potato starch to the irregular polygonal shaped granules of the Chinese taro (Jane *et al.,* 1994). In addition, different species and different organs have different numbers of granules per plastid. For example, maize endosperm amyloplasts contain only a single starch granule (McCullough *et al.,* 1992), while the amyloplasts in rice and oat endosperm contain multiple granules (Buttrose 1962; Hinchman and Gordon 1974).

In rice endosperm tissue, granule initiation and structure may be linked to amyloplast division. Yun and Kawagoe (2009) analysed the *arc5* mutant of rice, which, like the equivalent *Arabidopsis* mutant has a defect in plastid division. They found the altered amyloplast division had a significant effect on starch synthesis. Purified starch granules from amyloplasts were smaller and irregularly shaped compared to wild-type granules.

A future approach to understanding granule initiation in amyloplasts would be to find mutants in which there is a difference in the number or size of granules compared to

wild-type plants. A good starting point would be to examine the endosperm starch of cereal plants with mutations in genes that have previously been shown to affect starch granule initiation, for example a cereal *ss4* mutant. If SS4 plays a similar role in the initiation of storage starch and transitory starch then I would expect a reduction in the number of starch granules and an increase in granule size. No *ss4* mutant has been reported in cereals: such a mutant could be discovered in a diploid species by TILLING or transposon insertion mutagenesis (both available in rice), or generated by expression of RNAi. An alternative approach would be to screen mutant populations of diploid cereals for plants with altered granule numbers. For example discovery of a rice mutant with many fewer, larger granules in the endosperm would provide information about the proposal from Yun and Kawagoe (2010) that compound granules arise because of the existence of intra-plastidial "septa".

There is a strong argument for the genetic control of granule initiation in at least some circumstances. For example, as discussed in Chapter 1, members of the *Triticeae* grass family, which includes the cereals wheat and barley, contain two different types of starch granule in the endosperm amyloplasts. One disc shaped A-type granule (≥10µm) generally forms in the centre of the plastid, then the smaller more spherical B-type granules (≤10µm) form in the stromule regions, tubular projections that stem from the plastid and sometimes connect to other plastids (Bechtel and Wilson 2003; Bechtel *et al.,* 1990; Langeveld *et al.,* 2000; Parker 1985). The two types of granule initiate in two waves; A granules in the first 5-7 days following fertilisation and B granules 12-15 days after fertilisation (Briarty *et al.,* 1979). This tight regulation of initiation indicates a genetic and developmental control over starch granule initiation (Shewry and Morell 2001).

A recent study of the primitive wheat genus, *Aegilops,* supports a relatively simple genetic control over the initiation of B-granules. Like other members of the *Triticeae* grass family, most species of *Aegilops* have two waves of granule initiation in the endosperm. Howard *et al.,* (2010) identified accessions of three species of *Aegilops* which have no B-granules in the endosperm starch. Genetic analysis of one of these accessions led Howard *et al.,* (2010) to propose that a specific gene is responsible for the initiation of B-granules, the product of which is not required for A-granule synthesis and may be a previously uncharacterized starch biosynthetic protein. The discovery of

such a gene product is likely to provide information of great importance in understanding granule initiation in general. It is also of specific, applied value in wheat and barley breeding. As discussed in Howard *et al.,* (2010), B-granules can negatively affect both beer making from barley and flour processing from wheat, therefore identifying the gene responsible for their initiation and eliminating the protein responsible would improve both of these processes.

6.4 Broader implications

Ultimately, knowing what determines granule morphology and number would allow manipulation of these factors to produce the desired starch granule size and shape within the plant. Starch granule size is an important factor for many applications in food manufacturing (stabilisers, thickeners and emulsifiers) and industry (pharmaceuticals, paper and textile manufacturing). While desired sizes can be obtained via fractionation post harvest, this requires time and money. Therefore, if desired granule sizes could be produced within crops such as maize, wheat or potato, it would be beneficial to a large number of industries and reduce the production of waste material. For example, small starch granules can be used as a fat replacement in food or as coatings to reduce fat uptake during cooking. Large granules have applications in paper manufacturing for improving the finished appearance, strength, and printing properties.

Bibliography

Albrecht T, Koch A, Lode A, Greve B, Schneider-Mergener J, Steup M (2001) Plastidic (Pho1-type) phosphorylase isoforms in potato (*Solanum tuberosum* L.) plants: expression analysis and immunochemical characterization. Planta 213: 602-613.

Aldridge C, Maple J, Møller SG (2005) The molecular biology of plastid division in higher plants. Journal of Experimental Botany 56: 1061-1077.

Aldridge C, Møller SG (2005) The plastid division protein *At*MinD1 is a Ca^{2+}-ATPase stimulated by *At*MinE1. Journal of Biological Chemistry 280: 31673-31678.

Allaway WG, Setterfield G (1972) Ultrastructural observations on guard cells of *Vicia faba* and *Allium porrum*. Canadian Journal of Botany-Revue Canadienne de Botanique 50: 1405-1413.

Alonso MD, Lomako J, Lomako WM, Whelan WJ (1995) A new look at the biogenesis of glycogen. FASEB Journal 9: 1126-1137.

Ardila FJ, Tandecarz JS (1992) Potato tuber UDP-glucose - protein transglucosylase catalyzes its own glucosylation. Plant Physiology 99: 1342-1347.

Aronsson H, Jarvis P (2002) A simple method for isolating import-competent *Arabidopsis* chloroplasts. FEBS Letters 529: 215-220.

Artus NN, Ryberg M, Sundqvist C (1990) Plastid microtubule-like structures in wheat are insensitive to microtubule inhibitors. Physiologia Plantarum 79: 641-648.

Ashcroft RG, Preston C, Cleland RE, Critchley C (1986) Flow-cytometry of isolated chloroplasts and thylakoids. Photobiochemistry and Photobiophysics 13: 1-14.

Austin J, Webber AN (2005) Photosynthesis in *Arabidopsis thaliana* mutants with reduced chloroplast number. Photosynthesis Research 85: 373-384.

Baba T, Yoshii M, Kainuma K (1987) Acceptor molecule of granular-bound starch synthase from sweet-potato roots. Starch-Stärke 39: 52-56.

Badenhuizen NP (1963) Formation and distribution of amylose and amylopectin in the starch granule. Nature 197: 464-467.

Badenhuizen NP (1966) An electron microscopic investigation of amylolytic corrosion of starch granules in relation to fat formation. Protoplasma 62: 306-316.

Badenhuizen NP (1969) The biogenesis of starch granules in higher plants. Meredith Corporation, New York, 121 pp.

Badenhuizen NP, Dutton RW (1956) Growth of ^{14}C-labelled starch granules in potato tubers as revealed by autoradiographs. Protoplasma 47: 156-163.

Baker AA, Miles MJ, Helbert W (2001) Internal structure of the starch granule revealed by AFM. Carbohydrate Research 330: 249-256.

Ball S, Guan HP, James M, Myers A, Keeling P, Mouille G, Buleon A, Colonna P, Preiss J (1996) From glycogen to amylopectin: A model for the biogenesis of the plant starch granule. Cell 86: 349-352.

Ball SG, Morell MK (2003) From bacterial glycogen to starch: Understanding the biogenesis of the plant starch granule. Annual Review of Plant Biology 54: 207-233.

Ballicora MA, Frueauf JB, Fu YB, Schurmann P, Preiss J (2000) Activation of the potato tuber ADP-glucose pyrophosphorylase by thioredoxin. Journal of Biological Chemistry 275: 1315-1320.

Ballicora MA, Iglesias AA, Preiss J (2004) ADP-glucose pyrophosphorylase: a regulatory enzyme for plant starch synthesis. Photosynthesis Research 79: 1-24.

Balmer Y, Vensel WH, Cai N, Manieri W, Schurmann P, Hurkman WJ, Buchanan BB (2006) A complete ferredoxin/thioredoxin system regulates fundamental processes in amyloplasts. Proceedings of the National Academy of Sciences of the United States of America 103: 2988-2993.

Baroja-Fernandez E, Munoz FJ, Zandueta-Criado A, Moran-Zorzano MT, Viale AM, Alonso-Casajus N, Pozueta-Romero J (2004) Most of ADP-glucose linked to starch biosynthesis occurs outside the chloroplast in source leaves. Proceedings of the National Academy of Sciences of the United States of America 101: 13080-13085.

Barratt DHP, Derbyshire P, Findlay K, Pike M, Wellner N, Lunn J, Feil R, Simpson C, Maule AJ, Smith AM (2009) Normal growth of *Arabidopsis* requires cytosolic invertase but not sucrose synthase. Proceedings of the National Academy of Sciences of the United States of America 106: 13124-13129.

Batz O, Scheibe R, Neuhaus HE (1995) Purification of chloroplasts from fruits of green pepper (*Capsicum annuum* L.) and characterization of starch synthesis - Evidence for a functional chloroplastic hexose-phosphate translocator. Planta 196: 50-57.

Baunsgaard L, Lutken H, Mikkelsen R, Glaring MA, Pham TT, Blennow A (2005) A novel isoform of glucan, water dikinase phosphorylates pre-phosphorylated α-glucans and is involved in starch degradation in *Arabidopsis*. Plant Journal 41: 595-605.

Bechtel DB, Wilson JD (2003) Amyloplast formation and starch granule development in hard red winter wheat. Cereal Chemistry 80: 175-183.

Bechtel DB, Zayas I, Kaleikau L, Pomeranz Y (1990) Size distribution of wheat starch granules during endosperm development. Cereal Chemistry 67: 59-63.

Beckles DM, Smith AM, ap Rees T (2001) A cytosolic ADP-glucose pyrophosphorylase is a feature of graminaceous endosperms, but not of other starch-storing organs. Plant Physiology 125: 818-827.

Bergounioux C, Brown SC, Petit PX (1992) Flow-cytometry and plant protoplast cell biology. Physiologia Plantarum 85: 374-386.

Bernier G, Havelange A, Houssa C, Petitjean A, Lejeune P (1993) Physiological signals that induce flowering. Plant Cell 5: 1147-1155.

Bhattacharyya MK, Smith A, Ellis THN, Hedley CL, Martin C (1990) The wrinkled-seed character of pea described by Mendel is caused by a transposon-like insertion in a gene encoding starch-branching enzyme. Cell 60: 115-122.

Blancaflor EB, Fasano JM, Gilroy S (1998) Mapping the functional roles of cap cells in the response of *Arabidopsis* primary roots to gravity. Plant Physiology 116: 213-222.

Blauth SL, Kim KN, Klucinec J, Shannon JC, Thompson D, Guiltinan M (2002) Identification of mutator insertional mutants of starch-branching enzyme 1 (*sbe1*) in *Zea mays* L. Plant Molecular Biology 48: 287-297.

Blauth SL, Yao Y, Klucinec JD, Shannon JC, Thompson DB, Guilitinan MJ (2001) Identification of mutator insertional mutants of starch-branching enzyme 2a in corn. Plant Physiology 125: 1396-1405.

Borem A, Mather DE, Rasmusson DC, Fulcher RG, Hayes PM (1999) Mapping quantitative trait loci for starch granule traits in barley. Journal of Cereal Science 29: 153-160.

Borovsky D, Smith EE, Whelan WJ (1975) Purification and properties of potato 1,4-α-D-glucan - 1,4-α-D-glucan 6-α-(1,4-α-glucano)- transferase - evidence against a dual catalytic function in amylose-branching enzyme. European Journal of Biochemistry 59: 615-625.

Bouchet B, Rey L, Gallant DJ, Buvat R (1984) Use of colloidal gold labelled concanavalin A as a marker for the starch granule. Comptes Rendus de L'Academie des Sciences (Série III Science de la Vie) 299: 813-818.

Boyer CD, Daniels RR, Shannon JC (1976) Abnormal starch granule formation in *Zea mays* L. endosperms possessing the *amylose-extender* mutant. Crop Science 16: 298-301.

Boyes DC, Zayed AM, Ascenzi R, McCaskill AJ, Hoffman NE, Davis KR, Gorlach J (2001) Growth stage-based phenotypic analysis of *Arabidopsis*: A model for high throughput functional genomics in plants. Plant Cell 13: 1499-1510.

Brandao I, Salema R (1974) Microtubules in chloroplasts of higher plant (*Sedum sp*.). Journal of Submicroscopic Cytology and Pathology 6: 381-390.

Briarty LG, Hughes CE, Evers AD (1979) Developing endosperm of wheat - a stereological analysis. Annals of Botany 44: 641-658.

Brouquisse R, Gaudillere JP, Raymond P (1998) Induction of a carbon-starvation-related proteolysis in whole maize plants submitted to light/dark cycles and to extended darkness. Plant Physiology 117: 1281-1291.

Buléon A, Colonna P, Planchot V, Ball S (1998) Starch granules: structure and biosynthesis. International Journal of Biological Macromolecules 23: 85-112.

Buléon A, Gallant DJ, Bouchet B, Mouille G, D'Hulst C, Kossmann J, Ball S (1997) Starches from A to C. Plant Physiology 115: 949-957.

Burton RA, Bewley JD, Smith AM, Bhattacharyya MK, Tatge H, Ring S, Bull V, Hamilton WDO, Martin C (1995) Starch branching enzymes belonging to distinct enzyme families are differentially expressed during pea embryo development. Plant Journal 7: 3-15.

Burton RA, Jenner H, Carrangis L, Fahy B, Fincher GB, Hylton C, Laurie DA, Parker M, Waite D, van Wegen S, Verhoeven T, Denyer K (2002) Starch granule initiation and growth are altered in barley mutants that lack isoamylase activity. Plant Journal 31: 97-112.

Busi MV, Palopoli N, Valdez HA, Fornasari MS, Wayllace NZ, Gomez-Casati DF, Parisi G, Ugalde RA (2008) Functional and structural characterization of the catalytic domain of the starch synthase III from *Arabidopsis thaliana*. Proteins-Structure Function and Bioinformatics 70: 31-40.

Bustos R, Fahy B, Hylton CM, Seale R, Nebane NM, Edwards A, Martin C, Smith AM (2004) Starch granule initiation is controlled by a heteromultimeric isoamylase in potato tubers. Proceedings of the National Academy of Sciences of the United States of America 101: 2215-2220.

Butterfass T (1979) Patterns of chloroplast reproduction. Springer-Verlag, Berlin and New York. Volume 6. 205 pp.

Buttrose MS (1962) Formation of rice starch granules. Naturwissenschaften 49: 307-308.

Carmi A, Shomer I (1979) Starch accumulation and photosynthetic activity in primary leaves of bean (*Phaseolus vulgaris* L.). Annals of Botany 44: 479-484.

Caspar T, Huber SC, Somerville C (1985) Alterations in growth, photosynthesis, and respiration in a starchless mutant of *Arabidopsis thaliana* (L.) deficient in chloroplast phosphoglucomutase activity. Plant Physiology 79: 11-17.

Caspar T, Lin TP, Kakefuda G, Benbow L, Preiss J, Somerville C (1991) Mutants of *Arabidopsis* with altered regulation of starch degradation. Plant Physiology 95: 1181-1188.

Caspar T, Pickard BG (1989) Gravitropism in a starchless mutant of *Arabidopsis* - Implications for the starch-statolith theory of gravity sensing. Planta 177: 185-197.

Cavalier-Smith T (1999) Zooflagellate phylogeny and the systematics of Protozoa. Biological Bulletin 196: 393-395.

Chaly N, Possingham JV, Thomson WW (1980) Chloroplast division in spinach leaves examined by scanning electron microscopy and freeze etching. Journal of Cell Science 46: 87-96.

Chatterjee M, Berbezy P, Vyas D, Coates S, Barsby T (2005) Reduced expression of a protein homologous to glycogenin leads to reduction of starch content in *Arabidopsis* leaves. Plant Science 168: 501-509.

Cheetham ME, Caplan AJ (1998) Structure, function and evolution of DnaJ: conservation and adaptation of chaperone function. Cell Stress and Chaperones 3: 28-36.

Cheng C, Mu J, Farkas I, Huang DQ, Goebl MG, Roach PJ (1995) Requirement of the self-glucosylating initiator proteins Glg1p and Glg2p for glycogen accumulation in *Saccharomyces cerevisiae*. Molecular and Cellular Biology 15: 6632-6640.

Chia T, Thorneycroft D, Chapple A, Messerli G, Chen J, Zeeman SC, Smith SM, Smith AM (2004) A cytosolic glucosyltransferase is required for conversion of starch to sucrose in *Arabidopsis* leaves at night. Plant Journal 37: 853-863.

Christiansen C, Abou Hachem M, Glaring MA, Vikso-Nielsen A, Sigurskjold BW, Svensson B, Blennow A (2009) A CBM20 low-affinity starch-binding domain from glucan, water dikinase. FEBS Letters 583: 1159-1163.

Clough SJ, Bent AF (1998) Floral dip: A simplified method for *Agrobacterium*-mediated transformation of *Arabidopsis thaliana*. Plant Journal 16: 735-743.

Colleoni C, Dauvillée D, Mouille G, Buléon A, Gallant DJ, Bouchet B, Morell M, Samuel MS, Delrue B, D'Hulst C, Bliard C, Nuzillard JM, Ball S (1999a) Genetic and biochemical evidence for the involvement of α-1,4 glucanotransferases in amylopectin synthesis. Plant Physiology 120: 993-1003.

Colleoni C, Dauvillée D, Mouille G, Morell M, Samuel M, Slomianny MC, Lienard L, Wattebled F, D'Hulst C, Ball S (1999b) Biochemical characterisation of the *Chlamydomonas reinhardtii* α-1,4 glucanotransferase supports a direct function in amylopectin biosynthesis. Plant Physiology 120: 1005-1014.

Colletti KS, Tattersall EA, Pyke KA, Froehlich JE, Stokes KD, Osteryoung KW (2000) A homologue of the bacterial cell division site-determining factor MinD mediates placement of the chloroplast division apparatus. Current Biology 10: 507-516.

Commuri PD, Jones RJ (2001) High temperatures during endosperm cell division in maize: A genotypic comparison under in vitro and field conditions. Crop Science 41: 1122-1130.

Commuri PD, Keeling PL (2001) Chain-length specificities of maize starch synthase I enzyme: studies of glucan affinity and catalytic properties. Plant Journal 25: 475-486.

Comparot-Moss S, Kötting O, Stettler M, Edner C, Graf A, Weise SE, Streb S, Lue WL, MacLean D, Mahlow S, Ritte G, Steup M, Chen J, Zeeman SC, Smith AM (2010) A putative phosphatase, LSF1, is required for normal starch turnover in *Arabidopsis* leaves. Plant Physiology 152: 685-697.

Coppin A, Varré JS, Lienard L, Dauvillée D, Guérardel Y, Soyer-Gobillard MO, Buléon A, Ball S, Tomavo S (2005) Evolution of plant like crystalline storage polysaccharide in the protozoan parasite *Toxoplasma gondii* argues for a red alga ancestry. Journal of Molecular Evolution 60: 257-267.

Corbesier L, Lejeune P, Bernier G (1998) The role of carbohydrates in the induction of flowering in *Arabidopsis thaliana*: comparison between the wild type and a starchless mutant. Planta 206: 131-137.

Craft J, Samalova M, Baroux C, Townley H, Martinez A, Jepson I, Tsiantis M, Moore I (2005) New pOp/LhG4 vectors for stringent glucocorticoid-dependent transgene expression in *Arabidopsis*. Plant Journal 41: 899-918.

Craig J, Lloyd JR, Tomlinson K, Barber L, Edwards A, Wang TL, Martin C, Hedley CL, Smith AM (1998) Mutations in the gene encoding starch synthase II profoundly alter amylopectin structure in pea embryos. Plant Cell 10: 413-426.

Critchley JH, Zeeman SC, Takaha T, Smith AM, Smith SM (2001) A critical role for disproportionating enzyme in starch breakdown is revealed by knock-out mutation in *Arabidopsis*. Plant Journal 26: 89-100.

D'Hulst C, Merida A (2010) The priming of storage glucan synthesis from bacteria to plants: current knowledge and new developments. New Phytologist 188: 13-21.

Damager I, Engelsen SB, Blennow A, Møller BL, Motawia MS (2010) First principles insight into the α-glucan structures of starch: their synthesis, conformation, and hydration. Chemical Reviews 110: 2049-2080.

Dauvillee D, Chochois V, Steup M, Haebel S, Eckermann N, Ritte G, Ral JP, Colleoni C, Hicks G, Wattebled F, Deschamps P, D'Hulst C, Lienard L, Cournac L, Putaux JL, Dupeyre D, Ball SG (2006) Plastidial phosphorylase is required for normal starch synthesis in *Chlamydomonas reinhardtii*. Plant Journal 48: 274-285.

Dauvillée D, Colleoni C, Mouille G, Buléon A, Gallant DJ, Bouchet B, Morell MK, D'Hulst C, Myers AM, Ball SG (2001) Two loci control phytoglycogen production in the monocellular green alga *Chlamydomonas reinhardtii*. Plant Physiology 125: 1710-1722.

de Pater S, Caspers M, Kottenhagen M, Meima H, ter Stege R, de Vetten N (2006) Manipulation of starch granule size distribution in potato tubers by modulation of plastid division. Plant Biotechnology Journal 4: 123-134.

Decker K, Peist R, Reidl J, Kossmann M, Brand B, Boos W (1993) Maltose and maltotriose can be formed endogenously in *Escherichia coli* from glucose and glucose-1-phosphate independently of enzymes of the maltose system. Journal of Bacteriology 175: 5655-5665.

Delatte T, Trevisan M, Parker ML, Zeeman SC (2005) *Arabidopsis* mutants *Atisa1* and *Atisa2* have identical phenotypes and lack the same multimeric isoamylase, which influences the branch point distribution of amylopectin during starch synthesis. Plant Journal 41: 815-830.

Delatte T, Umhang M, Trevisan M, Eicke S, Thorneycroft D, Smith SM, Zeeman SC (2006) Evidence for distinct mechanisms of starch granule breakdown in plants. Journal of Biological Chemistry 281: 12050-12059.

Delgado IJ, Wang ZH, de Rocher A, Keegstra K, Raikhel NV (1998) Cloning and characterization of AtRGP1 - A reversibly autoglycosylated *Arabidopsis* protein implicated in cell wall biosynthesis. Plant Physiology 116: 1339-1349.

Delrue B, Fontaine T, Routier F, Decq A, Wieruszeski J-M, Van den Koornhuyse N, Maddelein M-L, Fournet B, Ball S (1992) Waxy *Chlamydomonas reinhardtii*:

Monocellular algal mutants defective in amylose biosynthesis and granule-bound starch synthase activity accumulate a structurally modified amylopectin. Journal of Bacteriology 174: 3612-3620.

Delvallé D, Dumez S, Wattebled F, Roldan I, Planchot V, Berbezy P, Colonna P, Vyas D, Chatterjee M, Ball S, Merida A, D'Hulst C (2005) Soluble starch synthase I: A major determinant for the synthesis of amylopectin in *Arabidopsis thaliana* leaves. Plant Journal 43: 398-412.

Dengate HN, Baruch DW, Meredith P (1978) The density of wheat starch granules: A tracer dilution procedure for determining the density of an immiscible dispersed phase. Starch-Stärke 30: 80-84.

Denyer K, Barber LM, Burton R, Hedley CL, Hylton CM, Johnson S, Jones DA, Marshall J, Smith AM, Tatge H, Tomlinson K, Wang TL (1995) The isolation and characterization of novel low-amylose mutants of *Pisum sativum* L. Plant Cell and Environment 18: 1019-1026.

Denyer K, Clarke B, Hylton C, Tatge H, Smith AM (1996a) The elongation of amylose and amylopectin chains in isolated starch granules. Plant Journal 10: 1135-1143.

Denyer K, Dunlap F, Thorbjornsen T, Keeling P, Smith AM (1996b) The major form of ADP-glucose pyrophosphorylase in maize endosperm is extra-plastidial. Plant Physiology 112: 779-785.

Denyer K, Sidebottom C, Hylton CM, Smith AM (1993) Soluble isoforms of starch synthase and starch-branching enzyme also occur within starch granules in developing pea embryos. Plant Journal 4: 191-198.

Denyer K, Smith AM (1992) The purification and characterization of the two forms of soluble starch synthase from developing pea embryos. Planta 186: 609-617.

Denyer K, Waite D, Motawia S, Møller BL, Smith AM (1999) Granule-bound starch synthase I in isolated starch granules elongates malto-oligosaccharides processively. Biochemical Journal 340: 183-191.

Deschamps P, Haferkamp I, Dauvillée D, Haebel S, Steup M, Buléon A, Putaux JL, Colleoni C, D'Hulst C, Plancke C, Gould S, Maier U, Neuhaus HE, Ball S (2006) Nature of the periplastidial pathway of starch synthesis in the cryptophyte *Guillardia theta*. Eukaryotic Cell 5: 954-963.

Deschamps P, Moreau H, Worden AZ, Dauvillee D, Ball SG (2008) Early gene duplication within chloroplastida and its correspondence with relocation of starch metabolism to chloroplasts. Genetics 178: 2373-2387.

Dhugga KS, Tiwari SC, Ray PM (1997) A reversibly glycosylated polypeptide (RGP1) possibly involved in plant cell wall synthesis: Purification, gene cloning, and trans-Golgi localization. Proceedings of the National Academy of Sciences of the United States of America 94: 7679-7684.

Dian WM, Jiang HW, Wu P (2005) Evolution and expression analysis of starch synthase III and IV in rice. Journal of Experimental Botany 56: 623-632.

Dinges JR, Colleoni C, James MG, Myers AM (2003) Mutational analysis of the pullulanase-type debranching enzyme of maize indicates multiple functions in starch metabolism. Plant Cell 15: 666-680.

Dinges JR, Colleoni C, Myers AM, James MG (2001) Molecular structure of three mutations at the maize *sugary1* locus and their allele-specific phenotypic effects. Plant Physiology 125: 1406-1418.

Dodd JL, McCracken DA (1972) Starch in fungi - Its molecular structure in three genera and an hypothesis concerning its physiological role. Mycologia 64: 1341-1343.

Dodge JD, Lee JJ (2000) Phylum Dinoflagellata. In: Lee JJ, Leedale GF, Bradbury P eds) The illustrated guide to the protozoa. Wiley-Blackwell, Lawrence, Kansas, USA, pp 656-689.

Doi K (1965) Formation of amylopectin granules in gelatin gel as a model of starch precipitation in plant plastids. Biochimica et Biophysica Acta 94: 557-565.

Donald AM (2001) Plasticization and self assembly in the starch granule. Cereal Chemistry 78: 307-314.

Dorion S, Parveen, Jeukens J, Matton DP, Rivoal J (2005) Cloning and characterization of a cytosolic isoform of triosephosphate isomerase developmentally regulated in potato leaves. Plant Science 168: 183-194.

Dumez S, Wattebled F, Dauvillée D, Delvallé D, Planchot R, Ball SG, D'Hulst C (2006) Mutants of *Arabidopsis* lacking starch branching enzyme II substitute starch synthesis by cytoplasmic maltose accumulation. Plant Cell 18: 2694-2709.

Edner C, Li J, Albrecht T, Mahlow S, Hejazi M, Hussain H, Kaplan F, Guy C, Smith SM, Steup M, Ritte G (2007) Glucan, water dikinase activity stimulates breakdown of starch granules by plastidial β-amylases. Plant Physiology 145: 17-28.

Edwards A, Fulton DC, Hylton C, Jobling S, Gibley M, Rössner U, Martin C, Smith A (1999) A combined reduction in activity of starch synthases II and III of potato has novel effects on the starch of tubers. Plant Journal 17: 251-261.

Edwards A, Marshall J, Denyer K, Sidebottom C, Visser RGF, Martin C, Smith AM (1996) Evidence that a 77-kilodalton protein from the starch of pea embryos is an isoform of starch synthase that is both soluble and granule bound. Plant Physiology 112: 89-97.

Edwards A, Marshall J, Sidebottom C, Visser RGF, Smith AM, Martin C (1995) Biochemical and molecular characterization of a novel starch synthase from potato tubers. Plant Journal 8: 283-294.

Edwards A, Vincken JP, Suurs L, Visser RGF, Zeeman S, Smith A, Martin C (2002) Discrete forms of amylose are synthesized by isoforms of GBSSl in pea. Plant Cell 14: 1767-1785.

Eichelmann H, Laisk A (1994) CO_2 uptake and electron-transport rates in wild-type and a starchless mutant of *Nicotiana sylvestris* - The role and regulation of starch synthesis at saturating CO_2 concentrations. Plant Physiology 106: 679-687.

El-Kafafi ES, Karamoko M, Pignot-Paintrand I, Grunwald D, Mandaron P, Lerbs-Mache S, Falconet D (2008) Developmentally regulated association of plastid division protein FtsZ1 with thylakoid membranes in *Arabidopsis thaliana*. Biochemical Journal 409: 87-94.

Ellis RJ, Macdonald IR (1970) Specificity of cycloheximide in higher plant systems. Plant Physiology 46: 227-232.

Fettke J, Albrecht T, Hejazi M, Mahlow S, Nakamura Y, Steup M (2010) Glucose 1-phosphate is efficiently taken up by potato (*Solanum tuberosum*) tuber parenchyma cells and converted to reserve starch granules. New Phytologist 185: 663-675.

Fettke J, Chia T, Eckermann N, Smith A, Steup M (2006) A transglucosidase necessary for starch degradation and maltose metabolism in leaves at night acts on cytosolic heteroglycans (SHG). Plant Journal 46: 668-684.

Fitting C, Doudoroff M (1952) Phosphorolysis of maltose by enzyme preparations from *Neisseria meningitidis*. Journal of Biological Chemistry 199: 153-163.

Fitzpatrick LM, Keegstra K (2001) A method for isolating a high yield of *Arabidopsis* chloroplasts capable of efficient import of precursor proteins. Plant Journal 27: 59-65.

Flipse E, Keetels C, Jacobsen E, Visser RGF (1996) The dosage effect of the wildtype GBSS allele is linear for GBSS activity but not for amylose content: Absence of amylose has a distinct influence on the physico-chemical properties of starch. Theoretical and Applied Genetics 92: 121-127.

French D (1984) Organisation of starch granules. In: Whistler RL, BeMiller JN, Paschall JF eds) Starch, Chemistry and Technology. Academic Press, Orlando, FL, pp 183-247.

Fujita N, Yoshida M, Kondo T, Saito K, Utsumi Y, Tokunaga T, Nishi A, Satoh H, Park JH, Jane JL, Miyao A, Hirochika H, Nakamura Y (2007) Characterization of SSIIIa-deficient mutants of rice: The function of SSIIIa and pleiotropic effects by SSIIIa deficiency in the rice endosperm. Plant Physiology 144: 2009-2023.

Fujiwara M, Yoshida S (2001) Chloroplast targeting of chloroplast division FtsZ2 proteins in *Arabidopsis*. Biochemical and Biophysical Research Communications 287: 462-467.

Fujiwara MT, Hashimoto H, Kazama Y, Abe T, Yoshida S, Sato N, Itoh RD (2008) The assembly of the FtsZ ring at the mid-chloroplast division site depends on a balance between the activities of *At*MinE1 and ARC11/*At*MinD1. Plant and Cell Physiology 49: 345-361.

Fujiwara MT, Li DL, Kazama Y, Abe T, Uno T, Yamagata H, Kanamaru K, Itoh RD (2009) Further evaluation of the localization and functionality of hemagglutinin epitope- and fluorescent protein-tagged *At*minD1 in *Arabidopsis thaliana*. Bioscience Biotechnology and Biochemistry 73: 1693-1697.

Fujiwara MT, Nakamura A, Itoh RD, Shimada Y, Yoshida S, Møller SG (2004) Chloroplast division site placement requires dimerisation of the ARC11/*At*MinD1 protein in *Arabidopsis*. Journal of Cell Science 117: 2399-2410.

Fulton DC, Edwards A, Pilling E, Robinson HL, Fahy B, Seale R, Kato L, Donald AM, Geigenberger P, Martin C, Smith AM (2002) Role of granule-bound starch synthase in determination of amylopectin structure and starch granule morphology in potato. Journal of Biological Chemistry 277: 10834-10841.

Fulton DC, Stettler M, Mettler T, Vaughan CK, Li J, Francisco P, Gil D, Reinhold H, Eicke S, Messerli G, Dorken G, Halliday K, Smith AM, Smith SM, Zeeman SC (2008) β-AMYLASE4, a noncatalytic protein required for starch breakdown, acts upstream of three active β-amylases in *Arabidopsis* chloroplasts. Plant Cell 20: 1040-1058.

Gallant DJ, Bouchet B, Baldwin PM (1997) Microscopy of starch: evidence of a new level of granule organisation. Carbohydrate Polymers 32: 177-191.

Gallant DJ, Bouchet B, Buléon A, Perez S (1992) Physical characteristics of starch granules and susceptibility to enzymatic degradation. European Journal of Clinical Nutrition 46: S3-S16.

Gambardella R, Alfano F (1991) Plastid tubules in the sporogenous lineage of the moss *Timmiella barbuloides* (Bryophyta) - An ultrastructural study. Annals of Botany 67: 555-559.

Gao H, Kadirjan-Kalbach D, Froehlich JE, Osteryoung KW (2003) ARC5, a cytosolic dynamin-like protein from plants, is part of the chloroplast division machinery. Proceedings of the National Academy of Sciences of the United States of America 100: 4328-4333.

Geddes R, Greenwood CT (1969) Observations on the biosynthesis of the starch granule. Starch-Stärke 6: 148-153.

Geiger DR, Batey JW (1967) Translocation of ^{14}C sucrose in sugar beet during darkness. Plant Physiology 42: 1743-1749.

Geiger DR, Servaites JC, Fuchs MA (2000) Role of starch in carbon translocation and partitioning at the plant level. Australian Journal of Plant Physiology 27: 571-582.

Gentry MS, Dowen RH, Worby CA, Mattoo S, Ecker JR, Dixon JE (2007) The phosphatase laforin crosses evolutionary boundaries and links carbohydrate metabolism to neuronal disease. Journal of Cell Biology 178: 477-488.

Gibon Y, Blaesing OE, Palacios-Rojas N, Pankovic D, Hendriks JHM, Fisahn J, Hohne M, Gunther M, Stitt M (2004) Adjustment of diurnal starch turnover to short days: depletion of sugar during the night leads to a temporary inhibition of carbohydrate utilization, accumulation of sugars and post-translational activation of ADP-glucose pyrophosphorylase in the following light period. Plant Journal 39: 847-862.

Gibon Y, Pyl ET, Sulpice R, Lunn JE, Hohne M, Gunther M, Stitt M (2009) Adjustment of growth, starch turnover, protein content and central metabolism to a decrease of the carbon supply when *Arabidopsis* is grown in very short photoperiods. Plant Cell and Environment 32: 859-874.

Gibon Y, Usadel B, Blaesing OE, Kamlage B, Hoehne M, Trethewey R, Stitt M (2006) Integration of metabolite with transcript and enzyme activity profiling during diurnal cycles in *Arabidopsis* rosettes. Genome Biology 7: R76.1-R76.23.

Glynn JM, Froehlich JE, Osteryoung KW (2008) *Arabidopsis* ARC6 coordinates the division machineries of the inner and outer chloroplast membranes through interaction with PDV2 in the intermembrane space. Plant Cell 20: 2460-2470.

Glynn JM, Miyagishima S-Y, Yoder DW, Osteryoung KW, Vitha S (2007) Chloroplast division. Traffic 8: 451-461.

Glynn JM, Yang Y, Vitha S, Schmitz AJ, Hemmes M, Miyagishima SY, Osteryoung KW (2009) PARC6, a novel chloroplast division factor, influences FtsZ assembly and is required for recruitment of PDV1 during chloroplast division in *Arabidopsis*. Plant Journal 59: 700-711.

Gould SB, Waller RF, McFadden GI (2008) Plastid evolution. Annual Review of Plant Biology 59: 491-517.

Graf A (2009) The regulation of starch degradation in *Arabidopsis thaliana* leaves at night. PhD thesis. University of East Anglia, Norwich, UK.

Graf A, Schlereth A, Stitt M, Smith AM (2010) Circadian control of carbohydrate availability for growth in *Arabidopsis* plants at night. Proceedings of the National Academy of Sciences of the United States of America 107: 9458-9463.

Grange RI, Hammond JBW, Andrews J (1989a) Characteristics of starch grains isolated form mature pepper leaves grown under different irradiances and daylengths. Journal of Experimental Botany 40: 1045-1052.

Grange RI, Hammond JBW, Andrews J (1989b) Characteristics of starch grains isolated from mature pepper leaves grown under different irradiances and daylengths. Journal of Experimental Botany 40: 1045-1052.

Graumann PL (2007) Cytoskeletal elements in bacteria. Annual Review of Microbiology 61: 589-618.

Gray MW (1999) Evolution of organellar genomes. Current Opinion in Genetics and Development 9: 678-687.

Gremillon L, Kiessling J, Hause B, Decker EL, Reski R, Sarnighausen E (2007) Filamentous temperature-sensitive Z (FtsZ) isoforms specifically interact in the chloroplasts and in the cytosol of *Physcomitrella patens*. New Phytologist 176: 299-310.

Guan HP, Kuriki T, Sivak M, Preiss J (1995) Maize branching enzyme catalyzes synthesis of glycogen-like polysaccharide in *glgB*-deficient *Escherichia coli* Proceedings of the National Academy of Sciences of the United States of America 92: 964-967.

Guan HP, Preiss J (1993) Differentiation of the properties of the branching isozymes from maize (*Zea Mays*). Plant Physiology 102: 1269-1273.

Guérardel Y, Leleu D, Coppin A, Lienard L, Slomianny MC, Strecker G, Ball S, Tomavo S (2005) Amylopectin biogenesis and characterisation in the protozoan parasite *Toxoplasma gondii,* the intracellular development of which is restricted in the HepG2 cell line. Microbes and Infection 7: 41-48.

Haapala H (1968) Accumulation and disintegration of starch in the chloroplasts of *Stellaria media* grown under constant illumination. Physiologia Plantarum 21: 868-871.

Haapala H (1969) Photosynthesis and starch metabolism of chloroplasts during prolonged illumination. Planta 86: 259-266.

Hamilton AJ, Baulcombe DC (1999) A species of small antisense RNA in posttranscriptional gene silencing in plants. Science 286: 950-952.

Hanashiro I, Tagawa M, Shibahara S, Iwata K, Takeda Y (2002) Examination of molar-based distribution of A, B and C chains of amylopectin by fluorescent labeling with 2-aminopyridine. Carbohydrate Research 337: 1211-1215.

Hansen PI, Spraul M, Dvortsak P, Larsen FH, Blennow A, Motawia MS, Engelsen SB (2009) Starch phosphorylation - Maltosidic restrains upon 3 '- and 6 '-phosphorylation investigated by chemical synthesis, molecular dynamics and NMR spectroscopy. Biopolymers 91: 179-193.

Hargreaves JA, ap Rees T (1988) Turnover of starch and sucrose in roots of *Pisum sativum*. Phytochemistry 27: 1627-1629.

Harmer SL, Hogenesch LB, Straume M, Chang HS, Han B, Zhu T, Wang X, Kreps JA, Kay SA (2000) Orchestrated transcription of key pathways in *Arabidopsis* by the circadian clock. Science 290: 2110-2113.

Harrison CJ, Hedley CL, Wang TL (1998) Evidence that the *rug3* locus of pea (*Pisum sativum* L.) encodes plastidial phosphoglucomutase confirms that the imported substrate for starch synthesis in pea amyloplasts is glucose-6-phosphate. Plant Journal 13: 753-762.

Hartley JL, Temple GF, Brasch MA (2000) DNA cloning using in vitro site-specific recombination. Genome Research 10: 1788-1795.

Hashimoto H (1986) Double ring structure around the constricting neck of dividing plastids of *Avena sativa*. Protoplasma 135: 166-172.

Haswell ES, Meyerowitz EM (2006) MscS-like proteins control plastid size and shape in *Arabidopsis thaliana*. Current Biology 16: 1-11.

Haughn GW, Somerville C (1986) Sulfonylurea-resistant mutants of *Arabidopsis thaliana*. Molecular and General Genetics 204: 430-434.

Heitz E (1922) Untersuchungen uber die Teilung der Chloroplasten nebst Beobachtungen uber Zellgrosse und Chromatophorengrosse. PhD thesis; Heidelberg University, Germany.

Hejazi M, Fettke J, Haebel S, Edner C, Paris O, Frohberg C, Steup M, Ritte G (2008) Glucan, water dikinase phosphorylates crystalline maltodextrins and thereby initiates solubilization. Plant Journal 55: 323-334.

Hejazi M, Fettke J, Kötting O, Zeeman SC, Steup M (2010) The laforin-like dual-specificity phosphatase SEX4 from *Arabidopsis* hydrolyzes both C6-and C3-phosphate

esters introduced by starch-related dikinases and thereby affects phase transition of α-glucans. Plant Physiology 152: 711-722.

Helbert W, Chanzy H, Planchot V, Buleon A, Colonna P (1993) Morphological and structural features of amylose spherocrystals of A-Type. International Journal of Biological Macromolecules 15: 183-187.

Hendriks JHM, Kolbe A, Gibon Y, Stitt M, Geigenberger P (2003) ADP-glucose pyrophosphorylase is activated by posttranslational redox-modification in response to light and to sugars in leaves of *Arabidopsis* and other plant species. Plant Physiology 133: 838-849.

Hennen-Bierwagen TA, Lin Q, Grimaud F, Planchot V, Keeling PL, James MG, Myers AM (2009) Proteins from multiple metabolic pathways associate with starch biosynthetic enzymes in high molecular weight complexes: A model for regulation of carbon allocation in maize amyloplasts. Plant Physiology 149: 1541-1559.

Hennen-Bierwagen TA, Liu F, Marsh RS, Kim S, Gan Q, Tetlow IJ, Emes MJ, James MG, Myers AM (2008) Starch biosynthetic enzymes from developing maize endosperm associate in multisubunit complexes. Plant Physiology 146: 1892-1908.

Hennessy F, Cheetham ME, Dirr HW, Blatch GL (2000) Analysis of the levels of conservation of the J domain among the various types of DnaJ-like proteins. Cell Stress and Chaperones 5: 347-358.

Herold A, Leegood RC, McNeil PH, Robinson SP (1981) Accumulation of maltose during photosynthesis in protoplasts isolated from spinach leaves treated with mannose. Plant Physiology 67: 85-88.

Hicks GR, Hironaka CM, Dauvillée D, Funke RP, D'Hulst C, Waffenschmidt S, Ball SG (2001) When simpler is better. Unicellular green algae for discovering new genes and functions in carbohydrate metabolism. Plant Physiology 127: 1334-1338.

Hill LM, Smith AM (1991) Evidence that glucose-6-phosphate is imported as the substrate for starch synthesis by the plastids of developing pea embryos. Planta 185: 91-96.

Hinchman RR, Gordon SA (1974) Amyloplast size and number in gravity-compensated oat seedlings. Plant Physiology 53: 398-401.

Hizukuri S (1986) Polymodal distribution of the chain lengths of amylopectin, and its significance. Carbohydrate Research 147: 342-347.

Hoffman LR (1967) Observations on fine structure of *Oedogonium*. III. Microtubular elements in chloroplasts of *O. cardiacum*. Journal of Phycology 3: 212-221.

Hovenkamp-Hermelink JHM, Jacobsen E, Ponstein AS, Visser RGF, Vos-Scheperkeuter GH, Bijmolt EW, de Vries JN, Witholt B, Feenstra WJ (1987) Isolation of an amylose-free starch mutant of the potato (*Solanum tuberosum* L.). Theoretical and Applied Genetics 75: 217-221.

Howard T, Rejab NA, Griffiths S, Leigh F, Simmonds J, Uauy C, Leverington-Waite M, Trafford K (2010) Identification of a major QTL controlling the content of B-type starch granules in *Aegilops*. Soon to be published.

Howitt CA, Rahman S, Morell MK (2006) Expression of bacterial starch-binding domains in *Arabidopsis* increases starch granule size. Functional Plant Biology 33: 257-266.

Hu Y, Chen ZW, Liu WZ, Liu XL, He YK (2008) Chloroplast division is regulated by the circadian expression of *FTSZ* and *MIN* genes in *Chlamydomonas reinhardtii*. European Journal of Phycology 43: 207-215.

Huber SC, Huber JL (1996) Role and regulation of sucrose-phosphate synthase in higher plants. Annual Review of Plant Physiology and Plant Molecular Biology 47: 431-444.

Hussain H, Mant A, Seale R, Zeeman S, Hinchliffe E, Edwards A, Hylton C, Bornemann S, Smith AM, Martin C, Bustos R (2003) Three isoforms of isoamylase contribute different catalytic properties for the debranching of potato glucans. Plant Cell 15: 133-149.

Imaizumi T (2010) *Arabidopsis* circadian clock and photoperiodism: time to think about location. Current Opinion in Plant Biology 13: 83-89.

Ishizaki Y, Taniguchi H, Maruyama Y, Nakamura M (1983) Debranching enzymes of potato tubers (*Solanum tuberosum* L.). 1. Purification and some properties of potato isoamylase. Agricultural and Biological Chemistry 47: 771-779.

Itoh R, Fujiwara M, Nagata N, Yoshida S (2001) A chloroplast protein homologous to the eubacterial topological specificity factor MinE plays a role in chloroplast division. Plant Physiology 127: 1644-1655.

Izumo A, Fujiwara S, Oyama Y, Satoh A, Fujita N, Nakamura Y, Tsuzuki M (2007) Physicochemical properties of starch in *Chlorella* change depending on the CO_2 concentration during growth: Comparison of structure and properties of pyrenoid and stroma starch. Plant Science 172: 1138-1147.

James MG, Robertson DS, Myers AM (1995) Characterisation of the maize gene *sugary1*, a determinant of starch composition in kernels. Plant Cell 7: 417-429.

Jane J, Kasemsuwan T, Leas S, Ames IA, Zobel H, Darien IL, Robyt JF (1994) Anthology of starch granule morphology by scanning electron microscopy. Starch-Stärke 46: 121-129.

Jane J, Xu A, Radosavljevic M, Seib PA (1992) Location of amylose in normal starch granules. 1. Susceptibility of amylose and amylopectin to cross-linking reagents. Cereal Chemistry 69: 405-409.

Jane JL, Wong KS, McPherson AE (1997) Branch-structure difference in starches of A- and B-type X-ray patterns revealed by their Naegeli dextrins. Carbohydrate Research 300: 219-227.

Jenkins PJ, Cameron RE, Donald AM (1993) A universal feature in the structure of starch granules from different botanical sources. Starch-Stärke 45: 417-420.

Jhamb S, Zalik S (1975) Plastid development in a *virescens* barley mutant and chloroplast microtubules. Canadian Journal of Botany-Revue Canadienne de Botanique 53: 2014-2025.

Ji Q, Oomen RJF, Vincken JP, Bolam DN, Gilbert HJ, Suurs L, Visser RGF (2004) Reduction of starch granule size by expression of an engineered tandem starch-binding domain in potato plants. Plant Biotechnology Journal 2: 251-260.

Jobling SA, Schwall GP, Westcott RJ, Sidebottom CM, Debet M, Gidley MJ, Jeffcoat R, Safford R (1999) A minor form of starch branching enzyme in potato (*Solanum tuberosum* L.) tubers has a major effect on starch structure: cloning and characterisation of multiple forms of SBE A. Plant Journal 18: 163-171.

Jones RJ, Srienc F, Roessler J (1992) Flow cytometric determination of light-scattering and absorbency properties of starch granules. Starch-Stärke 44: 243-247.

Jossier M, Bouly JP, Meimoun P, Arjmand A, Lessard P, Hawley S, Hardie DG, Thomas M (2009) SnRK1 (SNF1-related kinase 1) has a central role in sugar and ABA signalling in *Arabidopsis thaliana*. Plant Journal 59: 316-328.

Kahn LD (1983) The poisively cooperative binding of concanavalin A to corn starch: The isotherm of binding and a measure of the cooperativity. Carbohydrate Research 113: 133-139.

Kammerer B, Fischer K, Hilpert B, Schubert S, Gutensohn M, Weber A, Flugge UI (1998) Molecular characterization of a carbon transporter in plastids from heterotrophic tissues: The glucose 6-phosphate phosphate antiporter. Plant Cell 10: 105-117.

Kasten B, Reski R (1997) β-lactam antibiotics inhibit chloroplast division in a moss (*Physcomitrella patens*) but not in tomato (*Lycopersicon esculentum*). Journal of Plant Physiology 150: 137-140.

Kerk D, Conley TR, Rodriguez FA, Tran HT, Nimick M, Muench DG, Moorhead GBG (2006) A chloroplast-localized dual-specificity protein phosphatase in *Arabidopsis* contains a phylogenetically dispersed and ancient carbohydrate-binding domain, which binds the polysaccharide starch. Plant Journal 46: 400-413.

Kerschen A, Napoli CA, Jorgensen RA, Müller AE (2004) Effectiveness of RNA interference in transgenic plants. FEBS Letters 566: 223-228.

Kiessling J, Kruse S, Rensing SA, Harter K, Decker EL, Reski R (2000) Visualisation of a cytoskeleton-like FtsZ network in chloroplasts. Journal of Cell Biology 151: 945-950.

Kim W, Johnson JW, Graybosch RA, Gaines CS (2003) Physicochemical properties and end-use quality of wheat starch as a function of waxy protein alleles. Journal of Cereal Science 37: 195-204.

Kinsman EA, Pyke KA (1998) Bundle sheath cells and cell specific plastid development in *Arabidopsis* leaves. Development 125: 1815-1822.

Kiss JZ, Edelmann RE (1999) Spaceflight experiments with *Arabidopsis* starch-deficient mutants support a statolith-based model for graviperception. Advanced Space Research 24: 755-762.

Kiss JZ, Guisinger MM, Miller AJ (1998a) What is the threshold amount of starch necessary for full gravitropic sensitivity? In: Montufar Solis D, Barlow PW, Moore D, Hader DP, Ishay JS eds) Life Sciences: Microgravity Research. pp 1197-1202.

Kiss JZ, Hertel R, Sack FD (1989) Amyloplasts are necessary for full gravitropic sensitivity in roots of *Arabidopsis thaliana*. Planta 177: 198-206.

Kiss JZ, Katembe J, Edelmann RE (1998b) Gravitropism and development of wild-type and starch-deficient mutants of *Arabidopsis* during spaceflight. Physiologia Plantarum 102: 493-502.

Kiss JZ, Sack FD (1990) Severely reduced gravitropism in dark-grown hypocotyls of a starch-deficient mutant of *Nicotiana sylvestris*. Plant Physiology 94: 1867-1873.

Kitahata S, Murakami H, Okada S (1989) Purification and some properties of amylomaltase from *Escherichia coli* Ifo-3806. Agricultural and Biological Chemistry 53: 2653-2659.

Kleczkowski LA (1999) A phosphoglycerate to inorganic phosphate ratio is the major factor in controlling starch levels in chloroplasts via ADP-glucose pyrophosphorylase regulation. FEBS Letters 448: 153-156.

Kofler H, Hausler RE, Schulz B, Groner F, Flügge U-I, Weber A (2000) Molecular characterisation of a new mutant allele of the plastid phosphoglucomutase in *Arabidopsis,* and complementation of the mutant with the wild-type cDNA. Molecular Genomics and Genetics 263: 978-986.

Koksharova OA, Wolk CP (2002) A novel gene that bears a DnaJ motif influences cyanobacterial cell division. Journal of Bacteriology 184: 5524-5528.

Kolasa A (2007) Glycogenins in plants? Starch granule and polymer initiation. Comparative Biochemistry and Physiology, Part A 146: S272.

Kolbe A, Tiessen A, Schluepmann H, Paul M, Ulrich S, Geigenberger P (2005) Trehalose 6-phosphate regulates starch synthesis via posttranslational redox activation of ADP-glucose pyrophosphorylase. Proceedings of the National Academy of Sciences of the United States of America 102: 11118-11123.

Komor E (2000) Source physiology and assimilate transport: the interaction of sucrose metabolism, starch storage and phloem export in source leaves and the effects on sugar status in phloem. Australian Journal of Plant Physiology 27: 497-505.

Koniger M, Delamaide JA, Marlow ED, Harris GC (2008) *Arabidopsis thaliana* leaves with altered chloroplast numbers and chloroplast movement exhibit impaired adjustments to both low and high light. Journal of Experimental Botany 59: 2285-2297.

Kossmann J, Lloyd J (2000) Understanding and influencing starch biochemistry. Critical Reviews in Plant Sciences 19: 171-226.

Kötting O, Pusch K, Tiessen A, Geigenberger P, Steup M, Ritte G (2005) Identification of a novel enzyme required for starch metabolism in *Arabidopsis* leaves. The phosphoglucan, water dikinase. Plant Physiology 137: 242-252.

Kötting O, Santelia D, Edner C, Eicke S, Marthaler T, Gentry MS, Comparot-Moss S, Chen J, Smith AM, Steup M, Ritte G, Zeeman SC (2009) STARCH-EXCESS4 is a laforin-like phosphoglucan phosphatase required for starch degradation in *Arabidopsis thaliana*. Plant Cell 21: 334-346.

Kouri T, Gyory A, Rowan RM (2003) ISLH recommended reference procedure for the enumeration of particles in urine. Laboratory Hematology 9: 58-63.

Kruger NJ, ap Rees T (1983) Maltose metabolism by pea chloroplasts. Planta 158: 179-184.

Kubo A, Colleoni C, Dinges JR, Lin Q, Lappe R, Rivenbark J, Meyer A, Ball SG, James MG, Hennen-Bierwagen TA, Myers AM (2010) Functions of heteromeric and homomeric isoamylase-type starch debranching enzymes in developing maize endosperm. Plant Physiology 153: 956-969.

Kubo A, Fujita N, Harada K, Matsuda T, Satoh H, Nakamura Y (1999) The starch-debranching enzymes isoamylase and pullulanase are both involved in amylopectin biosynthesis in rice endosperm. Plant Physiology 121: 399-409.

Kugrens P, Lee RE, Hill DRA (2000) Order Cryptomonadida. In: Lee JJ, Leedale GF, Bradbury P eds) The illustrated guide to the protozoa. Wiley-Blackwell, Lawrence, Kansas, USA, pp 1111-1125.

Kuipers AGJ, Jacobsen E, Visser RGF (1994) Formation and deposition of amylose in the potato tuber starch granule are affected by the reduction of granule-bound starch synthase gene expression. Plant Cell 6: 43-52.

Kutík J (1989) Ultrastructure of chloroplasts in palisade and spongy parenchyma cells during development of primary bean leaves. Photosynthetica 23: 678-681.

Langeveld SMJ, van Wijk R, Stuurman N, Kijne JW, de Pater S (2000) B-type granule containing protrusions and interconnections between amyloplasts in developing wheat endosperm revealed by transmission electron microscopy and GFP expression. Journal of Experimental Botany 51: 1357-1361.

Langeveld SMJ, Vennik M, Kottenhagen M, van Wijk R, Buijk A, Kijne JW, de Pater S (2002) Glucosylation activity and complex formation of two classes of reversibly glycosylated polypeptides. Plant Physiology 129: 278-289.

Lao NT, Schoneveld O, Mould RM, Hibberd JM, Gray JC, Kavanagh TA (1999) An *Arabidopsis* gene encoding a chloroplast-targeted β-amylase. Plant Journal 20: 519-527.

Lavintman N, Cardini CE (1973) Particulate UDPglucose - protein transglucosylase from potato tuber. FEBS Letters 29: 43-46.

Lavintman N, Tandecarz J, Carceller M, Mendiara S, Cardini CE (1974) Role of uridine-diphosphate glucose in biosynthesis of starch - Mechanism of formation and enlargement of a glucoproteic acceptor. European Journal of Biochemistry 50: 145-155.

Lawrence ME, Possingham JV (1984) Observations of microtubule-like structures within spinach plastids. Biology of the Cell 52: 77-82.

Leonard JM, Rose RJ (1979) Sensitivity of the chloroplast division cycle to chloramphenicol and cycloheximide in cultured spinach leaves. Plant Science Letters 14: 159-167.

Leterrier M, Holappa LD, Broglie KE, Beckles DM (2008) Cloning, characterisation and comparative analysis of a starch synthase IV gene in wheat: functional and evolutionary implications. BMC Plant Biology 8: Article 98.

Libessart N, Maddelein ML, Vandenkoornhuyse N, Decq A, Delrue B, Mouille G, D'Hulst C, Ball S (1995) Storage, photosynthesis, and growth - the conditional nature of mutations affecting starch synthesis and structure in *Chlamydomonas*. Plant Cell 7: 1117-1127.

Lin TP, Caspar T, Somerville C, Preiss J (1988) Isolation and characterisation of a starchless mutant of *Arabidopsis thaliana* (L.) Heynh lacking ADPglucose pyrophosphorylase activity. Plant Physiology 86: 1131-1135.

Lindeboom N, Chang PR, Tyler RT (2004) Analytical, biochemical and physicochemical aspects of starch granule size, with emphasis on small granule starches: A review. Starch-Stärke 56: 89-99.

Linden JC, Schilling N (1984) De novo maltotriose biosynthesis from the reducing end by *Spinacia oleracea* L. chloroplasts. Plant Physiology 74: 795-799.

Linden JC, Schilling N, Brackenhofer H, Kandler O (1975) Asymmetric labeling of maltose during photosynthesis in $^{14}CO_2$. Zeitschrift Fur Pflanzenphysiologie 76: 176-181.

Lizotte PA, Henson CA, Duke SH (1990) Purification and characterization of pea epicotyl β-amylase. Plant Physiology 92: 615-621.

Lloyd JR, Blennow A, Burhenne K, Kossmann J (2004) Repression of a novel isoform of disproportionating enzyme (stDPE2) in potato leads to inhibition of starch degradation in leaves but not tubers stored at low temperature. Plant Physiology 134: 1347-1354.

Lohmeier-Vogel EM, Kerk D, Nimick M, Wrobel S, Vickerman L, Muench DG, Moorhead GBG (2008) *Arabidopsis* At5g39790 encodes a chloroplast-localized, carbohydrate-binding, coiled-coil domain-containing putative scaffold protein. Bmc Plant Biology 8: 120.

Lomako J, Lomako WM, Whelan WJ (1992) The substrate specificity of isoamylase and the preparation of apo-glycogenin. Carbohydrate Research 227: 331-338.

Lomako J, Lomako WM, Whelan WJ, Dombro RS, Neary JT, Norenberg MD (1993) Glycogen synthesis in the astrocyte - from glycogenin to proglycogen to glycogen. FASEB Journal 7: 1386-1393.

Lopez-Juez E, Pyke KA (2005) Plastids unleashed: their development and their integration in plant development. International Journal of Developmental Biology 49: 557-577.

Lu Y, Gehan JP, Sharkey TD (2005) Daylength and circadian effects on starch degradation and maltose metabolism. Plant Physiology 138: 2280-2291.

Lu Y, Savage LJ, Ajjawi I, Imre KM, Yoder DW, Benning C, DellaPenna D, Ohlrogge JB, Osteryoung KW, Weber AP, Wilkerson CG, Last RL (2008) New connections across pathways and processes: Industrialised mutant screening reveals novel associations between diverse phenotypes in *Arabidopsis*. Plant Physiology 146: 1482-1500.

Lu Y, Sharkey TD (2004) The role of amylomaltase in maltose metabolism in the cytosol of photosynthetic cells. Planta 218: 466-473.

Lu Y, Sharkey TD (2006) The importance of maltose in transitory starch breakdown. Plant Cell and Environment 29: 353-366.

Lu Y, Steichen JM, Yao J, Sharkey TD (2006) The role of cytosolic α-glucan phosphorylase in maltose metabolism and the comparison of amylomaltase in *Arabidopsis* and *Escherichia coli*. Plant Physiology 142: 878-889.

Lunn JE, Feil R, Hendriks JHM, Gibon Y, Morcuende R, Osuna D, Scheible WR, Carillo P, Hajirezaei MR, Stitt M (2006) Sugar-induced increases in trehalose 6-phosphate are correlated with redox activation of ADPglucose pyrophosphorylase and higher rates of starch synthesis in *Arabidopsis thaliana*. Biochemical Journal 397: 139-148.

Lunn JE, Hatch MD (1997) The role of sucrose-phosphate synthase in the control of photosynthate partitioning in *Zea mays* leaves. Australian Journal of Plant Physiology 24: 1-8.

Lupas AN, Gruber M (2005) The structure of α-helical coiled coils. In: Fibrous Proteins: Coiled-Coils, Collagen and Elastomers. pp 37-38.

Lytovchenko A, Bieberich K, Willmitzer L, Fernie AR (2002) Carbon assimilation and metabolism in potato leaves deficient in plastidial phosphoglucomutase. Planta 215: 802-811.

MacDonald FD, Preiss J (1985) Partial purification and characterisation of granule-bound starch synthases from normal and *waxy* maize. Plant Physiology 78: 849-852.

Macdonald IR, Ellis RJ (1969) Does cycloheximide inhibit protein synthesis specifically in plant tissues. Nature 222: 791-792.

Macmasters MM, Hilbert GE, Cox MJ, Eck JW, Bice CW (1946) Coacervation of starch. Quartermaster Corps Report 17: Referenced in Badenhuizen (1963) (Note: Original article was unavailable through the British Library or alternative sources).

Maple J, Aldridge C, Møller SG (2005) Plastid division is mediated by combinatorial assembly of plastid division proteins. Plant Journal 43: 811-823.

Maple J, Chua N-H, Møller SG (2002) The topological specificity factor *At*MinE1 is essential for correct plastid division site placement in *Arabidopsis*. Plant Journal 31: 269-277.

Maple J, Fujiwara MT, Kitahata N, Lawson T, Baker NR, Yoshida S, Møller SG (2004) Giant chloroplast1 is essential for correct plastid division in *Arabidopsis*. Current Biology 14: 776-781.

Maple J, Moller SG (2010) The complexity and evolution of the plastid division machinery. Biochemical Society Transactions 38: 783-788.

Maple J, Møller SG (2007a) Interdependency of formation and localisation of the Min complex controls symmetric plastid division. Journal of Cell Science 120: 3446-3456.

Maple J, Møller SG (2007b) Plastid division coordination across a double-membraned structure. Febs Letters 581: 2162-2167.

Maple J, Møller SG (2007c) Plastid division: Evolution, mechanism and complexity. Annals of Botany 99: 565-579.

Maple J, Vojta L, Soll J, Møller SG (2007) ARC3 is a stromal Z-ring accessory protein essential for plastid division. EMBO Reports 8: 293-299.

Marrison JL, Rutherford SM, Robertson EJ, Lister C, Dean C, Leech RM (1999) The distinctive roles of five different ARC genes in the chloroplast division process in *Arabidopsis*. Plant Journal 18: 651-662.

Martin A, Lang D, Hanke ST, Mueller SJX, Sarnighausen E, Vervliet-Scheebaum M, Reski R (2009) Targeted gene knockouts reveal overlapping functions of the five *Physcomitrella patens* FtsZ isoforms in chloroplast division, chloroplast shaping, cell patterning, plant development, and gravity sensing. Molecular Plant 2: 1359-1372.

Mason JM, Arndt KM (2004) Coiled coil domains: Stability, specificity, and biological implications. ChemBioChem. 5: 170-176.

Masuda HP, Ramos GBA, de Almeida-Engler J, Cabral LM, Coqueiro VM, Macrini CMT, Ferreira PCG, Hemerly AS (2004) Genome based identification and analysis of the pre-replicative complex of *Arabidopsis thaliana*. FEBS Letters 574: 192-202.

Matheson NK (1996) The chemical structure of amylose and amylopectin fractions of starch from tobacco leaves during development and diurnally-nocturnally. Carbohydrate Research 282: 247-262.

McAndrew RS, Froehlich JE, Vitha S, Stokes KD, Osteryoung KW (2001) Colocalization of plastid division proteins in the chloroplast stromal compartment establishes a new functional relationship between FtsZ1 and FtsZ2 in higher plants. Plant Physiology 127: 1656-1666.

McAndrew RS, Olson B, Kadirjan-Kalbach DK, Chi-Ham CL, Vitha S, Froehlich JE, Osteryoung KW (2008) In vivo quantitative relationship between plastid division proteins FtsZ1 and FtsZ2 and identification of ARC6 and ARC3 in a native FtsZ complex. Biochemical Journal 412: 367-378.

McClung CR (2001) Circadian rhythms in plants. Annual Review of Plant Physiology and Plant Molecular Biology 52: 139-162.

McCracken DA, Dodd JL (1971) Molecular structure of starch-type polysaccharides from *Hericium ramosum* and *Hericium coralloides*. Science 174: 419.

McCullough AJ, Kangasjarvi J, Gengenbach BG, Jones RJ (1992) Plastid DNA in developing maize endosperm - Genome structure, methylation, and transcript accumulation patterns. Plant Physiology 100: 958-964.

McFadden GI (2001) Chloroplast origin and integration. Plant Physiology 125: 50-53.

McKibbin RS, Muttucumaru N, Paul MJ, Powers SJ, Burrell MM, Coates S, Purcell PC, Tiessen A, Geigenberger P, Halford NG (2006) Production of high-starch, low-glucose potatoes through over-expression of the metabolic regulator SnRK1. Plant Biotechnology Journal 4: 409-418.

Meeuse BJD, Hall DM (1973) Studies on cell wall starch of *Hericium*. Annals of the New York Academy of Sciences 210: 39-45.

Mikkelsen R, Mutenda KE, Mant A, Schurmann P, Blennow A (2005) α-Glucan, water dikinase (GWD): A plastidic enzyme with redox-regulated and coordinated catalytic activity and binding affinity. Proceedings of the National Academy of Sciences of the United States of America 102: 1785-1790.

Mikkelsen R, Suszkiewicz K, Blennow A (2006) A novel type carbohydrate-binding module identified in α-glucan, water dikinases is specific for regulated plastidial starch metabolism. Biochemistry 45: 4674-4682.

Miyagishima SY, Froehlich JE, Osteryoung KW (2006) PDV1 and PDV2 mediate recruitment of the dynamin-related protein ARC5 to the plastid division site. Plant Cell 18: 2517-2530.

Miyagishima SY, Kuwayama H, Urushihara H, Nakanishi H (2008) Evolutionary linkage between eukaryotic cytokinesis and chloroplast division by dynamin proteins. Proceedings of the National Academy of Sciences of the United States of America 105: 15202-15207.

Miyake H, Maeda E (1975) Development of bundle sheath chloroplasts in rice seedlings. Canadian Journal of Botany-Revue Canadienne de Botanique 54: 556-565.

Miyake H, Maeda E (1978) Starch accumulation in bundle sheath chloroplasts during leaf development of C_3 and C_4 plants of *Gramineae*. Canadian Journal of Botany-Revue Canadienne de Botanique 56: 880-882.

Mizuno K, Kawasaki T, Shimada H, Satoh H, Kobayashi E, Okumura S, Arai Y, Baba T (1993) Alteration of the structural properties of starch components by the lack of an isoform of starch branching enzyme in rice seeds. Journal of Biological Chemistry 268: 19084-19091.

Modrusan Z, Wrischer M (1990) Studies on chloroplast division in young leaf tissues of some higher plants. Protoplasma 154: 1-7.

Mohammadkhani A, Stoddard FL, Marshall DR (1998) Survey of amylose content in *Secale cereale*, *Triticum monococcum*, *T. turgidum* and *T. tauschii*. Journal of Cereal Science 28: 273-280.

Molas ML, Kiss JZ (2009) Phototropism and gravitropism in plants. In: Advances in Botanical Research, Vol 49. pp 1-34.

Molin WT, Meyers SP, Baer GR, Schrader LE (1982) Ploidy effects in isogenic populations of alfalfa. Plant Physiology 70: 1710-1714.

Moore B, Zhou L, Rolland F, Hall Q, Cheng WH, Liu YX, Hwang I, Jones T, Sheen J (2003) Role of the *Arabidopsis* glucose sensor HXK1 in nutrient, light, and hormonal signaling. Science 300: 332-336.

Morden CW, Sherwood AR (2002) Continued evolutionary surprises among dinoflagellates. Proceedings of the National Academy of Sciences of the United States of America 99: 11558-11560.

Morell MK, Blennow A, Kosar-Hashemi B, Samuel MS (1997) Differential expression and properties of starch branching enzyme isoforms in developing wheat endosperm. Plant Physiology 113: 201-208.

Mori T, Kuroiwa H, Takahara M, Miyagishima S, Kuroiwa T (2001) Visualization of an FtsZ ring in chloroplasts of *Lilium longiflorum* leaves. Plant and Cell Physiology 42: 555-559.

Mouille G, Maddelein ML, Libessart N, Talaga P, Decq A, Delrue B, Ball S (1996) Preamylopectin processing: A mandatory step for starch biosynthesis in plants. Plant Cell 8: 1353-1366.

Mukerjea R, Mukerjea R, Robyt JF (2009) Starch biosynthesis: experiments on how starch granules grow in vivo. Carbohydrate Research 344: 67-73.

Munck L, Rexen F, Haastrup L (1988) Cereal starches within the European Community - Agricultural production, dry and wet milling and potential use in industry. Starch-Stärke 40: 81-87.

Munoz FJ, Baroja-Fernandez E, Moran-Zorzano MT, Viale AM, Etxeberria E, Alonso-Casajus N, Pozueta-Romero J (2005) Sucrose synthase controls both intracellular ADP glucose levels and transitory starch biosynthesis in source leaves. Plant and Cell Physiology 46: 1366-1376.

Munoz FJ, Zorzano MTM, Alonso-Casajus N, Baroja-Fernandez E, Etxeberria E, Pozueta-Romero J (2006) New enzymes, new pathways and an alternative view on starch biosynthesis in both photosynthetic and heterotrophic tissues of plants. Biocatalysis and Biotransformation 24: 63-76.

Myers AM, Morell MK, James MG, Ball SG (2000) Recent progress toward understanding biosynthesis of the amylopectin crystal. Plant Physiology 122: 989-997.

Naegele T, Henkel S, Hoermiller I, Sauter T, Sawodny O, Ederer M, Heyer AG (2010) Mathematical modelling of the central carbohydrate metabolism in *Arabidopsis thaliana*

reveals a substantial regulatory influence of vacuolar invertase on whole plant carbon metabolism. Plant Physiology 153: 260-272.

Nakamura Y (2002) Towards a better understanding of the metabolic system for amylopectin biosynthesis in plants: Rice endosperm as a model tissue. Plant and Cell Physiology 43: 718-725.

Nakamura Y, Kubo A, Shimamune T, Matsuda T, Harada K, Satoh H (1997) Correlation between activities of starch debranching enzyme and α-polyglucan structure in endosperms of *sugary1* mutants of rice. Plant Journal 12: 143-153.

Nakanishi H, Suzuki K, Kabeya Y, Miyagishima S (2009) Plant specific protein MCD1 determines the site of chloroplast division in concert with bacteria-derived MinD. Current Biology 19: 151-156.

Nelson OE, Rines HW (1962) The enzymatic deficiency in the waxy mutant of maize. Biochemical and Biophysical Research Communications 9: 297-300.

Neuhaus HE, Häusler RE, Sonnewald U (2005) No need to shift the paradigm on the metabolic pathway to transitory starch in leaves. Trends in Plant Science 10: 154-156.

Neuhaus HE, Henrichs G, Scheibe R (1993) Characterization of glucose-6-phosphate incorporation into starch by isolated intact cauliflower bud plastids. Plant Physiology 101: 573-578.

Neuhaus HE, Kruckeberg AL, Feil R, Stitt M (1989) Reduced-activity mutants of phosphoglucose isomerase in the cytosol and chloroplast of *Clarkia xantiana*. 2. Study of the mechanisms which regulate photosynthate partitioning. Planta 178: 110-122.

Neuhaus HE, Stitt M (1990) Control analysis of photosynthate partitioning - Impact of reduced activity of ADP-glucose pyrophosphorylase or plastid phosphoglucomutase on the fluxes to starch and sucrose in *Arabidopsis thaliana* (L.) Heynh. Planta 182: 445-454.

Ni ZF, Kim ED, Ha MS, Lackey E, Liu JX, Zhang YR, Sun QX, Chen ZJ (2009) Altered circadian rhythms regulate growth vigour in hybrids and allopolyploids. Nature 457: 327-331.

Nielsen TH, Baunsgaard L, Blennow A (2002) Intermediary glucan structures formed during starch granule biosynthesis are enriched in short side chains, a dynamic pulse labeling approach. Journal of Biological Chemistry 277: 20249-20255.

Niittylä T, Comparot-Moss S, Lue WL, Messerli G, Trevisan M, Seymour MDJ, Gatehouse JA, Villadsen D, Smith SM, Chen JC, Zeeman SC, Smith AM (2006) Similar protein phosphatases control starch metabolism in plants and glycogen metabolism in mammals. Journal of Biological Chemistry 281: 11815-11818.

Niittylä T, Messerli G, Trevisan M, Chen J, Smith AM, Zeeman SC (2004) A previously unknown maltose transporter essential for starch degradation in leaves. Science 303: 87-89.

Niittylä TJK (2003) The role of malto-oligosaccharides in starch metabolism of *Arabidopsis thaliana* (L.) leaves. In: PhD thesis. University of East Anglia, Norwich, UK.

Nordmark TS, Ziegler GR (2002a) Spherulitic crystallization of gelatinized maize starch and its fractions. Carbohydrate Polymers 49: 439-448.

Nordmark TS, Ziegler GR (2002b) Structural features of non-granular spherulitic maize starch. Carbohydrate Research 337: 1467-1475.

Okazaki K, Kabeya Y, Suzuki K, Mori T, Ichikawa T, Matsui M, Nakanishi H, Miyagishima S (2009) The PLASTID DIVISION1 and 2 components of the chloroplast division machinery determine the rate of chloroplast division in land plant cell differentiation. Plant Cell 21: 1769-1780.

Oostergetel ET, van Bruggen EFJ (1993) The crystalline domains in potato starch granules are arranged in a helical fashion. Carbohydrate Polymers 21: 7-12.

Oross JW, Possingham JV (1989) Ultrastructural features of the constricted region of dividing plastids. Protoplasma 150: 131-138.

Oross JW, Possingham JV (1991) Tubular structures in developing plastids of three dicotyledonous species. Canadian Journal of Botany-Revue Canadienne de Botanique 69: 136-139.

Osteryoung KW, Nunnari J (2003) The division of endosymbiotic organelles. Science 302: 1698-1704.

Osteryoung KW, Stokes KD, Rutherford SM, Percival AL, W.Y. L (1998) Chloroplast division in higher plants requires members of two functionally divergent gene families with homology to bacterial *FtsZ*. Plant Cell 10: 1991-2004.

Ottesen E, Zhong R, Lamppa GK (2010) Identification of a chloroplast division mutant coding for ARC6H, an ARC6 homolog that plays a nonredundant role. Plant Science 178: 114-122.

Pallas JE (1964) Guard-cell starch retention and accumulation in the dark. Botanical Gazette 125: 102-107.

Palmer TN, Ryman BE, Whelan WJ (1976) Action pattern of amylomaltase from *Escherichia coli*. European Journal of Biochemistry 69: 105-115.

Pan D, Nelson OE (1984) A debranching enzyme deficiency in endosperms of the *sugary-1* mutants of maize. Plant Physiology 74: 324-328.

Parker ML (1985) The relationship between A-type and B-type starch granules in the developing endosperm of wheat. Journal of Cereal Science 3: 271-278.

Patron NJ, Keeling PJ (2005) Common evolutionary origin of starch biosynthetic enzymes in green and red algae. Journal of Phycology 41: 1131-1141.

Paul MJ, Foyer CH (2001) Sink regulation of photosynthesis. Journal of Experimental Botany 52: 1383-1400.

Petit PX, Diolez P, de Kouchkovsky Y (1989) Flow cytometric analysis of energy transducing organelles: mitochondria and chloroplasts. In: Yen A (ed) Flow Cytometry: Advanced Research and Clinical Applications; Volume 1. CRC Press, Boca Raton, pp 271-303.

Pickett-Heaps J (1968) Microtubule-like structures in growing plastids or chloroplasts of two algae. Planta 81: 193-200.

Pilling E, Smith SM (2003) Growth ring formation in the starch granules of potato tubers. Plant Physiology 132: 365-371.

Pitcher J, Smythe C, Campbell DG, Cohen P (1987) Identification of the 38 kDa subunit of rabbit skeletal muscle glycogen synthase as glycogenin. European Journal of Biochemistry 169: 497-502.

Pitcher J, Smythe C, Cohen P (1988) Glycogenin is the priming glucosyltransferase required for the initiation of glycogen biogenesis in rabbit skeletal muscle. European Journal of Biochemistry 176: 391-395.

Pizzolato TD, Frick H (1979) Pyrimidine metabolism in *Lemna minor*. 2. Specific inhibition of plastid replication in a higher plant by cytidine deoxyriboside. Plant Physiology 63: 979-983.

Pogliano J (2008) The bacterial cytoskeleton. Current Opinion in Cell Biology 20: 19-27.

Posewitz MC, Smolinski SL, Kanakagiri S, Melis A, Seibert M, Ghirardi ML (2004) Hydrogen photoproduction is attenuated by disruption of an isoamylase gene in *Chlamydomonas reinhardtii*. Plant Cell 16: 2151-2163.

Possingham JV, Lawrence ME (1983) Controls of plastid division. International Journal of Cytology 84: 1-56.

Possingham JV, Saurer W (1969) Changes in chloroplast number per cell during leaf development in spinach. Planta 86: 186-194.

Preiss J (1988) Biosynthesis of starch and its regulation. In: Preiss J (ed) The biochemistry of plants. Volume 14. Academic Press, San Diego, pp 181-254.

Pritchard SG, Peterson CM, Prior SA, Rogers HH (1997) Elevated atmospheric CO_2 differentially affects needle chloroplast ultrastructure and phloem anatomy in *Pinus palustris*: Interactions with soil resource availability. Plant Cell and Environment 20: 461-471.

Pyke K (2006) Plastid division: The squeezing gets tense. Current Biology 16: R60-R62.

Pyke KA, Leech RM (1991) Rapid image analysis screening procedure for identifying chloroplast number mutants in mesophyll cells of *Arabidopsis thaliana* (L.) Heynh. Plant Physiology 96: 1193-1195.

Pyke KA, Leech RM (1992) Chloroplast division and expansion is radically altered by nuclear mutations in *Arabidopsis thaliana*. Plant Physiology 99: 1005-1008.

Pyke KA, Leech RM (1994) A genetic analysis of chloroplast division and expansion in *Arabidopsis thaliana* Plant Physiology 104: 201-207.

Pyke KA, Marrison JL, Leech RM (1991) Temporal and spatial development of the cells of the expanding first leaf of *Arabidopsis thaliana* (L) Heynh. Journal of Experimental Botany 42: 1407-1416.

Pyke KA, Rutherford SM, Robertson EJ, Leech RM (1994) *arc6*, a fertile *Arabidopsis* mutant with only two mesophyll cell chloroplasts. Plant Physiology 106: 1169-1177.

Qiu XB, Shao YM, Miao S, Wang L (2006) The diversity of the DnaJ/Hsp40 family, the crucial partners for Hsp70 chaperones. Cellular and Molecular Life Sciences 63: 2560-2570.

Quentmeier H, Ingold E, Seitz HU (1987) Purification of an autocatalytic protein-glycosylating enzyme from cell-suspensions of *Daucus carota* L. Planta 171: 483-488.

Raeker MO, Gaines CS, Finney PL, Donelson T (1998) Granule size distribution and chemical composition of starches from 12 soft wheat cultivars. Cereal Chemistry 75: 721-728.

Rahman S, Nakamura Y, Li Z, Clarke B, Fujita N, Mukai Y, Yamamoto M, Regina A, Tan Z, Kawasaki S, Morell M (2003) The sugary-type isoamylase gene from rice and *Aegilops tauschii*: characterization and comparison with maize and *Arabidopsis*. Genome 46: 496-506.

Rahman S, Regina A, Li ZY, Mukai Y, Yamamoto M, Kosar-Hashemi B, Abrahams S, Morell MK (2001) Comparison of starch-branching enzyme genes reveals evolutionary relationships among isoforms. Characterization of a gene for starch-branching enzyme IIa from the wheat D genome donor *Aegilops tauschii*. Plant Physiology 125: 1314-1324.

Ral JP, Derelle E, Ferraz C, Wattebled F, Farinas B, Corellou F, Buléon A, Slomianny MC, Delvallé D, D'Hulst C, Rombauts S, Moreau H, Ball S (2004) Starch division and partitioning. A mechanism for granule propagation and maintenance in the picophytoplanktonic green alga *Ostreococcus tauri*. Plant Physiology 136: 3333-3340.

Rasse DP, Tocquin P (2006) Leaf carbohydrate controls over *Arabidopsis* growth and response to elevated CO2: an experimentally based model. New Phytologist 172: 500-513.

Raynaud C, Perennes C, Reuzeau C, Catrice O, Brown S, Bergounioux C (2005) Cell and plastid division are coordinated through the prereplication factor *At*CDT1. Proceedings of the National Academy of Sciences of the United States of America 102: 8216-8221.

Recondo E, Leloir LF (1961) Adenosine diphosphate glucose and starch synthesis. Biochemical and Biophysical Research Communications 6: 85-88.

Regina A, Kosar-Hashemi B, Ling S, Li ZY, Rahman S, Morell M (2010) Control of starch branching in barley defined through differential RNAi suppression of starch branching enzyme IIa and IIb. Journal of Experimental Botany 61: 1469-1482.

Reibach PH, Benedict CR (1982) Biosynthesis of starch in proplastids of germinating *Ricinus communis* endosperm tissue. Plant Physiology 70: 252-256.

Reski R (2002) Rings and networks: the amazing complexity of FtsZ in chloroplasts. Trends in Plant Science 7: 103-105.

Reski R (2009) Challenges to our current view on chloroplasts. Biological Chemistry 390: 731-738.

Ridout MJ, Gunning AP, Parker ML, Wilson RH, Morris VJ (2002) Using AFM to image the internal structure of starch granules. Carbohydrate Polymers 50: 123-132.

Ridout MJ, Parker ML, Hedley CL, Bogracheva TY, Morris VJ (2003) Atomic force microscopy of pea starch granules: Granule architecture of wild-type parent, *r* and *rb* single mutants, and the *rrb* double mutant. Carbohydrate Research 338: 2135-2147.

Ring SG, Miles MJ, Morris VJ, Turner R, Colonna P (1987) Spherulitic crystallization of short chain amylose. International Journal of Biological Macromolecules 9: 158-160.

Ritte G, Heydenreich M, Mahlow S, Haebel S, Kötting O, Steup M (2006) Phosphorylation of C6- and C3-positions of glucosyl residues in starch is catalysed by distinct dikinases. FEBS Letters 580: 4872-4876.

Rivera ER, Arnott HJ (1982) Tubular structures in the plastids of *Echinomastus intertextus* Brit and Rose (Cactaceae). New Phytologist 90: 551-561.

Robertson EJ, Rutherford SM, Leech RM (1996) Characterization of chloroplast division using the *Arabidopsis* mutant *arc5*. Plant Physiology 112: 149-159.

Roldan I, Wattebled F, Lucas MM, Delvallé D, Planchot V, Jimenez S, Perez R, Ball S, D'Hulst C, Merida A (2007) The phenotype of soluble starch synthase IV defective mutants of *Arabidopsis thaliana* suggests a novel function of elongation enzymes in the control of starch granule formation. Plant Journal 49: 492-504.

Rolland F, Baena-Gonzalez E, Sheen J (2006) Sugar sensing and signaling in plants: Conserved and novel mechanisms. Annual Review of Plant Biology 57: 675-709.

Romberg L, Levin PA (2003) Assembly dynamics of the bacterial cell division protein FtsZ: Poised at the edge of stability. Annual Review of Microbiology 57: 125-154.

Rose A, Manikantan S, Schraegle SJ, Maloy MA, Stahlberg EA, Meier I (2004) Genome-wide identification of *Arabidopsis* coiled-coil proteins and establishment of the ARABI-COIL database. Plant Physiology 134: 927-939.

Rothschild A, Tandecarz JS (1994) UDP-glucose-protein transglucosylase in developing maize endosperm. Plant Science 97: 119-127.

Rutherford SM (1996) The genetic and physical analysis of mutants of chloroplast number and size in *Arabidopsis thaliana*. In: PhD thesis; University of York, UK.

Ryley JF, Bentley M, Manners DJ, Stark JR (1969) Amylopectin, the storage polysaccharide of the coccidia *Eimeria brunetti* and *E. tenella*. Journal of Parasitology 55: 839-845.

Ryoo N, Yu C, Park CS, Baik MY, Park IM, Cho MH, Bhoo SH, An G, Hahn TR, Jeon JS (2007) Knockout of a starch synthase gene OsSSIIIa/Flo5 causes white-core floury endosperm in rice (*Oryza sativa* L.). Plant Cell Reports 26: 1083-1095.

Sack FD (1997) Plastids and gravitropic sensing. Planta 203: S63-S68.

Saether N, Iversen TH (1991) Gravitropism and starch statoliths in an *Arabidopsis* mutant. Planta 184: 491-497.

Safford R, Jobling SA, Sidebottom CM, Westcott RJ, Cooke D, Tober KJ, Strongitharm BH, Russell AL, Gidley MJ (1998) Consequences of antisense RNA inhibition of starch branching enzyme activity on properties of potato starch. Carbohydrate Polymers 35: 155-168.

Sagisaka S, Akita T, Akase T, Matsumoto K, Nozaki K, Matsui H, Ito H, Honma M (1999) Trafficking of starch synthase from the cytosol to functional sites in younger and older proplastids in developing stolons of potato. Journal of Plant Physiology 154: 310-318.

Sakai A, Kawano S, Kuroiwa T (1992) Conversion of proplastids to amyloplasts in tobacco cultured cells is accompanied by changes in the transcriptional activities of plastid genes. Plant Physiology 100: 1062-1066.

Sakamoto W, Uno Y, Zhang Q, Miura E, Kato Y, Sodmergen (2009) Arrested differentiation of proplastids into chloroplasts in variegated leaves characterized by plastid ultrastructure and nucleoid morphology. Plant and Cell Physiology 50: 2069-2083.

Santacruz S, Koch K, Andersson R, Aman P (2004) Characterization of potato leaf starch. Journal of Agricultural and Food Chemistry 52: 1985-1989.

Satoh H, Nishi A, Yamashita K, Takemoto Y, Tanaka Y, Hosaka Y, Sakurai A, Fujita N, Nakamura Y (2003) Starch-branching enzyme I-deficient mutation specifically affects the structure and properties of starch in rice endosperm. Plant Physiology 133: 1111-1121.

Satoh H, Shibahara K, Tokunaga T, Nishi A, Tasaki M, Hwang SK, Okita TW, Kaneko N, Fujita N, Yoshida M, Hosaka Y, Sato A, Utsumi Y, Ohdan T, Nakamura Y (2008) Mutation of the plastidial α-glucan phosphorylase gene in rice affects the synthesis and structure of starch in the endosperm. Plant Cell 20: 1833-1849.

Schafer G, Heber U, Heldt HW (1977) Glucose transport into spinach chloroplasts. Plant Physiology 60: 286-289.

Schaffer R, Landgraf J, Accerbi M, Simon V, Larson M, Wisman E (2001) Microarray analysis of diurnal and circadian-regulated genes in *Arabidopsis*. Plant Cell 13: 113-123.

Scheidig A, Frohlich A, Schulze S, Lloyd JR, Kossmann J (2002) Downregulation of a chloroplast-targeted beta-amylase leads to a starch-excess phenotype in leaves. Plant Journal 30: 581-591.

Schilling N (1982) Characterization of maltose biosynthesis from α-D-glucose-1-phosphate in *Spinacia oleracea* L. Planta 154: 87-93.

Schilling N, Kandler O (1975) α-glucose 1-phosphate, a precursor in biosynthesis of maltose in higher plants. Biochemical Society Transactions 3: 985-987.

Schluepmann H, Pellny T, van Dijken A, Smeekens S, Paul M (2003) Trehalose 6-phosphate is indispensable for carbohydrate utilization and growth in Arabidopsis thaliana. Proceedings of the National Academy of Sciences of the United States of America 100: 6849-6854.

Schmitz AJ, Glynn JM, Olson BJSC, Stokes KD, Osteryoung KW (2009) *Arabidopsis* FtsZ2-1 and FtsZ2-2 are functionally redundant, but FtsZ-based plastid division is not essential for chloroplast partitioning or plant growth and development. Molecular Plant 2: 1211-1222.

Schneider EM, Sievers A (1981) Concanavalin A binds to the endoplasmic reticulum and the starch grain surface of root statocytes. Planta 152: 177-180.

Schroder WP, Petit PX (1992) Flow cytometry of spinach chloroplasts - Determination of intactness and lectin-binding properties of the envelope and the thylakoid membranes. Plant Physiology 100: 1092-1102.

Schulze W, Schulze ED, Stadler J, Heilmeier H, Stitt M, Mooney HA (1994) Growth and reproduction of *Arabidopsis thaliana* in relation to storage of starch and nitrate in the wild-type and in starch-deficient and nitrate-uptake-deficient mutants. Plant, Cell and Environment 17: 795-809.

Schulze W, Stitt M, Schulze ED, Neuhaus HE, Fichtner K (1991) A quantification of the significance of assimilatory starch for growth of *Arabidopsis thaliana* (L.) Heynh. Plant Physiology 95: 890-895.

Schupp N, Ziegler P (2004) The relation of starch phosphorylases to starch metabolism in wheat. Plant and Cell Physiology 45: 1471-1484.

Seo B-S, Kim S, Scott MP, Singletary GW, Wong KS, James MG, Myers AM (2002) Functional interactions between heterologously expressed starch-branching enzymes of maize and the glycogen synthases of brewer's yeast. Plant Physiology 128: 1189-1199.

Servaites JC, Geiger DR (2002) Kinetic characteristics of chloroplast glucose transport. Journal of Experimental Botany 53: 1581-1591.

Shannon JC, Pien FM, Cao HP, Liu KC (1998) Brittle-1, an adenylate translocator, facilitates transfer of extraplastidial synthesized ADP-glucose into amyloplasts of maize endosperms. Plant Physiology 117: 1235-1252.

Sheffield HG, Frenkel JK, Ruiz A (1977) Ultrastructure of the cyst of *Sarcocystis muris*. Journal of Parasitology 63: 629-641.

Sheu JJ, Jan SP, Lee HT, Yu SM (1994) Control of transcription and messenger-RNA turnover as mechanisms of metabolic repression of α-amylase gene expression. Plant Journal 5: 655-664.

Shewry PR, Morell M (2001) Manipulating cereal endosperm structure, development and composition to improve end-use properties. Advances in Botanical Research 34: 165-236.

Shimada H, Koizumi M, Kuroki K, Mochizuki M, Fujimoto H, Ohta H, Masuda T, Takamiya K (2004) ARC3, a chloroplast division factor, is a chimera of prokaryotic FtsZ and part of eukaryotic phosphatidylinositol-4-phosphate 5-kinase. Plant and Cell Physiology 45: 960-967.

Shure M, Wessler S, Fedoroff N (1983) Molecular identification and isolation of the *Waxy* locus in maize. Cell 35: 225-233.

Singh DG, Lomako J, Lomako WM, Whelan WJ, Meyer HE, Serwe M, Metzger JW (1995) β-Glucosylarginine: a new glucose-protein bond in a self-glycosylating protein from sweet corn. FEBS Letters 376: 61-64.

Sivak MN (1992) (1-4)-α-D-Glucan synthesis by a chloroplastic phosphorylase isolated from spinach leaves is independent of added primer. Carbohydrate Research 227: 241-255.

Sivak MN, Wagner M, Preiss J (1993) Biochemical evidence for the role of the waxy protein from pea (*Pisum sativum* L.) as a granule-bound starch synthase. Plant Physiology 103: 1355-1359.

Skurat AV, Dietrich AD, Roach PJ (2006) Interaction between glycogenin and glycogen synthase. Archives of Biochemistry and Biophysics 456: 93-97.

Skurat AV, Lim SS, Roach PJ (1997) Glycogen biogenesis in rat 1 fibroblasts expressing rabbit muscle glycogenin. European Journal of Biochemistry 245: 147-155.

Smith A, Denyer K, Martin C (1997) The synthesis of the starch granule. Annual Review of Plant Physiology and Plant Molecular Biology 48: 67-87.

Smith AM (2001) The biosynthesis of starch granules. Biomacromolecules 2: 335-341.

Smith AM, Neuhaus HE, Stitt M (1990) The impact of decreased activity of starch-branching enzyme on photosynthetic starch synthesis in leaves of wrinkled-seeded peas. Planta 181: 310-315.

Smith AM, Stitt M (2007) Coordination of carbon supply and plant growth. Plant, Cell and Environment 30: 1126-1149.

Smith AM, Zeeman SC (2006) Quantification of starch in plant tissues. Nature Protocols 1: 1342-1345.

Smith AM, Zeeman SC, Smith SM (2005) Starch degradation. Annual Review of Plant Biology 56: 73-98.

Smith SM, Fulton DC, Chia T, Thorneycroft D, Chapple A, Dunstan H, Hylton C, Zeeman SC, Smith AM (2004) Diurnal changes in the transcriptome encoding enzymes of starch metabolism provide evidence for both transcriptional and posttranscriptional regulation of starch metabolism in *Arabidopsis* leaves. Plant Physiology 136: 2687-2699.

Smythe C, Cohen P (1991) The discovery of glycogenin and the priming mechanism for glycogen biosynthesis. European Journal of Biochemistry 200: 625-631.

Sokolov LN, Dominguez-Solis JR, Allary AL, Buchanan BB, Luan S (2006) A redox-regulated chloroplast protein phosphatase binds to starch diurnally and functions in its accumulation. Proceedings of the National Academy of Sciences of the United States of America 103: 9732-9737.

Sonnewald U, Basner A, Greve B, Steup M (1995) A second L-type isozyme of potato glucan phosphorylase - cloning, antisense inhibition and expression analysis. Plant Molecular Biology 27: 567-576.

Sparla F, Costa A, Lo Schiavo F, Pupillo P, Trost P (2006) Redox regulation of a novel plastid-targeted beta-amylase of Arabidopsis. Plant Physiology 141: 840-850.

Sprey B (1968) Fine structure of plastid stroma of *Hordeum vulgare* L. Protoplasma 66: 469-479.

Steichen JM, Petty RV, Sharkey TD (2008) Domain characterization of a 4-α-glucanotransferase essential for maltose metabolism in photosynthetic leaves. Journal of Biological Chemistry 283: 20797-20804.

Stettler M, Eicke S, Mettler T, Messerli G, Hortensteiner S, Zeeman SC (2009) Blocking the metabolism of starch breakdown products in *Arabidopsis* leaves triggers chloroplast degradation. Molecular Plant 2: 1233-1246.

Steup M, Robenek H, Melkonian M (1983) In vitro degradation of starch granules isolated from spinach chloroplasts. Planta 158: 428-436.

Stitt M (1990) Fructose-2,6-bisphosphate as a regulatory molecule in plants. Annual Review of Plant Physiology and Plant Molecular Biology 41: 153-185.

Stitt M, Huber S, Kerr P (1987) Control of photosynthetic sucrose synthesis. In: Hatch MD, Boardman NK eds) The biochemistry of plants. Academic Press, San Diego, pp 327-409.

Stitt M, Lunn J, Usadel B (2010) *Arabidopsis* and primary photosynthetic metabolism - more than the icing on the cake. Plant Journal 61: 1067-1091.

Stitt M, Quick P (1989) Photosynthetic carbon partitioning - Its regulation and possibilities for manipulation. Physiologia Plantarum 77: 633-641.

Stokes KD, Osteryoung KW (2003) Early divergence of the FtsZ1 and FtsZ2 plastid division gene families in photosynthetic eukaryotes. Gene 320: 97-108.

Streb S, Delatte T, Umhang M, Eicke S, Schorderet M, Reinhardt D, Zeeman SC (2008) Starch granule biosynthesis in *Arabidopsis* is abolished by removal of all debranching enzymes but restored by the subsequent removal of an endoamylase. Plant Cell 20: 3448-3466.

Streb S, Egli B, Eicke S, Zeeman SC (2009) The debate on the pathway of starch synthesis: A closer look at low-starch mutants lacking plastidial phosphoglucomutase supports the chloroplast-localized pathway. Plant Physiology 151: 1769-1772.

Sun J, Gibson KM, Kiirats O, Okita TW, Edwards GE (2002) Interactions of nitrate and CO_2 enrichment on growth, carbohydrates, and Rubisco in *Arabidopsis* starch mutants. Significance of starch and hexose. Plant Physiology 130: 1573-1583.

Suzuki K, Nakanishi H, Bower J, Yoder DW, Osteryoung KW, Miyagishima SY (2009) Plastid chaperonin proteins Cpn60-α and Cpn60-β are required for plastid division in *Arabidopsis thaliana*. BMC Plant Biology 9: 38.

Szydlowski N, Ragel P, Raynaud S, Lucas MM, Roldan I, Montero M, Munoz FJ, Ovecka M, Bahaji A, Planchot V, Pozueta-Romero J, D'Hulst C, Merida A (2009) Starch granule initiation in *Arabidopsis* requires the presence of either class IV or class III starch synthases. Plant Cell 21: 2443-2457.

Szymonska J, Krok F (2003) Potato starch granule nanostructure studied by high resolution non-contact AFM. International Journal of Biological Macromolecules 33: 1-7.

Takaha T, Critchley J, Okada S, Smith SM (1998) Normal starch content and composition in tubers of antisense potato plants lacking D-enzyme (4-α-glucanotransferase). Planta 205: 445-451.

Takaha T, Yanase M, Okada S, Smith SM (1993) Disproportionating enzyme (4-α-glucanotransferase - EC 2.4.1.25) of potato - Purification, molecular-cloning, and potential role in starch metabolism. Journal of Biological Chemistry 268: 1391-1396.

Takashima Y, Senoura T, Yoshizaki T, Haniada S, Ito H, Matsui H (2007) Differential chain-length specificities of two isoamylase-type starch-debranching enzymes from developing seeds of kidney bean. Bioscience Biotechnology and Biochemistry 71: 2308-2312.

Takeda Y, Guan HP, Preiss J (1993) Branching of amylose by the branching isoenzymes of maize endosperm. Carbohydrate Research 240: 253-263.

Takisawa H, Mimura S, Kubota Y (2000) Eukaryotic DNA replication: from pre-replication complex to initiation complex. Current Opinion in Cell Biology 12: 690-696.

Tang H, Ando H, Watanabe K, Takeda Y, Mitsunaga T (2001a) Fine structures of amylose and amylopectin from large, medium, and small waxy barley starch granules. Cereal Chemistry 78: 111-115.

Tang H, Mitsunaga T, Kawamura Y (2006) Molecular arrangement in blocklets and starch granule architecture. Carbohydrate Polymers 63: 555-560.

Tang H, Watanabe K, Mitsunaga T (2002) Characterization of storage starches from quinoa, barley and adzuki seeds. Carbohydrate Polymers 49: 13-22.

Tang HJ, Ando H, Watanabe K, Takeda Y, Mitsunaga T (2001b) Physicochemical properties and structure of large, medium and small granule starches in fractions of normal barley endosperm. Carbohydrate Research 330: 241-248.

Tatge H, Marshall J, Martin C, Edwards EA, Smith AM (1999) Evidence that amylose synthesis occurs within the matrix of the starch granule in potato tubers. Plant, Cell and Environment 22: 543-550.

Tauberger E, Fernie AR, Emmermann M, Renz A, Kossmann J, Willmitzer L, Trethewey RN (2000) Antisense inhibition of plastidial phosphoglucomutase provides compelling evidence that potato tuber amyloplasts import carbon from the cytosol in the form of glucose-6-phosphate. Plant Journal 23: 43-53.

Teng N, Jin B, Wang Q, Hao H, Ceulemans R, Kuang T, Lin J (2009) No detectable maternal effects of elevated CO_2 on *Arabidopsis thaliana* over 15 generations. PLoS One 4: e6035.

Terasawa K, Sato N (2005) Visualization of plastid nucleoids in situ using the PEND-GFP fusion protein. Plant and Cell Physiology 46: 649-660.

Tetlow IJ, Beisel KG, Cameron S, Makhmoudova A, Liu F, Bresolin NS, Wait R, Morell MK, Emes MJ (2008) Analysis of protein complexes in wheat amyloplasts reveals functional interactions among starch biosynthetic enzymes. Plant Physiology 146: 1878-1891.

Thomson WW, Foster P, Leech RM (1972) The isolation of proplastids from roots of *Vicia faba*. Plant Physiology 49: 270-272.

Tiessen A, Hendriks JHM, Stitt M, Branscheid A, Gibon Y, Farre EM, Geigenberger P (2002) Starch synthesis in potato tubers is regulated by post-translational redox modification of ADP-glucose pyrophosphorylase: A novel regulatory mechanism linking starch synthesis to the sucrose supply. Plant Cell 14: 2191-2213.

Tiessen A, Prescha K, Branscheid A, Palacios N, McKibbin R, Halford NG, Geigenberger P (2003) Evidence that SNF1-related kinase and hexokinase are involved in separate sugar-signalling pathways modulating post-translational redox activation of ADP-glucose pyrophosphorylase in potato tubers. Plant Journal 35: 490-500.

Tipping C, Murray DR (1999) Effects of elevated atmospheric CO_2 concentration on leaf anatomy and morphology in *Panicum* species representing different photosynthetic modes. International Journal of Plant Sciences 160: 1063-1073.

Tomlinson K, Denyer K (2003) Starch synthesis in cereal grains. Advances in Botanical Research 40: 1-61.

Tomlinson KL, Lloyd JR, Smith AM (1997) Importance of isoforms of starch-branching enzyme in determining the structure of starch in pea leaves. Plant Journal 11: 31-43.

Trevanion SJ, Castleden CK, Foyer CH, Furbank RT, Quick WP, Lunn JE (2004) Regulation of sucrose-phosphate synthase in wheat (*Triticum aestivum*) leaves. Functional Plant Biology 31: 685-695.

Tsai HL, Lue WL, Lu KJ, Hsieh MH, Wang SM, Chen J (2009) Starch synthesis in *Arabidopsis* is achieved by spatial co-transcription of core starch metabolism genes. Plant Physiology 151: 1582-1595.

Tsakraklides V, Bell SP (2010) Dynamics of pre-replicative complex assembly. Journal of Biological Chemistry 285: 9437-9443.

Ueda K, Kawaguchi T, Noguchi T (1994) Chloroplast microtubules in *Oedogonium capilliforme* (Chlorophyta). Journal of Phycology 30: 23-28.

Usadel B, Bläsing OE, Gibon Y, Retzlaff K, Hoehne M, Gunther M, Stitt M (2008) Global transcript levels respond to small changes of the carbon status during progressive exhaustion of carbohydrates in *Arabidopsis* rosettes. Plant Physiology 146: 1834-1861.

Utsumi Y, Nakamura Y (2006) Structural and enzymatic characterization of the isoamylase1 homo-oligomer and the isoamylase1-isoamylase2 hetero-oligomer from rice endosperm. Planta 225: 75-87.

van den Ent F, Amos L, Lowe J (2001) Bacterial ancestry of actin and tubulin. Current Opinion in Microbiology 4: 634-638.

Van Larebeke N, Zaenen I, Teuchy H, Schell J (1973) Circular DNA plasmids in *Agrobacterium* strains - Investigation of their role in induction of crown-gall tumors. Archives Internationales de Physiologie, de Biochimie et de Biophysique 81: 986-986.

Vaughn KC, Wilson KG (1981) Improved visualization of plastid fine structure - Plastid microtubules. Protoplasma 108: 21-27.

Viola R, Nyvall P, Pedersen M (2001) The unique features of starch metabolism in red algae. Proceedings of the Royal Society London B. 268: 1417-1422.

Vitha S, Froehlich JE, Koksharova O, Pyke KA, van Erp H, Osteryoung KW (2003) ARC6 is a J-domain plastid division protein and an evolutionary descendant of the cyanobacterial cell division protein Ftn2. Plant Cell 15: 1918-1933.

Vitha S, McAndrew RS, Osteryoung KW (2001) FtsZ ring formation at the chloroplast division site in plants. Journal of Cell Biology 153: 111-119.

Waigh TA, Donald AM, Heidelbach F, Riekel C, Gidley MJ (1999) Analysis of the native structure of starch granules with small angle X-ray microfocus scattering. Biopolymers 49: 91-105.

Waigh TA, Kato KL, Donald AM, Gidley MJ, Clarke CJ, Riekel C (2000) Side-chain liquid-crystalline model for starch. Starch-Stärke 52: 450-460.

Wan JX, Bringloe D, Lamppa GK (1998) Disruption of chloroplast biogenesis and plant development upon down-regulation of a chloroplast processing enzyme involved in the import pathway. Plant Journal 15: 459-468.

Wang SM, Lue WL, Yu TS, Long JH, Wang CN, Eimert K, Chen J (1998) Characterization of ADG1, an *Arabidopsis* locus encoding for ADPG pyrophosphorylase small subunit, demonstrates that the presence of the small subunit is required for large subunit stability. Plant Journal 13: 63-70.

Warner M (1989) The physical principles of side chain polymer liquid crystals. In: McArdle CB (ed) Side Chain Liquid Crystal Polymer. Kluwer Academic, New york, pp 7-30.

Wattebled F, Buléon A, Bouchet B, Ral JP, Lienard L, Delvallé D, Binderup K, Dauvillée D, Ball S, D'Hulst C (2002) Granule-bound starch synthase I - A major enzyme involved in the biogenesis of B-crystallites in starch granules. European Journal of Biochemistry 269: 3810-3820.

Wattebled F, Dong Y, Dumez S, Delvallé D, Planchot R, Berbezy P, Vyas D, Colonna P, Chatterjee M, Ball S, D'Hulst C (2005) Mutants of *Arabidopsis* lacking a chloroplastic isoamylase accumulate phytoglycogen and an abnormal form of amylopectin. Plant Physiology 138: 184-195.

Wattebled F, Ral JP, Dauvillée D, Myers AM, James MG, Schlichting R, Giersch C, Ball SG, D'Hulst C (2003) STA11, a *Chlamydomonas reinhardtii* locus required for normal starch granule biosynthesis, encodes disproportionating enzyme. Further evidence for a function of α-1,4 glucanotransferases during starch granule biosynthesis in green algae. Plant Physiology 132: 137-145.

Weber A, Servaites JC, Geiger DR, Kofler H, Hille D, Groner F, Hebbeker U, Flügge UI (2000) Identification, purification, and molecular cloning of a putative plastidic glucose translocator. Plant Cell 12: 787-801.

Weise SE, Schrader SM, Kleinbeck KR, Sharkey TD (2006) Carbon balance and circadian regulation of hydrolytic and phosphorolytic breakdown of transitory starch. Plant Physiology 141: 879-886.

Weise SE, Weber APM, Sharkey TD (2004) Maltose is the major form of carbon exported from the chloroplast at night. Planta 218: 474-482.

Whelan WJ (1998) Pride and prejudice: The discovery of the primer for glycogen synthesis. Protein Science 7: 2038-2041.

Wielopolska A, Townley H, Moore I, Waterhouse P, Helliwell C (2005) A high-throughput inducible RNAi vector for plants. Plant Biotechnology Journal 3: 583-590.

Wiese A, Christ MM, Virnich O, Schurr U, Walter A (2007) Spatio-temporal leaf growth patterns of *Arabidopsis thaliana* and evidence for sugar control of the diel leaf growth cycle. New Phytologist 174: 752-761.

Wildman SG, Jope CA, Atchison BA (1980) Light microscopic analysis of the 3-dimensional structure of higher plant chloroplasts - Position of starch grains and probable spiral arrangement of stroma lamellae and grana. Botanical Gazette 141: 24-36.

Williams ML, Farrar JF, Pollock CJ (1989) Cell specialization within the parenchymatous bundle sheath of barley. Plant Cell and Environment 12: 909-918.

Winter H, Robinson DG, Heldt HW (1993) Subcellular volumes and metabolite concentrations in barley leaves. Planta 191: 180-190.

Winter H, Robinson DG, Heldt HW (1994) Subcellular volumes and metabolite concentrations in spinach leaves. Planta 193: 530-535.

Witt W, Sauter JJ (1994) Starch metabolism in poplar wood ray cells during spring mobilization and summer deposition. Physiologia Plantarum 92: 9-16.

Yang Y, Glynn JM, Olson BJSC, Schmitz AJ, Osteryoung KW (2008) Plastid division: Across time and space. Current Opinion in Plant Biology 11: 577-584.

Yang YP, Juang YS, Hsu BD (2002) A quick method for assessing chloroplastic starch granules by flow cytometry. Journal of Plant Physiology 159: 103-106.

Yoder DW, Kadirjan-Kalbach D, Olsson BJSC, Miyagishima S, DeBlasio SL, Hangarter RP, Osteryoung KW (2007) Effects of mutations in *Arabidopsis* FtsZ1 on plastid division, FtsZ ring formation and positioning, and FtsZ filament morphology in vivo. Plant and Cell Physiology 48: 775-791.

Yoshida M, Fuji M, Nikuni Z, Maruo B (1958) The appositive growth of starch granules in beans as revealed by autoradiography. Bulletin of the Agricultural Chemical Society of Japan 22: 127-127.

Yoshida Y, Kuroiwa H, Misumi O, Nishida K, Yagisawa F, Fujiwara T, Nanamiya H, Kawamura F, Kuroiwa T (2006) Isolated chloroplast division machinery can actively constrict after stretching. Science 313: 1435-1438.

Yu SK, Blennow A, Bojko M, Madsen F, Olsen CE, Engelsen SB (2002) Physico-chemical characterization of floridean start of red algae. Starch-Stärke 54: 66-74.

Yu TS, Kofler H, Hausler RE, Hille D, Flugge UI, Zeeman SC, Smith AM, Kossmann J, Lloyd J, Ritte G, Steup M, Lue WL, Chen JC, Weber A (2001) The *Arabidopsis sex1* mutant is defective in the R1 protein, a general regulator of starch degradation in plants, and not in the chloroplast hexose transporter. Plant Cell 13: 1907-1918.

Yu TS, Lue WL, Wang SM, Chen JC (2000) Mutation of *Arabidopsis* plastid phosphoglucose isomerase affects leaf starch synthesis and floral initiation. Plant Physiology 123: 319-325.

Yu TS, Zeeman SC, Thorneycroft D, Fulton DC, Dunstan H, Lue WL, Hegemann B, Tung SY, Umemoto T, Chapple A, Tsai DL, Wang SM, Smith AM, Chen J, Smith SM (2005) α-Amylase is not required for breakdown of transitory starch in *Arabidopsis* leaves. Journal of Biological Chemistry 280: 9773-9779.

Yun M-S, Kawagoe Y (2009) Amyloplast division progresses simultaneously at multiple sites in the endosperm of rice. Plant and Cell Physiology 50: 1617-1626.

Yun M-S, Kawagoe Y (2010) Septum formation in amyloplasts produces compound granules in the rice endosperm and is regulated by plastid division proteins. Plant and Cell Physiology 51: 1469-1479.

Zeeman S, Northrop F, Smith A, ap Rees T (1998a) A starch-accumulating mutant of *Arabidopsis thaliana* deficient in a chloroplastic starch-hydrolysing enzyme. Plant Journal 16: 357-365.

Zeeman SC, ap Rees T (1999) Changes in carbohydrate metabolism and assimilate export in starch-excess mutants of *Arabidopsis*. Plant Cell and Environment 22: 1445-1453.

Zeeman SC, Delatte T, Messerli G, Umhang M, Stettler M, Mettler T, Streb S, Reinhold H, Kötting O (2007a) Starch breakdown: recent discoveries suggest distinct pathways and novel mechanisms. Functional Plant Biology 34: 465-473.

Zeeman SC, Smith SM, Smith AM (2002a) The priming of amylose synthesis in *Arabidopsis* leaves. Plant Physiology 128: 1069-1076.

Zeeman SC, Smith SM, Smith AM (2007b) The diurnal metabolism of leaf starch. Biochemical Journal 401: 13-28.

Zeeman SC, Thorneycroft D, Schupp N, Chapple A, Weck M, Dunstan H, Haldimann P, Bechtold N, Smith AM, Smith SM (2004) Plastidial α-glucan phosphorylase is not required for starch degradation in *Arabidopsis* leaves but has a role in the tolerance of abiotic stress. Plant Physiology 135: 849-858.

Zeeman SC, Tiessen A, Pilling E, Kato KL, Donald AM, Smith AM (2002b) Starch synthesis in *Arabidopsis*. Granule synthesis, composition, and structure. Plant Physiology 129: 516-529.

Zeeman SC, Umemoto T, Lue WL, Au-Yeung P, Martin C, Smith AM, Chen J (1998b) A mutant of *Arabidopsis* lacking a chloroplastic isoamylase accumulates both starch and phytoglycogen. Plant Cell 10: 1699-1711.

Zhang M, Hu Y, Jia JJ, Li DP, Zhang RJ, Gao HB, He YK (2009) CDP1, a novel component of chloroplast division site positioning system in *Arabidopsis*. Cell Research 19: 877-886.

Zhang XL, Myers AM, James MG (2005) Mutations affecting starch synthase III in *Arabidopsis* alter leaf starch structure and increase the rate of starch synthesis. Plant Physiology 138: 663-674.

Zhang XL, Szydlowski N, Delvalle D, D'Hulst C, James MG, Myers AM (2008) Overlapping functions of the starch synthases SSII and SSIII in amylopectin biosynthesis in *Arabidopsis*. BMC Plant Biology 8: Article Number 96

Ziegler GR, Creek JA, Runt J (2005) Spherulitic crystallization in starch as a model for starch granule initiation. Biomacromolecules 6: 1547-1554.